IDENTIFYING AND SEPARATING FROM A SEQUENCE OF MINE TREMORS

SERIES OF EVENTS GENERATED BY A SINGLE PROCESS

Final Report

Stanislaw Lasocki

University of Mining and Metallurgy

Faculty of Geology, Geophysics and Environmental Protection

al. Mickiewicza 30

30-059 Cracow, Poland

Special Contract SPC-95-4029

U.S. Department of the Air Force

European Office of Aerospace Research and Development, London

Kraków, September 1996

DISCLAIMER NOTICE

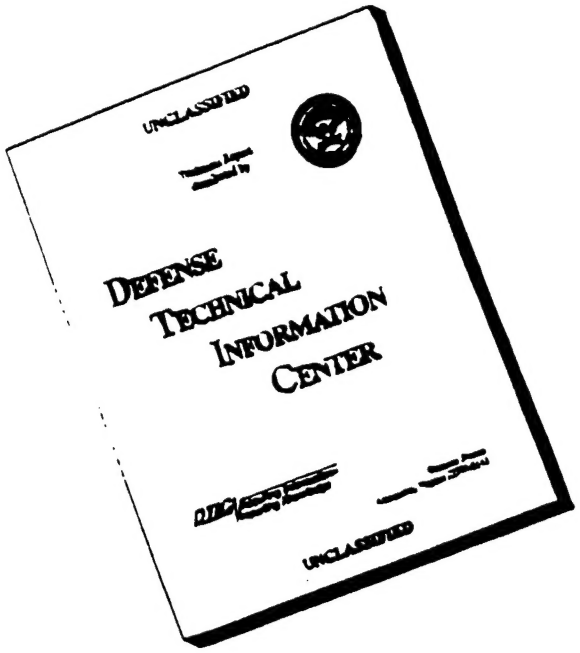

THIS DOCUMENT IS BEST QUALITY AVAILABLE. THE COPY FURNISHED TO DTIC CONTAINED A SIGNIFICANT NUMBER OF PAGES WHICH DO NOT REPRODUCE LEGIBLY.

REPORT DOCUMENTATION PAGE

Form Approved OMB No. 0704-0188

1. AGENCY USE ONLY (Leave blank)	2. REPORT DATE	3. REPORT TYPE AND DATES COVERED
	September 1996	Final

4. TITLE AND SUBTITLE

Identifying and Separating from a Sequence of Mine Tremors Series of Events Generated by a Single Process

5. FUNDING NUMBERS

SPC-95-4029

6. AUTHOR(S)

Stanislaw Lasocki

7. PERFORMING ORGANIZATION NAME(S) AND ADDRESS(ES)

University of Mining and Metallurgy
Faculty of Geology, Geophysics and Environmental Protection
al. Mickiewicza 30
30-059 Cracow, Poland

8. PERFORMING ORGANIZATION REPORT NUMBER

9. SPONSORING/MONITORING AGENCY NAME(S) AND ADDRESS(ES)

EOARD
PSC 802 BOX 14
FPO AE 09499-0200

10. SPONSORING/MONITORING AGENCY REPORT NUMBER

SPC-95-4029

11. SUPPLEMENTARY NOTES

12a. DISTRIBUTION/AVAILABILITY STATEMENT

Unlimited

12b. DISTRIBUTION CODE

13. ABSTRACT (Maximum 200 words)

Generation of induced seismicity in underground mines is controlled by various local and mine-wide factors, and the seismic series are usually composed of events of different origins. Although it is well known that seismicity in mines is a multimodal phenomenon, it is not easy to identify its various components. A set of statistical studies to study complexity of seismic series is proposed. These are the descriptive statistics analysis to recognize basic features of the seismic series, the extreme value method to identify modes of the energy distribution of events, to estimate the limiting energy values for these modes and to distinguish those event generating processes which have well separated modes of energy and the analysis of deflection to identify generating processes that are responsible for certain dominant directions in the seismic series. The dominant directions of the distribution of epicenters are described by the deflections of straight lines connecting the epicenters of every two consecutive events in a series, measured from the NS direction. The deflection then forms another set of time series. The series of deflections are analyzed by a nonparametric kernel estimation of the deflection probability density function; a novel, objective quantitative approach.

14. SUBJECT TERMS

15. NUMBER OF PAGES
132

16. PRICE CODE

17. SECURITY CLASSIFICATION OF REPORT	18. SECURITY CLASSIFICATION OF THIS PAGE	19. SECURITY CLASSIFICATION OF ABSTRACT	20. LIMITATION OF ABSTRACT
UNCLASSIFIED	UNCLASSIFIED	UNCLASSIFIED	UL

Abstract:

Generation of induced seismicity in underground mines is controlled by various local and mine-wide factors, and the seismic series are usually composed of events of different origins. Although it is well known that seismicity in mines is a multimodal phenomenon, it is not easy to identify its various components. A set of statistical methods to study complexity of seismic series is proposed. These are the descriptive statistics analysis to recognize basic features of the seismic series, the extreme value method to identify modes of the energy distribution of events, to estimat the limiting energy values for these modes and to distinguish those event generating processes which have well separated modes of energy and the analysis of deflection to identify generating processes that are responsible for certain dominant directions in the seismic series. The dominant directions of the distribution of epicenters are described by the deflections of straight lines connecting the epicenters of every two consecutive events in a series, measured from the NS direction. The deflection then forms another set of time series. The series of deflections are analyzed by a nonparametric kernel estimation of the deflection probability density function; a novel, objective quantitative approach.

The proposed methods were applied to the sets of events from Wujek coal mine, that occurred from 1988 to 1993 in different areas of the mine. Altogether 14297 events was analyzed. Their distribution is not random both in space and in energy. The analyses resulted in identification of likely processes of seismic event generation. The analysis of deflection applied in the pseudo-multivariate way can be used to separate, from the seismic series, events originated by these identified processes.

Contents:

1. Introduction

Generation of induced seismicity in underground mines is controlled by various local and mine-wide factors. Recorded series contain events originated by different processes of rockmass fracturing. Recognition of the complex structure of the series and separating of their components can be helpful for determining mechanisms governing the seismic event generation.

The research, made within the framework of the Special Contract SPC-95-4029, aimed to answer to the principal question: Is it possible, by the statistical analysis of standard seismic catalogs, to evidence the fact that the seismic series contain complex mixture of outcomes of different generating processes? When such the question is positively answered then it will be also possible to identify those processes and, after complementing the results of the statistical analysis with information from other sources, to conclude about possible factors controlling the identified processes.

Statistical inference applied to samples of events described by a number of parameters means that these parameters are regarded as random variables, having specific probability distributions. Their measured values are supposed to be the statistical samples representing features of the populations. If the problem set by us can be resolved by statistical analysis methods then the parameters of the seismic events, generated by different processes, must differ statistically, which means that they must have different probability distributions. In such the case the general probability distributions of parameters for the whole seismic series, which is a mixture of outcomes of different processes, are superpositions of the individual distributions related to the particular processes and are, in general, multimodal. In a simplified but feasible approach one can regard the modes of these generalized distributions as identifying their unimodal components, hence as identifying different generating processes.

The above presented concept of identification of different processes generating the seismic events can be realized in two ways. The first one is a univariate approach in which each of the parameters is studied individually, which leads to individual separating of the modes of its probability distribution. This approach is relatively simple, has a good theoretical background and, thanks to this, in many cases can be used in practice. Its main drawback stems from the fact that no crossing relations between parameters are taken into account. These crossing effects are

obviously present for the obvious reason that the parameters describe the same phenomenon. The second approach is multivariate in which the multidimensional distribution of all parameters is studied. It is conceptually more proper than the first one, however difficulties, that appear when attempting to determine exact characteristics of the multidimensional distribution from the sample, cause that this approach can be used only in a simplified way and only when the data satisfy very specific conditions. An important representation of the univariate approach is the cluster analysis. This analysis has been developed, however, for phenomena described with numerous random variables, which values can be measured repeatedly (Anderberg 1973). A version of the cluster analysis, the single-link clustering method was used to separate components of the seismic series (e.g. Frohlich and Davis 1986, Davis and Frohlich 1991). Our trials made in this work on the mining-induced seismicity for the time being disqualified this method for our purposes when so many events described by so few parameters were to be studied.

Within this study we decided to work out a compromise between the univariate and multivariate approaches, which we have called as the pseudo-multivariate approach. It relies on repetitions of the univariate analysis (the one parameter analysis) for subsets extracted from the whole set of data so that values of other parameter (or parameters) in the subsets are kept in selected intervals. Comparison of features of the analyzed random variable determined for different subsets reveals partially the crossing relations. Out of the parameters of seismic events, which are in our standard catalogs from mines: time of the event occurrence, coordinates of its epicenter and its seismic energy, the coordinates of epicenter and the energy have been used to split the catalog into the subsets. The reasons for choosing the first discriminator are obvious. We expect that the seismic events grouped in an area are more structurally homogeneous than the events that come from different clusters. The energy, from the other hand, according to world-wide studies of induced seismicity, most probably discriminates different kinds of the generating processes. Two classes of seismic induced events were distinguished, in general the small events, that are directly connected to mining works and, in general, the strong ones which are triggered by mining works but which are also controlled by tectonic and mining structures (Gibowicz 1992, Johnston and Einstein 1992).

Statistical analysis works on statistical samples that is the samples that are, simply speaking, constant in time. A considerable effort have been done in studying basic features of our data in order to test their time homogeneity. The results are presented in Section 4 of this report. The descriptive statistics studies allowed also to determine global variability of the event parameters, to verify correctness of the way of division of the catalog into subsets and to determine the intervals of coordinates and seismic energy for such the division.

Sometimes the problem of data decomposition, difficult for solving by methods directly dealing with measured values, can be significantly simplified by means of an indirect method that uses such data transformation which strongly reduces the original data set. This kind of method was in our study the method of the analysis of asymptotic distributions of the extreme values. Instead of studying of distributions of the seismic event energy the distributions of energy maxima, evaluated in constant time intervals, are analyzed. The method, presented in Section 5, was already used in studies of the seismic catalogs from mines (Kijko et al 1987). Here, however, is has been applied for the first time so widely with the use of statistical tests for assessing differences between the empirical distributions of the energy maxima.

On the basis of numerous works describing both natural as well as induced seismicity one can expect that the spatial distribution of events generated by a single process will have a distinct, more or less linear direction. For the purpose of studies of the directional character of the seismic series we have introduced a new parameter, called as deflection, constructed on mutual, bi-directional migrations of two consecutive events. Its definition and its basic statistical properties are given in Section 6.

We anticipated initially that it would be possible to identify modes of the distribution of deflections from the histograms. However subjectivity of histograms causes that such the identification would have been non-unique and of weakly reliable. As the things are we decided to find objective methods of estimation of the probability density function (p.d.f.) from the sample data. The nonparametric kernel estimation of p.d.f. turned out to suit to our purposes. This method, so far as we know for the first time used in the seismic series studies, is insufficiently developed from the point of view of specific practical applications. Therefore we had to make much effort, to carry out a lot of simulation and comparative experiments to be able

to use it for studying the multimodality of the distributions of deflection. The results of these studies are given in Section 7.

In Section 8 we present the detailed analysis of deflections for a number of subsets of our seismic catalog, the identification of generating processes of seismic events on the basis of modes of the distributions of deflection and some attempts of relating the dominant trends of the seismic series to tectonic and mining structures of the mine. The method of the directional character of seismic series analysis with the use of the nonparametric kernel estimation of p.d.f. will be presented on the 4th International Symposium on Rockburst and Seismicity in Mines in 1997 (Lasocki et al. 1996).

Section 9 contains an example of separating of seismic events that are outcomes of the generating process identified by the analysis of deflections. Finally, Section 10 presents conclusions which we could draw from the research made within this project.

2. The area of investigation

When selecting the area for investigations we considered a number of conditions that the data should satisfy.

1. Size of sample sets. Generation of induced seismicity in underground mines is controlled by various local, mine-wide and regional factors. However the majority of seismic events is directly linked to the mining operation. The seismicity connected with mining can hide effects of processes with lower event rate. We wanted to test whether it was possible to ascertain a complex character of seismic catalogs and separate its components from seismic series analysis and to develop suitable methods for such separation. Thus we had to possess initially huge data sets. In this way the statistical inference could deliver certain conclusions for samples reduced in course of separating.

2. Completeness and uniform quality of seismic catalogs. The requirement to have huge data set implies that the data will come from a considerable time period. For obvious reasons our studies could be performed only on complete and uniform quality catalogs. Therefore we had to be sure that, during a period selected for our study, all a seismological network layout, quality of recording and event parameter estimation techniques remained unchanged. These were only initial requirements and we also studied an internal structure of our data sets from a point of view of their completeness.

3. Wide energy range of the data. Polish standard seismic catalogs in mines contain limited number of parameters of recorded events. Each event is described by the time of event occurrence, epicenter coordinates, some, usually poor, information about the depth of focus and the seismic energy at the source. We expect that different generating processes result in differences in distributions of parameters of events. Following world-wide studies (e.g., Gibowicz 1990, Johnston and Einstein 1990), we can suspect a particular significance of energy distributions. Triggering processes are supposed to generate events with higher energy modes than processes directly controlled by mining. Therefore it was necessary to have data covering the widest possible energy range.

4. Complex mining and geological conditions of an area. We had to have data from an area where more than one generating processes were likely to happen. Studies on structure of

induced seismicity postulat that there are at least two different types of this phenomenon: the one directly connected with mining and the other triggered by faults and other weak zones (Gibowicz 1990, Gibowicz and Kijko 1994). Thus, to make our study feasibly, we wished to have, in the area under study, structures that could give rise to the second type of induced processes. This condition does not mean that developed methods for generating processes identification are limited to the processes originated by faults or similar structures. However we had to have chance to find more than one component in our data.

5. Availability of seismological and complementary data. In order to form reasonable basis for sample reduction and to validate conclusions concerning existence of different processes not only seismological data were required but we had to have mining and geological information about the area.

The given conditions were well satisfied by data from the Wujek coal mine. Wujek coal mine exploits seams in the central part of the Upper Silesian Coal Basin (USCB) located in southern Poland. Structurally the area of mine belongs to the main anticline of USCB. The area is bounded from the south by double Klodnicki fault, with some 125 and 120 meter throw, respectively, from the east by Wojciech fault, with 80 to 120 meter throw, and from the west by Srodkowy fault with 50 meter throw. The area is additionally fragmented by a number of secondary faults with general the N-S or NE-SW strike directions. According to some recent hypotheses the rockmass in this part of USCB is still not in equilibrium and the strongest mining tremors may be resulted by a superposition of a local stress field due to exploitation and non-relaxed remnant tectonic stresses (Teper et al. 1992). The faults present in the mine area divide it into the following five, more or less homogeneous, parts:

- The north-western (NW), the left uppermost part of the main, roughly below the line assigned by (17500, -8500) and (19000, -6000) coordinates;

- The south-western (SW), below NW part, enclosed from the east by the line assigned by (19500, -7400) and (18100, -7400) coordinates;

- The central (C), left to NW and SW parts, enclosed from the east roughly by the line of (19650, -8850) and (17500, -8700) coordinates. Mining has been carried on only in the southern part of this area;

- The south-eastern (SE), left to C part, enclosed from the north by the line of some (19000, -10500) and (18450, -8750) coordinates;

- The north-eastern (NE), bounded by the northern border of SE part and the eastern border of C part.

Because the mine is partially just under the town Katowice mining has been done by means of longwall technique in tabular excavations in some areas with hydraulic backfill and in other by caving.

The mine is old and there is a lot of interacting remnants of past works since 1920 (edges, pillars etc.) at various levels. The remnants definitely influence stability of the rockmass.

Both the recording system and the data collection method have remained, more or less, unchanged since 1988. Therefore we selected for our study a time period between 1988 and 1993.

During the period selected for our study mining works were carried on at five coal levels simultaneously, beneath other six already mined out. These productive levels are:

- The uppermost productive level 416 located at depths of 700 to 740 meters. Its thickness ranges from 4 to 5.5 m. During the studied period mining was carried on, at this level, only in C part in two slabs;

- The level 501 located at depth range from 770 to 810 m with thickness ranging from some 7 to 8.5m. Coal has been mined there in three slabs in NW, C and NE parts, and in two slabs in SW and SE parts, where the coal layer was thinner. During the studied period mining was carried on in all but SE parts. Exploitation of level 501 was the most endangered by rockbursts. Often strong tremors caused considerable damages to mining installations. In some cases the works had to be stopped and the longwalls rebuild;

- The level 504 located from 2.5 to 15 meters under the level 501. Its thickness varies from 1.6 to 2.4 m. The level in its productive parts was nearly mined out before the period selected for study. Only six longwalls were working in the years 1988-1993, three in NW part and three in C part;

- The level 507. It appears as a separate coal layer, with thickness some 1.5 meters, only in NW and SW parts of the mine, at depth of some 745 m. In other parts it joins the next level 510. During the studied period NW part of this level was being worked;

- The last level 510 is present in all parts of the mine at depth range from 800 to 850 m. The coal layer is thick, 5.3 to 6 m, and the coal has been mined in two slabs. In the years 1988-1993 the works were done in NW, SE and NE parts of the level.

Up to 50 meters thick layers of compact rigid sandstones dominate strata separating and overlaying the productive layers. The other strata are formed of shales of various kind with incidental intrusions of coal.

Maps of all slabs of all productive levels are given in Appendices 1-9. Dark areas denote parts worked out before 1988. Geometry of stopes active during the period selected for study, marked by thick black lines, is combined with longwall positions in selected days.

3. Seismological database

A local mine area wide seismic network was installed in 1975. Since 1982 the mine has been equipped with a 12 channel digital recording system called PCM G3, produced in Warsaw, Poland. The sensors (only vertical component) have been distributed all over the mine area at various depths ranging from 300 to 850m below the surface. Horizontal distances between the sensors do not exceed 3.5 km. An overall dynamics of the recording system is some 70 dB while the frequency range of flat response is form 0.1 to 27 Hz.

The network records events of energy from 10^2J. The recorded signals are immediately processed to evaluate their parameters and then stored in the mine catalog. Every event in the catalog is described by a time of its occurrence, coordinates of its epicenter, its seismic source energy, comments concerning the stope and the level where the event occurred and additional comments on mining works to that could have an influence on event creation (productive blasting, destressing blasting, water injection etc.). Various test have pointed out that the average accuracy of epicenter location is some 50 m while the precision of energy determination is roughly the half of order. Due to a flat distribution of sensors, the source depth cannot be estimated reliably. The only information about vertical positions of sources comes from the comments linking events to specific coal levels. In this connection we consider only vertical division of the data into different productive levels.

For some of the weakest events, usually of energy below 10^3J, even the epicenter coordinates are not determined. We use these data only in descriptive statistics analyses. For more sophisticated studies we need values of all parameters of events.

14297 events were recorded during the period selected for the study. Out of them 1524 occurred at the level 416, 7365 at the level 501, 642 at the level 504, 1345 at the level 1345, 2980 at the level 510, and for 441 the source location was not determined. The distribution of events among the mine parts is given in Figure 3.1. Zero level denotes events for which information about coal level was not provided. SW part of the level 501 was the most seismically active. Also E part at the level 510, C part at the level 501, C part at the level 416 and NW part at the level 507 experienced considerable activity.

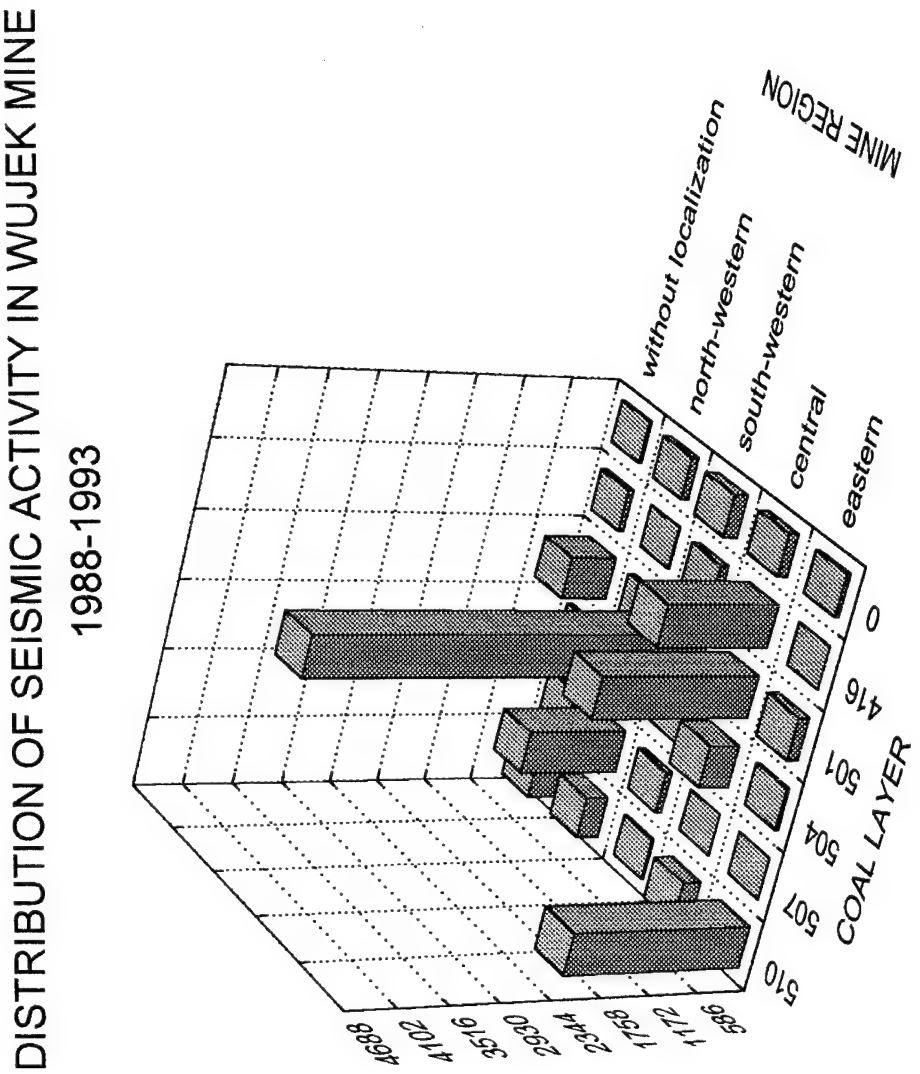

Figure 3.1 Distribution of seismic activity at the Wujek coal mine, in the years 1988-1993

As mentioned previously the catalog comprised events of energy from 10^2J. The strongest recorded event had energy of $5.4*10^8$J (Richter's magnitude some 3.6). It occurred at the coal level 501, by Arkona fault, well apart form mining works of longwall I. The cumulative frequency- energy distribution of all events is presented in Figure 3.2. The distribution is more or less linear from 10^3J. Hence, as far as energy is concerned, we can assume that the database is complete starting from this energy value. No significant differences in the distributions constructed for activity in each year can be seen. The fact suggests a time uniformity of energy evaluation.

The spatial distributions of seismicity associated with the level 416 during the studied period together, with contours of active excavations, are presented in Figures 3.3, 3.4, 3.5. Respective figures show positions of sources of all recorded events, of events that energy was greater than or equal to 10^4J and of events that energy was greater than or equal to 10^5J. Most of events occurred close to active stopes. There are, however, two opposite cases. The cluster located in SW part could be eventually a far effect of severe activity at the 501 level . Similar phenomenon at the same place is observed in the seismicity map of the levels 504 (Fig. 3.9) and 507 (Fig. 3.12). Since in this area both levels (416 and 501) are distanced vertically of some 60 meters the activity at the level 416 could be an example of a chaotic dynamic system behavior of rockmass in the subcritical state. Such hypotheses explaining strange appearance of both natural as well as induced seismicity can be found in a number of references (e.g., Grasso 1993, Morrison 1993). The other cluster located in NW part cannot be linked neither to active excavations nor to other seismically active areas at any productive level.

Generally the activity of level 416 during the studied period was not very hazardous. There were only three events of energy above 10^4J order.

The maps of seismic sources recorded at the level 501 are shown in Figures 3.6, 3.7, 3.8 respectively. The most active areas, with many strong tremors, were connected with mining in third slab of SW part, adjoining Arkona fault, and with mining in C part. The cluster whose center is at some (18600, -8600) cannot be linked to any mining or seismic activity at any level.

Figures 3.9, 3.10, 3.11 show maps of seismic sources recorded at the level 504. Apart from clusters linked to excavations in C and NW parts one may see a group of seismic events in SW part of possible similar origin to those at the level 416 in this part. This seismic activity is,

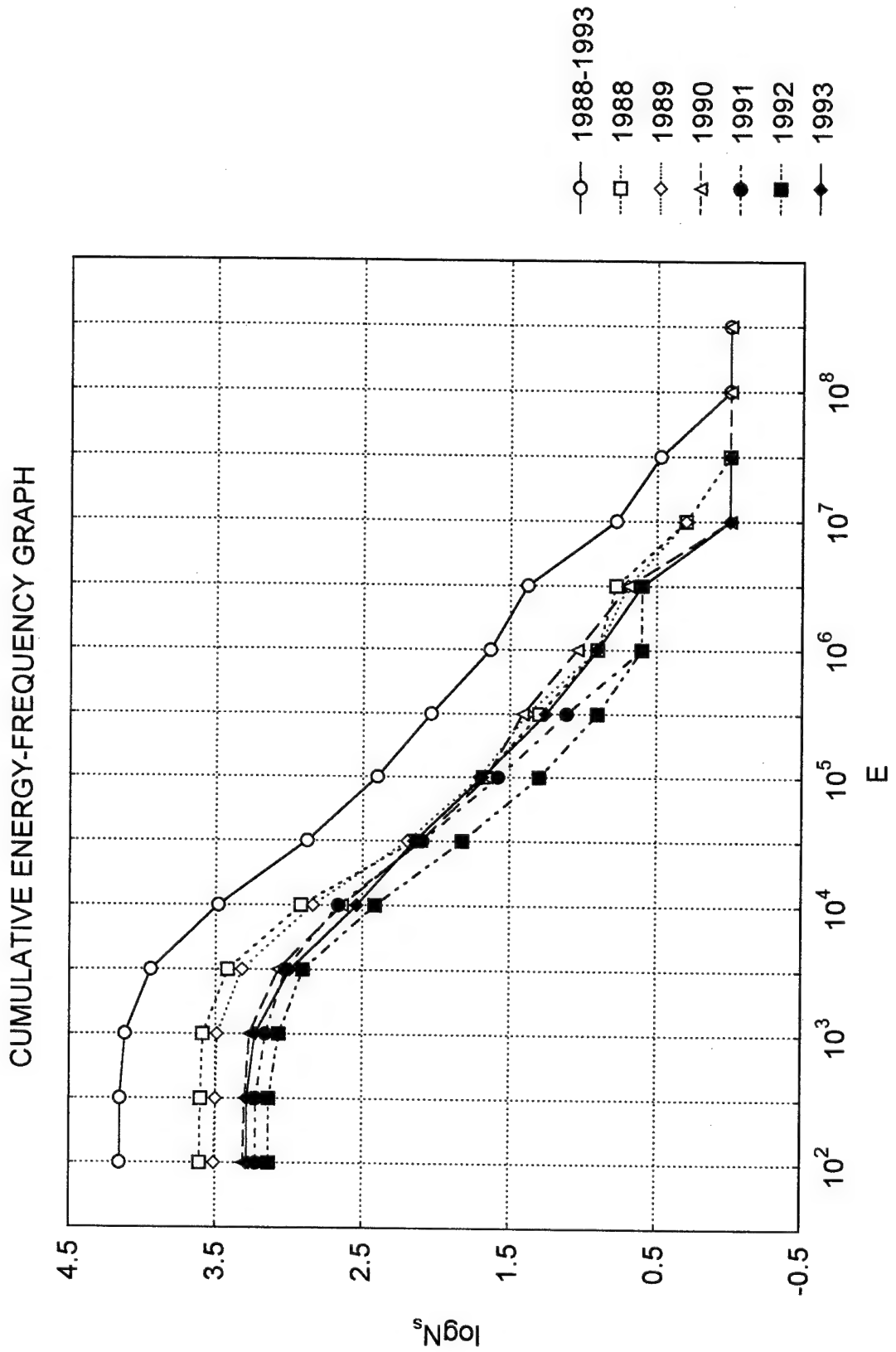

Figure 3.2 Cumulative energy-frequency graphs for events recorded at the Wujek coal mine, in the years 1988-1993

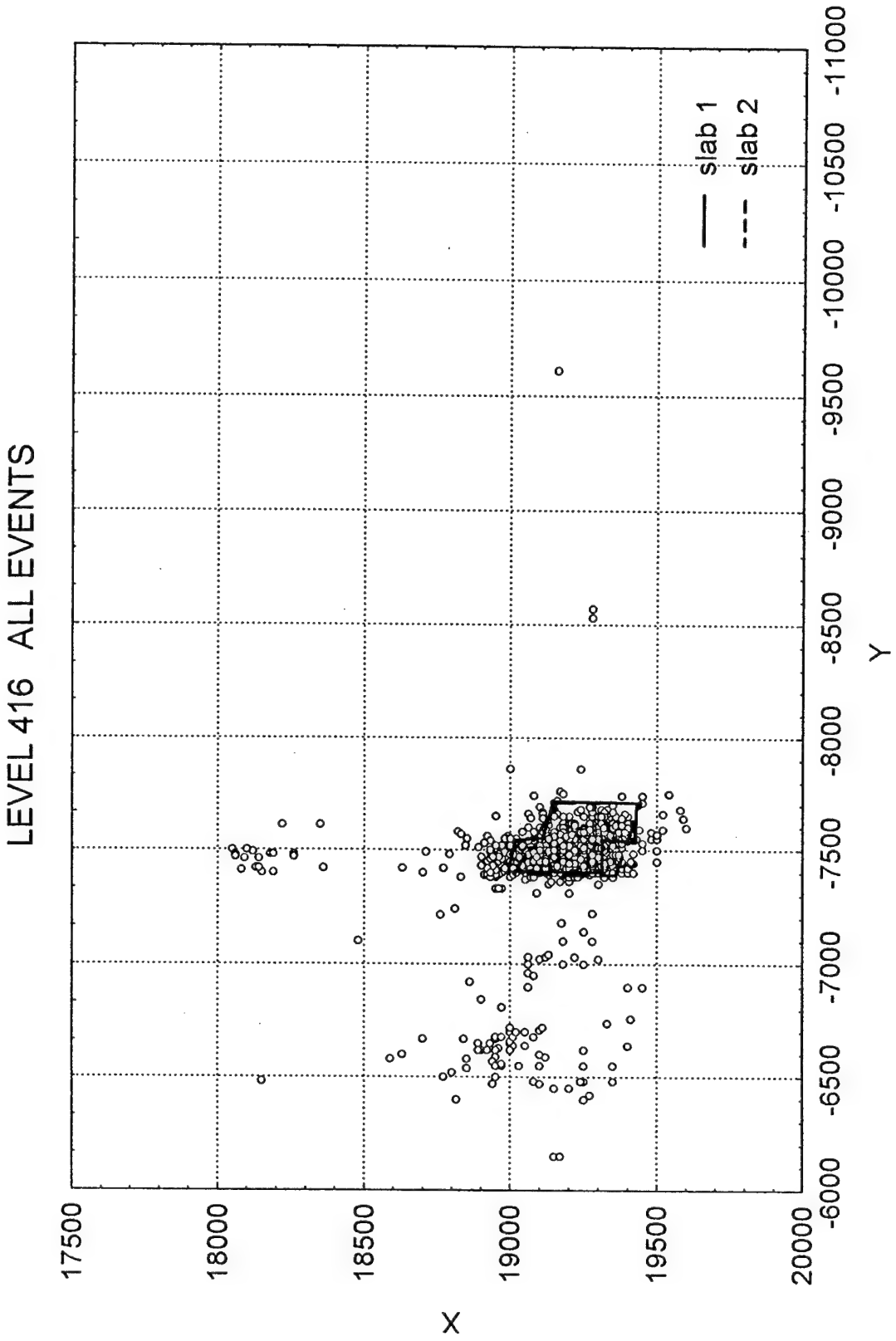

Figure 3.3 Spatial distribution of all seismic events associated with the coal level 416

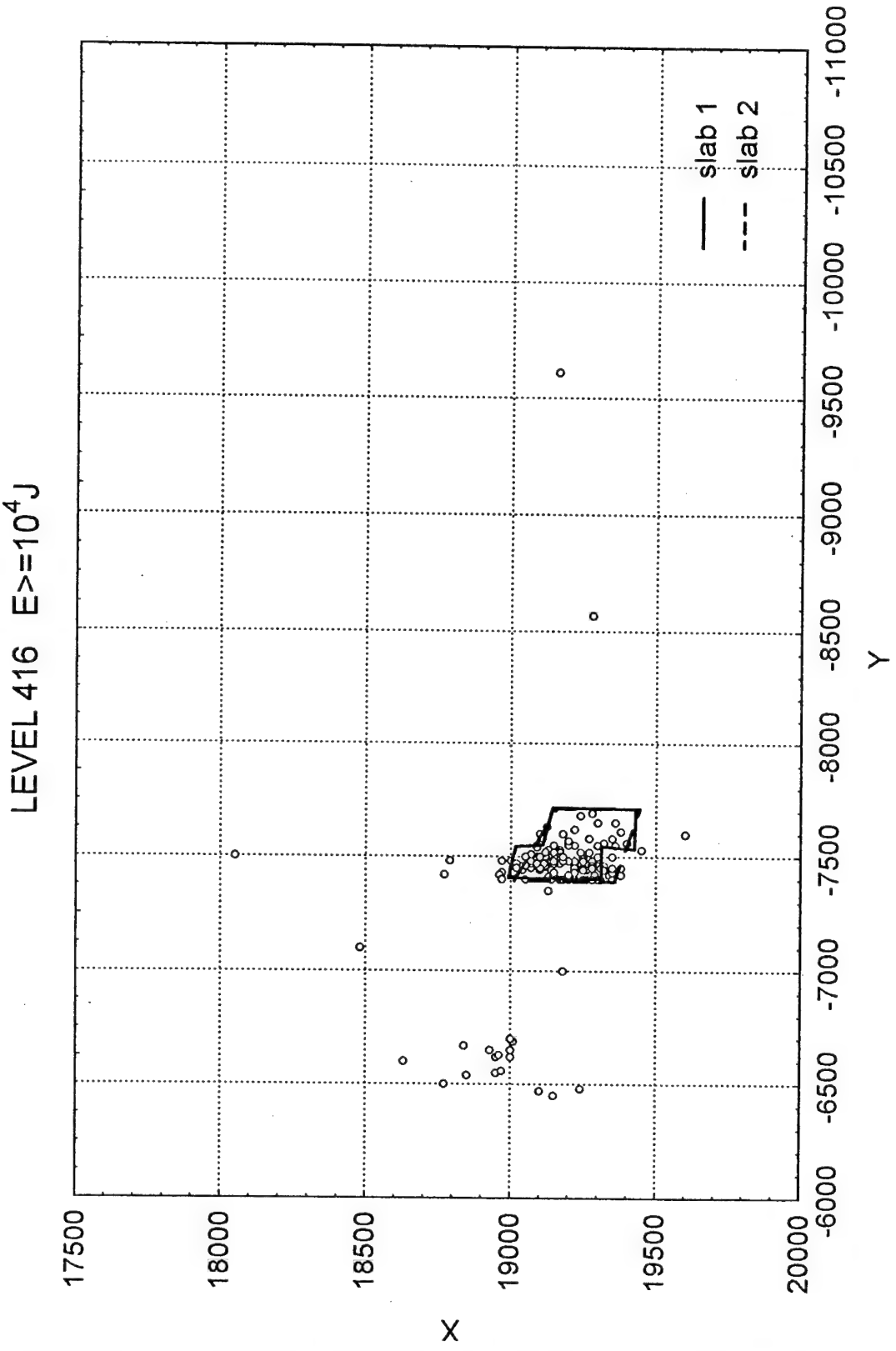

Figure 3.4 Spatial distribution of seismic events of energy ≥ 10^4 J associated with the coal level 416

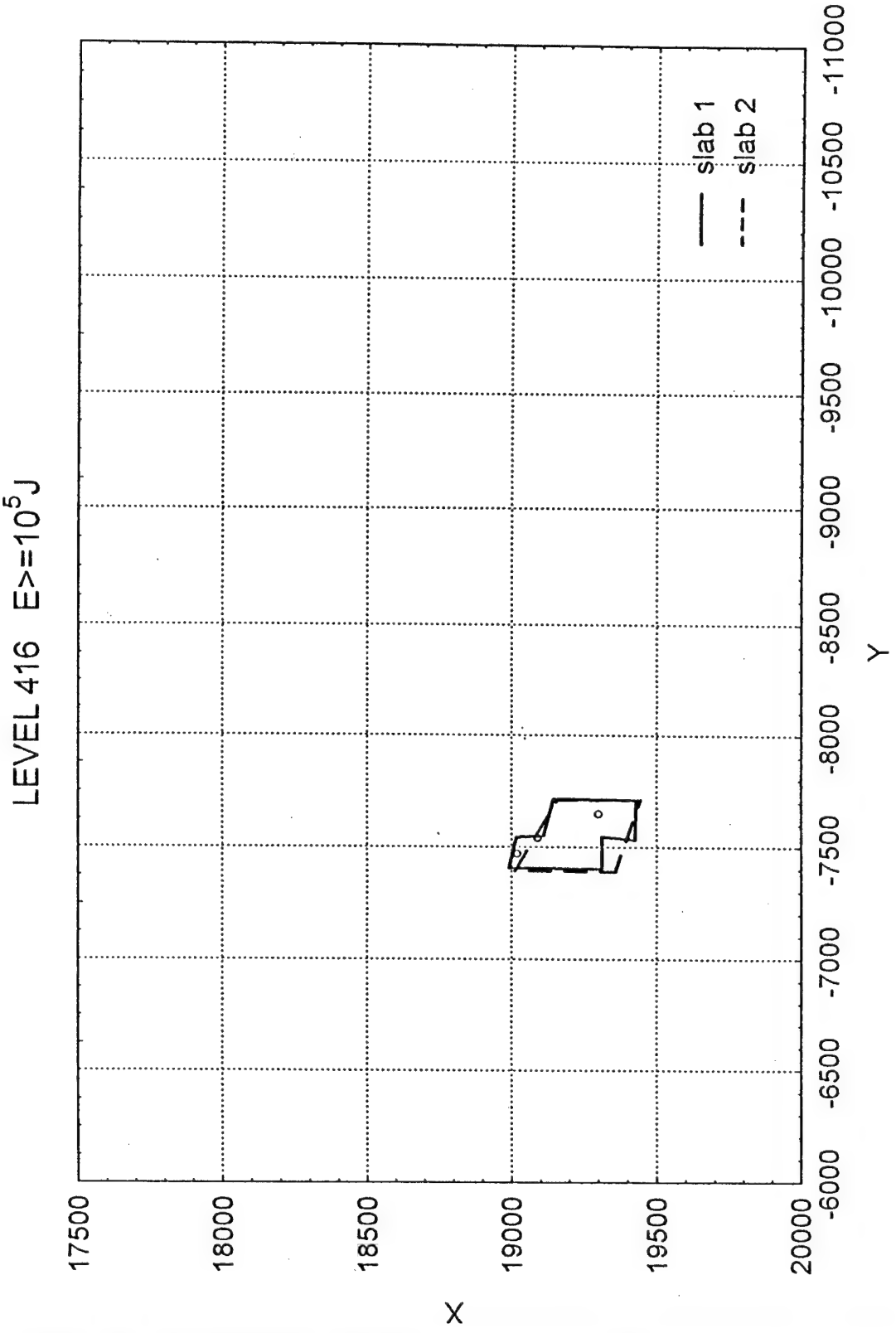

Figure 3.5 Spatial distribution of seismic events of energy ≥ 10^5 J associated with the coal level 416

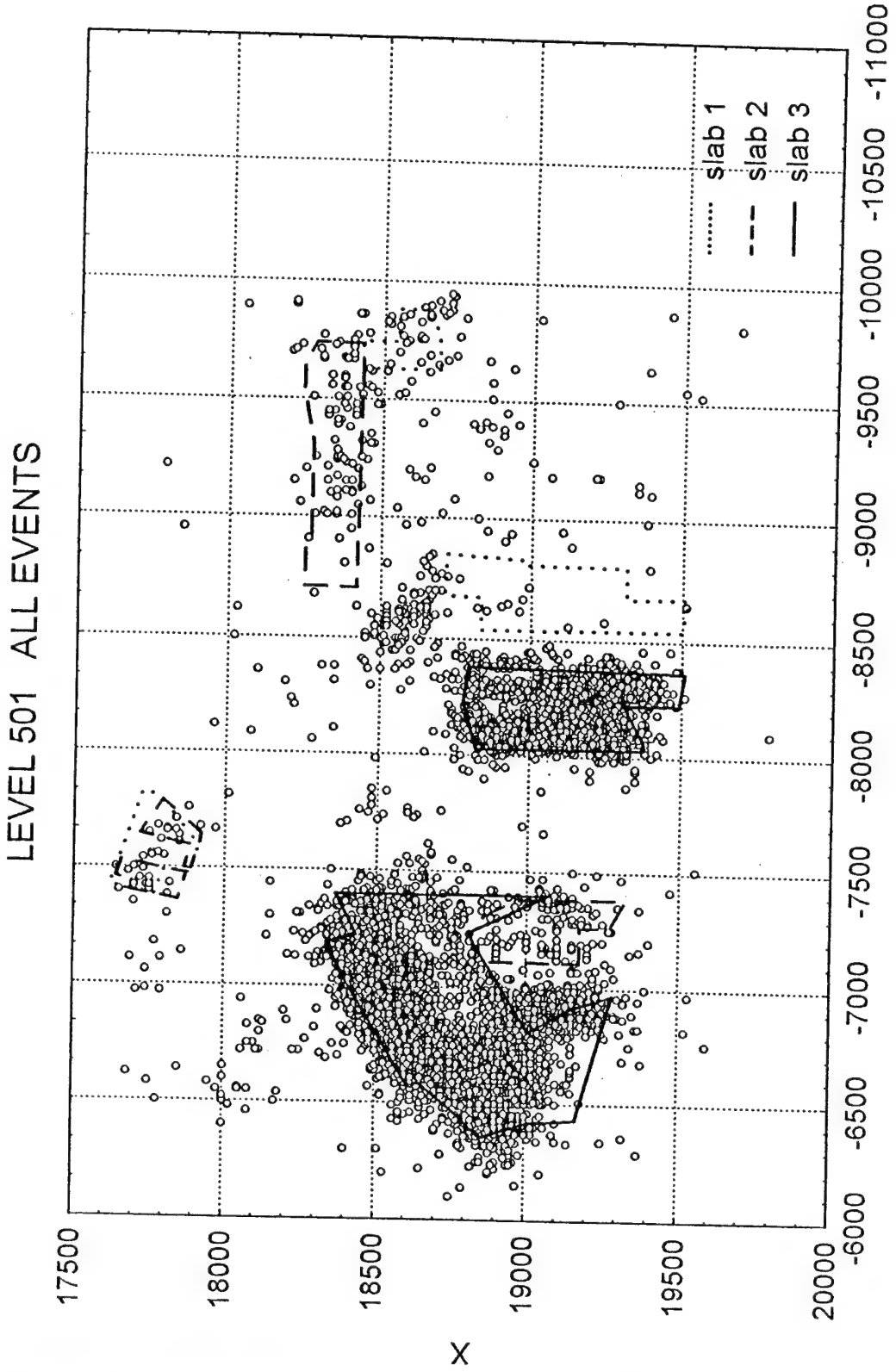

Figure 3.6 Spatial distribution of all seismic events associated with the coal level 501

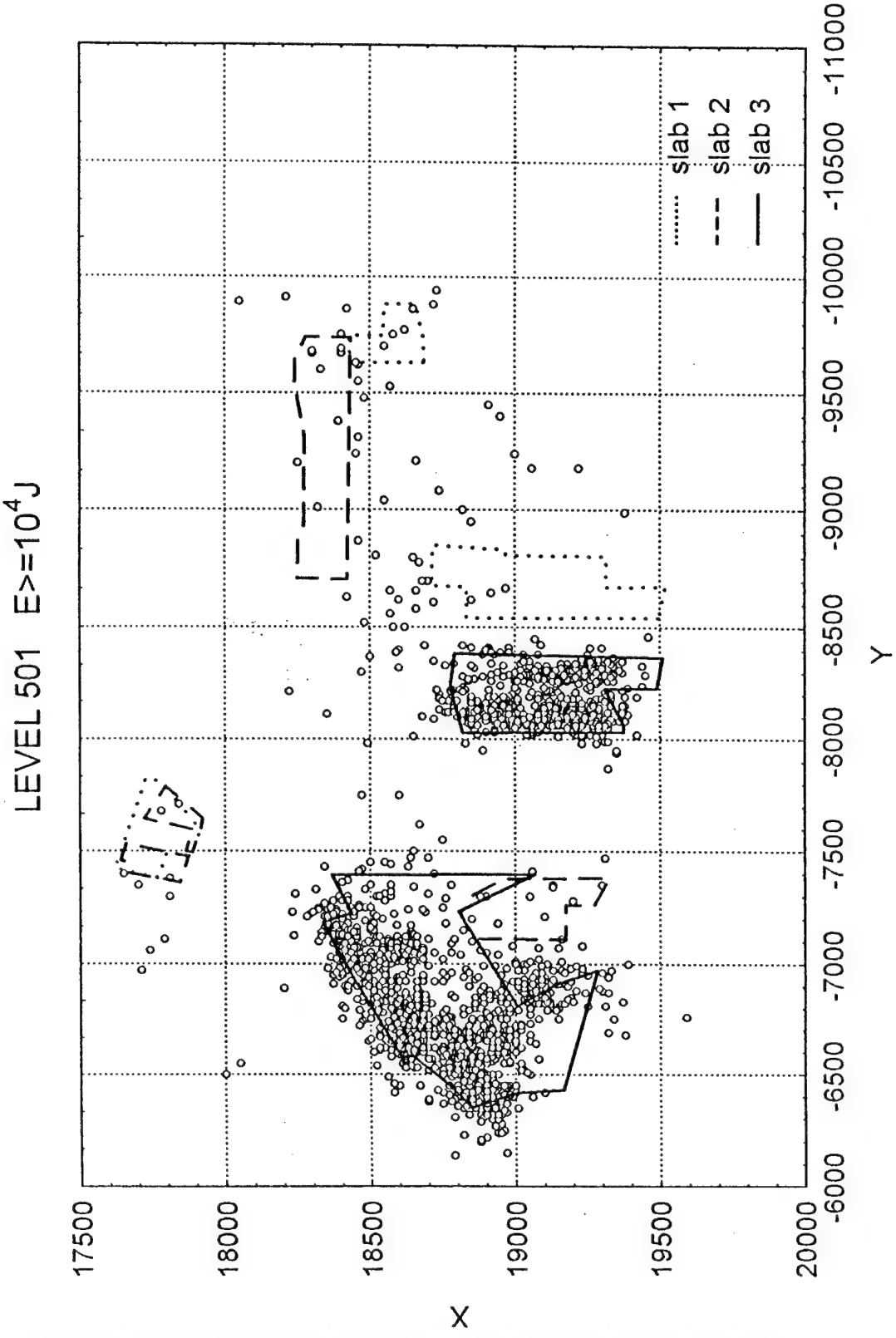

Figure 3.7 Spatial distribution of seismic events of energy ≥ 10^4 J associated with the coal level 501

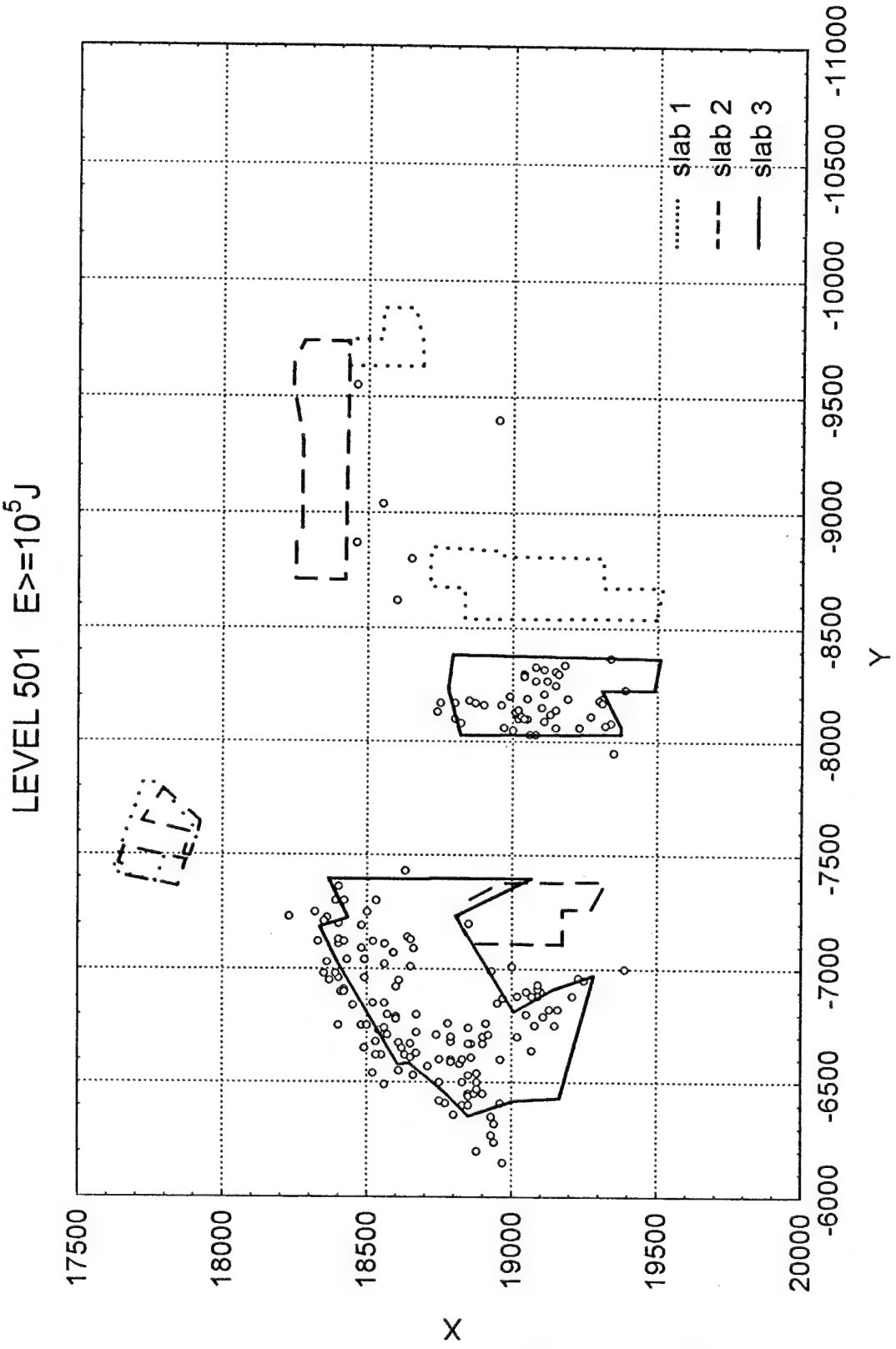

Figure 3.8 Spatial distribution of seismic events of energy $\geq 10^5$ J associated with the coal level 501

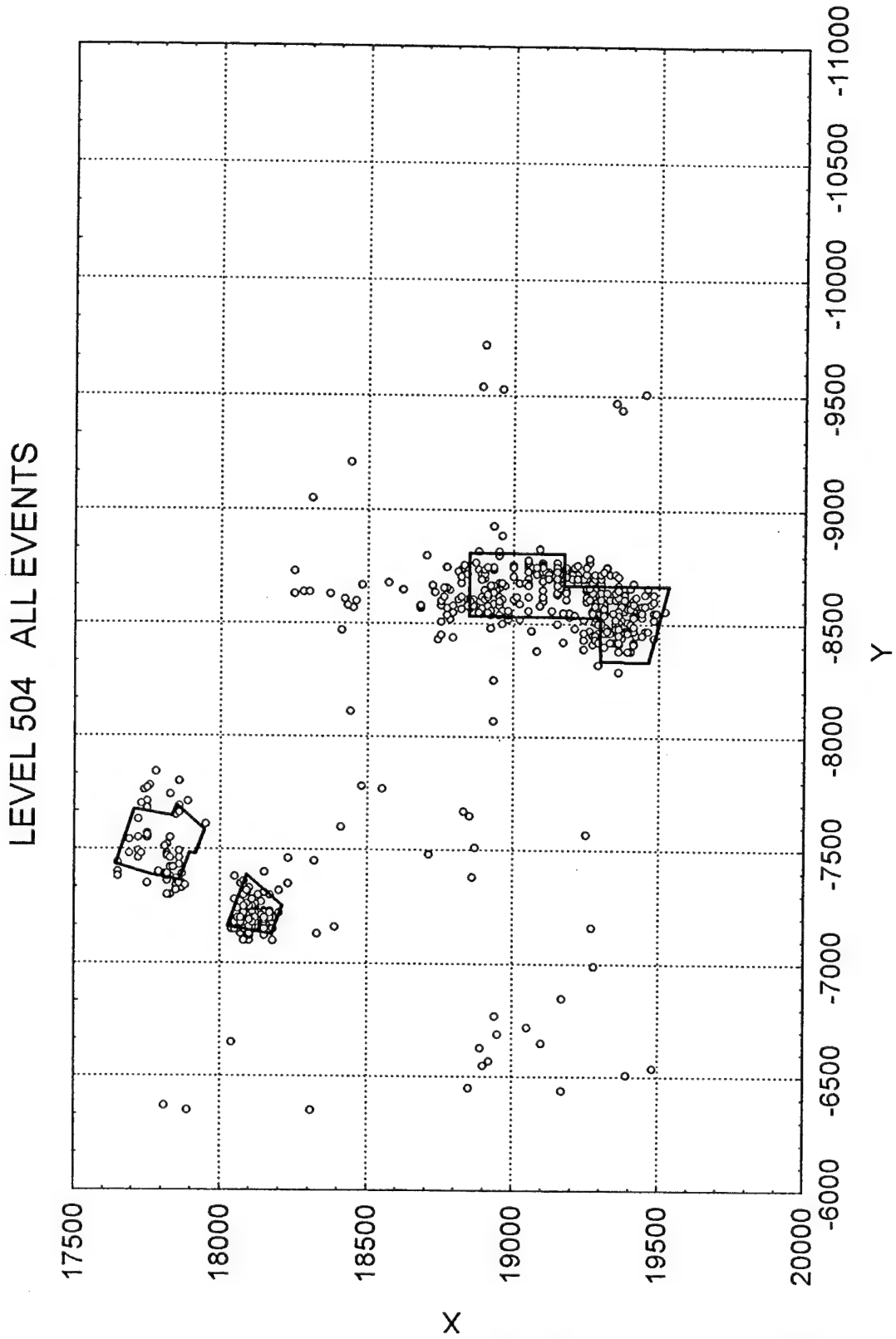

Figure 3.9 Spatial distribution of all seismic events associated with the coal level 504

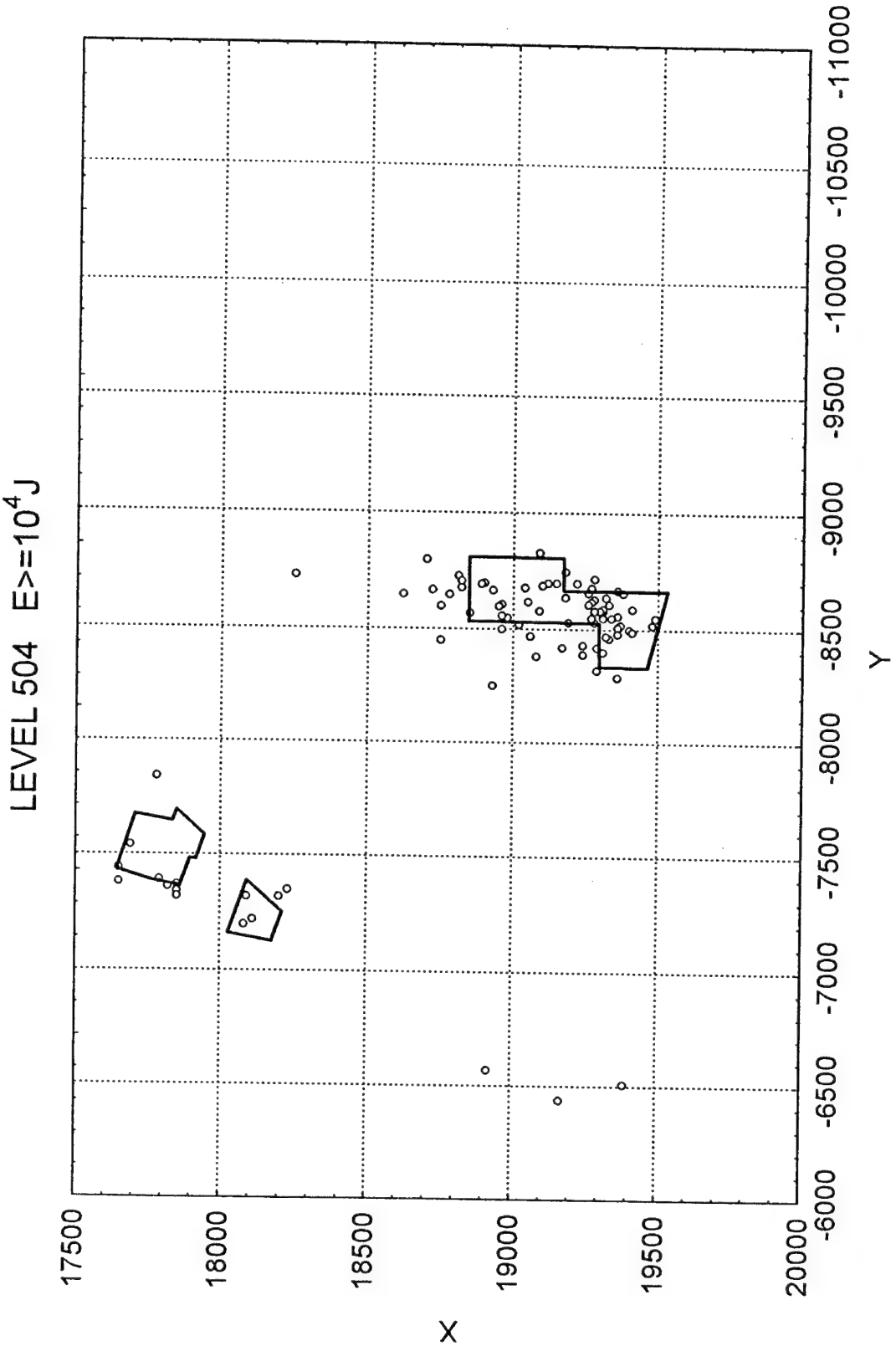

Figure 3.10 Spatial distribution of seismic events of energy ≥ 10^4 J associated with the coal level 504

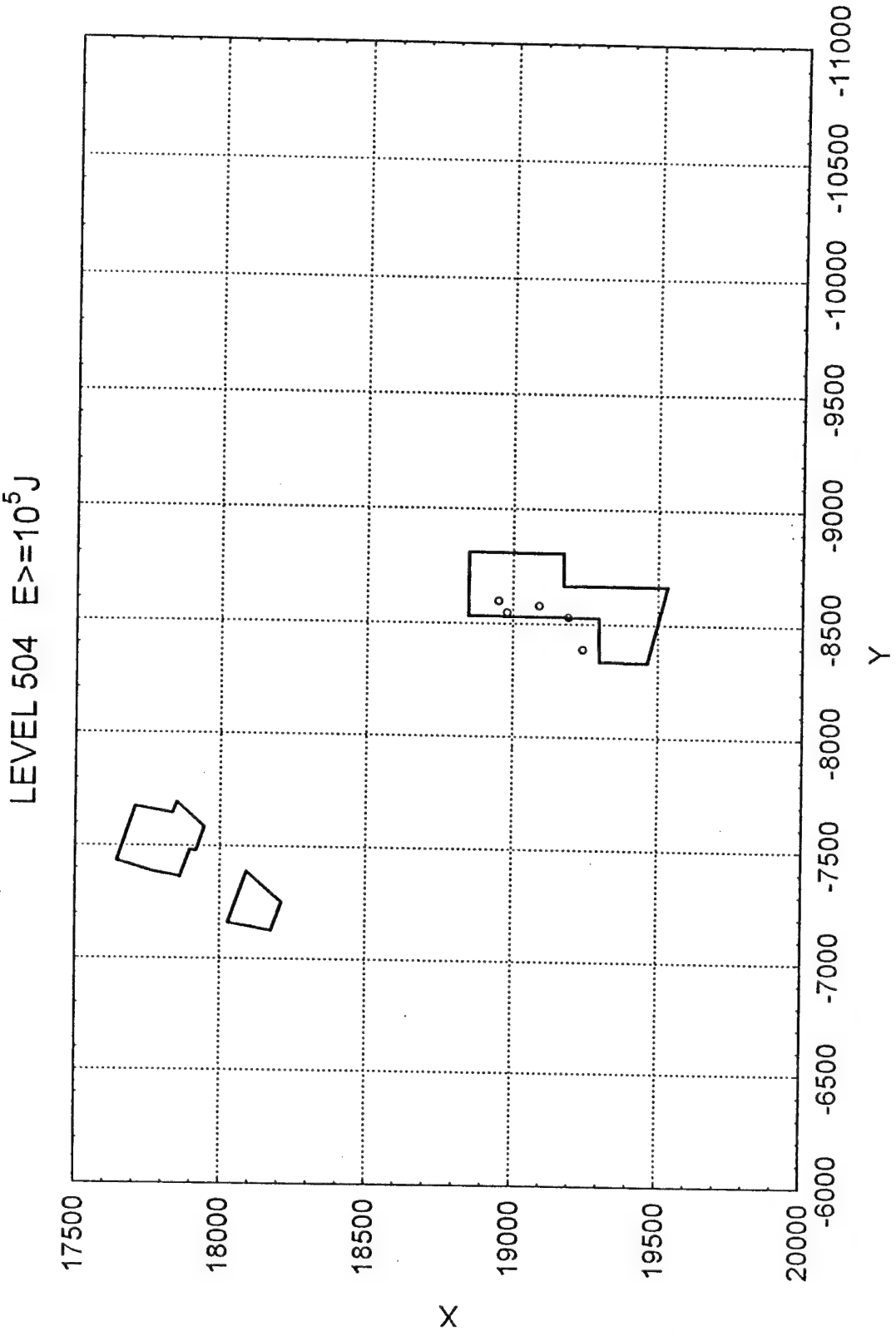

Figure 3.11 Spatial distribution of seismic events of energy ≥ 10^5 J associated with the coal level 504

however, much weaker than that at the level 416, although the level 504 is much closer to the level 501 than the level 416. Some slight activity in the northern part of C area also cannot be directly explained by mining works. In general energy of events was not very high. There were five events of energy above the 10^4J order, all close to excavations in C part.

The maps of seismic sources recorded at the level 507 are shown in Figures 3.12, 3.13, 3.14. The level exists only in the NW and SW parts but, to facilitate comparisons with other levels, the same scale of graphs has been maintained. The seismic activity concentrated in areas of active excavations. Events probably induced by seismic activity at the level 501 are seen in SW part. It should be noted that the level 507 is distanced form the level 501 of nearly 60 meters in this part of the mine. Despite considerable in number the overall seismicity associated with the level 507 was not very dynamic. Only nine events of energy above the 10^4J order were recorded.

The maps of spatial distributions of seismic events at the last level 510 are shown in Figures 3.15, 3.16, 3.17. One can see clusters connected with excavations in NW, SE and NE parts. Many events, however, were located beyond the active stopes, particularly in NE part of the mine. Some part of them could be correlated with mining works some 35 meters above, in the second slab of coal level 501. Still an open question remain why this area was more active at the level 510 than at the productive level 501. Also clusters with centers located at some (18150, -900) and (17950, -9600) cannot be directly linked to any excavations or any other seismically active parts of the mine. The level, in general, was the next, after the level 501, most active in high energy range. Many events of energy starting from 10^5J occurred in its SE part.

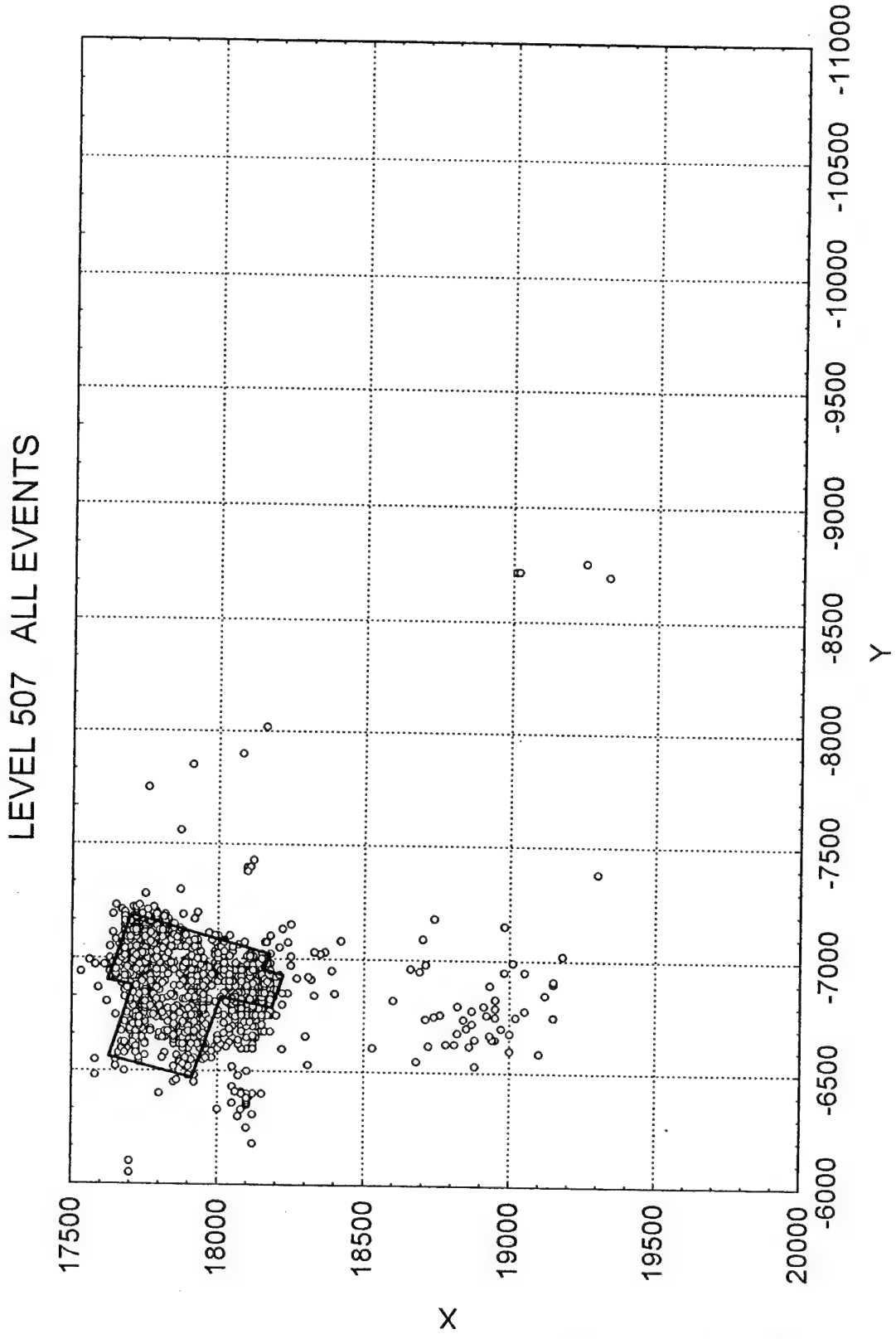

Figure 3.12 Spatial distribution of all seismic events associated with the coal level 507

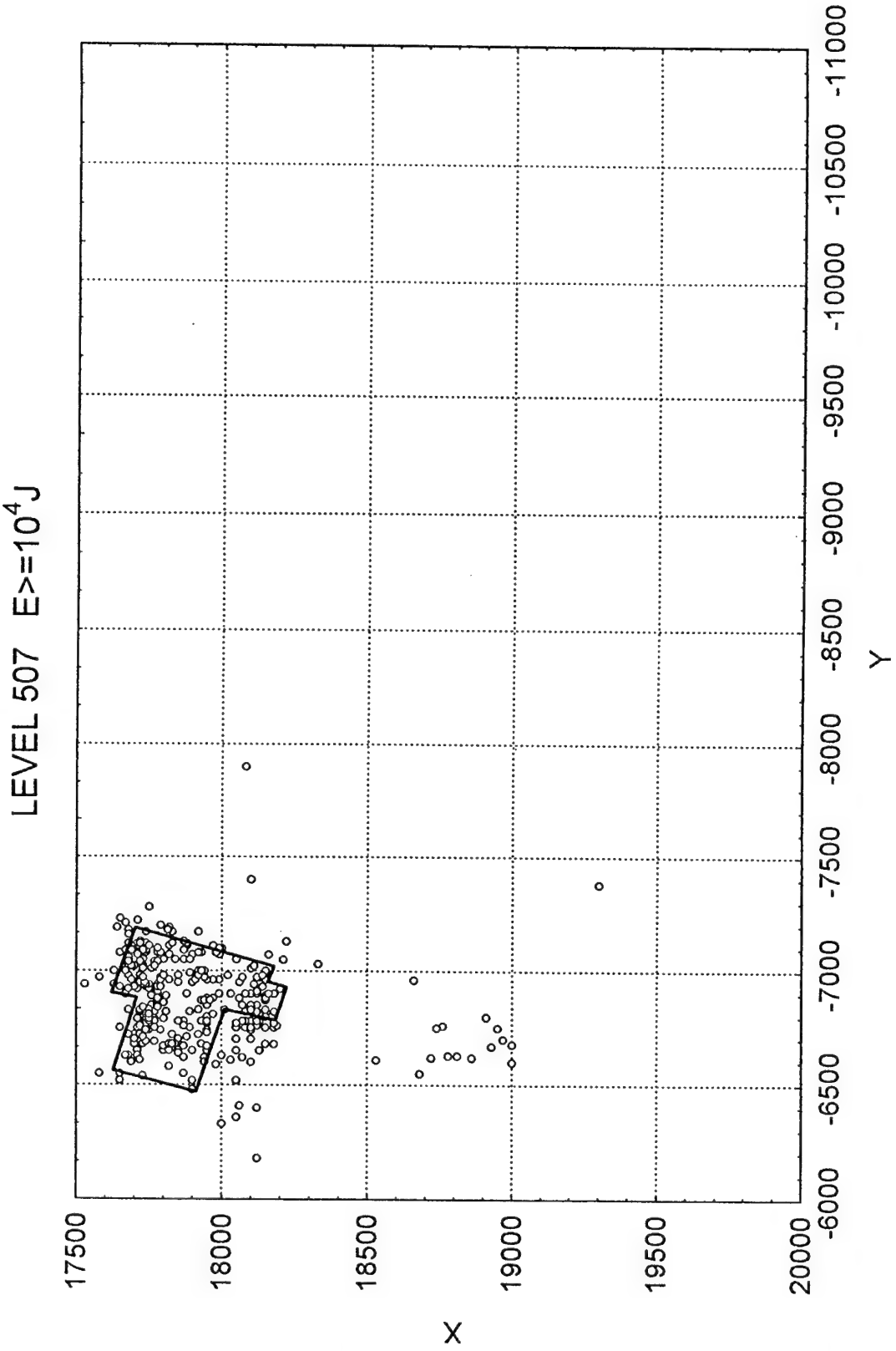

Figure 3.13 Spatial distribution of seismic events of energy ≥ 10^4 J associated with the coal level 507

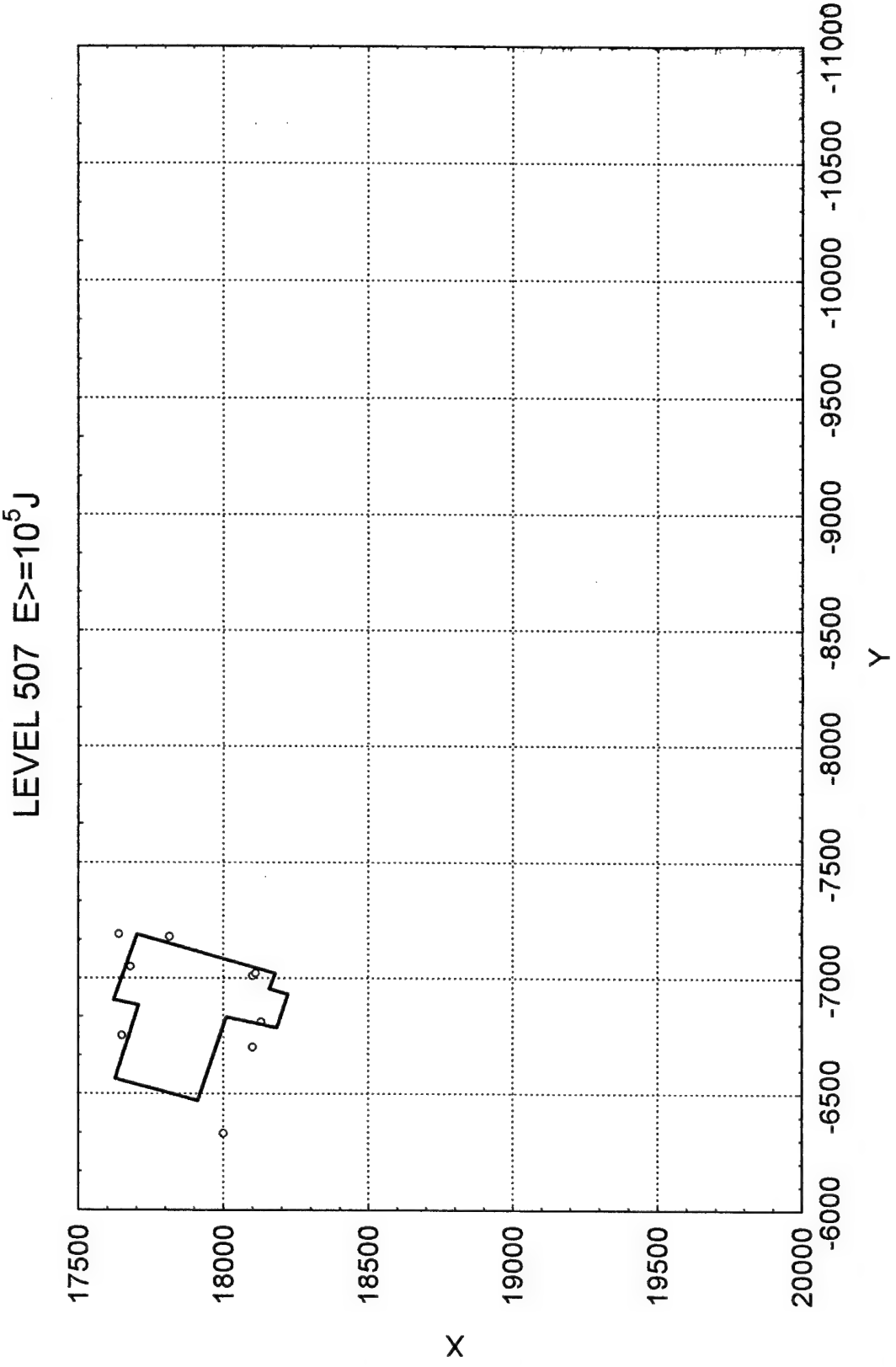

Figure 3.14 Spatial distribution of seismic events of energy ≥ 10^5 J associated with the coal level 507

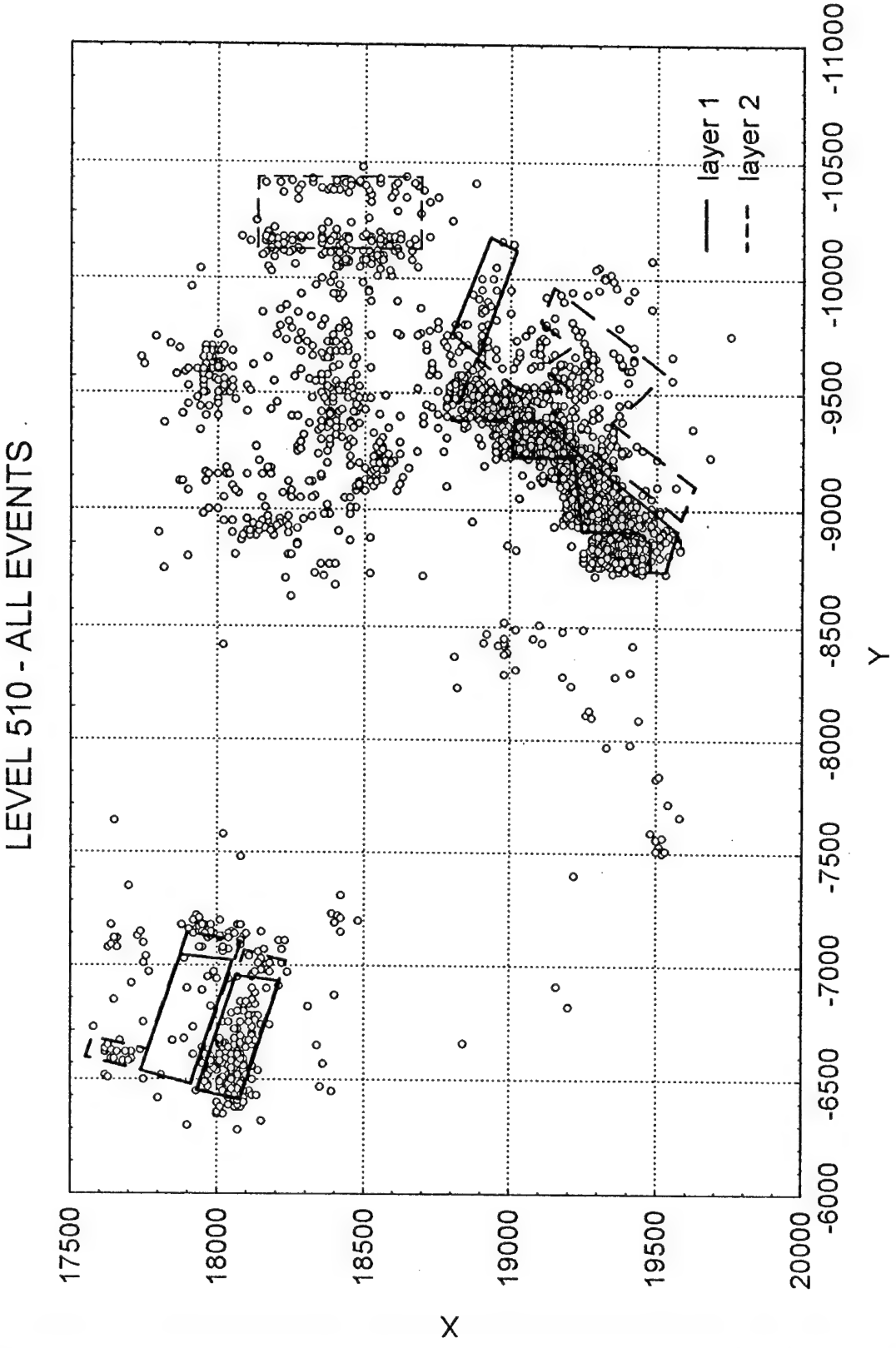

Figure 3.15 Spatial distribution of all seismic events associated with the coal level 510

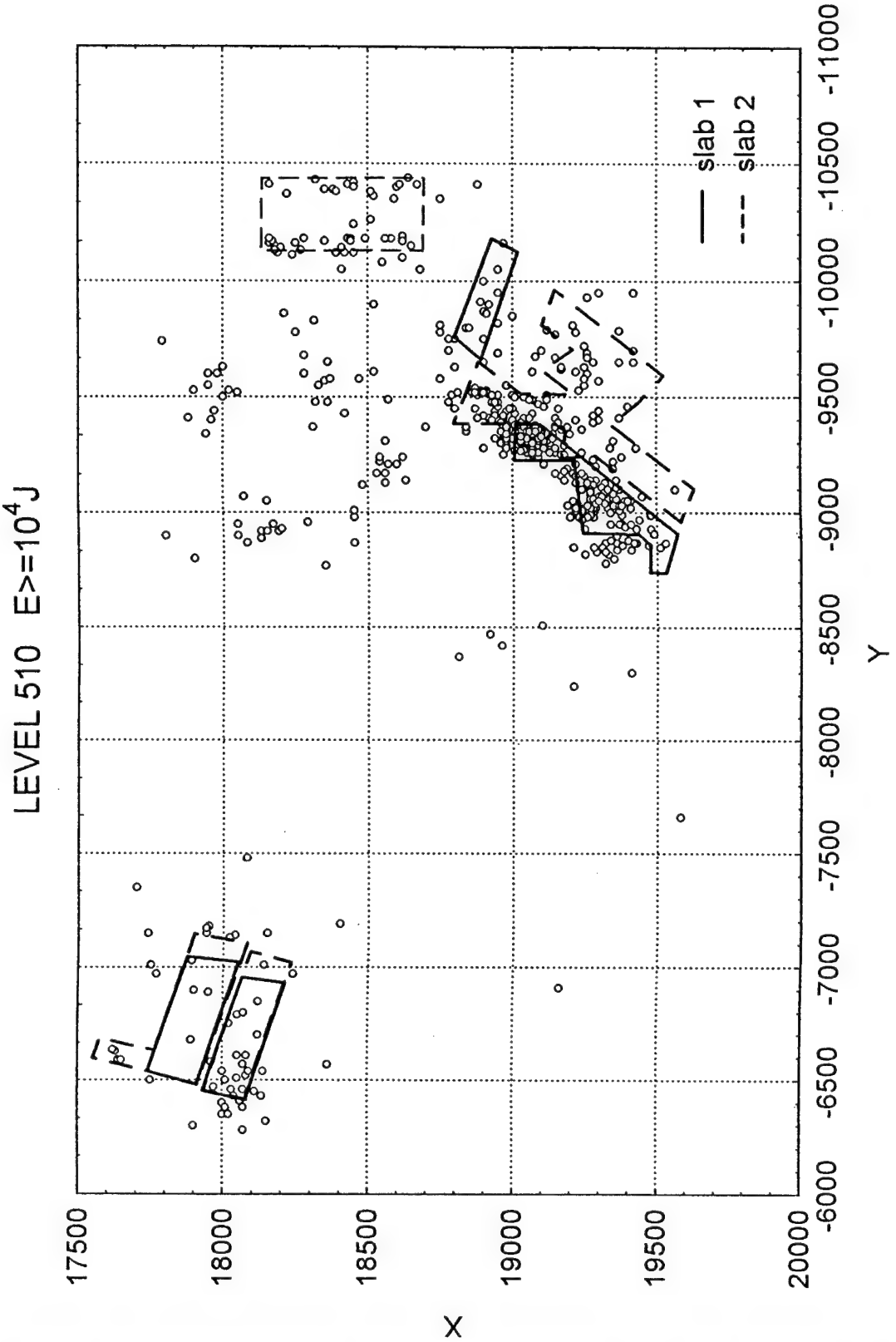

Figure 3.16 Spatial distribution of seismic events of energy ≥ 10^4 J associated with the coal level 510

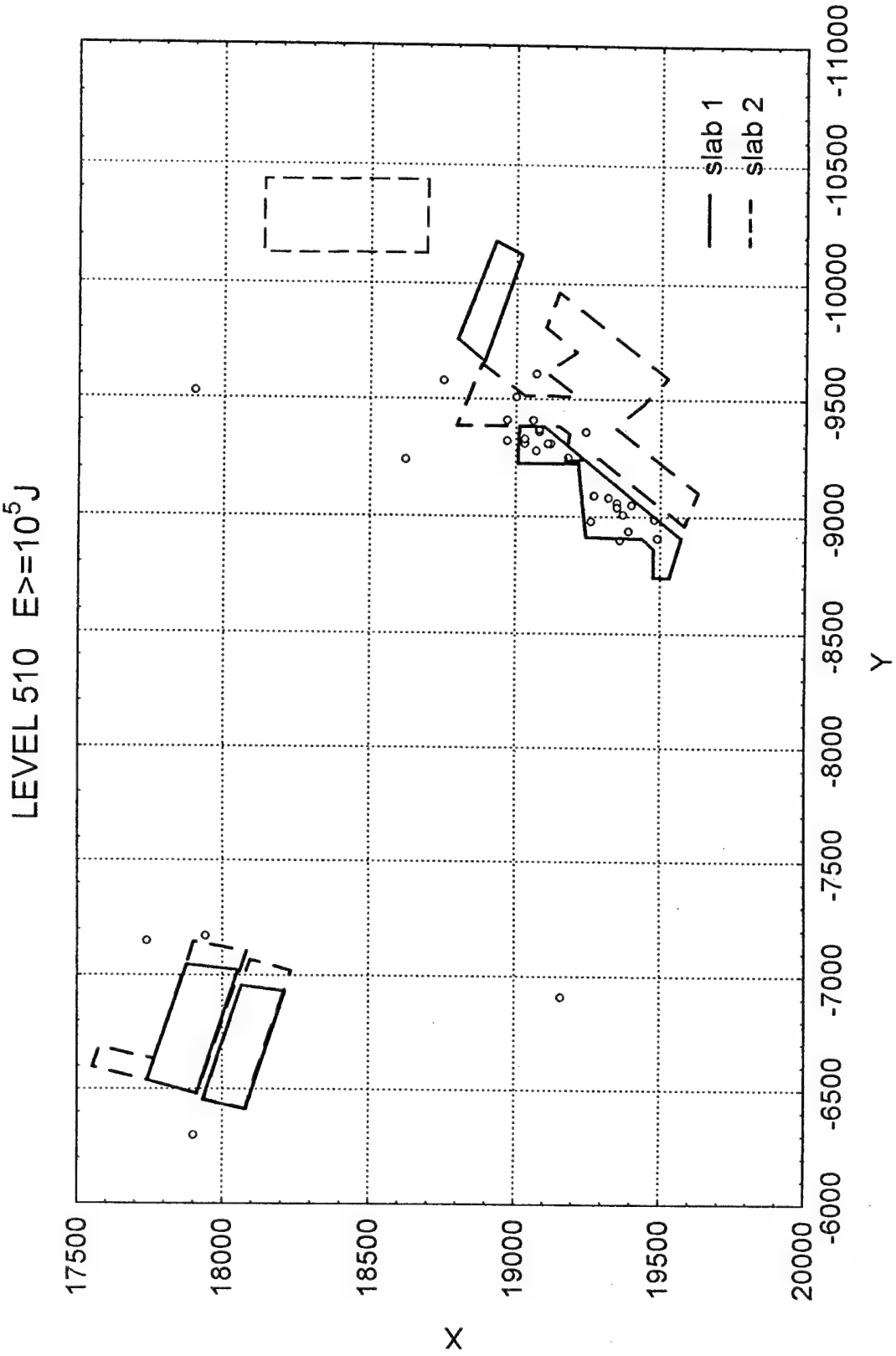

Figure 3.17 Spatial distribution of seismic events of energy ≥ 10^5 J associated with the coal level 510

4. Descriptive statistics

The aim of the descriptive statistics studies is the initial recognition of statistical properties of database. We intend to check whether the mining induced seismicity originated in various parts of the mine is so different that simple statistical tests can reveal these differences. Similar procedures ought to be used, in our opinion, while studying every large catalog of data, to divide it into coarsely homogenous parts before more developed methods are applied. Otherwise strong differences will be found by the methods designated to study detailed structure of the data and they can dominate results making detailed analyses impossible. Additionally the descriptive statistics comparisons of catalog parts from different time periods give chance to test indirectly completeness and an instrumental time homogeneity of the catalog. If we observed systematic time-ordered differences in distributions of a parameter (e.g. consecutively increasing mean value) we could suspect that the data acquisition changed over time.

Since major features of spatial distributions of sources are clearly visible from the maps (Figs. 3-17) here we concentrated ourselves onto time of event occurrence and event energy. The latter parameter is strongly non-linear. Technically it is much easier to study its logarithm. Conclusions drawn for the logarithm of energy obviously are also valid for energy.

As far as time of event occurrence is concerned we studied the interoccurrence time. For the pure Poissonian process of event generation the interoccurrence time has exponential distribution. It is, however, known that inducing processes in mines are not purely Poissonian (Lasocki 1992) and hence empirical distributions of this parameter does not match the theoretical exponential distribution. The feature, that does not agree with main event series behavior in earthquake seismology (Gardner and Knopoff 1974), comes from controlling influence of time-varying mining works over mining induced processes. The non-Poissonian structure of the induced seismicity was ascertained in full seismicity series. When the series were reduced to only strong events ($E \geq 10^5$J) it became Poissonian (Lasocki 1992).

Our descriptive statistics studies mainly concern testing differences in central tendency and empirical distributions of parameters. Since distributions of both the interoccurrence time as well as the logarithm of energy are unknown but surely are not normal we basically use nonparametric testing procedures. These are:

For the central tendency:

- The Mann-Withney U test. The test evaluates differences in medians between two samples. The test is computed based on rank sums of the data. It is regarded as the most powerful nonparametric alternative to the t-test for testing differences between means of normally distributed samples. The test was even found to be more powerful than the t-test in some cases;

- The Kruskall-Wallis ANOVA by Ranks and the median tests. The procedures are nonparametric alternatives to one-way analysis of variance and test for significant differences in medians. Having more than two samples to compare the use of these tests may be preferred over the univariate approach;

For the distribution:

- The Kolmogorov-Smirnov two sample test that assesses the hypothesis that two samples were drawn from different populations. Unlike the tests for central tendency it is also sensitive to differences in the general shapes of the distributions in the two samples;

- The Wald-Wolfowitz runs test. The test assesses the hypothesis that two samples were drawn from two populations that differ with respect to the central tendency and to the general shape of the distribution.

The detailed description of these tests can be found in a number of books on mathematical statistics (e.g., Hollander and Wolfe 1973, Box et all 1987).

Having in mind remarkable robustness to deviations from normality of the standard analysis of variance sometimes, to cross-validate our conclusions implied by nonparametric procedures. we use the one-way analysis of variance to study differences in means. We make use of the LSD (Least Significant Differences) test.

All mentioned procedures provide the probability of error when accepting the hypothesis about the existence of the difference. The probability is called the significance level. One usually accepts the hypothesis when the significance level is less than 0.05. However when the probability is greater than this value one cannot conclude that the samples were drawn from the same population (nor that they have the same central tendencies). If the probability of error when accepting the hypothesis about the existence of the difference is say 0.1 the probability of error when accepting the hypothesis about equality is 0.9.

Studies of the logarithm of seismic energy of events

Differences in location parameters (mean, median) of distributions of logarithm of seismic energy between samples containing events recorded at different coal levels in particular years of the studied period were studied by means of the Kruskal-Wallis test and the LSD test. The Kruskal-Wallis test proves significance of the differences between parts of the seismicity series due to the considered years, for all seismicity recorded in the whole mine, as well as for seismicity connected with the specific coal levels. The differences are very highly significant. The level of significance for all studied groups is less than 10^{-6}.

The detailed insight into these differences and the differences in the general shape of the logE distributions is assessed with the use of the LSD test for means and the Kolmogorov-Smirnov two sample test, respectively. The logE distribution is not normal but violation of the normality assumption has no significance for the LSD test results when samples are large. Table 4.1 presents results of the two tests. The results of the Kolmogorov-Smirnov testing procedure has been fully confirmed by the Wald-Wolfowitz test.

Similarities (non-significant differences) in both mean value and shape are randomly distributed among years of the studied period, however the slight tendency to decrease logE mean value with time can be picked. In some cases the samples that have similar mean have also similar shape of the energy distribution, in other they do not.

The differences in both the shape and the location of energy distributions between seismic series recorded in various years prove a strong link between seismic energy generation and mining works. The works changed in time both their location and their intensity. Some stopes were closed, in some other parts the exploitation was commenced. Irregular variations of mining activity caused irregularities in seismicity generation. Valuable information about a nature of mining works influence onto seismicity generation can be extracted, in our opinion, after confronting the obtained results with detailed data about mining works at particular levels.

Table 4.1. Significance of differences between means and distributions of logE for samples from different years

x				LSD test					
Year	Coal level	Sample size	Mean value	Significance level					
				1988	1989	1990	1991	1992	1993
1988	all levels	4038	3.69	x	0.13	0.03	0.98	$<10^{-6}$	$<10^{-6}$
	416	1269	3.57	x	0.003	0.54	-	-	-
	501	1670	3.78	x	0.0001	$<10^{-6}$	0.0007	$<10^{-6}$	$<10^{-6}$
	504	239	3.55	x	0.001	0.004	0.11	0.62	0.90
	507	525	3.71	x	$2x10^{-5}$	0.07	0.0002	0.011	0.04
	510	194	3.74	x	0.99	0.005	0.04	0.009	10^{-5}
1989	all levels	3219	3.70	>0.050	x	0.0009	0.23	$<10^{-6}$	$<10^{-6}$
	416	219	3.45	<0.001	x	0.08	-	-	-
	501	2024	3.71	<0.001	x	0.018	1.0	$<10^{-6}$	0.005
	504	98	3.34	<0.050	x	10^{-6}	0.0006	0.02	0.012
	507	438	3.85	<0.001	x	$<10^{-6}$	$<10^{-6}$	$3x10^{-5}$	0.0007
	510	326	3.74	>0.050	x	0.001	0.02	0.0018	$<10^{-6}$
1990	all levels	2052	3.65	<0.001	<0.001	x	0.08	0.003	$7x10^{-6}$
	416	34	3.63	>0.050	<0.050	x	-	-	-
	501	1380	3.66	<0.001	<0.001	x	0.03	0.0001	0.3
	504	73	3.75	<0.001	<0.001	x	0.61	0.036	0.011
	507	224	3.63	<0.050	<0.001	x	0.022	0.11	0.2
	510	299	3.60	<0.001	<0.010	x	0.58	0.48	0.21
1991	all levels	1680	3.69	<0.001	<0.001	<0.001	x	$8x10^{-6}$	$<10^{-6}$
	416	0	0	-	-	-	x	-	-
	501	1297	3.71	<0.001	<0.001	<0.001	x	$<10^{-6}$	0.008
	504	38	3.69	<0.001	<0.001	>0.050	x	0.25	0.13
	507	86	3.48	<0.001	<0.001	<0.050	x	0.089	0.14
	510	204	3.63	<0.001	<0.010	>0.050	x	0.43	0.11
1992	all levels	1371	3.60	<0.001	<0.001	<0.001	<0.001	x	0.29
	416	0	0	-	-	-	-	x	-
	501	453	3.55	<0.001	<0.001	<0.010	<0.001	x	0.015
	504	101	3.58	>0.050	<0.010	<0.050	<0.050	x	0.6
	507	39	3.49	>0.050	<0.001	>0.050	>0.050	x	0.97
	510	703	3.62	<0.010	<0.001	<0.010	>0.050	x	0.0057
1993	all levels	1940	3.58	<0.001	<0.001	<0.001	<0.001	<0.001	x
	416	0	0	-	-	-	-	-	x
	501	527	3.64	<0.001	<0.001	<0.001	<0.001	<0.050	x
	504	92	3.54	<0.010	>0.050	<0.050	>0.050	>0.050	x
	507	26	3.49	>0.050	<0.010	>0.050	>0.050	>0.050	x
	510	1252	3.55	<0.001	<0.001	<0.001	<0.050	<0.001	x
		Kolmogorov-Smirnov test							x

The general trend to lower mean energy in time could be due to a general decrease of number of strong events in time during the studied period. However, it is also possible, that the decreasing trend could be resulted by an enhancement of recording facilities in the mine. In this case, increasing in time number of weak events recorded could reduce the mean value. If the latter was true then the instrumental time-homogeneity of the database would not be preserved. The problem can be resolved through interoccurrence time studies. If the latter explanation is valid then a tendency to decrease interoccurrence time (increase the mean event rate) in consecutive years will be noted.

In order to study the same as previously properties of logE distributions in the series comprised only strong events we removed from the samples all events weaker than 3.2×10^4 J (half of order 10^4) and repeated the analysis of differences between parameters of location. The sample reduction decreases considerably sample sizes. In this case, due to not normal distribution of logE, only nonparametric procedures can be used. The applied Kruskall-Wallis and the median tests reject hypothesis about significant differences between the reduced samples associated with particular years of the studied period. The result pointes out that the strong event series are less variable in time, concerning energy of events, than the full series. Since we suspect that the variation of energy distribution in time is due to the variation of mining works we can conclude that generation of seismicity in higher energy range is less dependent upon the mining activity. This gives a strong suggestion that a controll of mining works over at least a considerable part of strong event generation is weaker. Thus the other than directly controlled by mining process takes place. As the things are an important conclusion may be put forward: There are probably more than one inducing processes and our induced seismicity series comprises mixture of their outcomes.

Besides time divided series studies also series due to particular coal levels and due to praticular areas of the mine are analysed. Because of limited sample sizes we use here the Mann-Withney U test to compare medians. The results of testing differences between samples associated with the coal level in the respective mine areas are presented in Table 4.2, whereas those between samples associated with the mine area at the respective coal levels are shown in Table 4.3. The results for full samples are above the diagonals of the tables while the values

assemblyed below the diagonals concern samples with events of energy equal to or greater than 10^4J. Relations only between samples of satisfactory size are presented.

As can be seen in the Table 4.2 the locations (medians) of logE distributions do not differ significantly between seismic series at the levels 416 and 504 and between the series at the levels 501 and 510. The first pair of levels comprises thin almost exploited coal layers. Seismicity associated with them neither had big rate nor was very dynamic. Coal layers of the second pair are thick and mining there was accompanied by considerable seismic activity in wide energy range.

The strong event series studies form another pairs with non-different logE locations. These are: (416, 507) , (501, 504) and (504, 510). The links cannot be explained on the basis of layer characteristics. The strong event generation is probably less dependent upon coal layers features but more controlled by local stress field due to structures located around the stopes and in, above and below the coal seam.

In general differences between distribution locations of the considered mine areas are stronger in full samples than in reduced data. The full seismic series from NW part, at the level 507 differs from all other full series from this part, at all other levels. Significant differences are also found between the full series from the levels 504 and 510 in NW part. Only two levels: 504 and 510 in C part are not different from the point of view of full series logE distributions.

The differences decreases after the energy threshold is applied. Neither full nor reduced series recorde in SW, NE and SE parts at different coal levels differ significantly.

Table 4.2. Significance of differences between medians of logE for samples from different coal levels

x				FULL SAMPLE SIGNIFICANCE LEVEL				
Coal level	**Region**	**Mean in full sample**	**Mean in reduced sample**	**416**	**501**	**504**	**507**	**510**
416	whole level	3.56	4.25	x	$<10^{-6}$	0.42	$<10^{-6}$	$<10^{-6}$
	SW	3.58	4.24	x	0.14	-	0.07	0.14
	C	3.58	4.25	x	$<10^{-6}$	0.04	-	0.046
501	whole level	3.70	4.42	$<10^{-6}$	x	$<10^{-6}$	$7x10^{-5}$	0.37
	NW	3.62	4.25	-	x	0.78	0.0002	0.22
	SW	3.77	4.43	0.05	x	-	0.35	0.89
	C	3.81	4.41	$3x10^{-6}$	x	$<10^{-6}$	-	$8x10^{-6}$
	NE	3.78	4.25	-	x	-	-	0.5
	SE	3.77	-	-	x	0.005	-	0.84
504	whole level	3.55	4.39	0.0008	0.83	x	$<10^{-6}$	$5x10^{-5}$
	NW	3.59	4.25	-	0.60	x	$<10^{-6}$	0.03
	C	3.66	4.41	0.0002	0.52	x	-	0.96
	SE	3.48	-	-	-	x	-	0.0003
507	whole level	3.72	4.25	0.78	$<10^{-6}$	0.0004	x	$<10^{-6}$
	NW	3.77	4.25	-	0.36	0.97	x	0.0001
	SW	3.78	4.31	0.17	0.64	-	x	0.6
510	whole level	3.61	4.34	0.01	$7x10^{-5}$	0.06	0.005	x
	NW	3.69	4.33	-	0.98	0.77	0.26	x
	C	3.64	4.30	0.35	0.12	-	-	x
	NE	3.74	4.23	-	0.82	-	-	x
	REDUCED SAMPLE SIGNIFICANCE LEVEL							x

Full seismic series from various parts of the mine (Table 4.3) turn out to be similar (not different) in a difficult to explain way. More obvious similarities, that can be correlated with geographical distribution of the studied areas are found for reduced samples. These similar pairs, from the point of view of seismic energy generation, are: (SW, C) , (NW, NE) and (SE, C). It is then likely that the full series generation, in which weak events dominate, is more level controlled while the stong event series generation is more region controlled. At particular levels the same blurring of differences between the seismic series from different parts of the mine after applying energy threshold can be observed in Table 4.3 as it was noted for the series from different coal levels at particular regions in table 4.2.

Table 4.3. Significance of differences between medians of logE for samples from different mine parts (regions)

x				FULL SAMPLE SIGNIFICANCE LEVEL				
Region	**Coal level**	**Mean in full sample**	**Mean in reduced sample**	**NW**	**SW**	**C**	**NE**	**SE**
NW	all levels	3.55	4.26	x	0.56	$<10^{-6}$	0.043	0.18
	501	3.62	4.25	x	0.011	0.002	0.001	0.11
	504	3.59	4.25	x	-	0.38	-	0.02
	507	3.77	4.25	x	0.91	-	-	-
	510	3.69	4.33	x	0.65	0.27	0.004	0.12
SW	all levels	3.77	4.43	$<10^{-6}$	x	$<10^{-6}$	0.011	0.27
	416	3.68	4.24	-	x	0.014	-	-
	501	3.77	4.43	0.38	x	0.0007	0.13	0.89
	507	3.78	4.31	0.09	x	-	-	-
	510	3.74	-	-	x	0.39	0.57	0.99
C	all levels	3.71	4.38	$<10^{-6}$	0.14	x	$<10^{-6}$	0.01
	416	3.58	4.25	-	0.60	x	-	-
	501	3.81	4.41	0.35	0.85	x	0.82	0.56
	504	3.66	4.41	0.14	-	x	-	0.015
	510	3.65	4.30	0.94	-	x	0.0002	0.008
NE	all levels	3.75	4.23	0.75	$5x10^{-5}$	$7x10^{-5}$	x	0.006
	501	3.79	4.25	0.49	0.08	0.06	x	0.41
	510	3.74	4.25	0.44	-	0.55	x	0.57
SE	all levels	3.73	4.37	0.003	0.03	0.28	0.02	x
	510	3.73	4.37	0.40	-	0.57	0.072	x
	REDUCED SAMPLE SIGNIFICANCE LEVEL							x

Interoccurrence time studies

Results of the Mann-Whitney U test of differences between interoccurrence time medians of events recorded in the whole mine area in particular years of the studied period are presented in Table 4.4. In all but one case differences are very highly significant. The medians show clear tendency of incrasing mean interoccurrence time during the period from 1988 to 1992. The central tendencies of the interoccurence times distributions represent the reciprocal of central tendencies of the event rates. Thus we reject the possibility, discussed in the previous subsection, that the seismicity time variation could be due to raising recording ability of the seismic network in the studied period. If this was true we would observe a reversed tendency of the interocurrence time median caused by a general increase of number of recorded events. We can then attribute both the logE distributions and the interoccurrence times distributions tendencies to the decrease of overal activity during the studied period..

Table 4.4. Results of median test for interoccurrence time of events recorded in the Wujek mine

Year	Sample size	Median	Significance level				
			1989	**1990**	**1991**	**1992**	**1993**
1988	4038	77	$<10^{-6}$	$<10^{-6}$	$<10^{-6}$	$<10^{-6}$	$<10^{-6}$
1989	3219	97	x	$<10^{-6}$	$<10^{-6}$	$<10^{-6}$	$<10^{-6}$
1990	2052	134		x	$<10^{-6}$	$<10^{-6}$	0.46
1991	1680	176			x	0.0001	$<10^{-6}$
1992	1371	208				x	$<10^{-6}$
1993	1940	125					x

Results of the U test of differences between interoccurrence time medians for events recorded at the particular mining levels, in particular years of the studied period are shown in Tables 4.5, 4.6, 4.7, 4.8, 4.9, respectively.

Table 4.5. Results of median test for interoccurrence time of events recorded in the coal level 416

Year	Sample size	Median	Significance level	
			1989	1990
1988	1272	145	$<10^{-6}$	$<10^{-6}$
1989	219	969	x	0.0001
1990	34	3025		x

Table 4.6. Results of median test for interoccurrence time of events recorded in the coal level 501

Year	Sample size	Median	Significance level				
			1989	1990	1991	1992	1993
1988	1673	196	$<10^{-6}$	0.012	$3x10^{-6}$	$<10^{-6}$	$<10^{-6}$
1989	2027	154	x	$<10^{-6}$	$<10^{-6}$	$<10^{-6}$	$<10^{-6}$
1990	1384	215		x	0.04	$<10^{-6}$	$<10^{-6}$
1991	1299	250			x	0.0001	$<10^{-6}$
1992	454	762				x	$6x10^{-5}$
1993	529	528					x

Table 4.7. Results of median test for interoccurrence time of events recorded in the coal level 504

Year	Sample size	Median	Significance level				
			1989	1990	1991	1992	1993
1988	239	378	$<10^{-6}$	10^{-6}	$<10^{-6}$	$<10^{-6}$	$<10^{-6}$
1989	98	1792	x	0.44	0.36	0.68	0.56
1990	73	1393		x	0.17	0.57	0.17
1991	38	2306			x	0.33	0.82
1992	101	1990				x	0.32
1993	93	2151					x

Table 4.8. Results of median test for interoccurrence time of events recorded in the coal level 507

Year	Sample size	Median	Significance level				
			1989	1990	1991	1992	1993
1988	528	538	0.40	0.12	$<10^{-6}$	$<10^{-6}$	$<10^{-6}$
1989	440	608	x	0.34	$<10^{-6}$	$<10^{-6}$	$<10^{-6}$
1990	227	661		x	$<10^{-6}$	$3x10^{-6}$	$<10^{-6}$
1991	86	2253			x	0.34	0.09
1992	39	4338				x	0.68
1993	26	4772					x

Table 4.9. Results of median test for interoccurrence time of events recorded in the coal level 510

Year	Sample size	Median	Significance level				
			1989	1990	1991	1992	1993
1988	194	886	0.04	0.09	0.14	$<10^{-6}$	$<10^{-6}$
1989	326	799	x	0.72	$8x10^{-5}$	$<10^{-6}$	$<10^{-6}$
1990	299	860		x	0.0004	$<10^{-6}$	$<10^{-6}$
1991	204	1150			x	$<10^{-6}$	$<10^{-6}$
1992	703	392				x	$<10^{-6}$
1993	1254	166					x

Significant or highly significant differences are found between medians of interoccurence times of seismic series recorded at the levels 416 and 501. The seismic activity of the level 501 varied irregularly.

No significant differences in the medians occurres between the series from the level 504 except the median for the series from 1988 that was considerable lower than those for the series from other years.

Two homogeneous groups of series concerning locations of interoccorrence times distributions are found for the level 507. One comprises the seismic series recorded in the years 1988-1990 while the other the series recorded in the years 1991-1993 when the seismic activity was very low.

The central location of interoccurrence time distribution of events associated with the level 510 turnes out to be not different in the years 1988-1990. Exploitation of the level 510 in slab 1 in NE part, that started by the end of 1992, caused considerable increase of the seismic activity in the level.

Conclusions

Although the descriptive statistics studies are a complementary tool in our work they justify the following suggestions and conclusions:

1. Seismicity is a complex, both time and place dependent phenomenon.

2. The event rate and the energy distribution of seismicity is time-varying due to time changes of mining works. The overal process tended towards lower energy and lower rate during the studied period. The tests do not evidence instrumental inhomegeneity of the database.

3. The distributions of energy of strong events do not vary significantly in time. This proves the existence of at least two inducing processes in the mine. The one, time-varying, controlled by mining works, generates, in general, weaker events. The other one, weakly dependent on time, i.e. mining activity, gives rise to stronger events.

4. Statistical features of series comprising events from the whole energy range show some correlation with properties of coal layers they are associated with. Statistical characteristics of series formed by only strong events are better correlated with the part of the mine they came from than with the coal level they were associated with. The process of generating weak events is predominantly dependent upon the coal layer and the stope characteristics. The process responsible for generating stronger events is more dependent upon joint influence of structures in an environment of the excavation than directly dependent upon the excavation itself.

5. The parameters of strong event series from various mine areas are less different than the parameters of full series from these areas. The generating process mainly responsible for strong events occurrences is less place dependent compared to the process of weak event generation. This is another suggestion that the process of strong event generation is controlled by some generlized superposition of geologic and mining structures of the mine area.

6. As mentioned the descriptive statistics studies enable preliminary data recognition thus the conclusions cannot be considered as finite and fully reliable. In particular, we are not allowed to state that there are only two generating processes. However, the studies evidence the fact that the induced seismicity is a multimodal process and its multimodality is reflected in the distribution of event energy.

5. Maximum value of energy studies

Studies of statistical properties of the largest annual magnitudes to assess characteristics of earthquake series have been presented in the number of papers (e.g., Nordquist 1945, Epstein and Lomnitz 1966, Yegulalp and Kuo 1974, Lomnitz 1974, Kijko and Sellevoll 1981, Campbell 1982, Kijko 1982, Gan and Tung 1983). This approach can also be met in the field of mining seismicity (e.g., Kushnir et al. 1984, Dessokey 1984, McGarr 1984, Lasocki 1993, Gibowicz and Kijko 1994, Kijko and Funk 1994). The popularity of the extreme value methods stems from the lowered requirements concerning the recording system, that should be able to record the strongest events.

Let x_i , $i=1,..,n$ be outcomes of the certain process, obtained during the certain time period, say $[t, t+\Delta T]$. Let the cumulative distribution function of the random variable X be F(x). When we divide the time period into m equally long intervals Δt $(\Delta T = m\Delta t)$ and we find $y_k = max(x_i \mid t+(k-1)\Delta t \le x_i \le t+k\Delta t)$, $k=1,..,m$ we shall have outcomes of another process of maximum generation with its own cumulative distribution function, say G(y). Gumbel (1962) has proved that there are only three possible forms of G(y) when n tends towards infinity. These asymptotic extreme value distributions are:

$$G(y) = \exp\left\{-\exp\left(-\frac{y-\xi}{\Theta}\right)\right\} \tag{5.1}$$

$$G(y) = \begin{cases} 0 & for \quad y < \xi \\ \exp\left[-\left(\frac{y-\xi}{\Theta}\right)^{-k}\right] & for \quad y \ge \xi \end{cases} \tag{5.2}$$

$$G(y) = \begin{cases} \exp\left[-\left(\frac{\xi-y}{\Theta}\right)^{k}\right] & for \quad y \le \xi \\ 1 & for \quad y > \xi \end{cases} \tag{5.3}$$

where: $\Theta > 0$ and $k > 0$.

The exact distribution of the extreme value Y can be reached only when the underlying distribution of the random variable X is known. The specific solutions (e.g., Lasocki 1993, Gibowicz and Kijko 1994, Kijko and Funk 1994) usually assume a kind of stationarity of the event series, which leads to the Poisson distribution of the number of events in a time interval. Since induced seismicity series, from such long time periods as studied in this work, are not Poissonian (Lasocki 1992) we had to use the asymptotic forms of the distribution of maxima.

The asymptotic distribution of extrema Y is related to the distribution of the random variable X (Johnson and Kotz 1970). The variable Y has type I asymptotic distribution if:

$$\lim_{n \to \infty} n\left\{1 - G\left(X_{1-n} - 1 + y\left[X_{1-(ne)^{-1}} - X_{1-n^{-1}}\right]\right)\right\} = \exp(-y) \tag{5.4}$$

where $X_z : G(X_z)=z$,

the type II distribution :

$$\lim_{x \to \infty} \frac{1 - G(x)}{1 - G(cx)} = c^k \tag{5.5}$$

where $c>0$ and $k>0$,

and type III distribution if:

$$\lim_{x \to 0} \frac{1 - G(cx + \omega)}{1 - G(x + \omega)} = c^k \tag{5.6}$$

The condition (5.4) is satisfied for unbounded distributions like normal and exponential, the condition (5.5) for distributions bounded from below and the condition (5.6) for those bounded form above. The energy of induced events has either the unlimited distribution assigned by the Gutenberg-Richter relation or a limited from above form (Cosentino et al. 1977, Lasocki 1993, 1993a, Kijko and Funk 1994). Thus the asymptotic distribution of logarithm of energy maxima is either of type I or of type III. In the first case the logarithmic function governs the relation between the logarithm of energy maxima and the logarithmized empirical cumulative distribution function of logE maxima. In the second case this relation is the power function asymptotically approaching a limiting value of logE. Every violation of the expected shapes by the empirical c.d.f. of energy maxima can be interpreted as multimodality of the underlying energy distribution, that is the sample contains mixture of outcomes of different generating processes. First attempts to use the extreme value methods to investigate complexity of the

seismic catalogs from mines were given by Kijko et al. (1987). The other applications for the regional seismicity of the Upper Silesian Coal Basin, Poland were presented by Idziak et al. (1991). The method would provide distinct results when the seismicity generation processes have different, well separated energy modes and the event rate of the high energy mode is lower than the others. The main drawback of the method is the use of the cumulative distribution function, that is the integral function, which screens local effects and insufficiently large peaks of the probability density function are not detectable. The method requires large size samples to reach the asymptotic distribution of maxima.

Identification of the seismicity generation processes by the extremum value statistics studies

Based on the theoretical development given above a number of logE maximum value studies were made. Figure 5.1 shows probability distribution of the 20-day maximum seismic energy release at the whole mine area, in the studied period. The size of our database, in average 130 events per 20-day interval, allowed to compare the empirical distributions with their asymptotic forms. The shape of the empirical distribution function is smooth. One can clearly see, however, at least two points of inflexion. These two most distinct points evidence at least three-mode structure of the seismic energy distribution of all events from the mine. Consequently they prove existence of at least three different generating processes, each of different energy mode. The low energy mode seems to tend asymptotically to the limiting value of energy at some $3x10^6$ J. The medium energy mode has the upper limit at some 10^7 J. The high energy mode limit exceeds 10^8 J.

The extreme value studies require the statistical structure of the sample of maxima. There cannot be any significant systematic time variations of the maximum distribution. The homogeneity of our maximum value set was tested by the Kruskal-Wallis and median tests of differences in locations and by the Kolmogorov-Smirnov test of differences in the shapes of distributions. Both tests rejected hypotheses about significant differences between the maximum energy distributions of seismic events series recorded in the particular years of the studied period.

As was proved by the descriptive statistics studies, the seismicity is a highly nonhomogeneous structure. The distributions of event parameters are different in different parts

of the mine. The distribution of energy maxima shown in Figure 5.1 represents a generalized form obtained while summing up local effects. There are secondary modes in the distribution, which, because of this summing, cannot be picked. To detail our studies we investigated the seismic series associated with the particular coal levels and the particular mine parts. In all further discussed cases we used the 20-day intervals to evaluate the logE maxima. The number of events per interval was set to be greater than 30, hence the distributions could be regarded as approaching their asymptotic forms.[1] The logE maxima from the intervals for which this condition was not satisfied, were not used to build the empirical distributions.

The probability distributions of maximum seismic energy release at the particular levels, in the studied period, are shown in Figures 5.2 - 5.6, respectively. The following modes of the distributions were identified:

- level 416: I - $E_{max} \approx 5 \times 10^4$ J , II - $E_{max} \approx 10^5$ J and possibly the third one with only one observation;
- level 501: possibly I - $E_{max} \approx 5 \times 10^5$ J , II - $E_{max} \approx 10^6$ J , III - $E_{max} \approx 5 \times 10^6$ J , IV - $E_{max} > 10^8$ J;
- level 504: I - $E_{max} \approx 5 \times 10^4$ J , II - $E_{max} \approx 10^5$ J. Limited number of observations makes this identification uncertain;
- level 507: possibly I - $E_{max} \approx 5 \times 10^4$ J , II - $E_{max} \approx 2 \times 10^5$ J;
- level 510: possibly I - $E_{max} \approx 5 \times 10^4$ J , II - $E_{max} \approx 2 \times 10^5$ J , III - $E_{max} \approx 5 \times 10^6$ J and possibly IV - $E_{max} > 10^8$ J with only one observation.

The mode with limiting value in the first half of order 10^5 J is present in distributions of logE maxima for seismic series from every level, although for the distribution associated with the level 501 it is obscured by the higher energy modes. Some traces of the possible mode of logE maximum distribution, with limiting value $\approx 5 \times 10^4$ J is also noticed for the series from every level except for that from the level 501. The levels 501 and 510 associated distributions display

---

[1] When the process of event occurrence is Poissonian, the exact distribution of maxima can be replaced by its asymptotic form if $\exp(-\lambda) \approx 0$, where λ is the average number of event per time interval. As stated, our process of seismic event occurrence is non-Poissonian but we hope that the same condition should be met to use the asymptotic distribution for maxima. 30 events per interval gives the value $\exp(-\lambda) < 10^{-14}$.

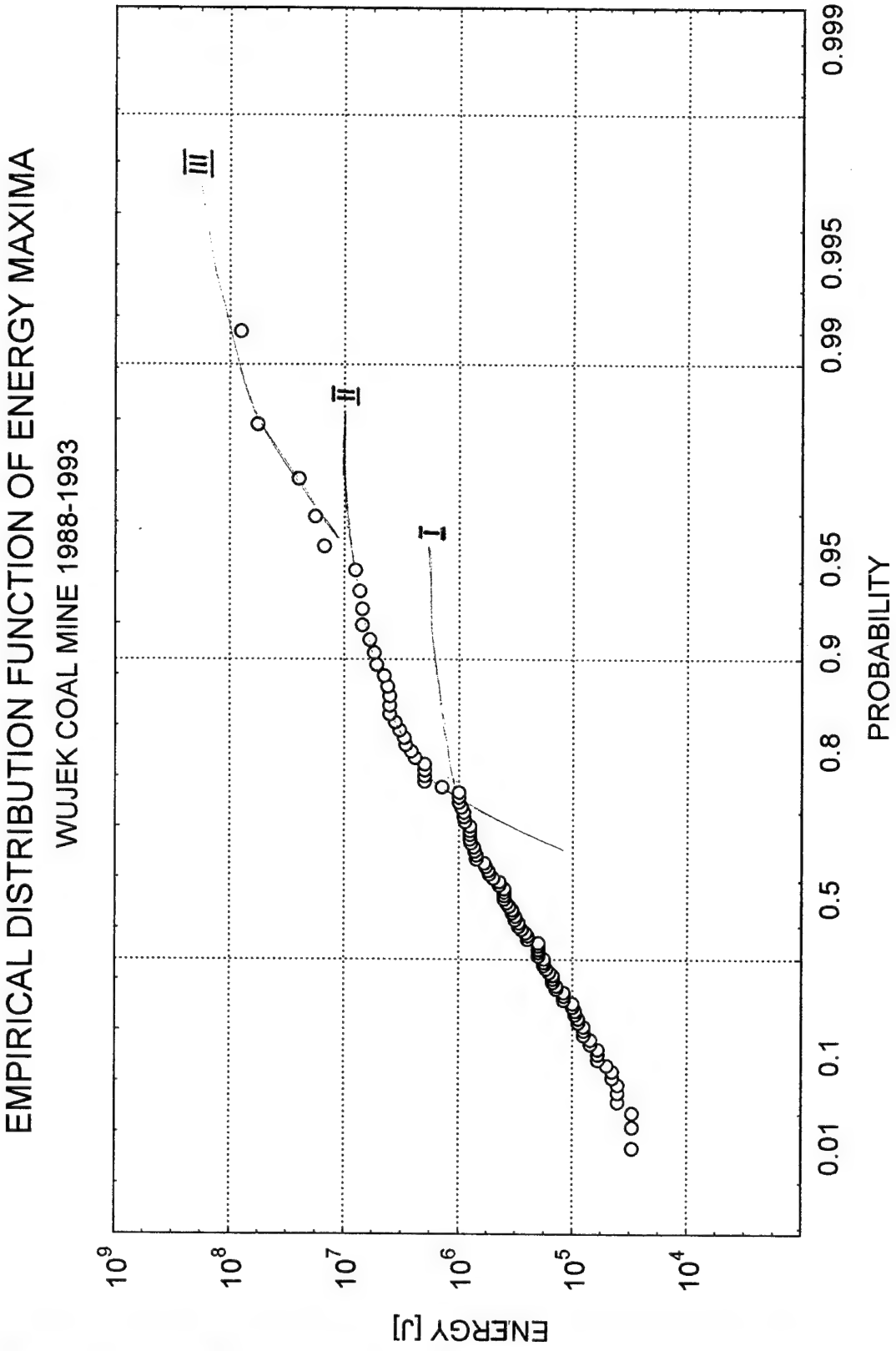

Figure 5.1 Probability distribution of the 20 days maximum seismic energy release at the Wujek mine, in the years 1988-1993

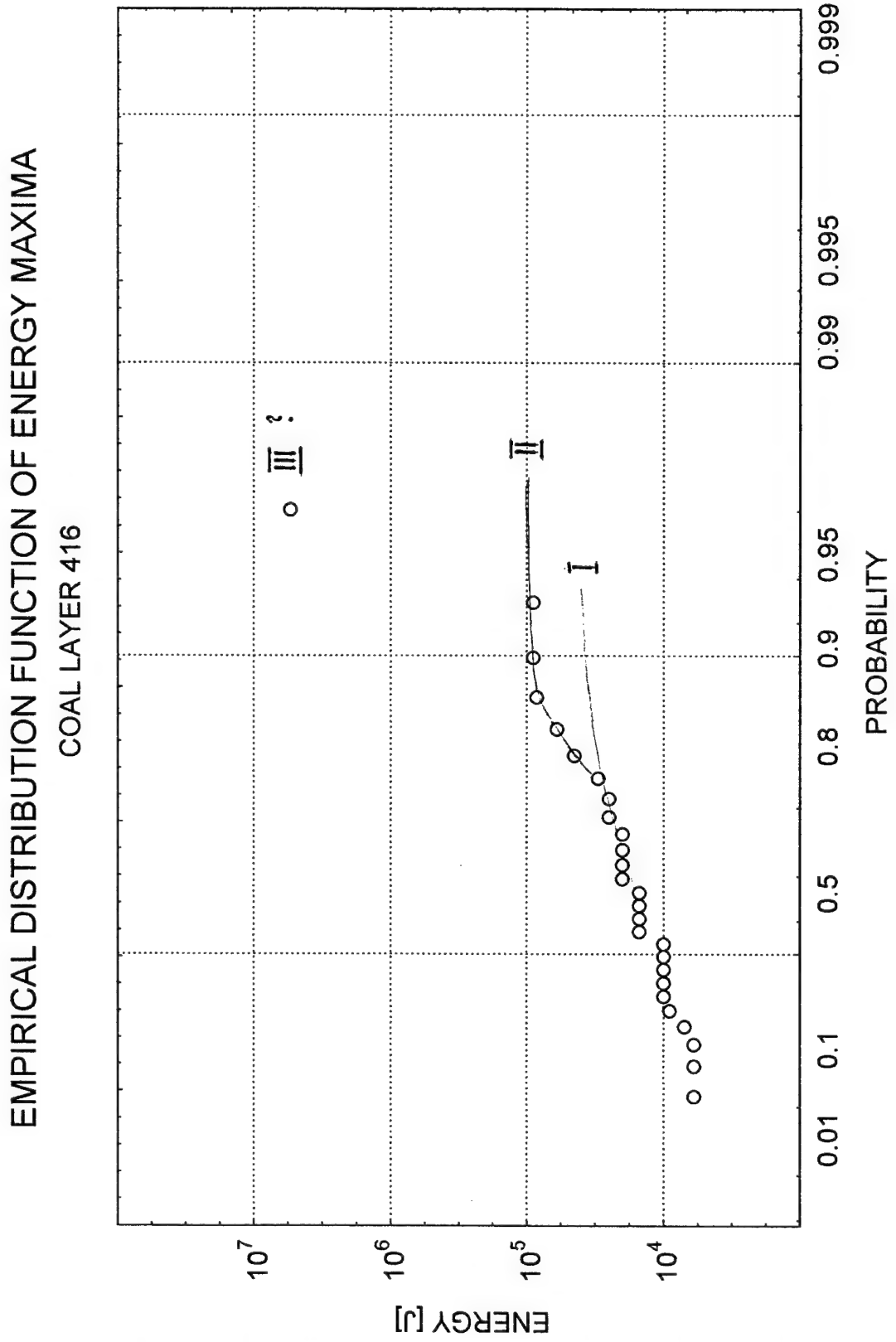

Figure 5.2 Probability distribution of the 20 days maximum seismic energy release at the coal level 416

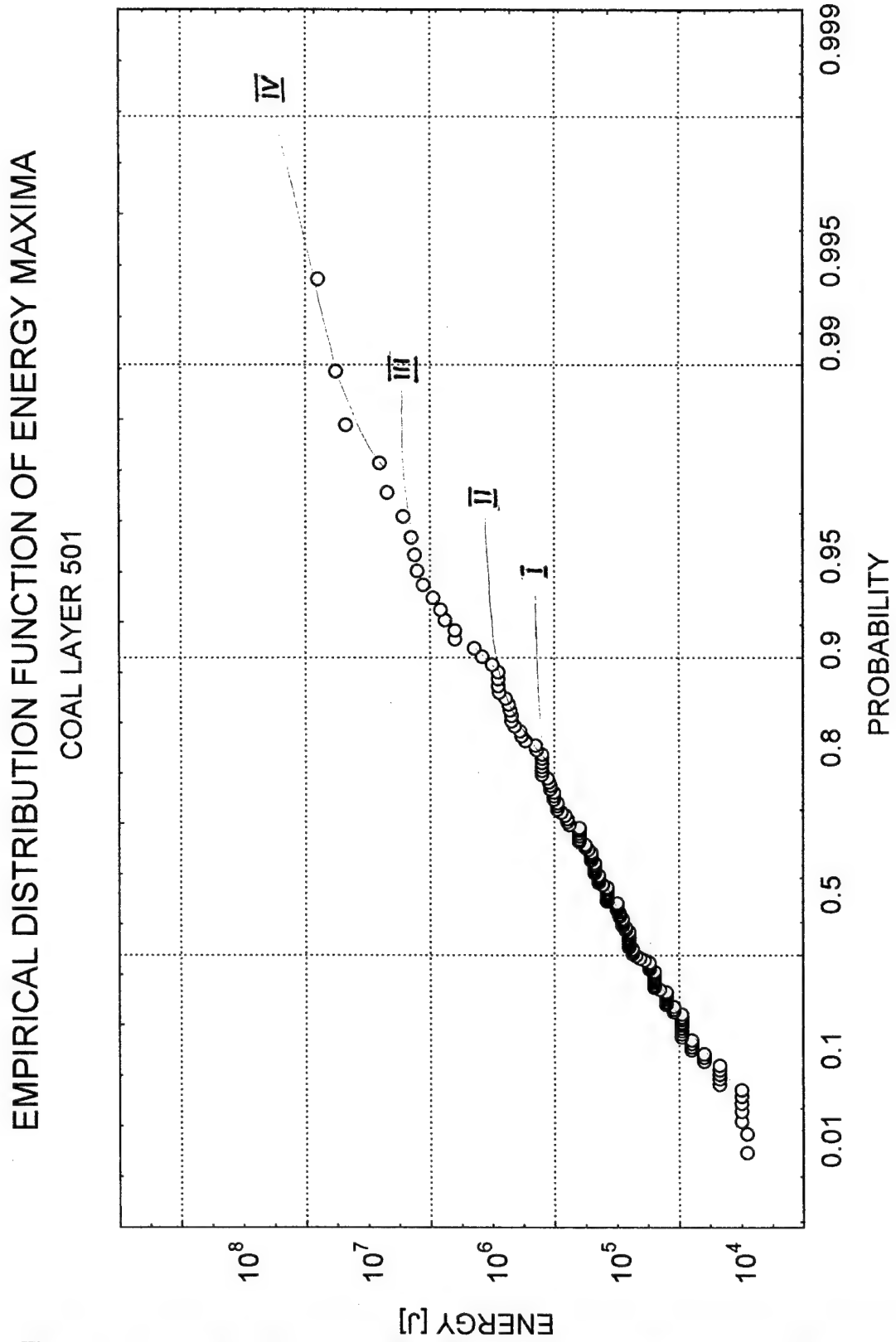

Figure 5.3 Probability distribution of the 20 days maximum seismic energy release at the coal level 501

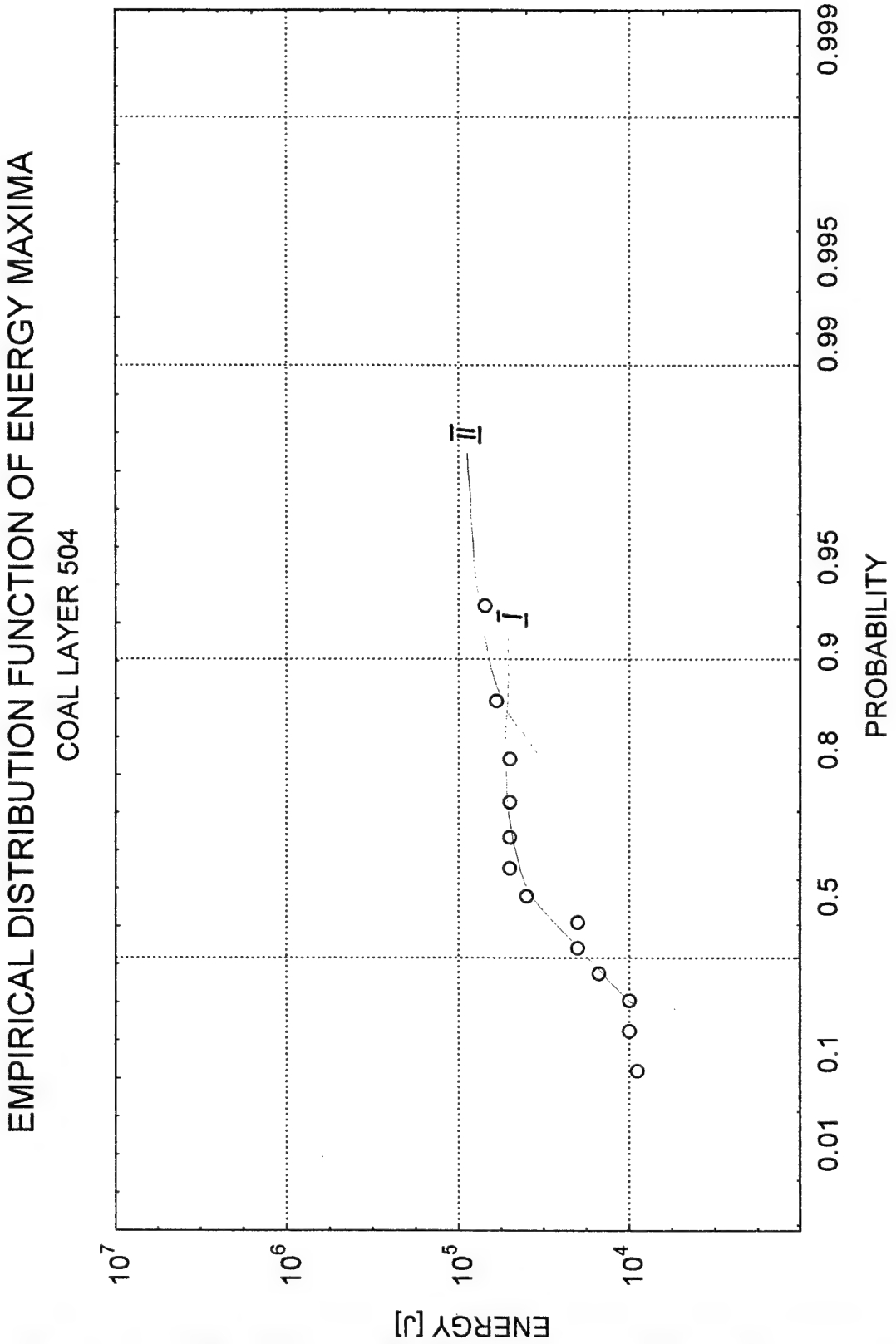

Figure 5.4 Probability distribution of the 20 days maximum seismic energy release at the coal level 504

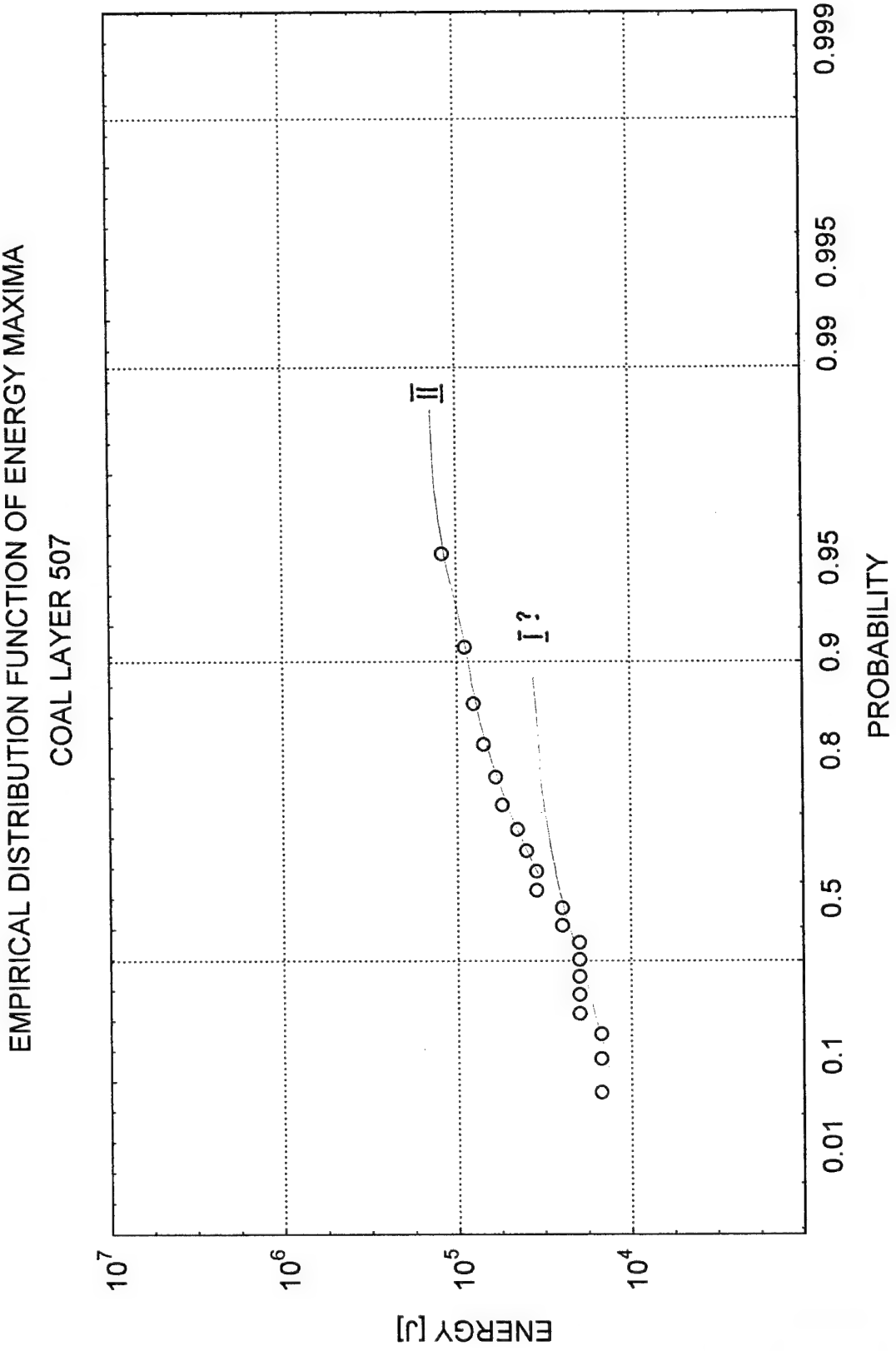

Figure 5.5 Probability distribution of the 20 days maximum seismic energy release at the coal level 507

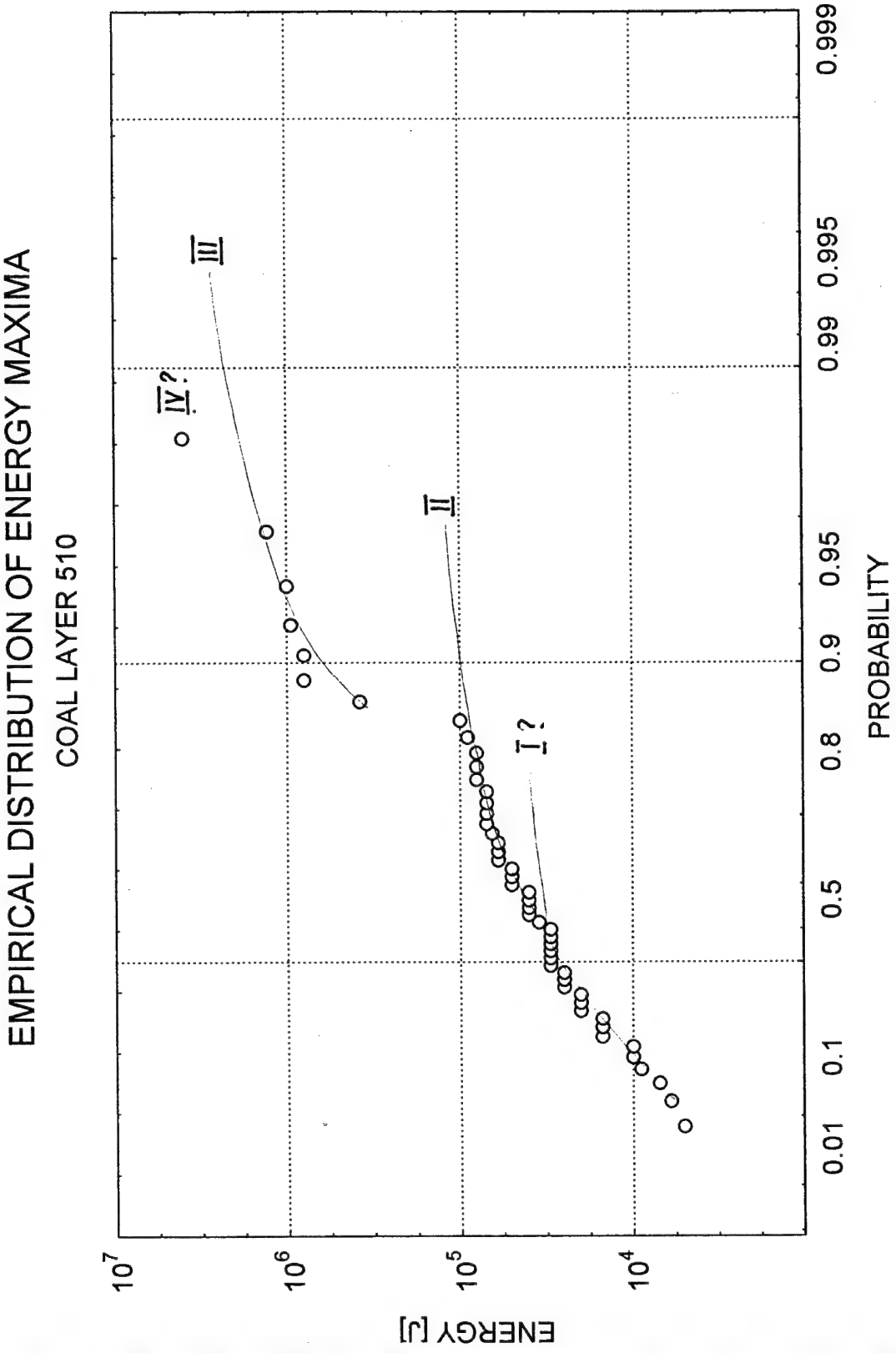

Figure 5.6 Probability distribution of the 20 days maximum seismic energy release at the coal level 510

complex structure with two more high energy modes. The limiting value of the first from these modes is located in the second half of order 10^6 J, and that of the second one exceeds 10^8 J.

The distributions of energy maxima, associated with the coal levels, were compared by means of the Kolmogorov-Smirnov two sample test. The results of the test are given in Table 5.1

Table 5.1. Results of Kolmogorov-Smirnov test for distributions of maximum seismic energy released at the coal levels

Coal level	No. of observations	Significance level				
		416	**501**	**504**	**507**	**510**
416	28	x	<0.001	>0.05	>0.05	<0.01
501	162		x	<0.001	<0.001	<0.001
504	14			x	>0.05	>0.05
507	21				x	>0.05
510	50					x

The test does not point out significant differences in the groups comprising the samples associated with the levels: 416, 504, 507 and comprising the samples associated with the levels: 504, 507, 510. The level 501 associated sample turnes out to be highly different from all other samples connected with all other levels. The similarities in the sample distributions form groups of vertically ordered levels. Thus it is likely that the process for energy maxima changes gradually with increasing depth of exploitation. The level 501, outstanding from the point of view of general rockbursts danger, turnes out to be also outstanding regarding the maximum energy generation.

The probability distributions of maximum seismic energy release at the particular mine region, in the studied period, are shown in Figures 5.7 - 5.11, respectively. The following modes of the distributions were identified:

- NW part: I - $E_{max} \approx 5 \times 10^4$ J , II - $E_{max} \approx 10^5$ J , III - $E_{max} \approx 5 \times 10^5$ J , IV - $E_{max} \approx 3 \times 10^6$ J and possibly V - $E_{max} > 10^7$ J with only one observation;
- SW part: possibly I - $E_{max} \approx 5 \times 10^4$ J , II - $E_{max} \approx 6 \times 10^5$ J , III - $E_{max} \approx 10^6$ J , IV - $E_{max} \approx 6 \times 10^6$ J , V - $E_{max} > 5 \times 10^7$ J ;

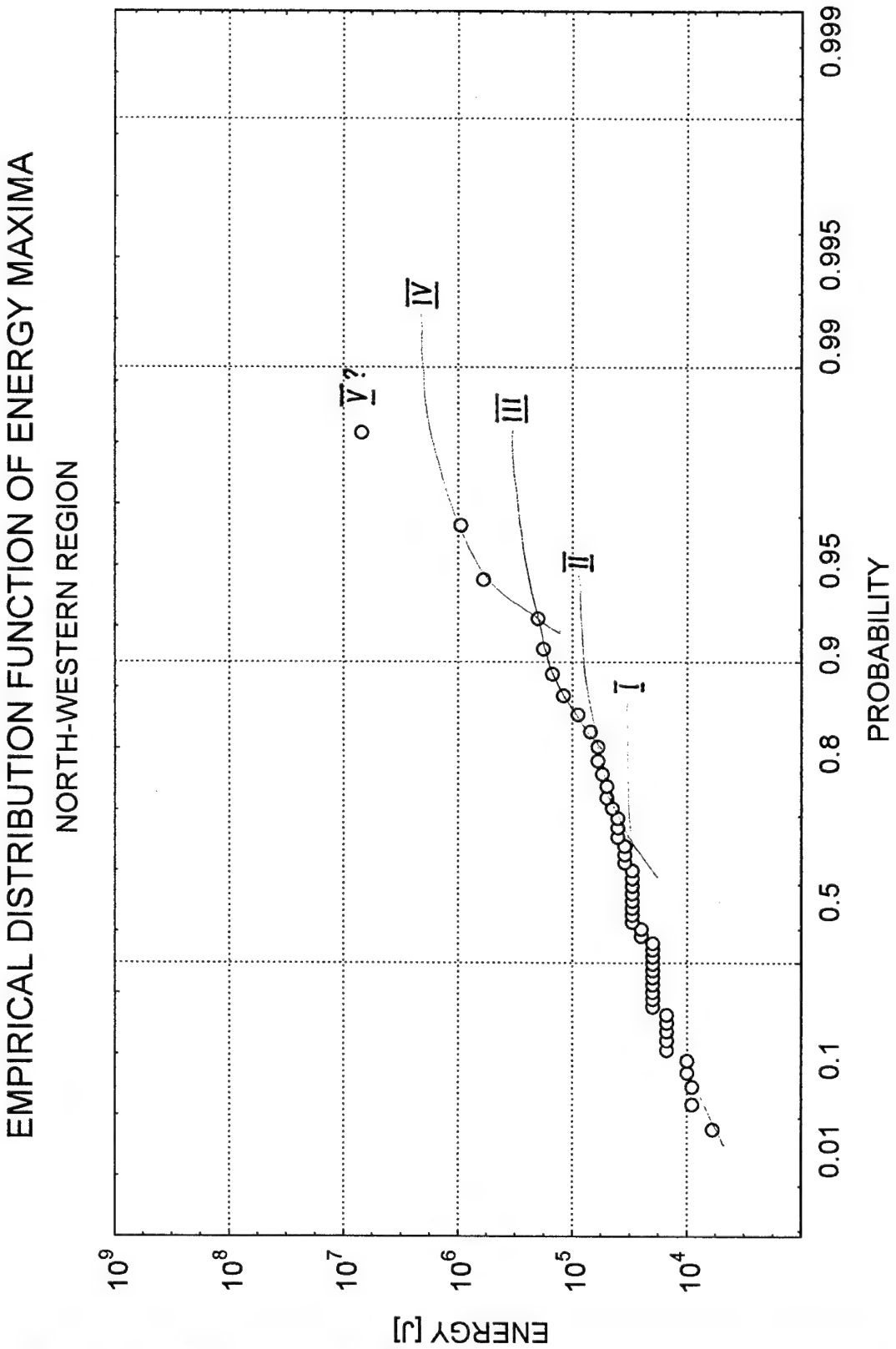

Figure 5.7 Probability distribution of the 20 days maximum seismic energy release in NW region of the Wujek mine

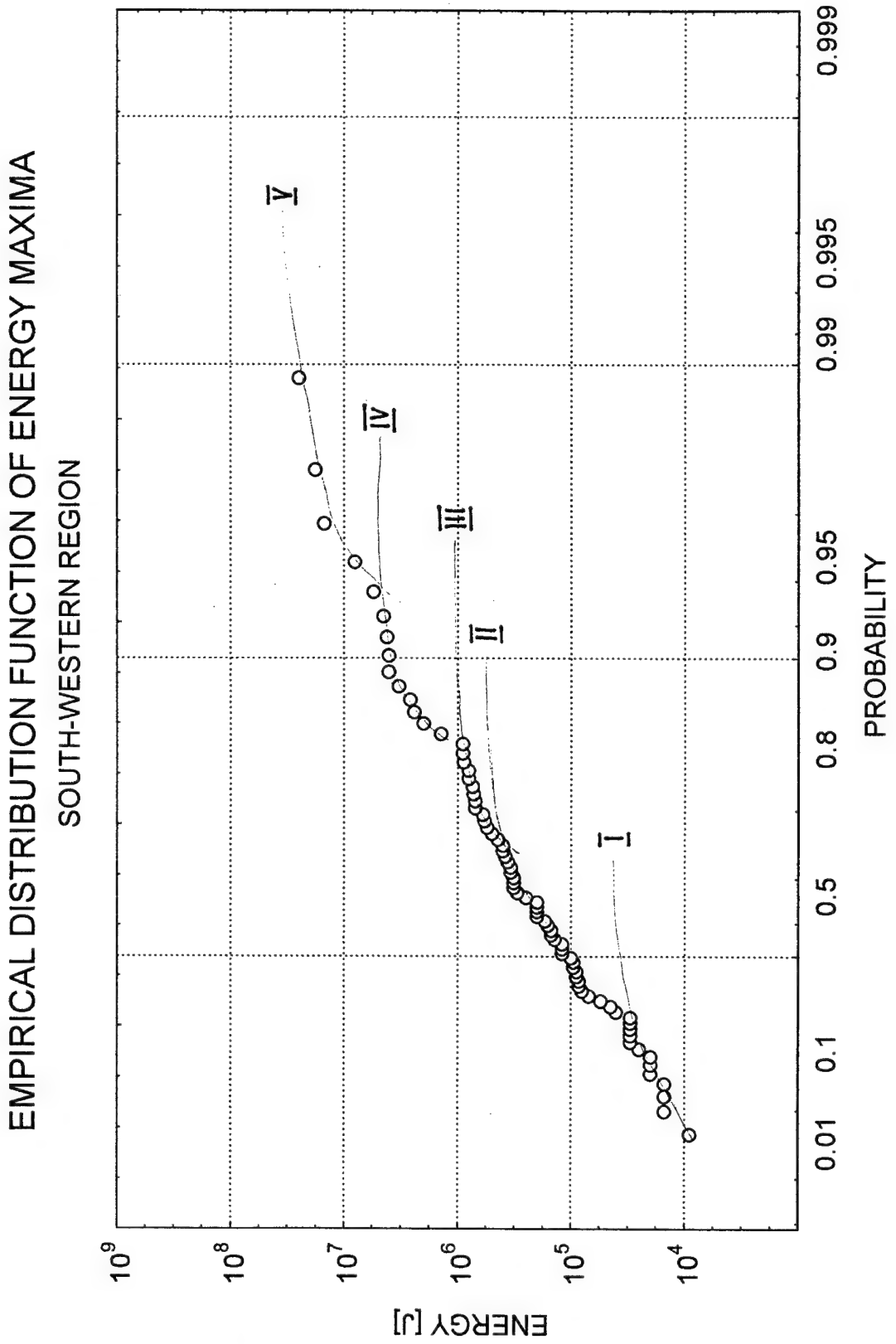

Figure 5.8 Probability distribution of the 20 days maximum seismic energy release in SW region of the Wujek mine

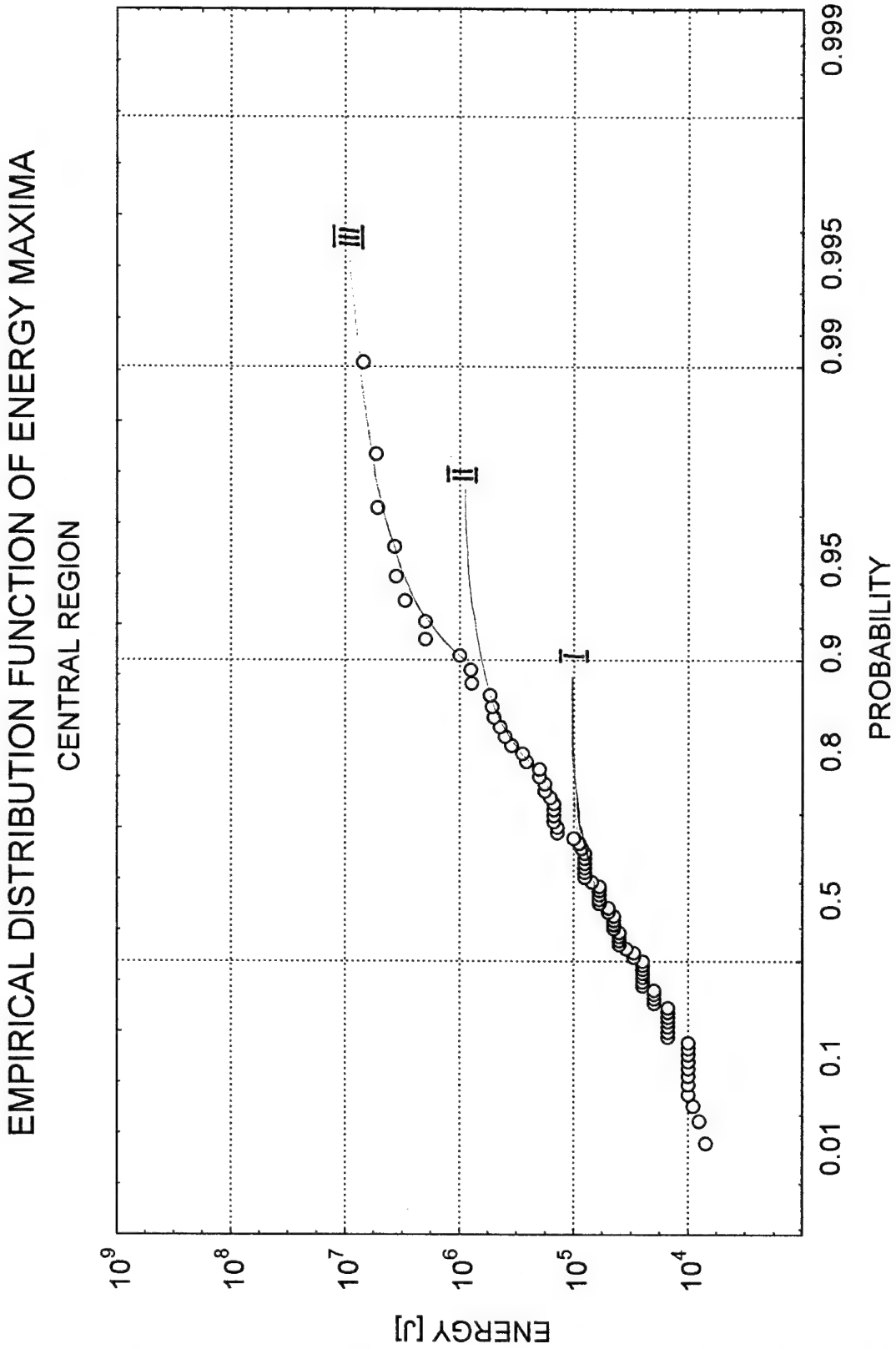

Figure 5.9 Probability distribution of the 20 days maximum seismic energy release in C region of the Wujek mine

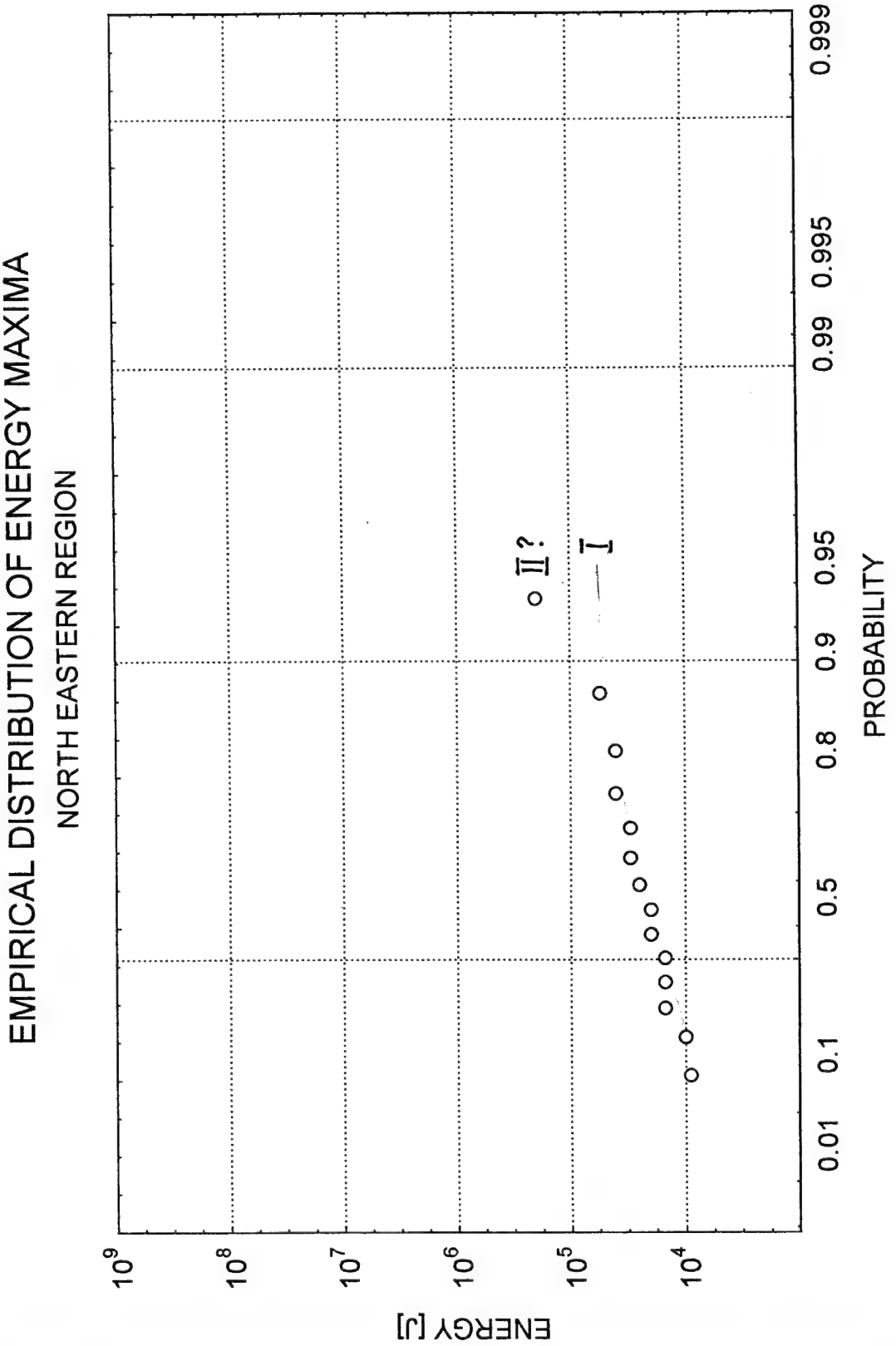

Figure 5.10 Probability distribution of the 20 days maximum seismic energy release in NE region of the Wujek mine

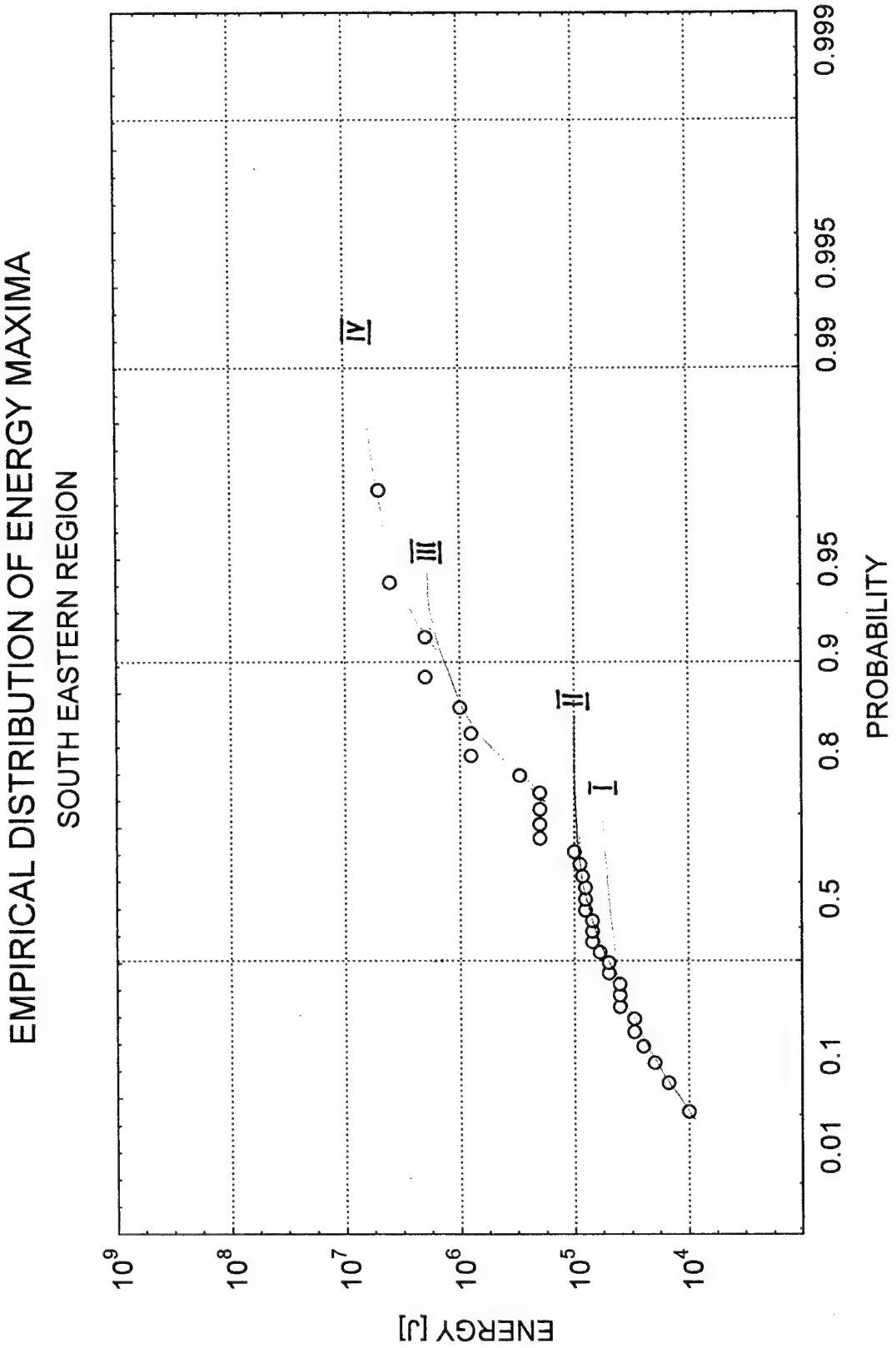

Figure 5.11 Probability distribution of the 20 days maximum seismic energy release in SE region of the Wujek mine

- C part: I - $E_{max} \approx 10^5$ J , II - $E_{max} \approx 10^6$ J , III - $E_{max} \approx 10^7$ J;

- NE part: I - $E_{max} \approx 5x10^4$ J , II - $E_{max} > 10^6$ J with only one observation;

- SE part: I - $E_{max} \approx 5x10^4$ J , II - $E_{max} \approx 10^5$ J , III - $E_{max} \approx 2x10^6$ J , IV - $E_{max} \approx 10^7$ J.

Like previously, these distributions of maxima were compared by means of the Kolmogorov-Smirnov two sample test. The results are given in Table 5.2.

Table 5.2. Results of Kolmogorov-Smirnov test for distributions of maximum seismic energy released at the mine regions

Mine region	No. of observations	Significance level				
		NW	SW	C	NE	SE
NW	28	x	<0.001	<0.01	>0.05	<0.001
SW	162		x	<0.001	<0.001	<0.05
504	14			x	<0.05	>0.05
507	21				x	<0.01
510	50					x

The distributions of logE maxima of the seismic series associated with NW and NE parts of the mine and the distributions of logE maxima associated with C and SE parts are similar (not significantly different).

The picture provided by this study of the regions associated distributions of logE maxima is less clear than that obtained from the previous, level associated samples study . The number of inflexions in the distributions increased, hence the estimates of the limiting values are less reliable. Doubtlessly the studies prove that there are different processes of event generation. It seems that they have different dynamics in different parts of the mine because the limiting values of the distributions of maxima are different. We can join these processes in crudely determined three classes. Class one of low energy mode processes contains modes I and II, with limiting values in the second half of the order 10^4 J or in the first half of the order 10^5 J. These are probably processes directly controlled by mining works in particular excavations, taking place in the coal layers or in their direct surrounding. The medium energy modes, with limiting values about 10^6 J assigne the second class. The second class processes are probably taking place in thick sandstone layers separating the coal seams and are controlled by the stress field resulted integrated effects of the active excavation, old workings geometry and local tectonic features.

The third class, which comprises high energy mode processes could be linked to generalized regional stress field variations.

We are unable to give the detailed explanation of the processes of seismic event generation upon the extreme value statistics study alone. Certainly the generating mechanisms are more complex than these mentioned here. Their better recognition needs complementing the statistical analysis with the rock mechanics modeling and the physics of rockmass fracturing studies.

Conclusions

1. The maximum energy value statistics method turnes out to be a valuable tool in studying complexity of the series of seismic events.
2. The results of the study prove that the energy distribution of seismic events induced by mining is multimodal in both mine-wide scale as well as at particular coal layers and in particular mine parts.
3. The maximum value studies enable to single out particular modes of event energy distributions and to estimate roughly their limiting values. It is expectable that different event generating processes are responsible for the different modes of energy distributions.
4. Some coal levels and some mine parts have similar distributions of maximum released energy, other ones have significantly different.
5. The distributions of energy of events recorded in strongly seismically active mine parts or at strongly active coal levels have more high energy modes than the distributions associated with mine regions where the seismic activity was moderate.
6. In general three classes of processes of seismic event generation are identified. The processes belonging to these classes are responsible for low, medium and high energy modes of event energy distribution, respectively. The limiting values of these processes depend upon the part of the mine they take place.
7. Determining of controlling factors and mechanisms of the identified processes will not be possible unless information from the rock mechanics and physics of fracturing studies complements results of the statistical analysis.

8. The extreme value statistics is an indirect way to identify processes of seismic event generation. It is not possible, on a basis of this method, to separate from the seismicity series events generated by specific identified processes.

6. Deflections. A preliminary analysis.

It is well known that series of mining induced events are not distributed randomly in space but have a certain geometrical time-varying structure. The seismic events tend to occur around plane structures like old workings edges, faults and other weak zones. Various methods have been applied to analyze geometrical distribution of sources in order to group events that are due to a single fracturing process. These are cluster analysis techniques where relations between events are inferred from their mutual distances, in a hope, that different generating processes would result in creating different clusters or different groups of clusters of induced seismicity (e.g., Frohlich and Davis 1986, Davis and Frohlich 1991, Kijko et al. 1993). According to our experience gained from trials made on the seismic catalog from Wujek mine, the clustering methods may work well when the catalog is of small or moderate size. For large series, and events which are described by only four - five parameters, the cluster classification leads to either trivial or non-unique results, difficult to interpret. It is also not still resolved how to define properly the distance in the time-space, to enable four dimension clustering, not mention about a higher order space like the time-location-energy one. We evidenced formerly that the mining-induced seismicity is nonstationary in both time and space. Hence significant clustering is expected rather in four, five-dimensional than in only the Euclidean space.

Geometrical approach is also represented by the fractal analysis of seismic source distribution (e.g., Smalley et al. 1987, Xie and Pariseau 1992, Idziak and Zuberek 1995, Lasocki and Mortimer 1996). Variations of the fractal dimensions among the seismic series, when the series have fractal character, or values of different order fractal dimensions, in case of multifractal structure of the series, are tried to be interpreted in terms of various generating processes. Still studies are needed concerning properties of the fractal dimension distributions which could enable distinguishing of the fractal dimensions (Cosentino et al. 1996). The other drawback of the fractal methods is the same as connected with the cluster analysis: the problem with defining distance in the multidimensional space.

Limited number of parameters of events limits, in our opinion, possibilities to study the complex structure of the seismic series. Therefore we have introduced and investigated a new parameter to describe the directional structure of the series. The trend of the seismic series is

characterized, in our study, by the distribution of deflection of straight lines connecting the epicenters of every two consecutive events. The deflection is measured from the NS direction. The sense of the vector connecting epicenters is not assessed and the identity

$$\alpha \equiv \begin{cases} \alpha + 180^o & for \quad \alpha \in \left[-180^o, -90^o\right] \\ \alpha - 180^o & for \quad \alpha \in \left[90^o, 180^o\right] \end{cases} \tag{6.1}$$

is set. In this way, the deflection varies in the range of [-90° , 90°].

The deflection is regarded as a random variable with a certain probability distribution. Modes of the probability distribution function of deflections show dominant trends of the studied seismic series. The parameter forms a time series, hence, in addition to information about geometrical assembly of epicenters, it kept also track of time ordering of events. Since, as it was mentioned, the plane structures (linear on the horizontal plane) are likely to play the major role in generating seismic events, we assume that the events building the specific dominant trend are outcomes of a single generating process.

For the N-event series we receive the (N-1)-point set of deflections. Thus, unlike in the maximum value studies, the analysis of deflection can be performed on particular seismicity clusters. The clusters of seismicity at Wujek mine were identified in Section 3. The descriptive statistics studies showed that these clusters differ in statistical properties. Therefore, the analysis of deflections was made on the selected clusters. In cases when the sample size was large enough for such the analysis, all complete series as well as their subsets, built by removing events below the prescribed energy thresholds, were considered. The studied data sets are presented in Table 6.1

The sets 1-3, 5-12, 14-19, 21-23, 16-30 were built form the seismic series that occurred in vicinity of active excavations (see: Figs. 3.3-3.17). Other sets concern cases of "strange" activity, which cannot be linked to mining works. C part, at the level 501, was divided with the W-S line at x=18700 into the southern area with mining stopes and the northern area where no exploitation could justify occurrence of seismic events (see: Fig. 3.6). Also NE part of the level 510 was split with the N-S line at y=-9850, and only its western part, that had no obvious connection with mining, was analyzed (see: Fig. 3.15).

Table 6.1 Data sets studied in the analysis of deflections

No	Coal level	Mine part	Energy threshold	Number of events
1	416	C	no	1342
2	416	C	$3.2x10^3$J	738
3	416	C	10^4J	134
4	416	SW	no	89
5	501	SW	no	4816
6	501	SW	10^4J	1207
7	501	SW	$3.2x10^4$J	344
8	501	SW	10^5J	49
9	501	southern part of C	no	1572
10	501	southern part of C	10^4J	524
11	501	southern part of C	$3.2x10^4$J	158
12	501	southern part of C	10^5J	49
13	501	northern part of C	no	112
14	504	C	no	367
15	504	C	$3.2x10^3$J	197
16	504	C	10^4J	71
17	507	NW	no	1199
18	507	NW	$3.2x10^3$J	889
19	507	NW	10^4J	314
20	507	SW	no	49
21	510	NW	no	272
22	510	NW	$3.2x10^3$J	168
23	510	NW	10^4J	52
24	510	western part of NE	no	357
25	510	western part of NE	$3.2x10^3$J	230
26	510	western part of NE	10^4J	56
27	510	SE	no	1677
28	510	SE	$3.2x10^3$J	1133
29	510	SE	10^4J	348
30	510	SE	$3.2x10^4$J	91

For each data set the respective set of deflections was prepared. Inspection of the histograms of deflections for the considered seismic series suggests their nonuniform distribution. At least one distinct mode of the distribution was visible in each histogram. Many histograms had also the secondary modes. In some cases neither the main nor secondary modes

were located at the same places for different subsets of the same data sets. Figure 6.1 shows, as an example, the histograms of deflections for sets 3 and 5, that is for the same seismicity cluster from SW part of the level 501, with no energy threshold and the threshold of 10^5J applied, respectively. The main mode of the distribution, located at some 50° for set 3, is shifted to some 65° for set 5. The strong event series (set 5) shows also the second trend of some -20°.

In order to verify the suggestion about the nonuniform distribution of deflections, the empirical distributions were compared with the theoretical uniform distribution by the chi-square and one-sample Kolmogorov-Smirnov tests. For all subsets both testing procedures have rejected, with high significance, the hypothesis about uniform character of the empirical distributions of deflections.

In practically all analyzed cases the histograms of deflections imply that the distribution of deflections of seismic events has complex multimodal structure. The identification of the modes is supposed to deliver valuable information about components of the data and, indirectly, about processes involved in the seismicity generation. Because of the subjective choice of a way of binding the histogram of random sample is always a subjective structure. The more complex and multimodal distribution of the variable is, the smaller sample is analyzed, the less certain shape of the distribution is assessed from the histogram. Although, in general, our study concerns large size samples we intend to work also with sets of some 50 or less points where a final shape of the histogram will dominantly depend upon the way of binding. We need, therefore, methods which can, more objectively than the histograms do, recover probability density functions from random samples. The nonparametric kernel estimation of probability density function, the technique, so far as we know, for the first time used in studies of seismicity, seems to fit to our purposes. A theoretical development of the method and results of various experiments necessary before applying the method to real data are given in the next section.

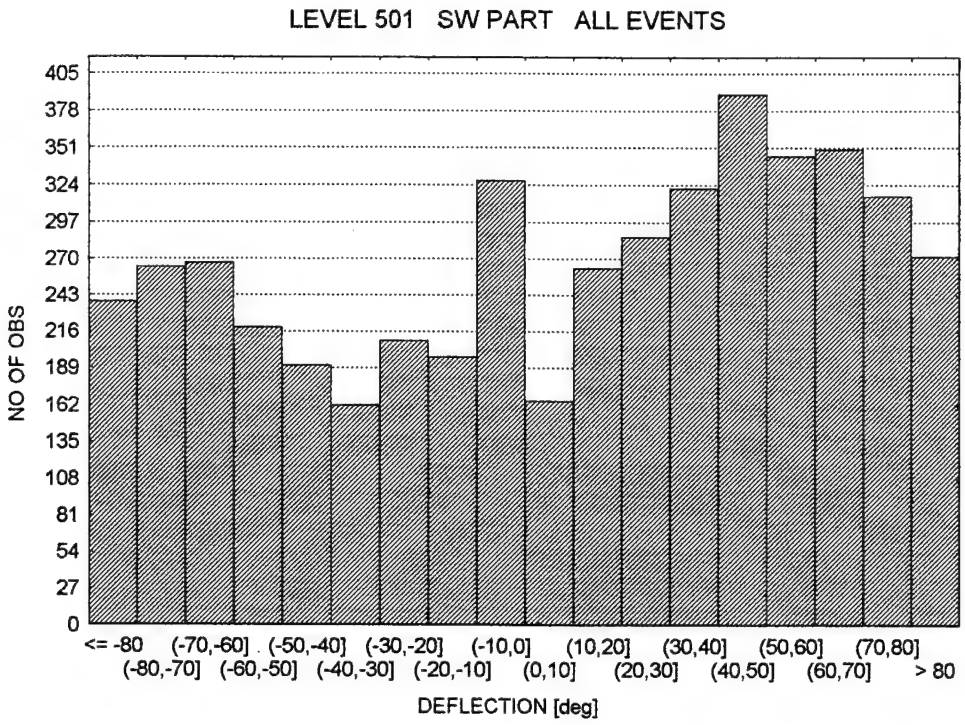

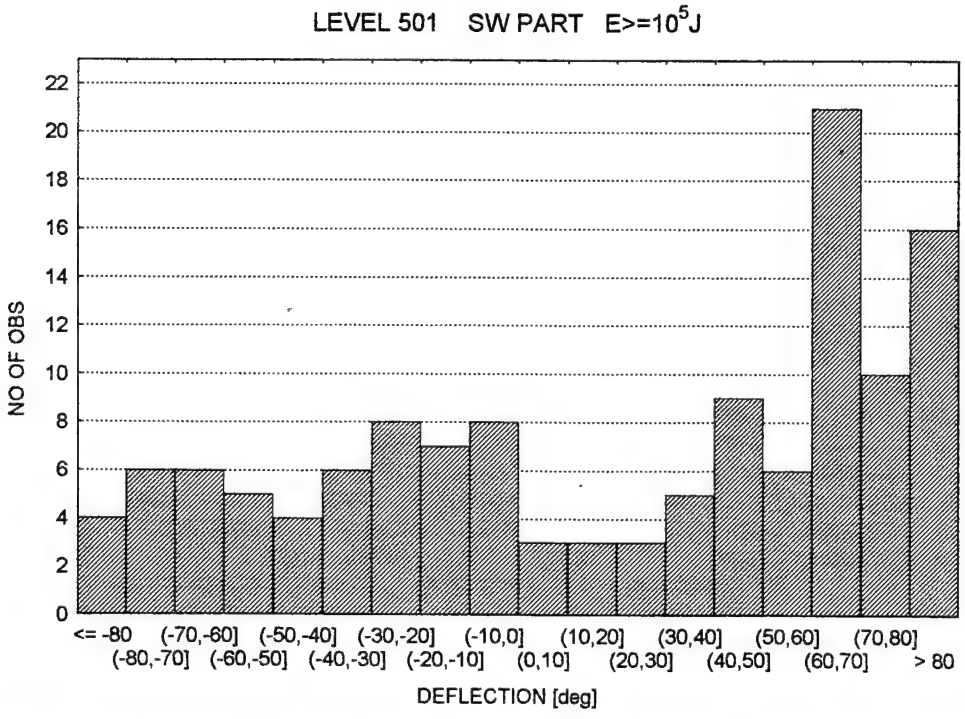

Figure 6.1 Histograms of deflections of seismic events recorded in SW part of the mine, at the level 501.

Summary and conclusions

1. A new way to study nonrandom character of the spatial distribution of seismic series was proposed. The method is based on the deflection of straight lines connecting epicenters of every two consecutive events, measured from the NS direction.

2. Distributions of deflection for seismic series from Wujek coal mine turned out to be complex and not uniform. There were clear dominant and sometimes also secondary directions. The modes of the distributions are expected to be formed by events originated by different generating processes.

3. The identification of modes of deflection distributions cannot be made from histograms because the histograms strongly depend on a subjective choice of binding. As an alternative approach the nonparametric kernel estimation of the probability density function is proposed. We think that this method can be used not only in the analysis of deflection but also to study structure of the seismic energy or logarithm of energy distributions.

7. Nonparametric kernel estimation of probability density functions

Statistical inference on a probability density function (p.d.f.), given random sample, is commonly made by assuming a function, estimating its parameters and assessing its validity using an adequate test. Then, for visual inspection rather than for other purposes, the estimated probability density function can be compared to a histogram. Unlike empirical probability distribution function or empirical probability exceedance function, histogram is a highly subjective structure and its resemblance to the true p.d.f. can always be criticized. Nevertheless, there is permanent need for developing methods enabling the user to construct a reliable estimator of a p.d.f., especially where rationale exists that the true p.d.f. is a multi-peak function. Of course, a p.d.f. can be derived from a given cumulative probability distribution function (cdf). Unfortunately, the latter is an integral function, which means that it screens local effects and insufficiently large peaks are not detectable.

Nonparametric kernel estimation, started with papers of Rosenblatt (1956) and Parzen (1962), is an approach which deals with direct estimation of unknown true p.d.f. using random sample data. Up to now, many estimators have been developed, their theoretical properties recognized. However, from practical point of view, the most important question has not been sufficiently answered yet: How, based on a random sample of real data, is to be selected the smoothing parameter h?. Because theory cannot and will not fully answer to this question, the only reasonable way is the experiment. It implies two possibilities complementing each other: (a) the Monte Carlo experiments enabling the researcher to investigate many features which he wants to know, and (b) applications of nonparametric methods to real data samples and using the physical information underlying the samples to verify (i.e. to confirm or reject) the statistical findings discovered by the nonparametric method used. However, although the possibility (a) is rather widely employed, real data are used for illustration purposes rather than as an additional source of information which qualitatively differs from generated pseudorandom numbers and, for this reason, is the information of special importance.

Our work is, on the one hand, connected with the possibility (a), when we illustrate how kernel methods work in cases which are of our interest, and, on the other hand, it also employs the possibility (b) in order to identify the real distributions of deflections and logarithms of energy of tremors, as well as in order to show how the relevant physical information correlates with the approximations obtained and justifies their use. It should be stressed here that while numerous papers have been published on theoretical and/or Monte

Carlo findings, papers dealing strictly with application problems of the p.d.f. nonparametric kernel estimation are rare and to our best knowledge this approach has not been yet used in seismicity.

Kernel estimation of probability density function

A kernel estimator $\hat{f}(x)$ of a p.d.f. $f(x)$ can be expressed (Parzen 1962) as

$$\hat{f}(x) = \frac{1}{nh}\sum_{i=1}^{n} K\left[\frac{x-x_i}{h}\right] \tag{7.1}$$

where x_i, $i=1,2,\ldots,n$, is a random sample, $K(.)$ is a given kernel function and h is a positive smoothing parameter (the terms bandwidth or window width are also used). Under conditions given in Parzen's (1962) paper, the $\hat{f}(x)$ is asymptotically unbiased and consistent. For the remainder of this section it is assumed that the sample x_i, $i=1,2,\ldots,n$, is nondecreasing.

In practice, both a kernel function and smoothing parameter have to be chosen. The choice of a kernel function is not very important and many symmetric unimodal functions can give similar efficiency of the method. For example, Silverman (1986) compared the efficiency *eff*(K) of five following symmetrical kernel functions $K(y)$:
a parabola:

$$K(y) = \begin{cases} \frac{3}{4\sqrt{5}}\left[1-\frac{y^2}{5}\right] & for\ |y| < 5^{1/2} \\ 0 & for\ |y| \geq 5^{1/2} \end{cases} \qquad eff(K) = 1 \tag{7.2}$$

a parabola of fourth order:

$$K(y) = \begin{cases} \frac{15}{16}(1-y^2)^2 & for\ |y| < 1 \\ 0 & for\ |y| \geq 1 \end{cases} \qquad eff(K) = 0.9939 \tag{7.3}$$

a triangle:

$$K(y) = \begin{cases} 1-|y| & for\ |y| < 1 \\ 0 & for\ |y| \geq 1 \end{cases} \qquad eff(K) = 0.9859 \tag{7.4}$$

a rectangle:

$$K(y) = \begin{cases} 1/2 & for\ |y| < 1 \\ 0 & for\ |y| \geq 1 \end{cases} \qquad eff(K) = 0.9295 \tag{7.5}$$

and a Gauss:

$$K(y) = \frac{1}{\sqrt{2\pi}} \exp\left[-\frac{y^2}{2}\right] \qquad eff(K) = 0.9512 \qquad (7.6)$$

Thus practically each symmetric unimodal function can be applied as a kernel function.

The choice of h is more crucial for performance of the method and several procedures exist for estimation of the smoothing parameter value (eg.: Scott and Factor 1981, Katkovnik 1985, Scott and Terrel 1987): method of minimization of integral mean square error, cross-validation (modified maximum likelihood function) method, k-nearest neighbor method, a method based on the Fourier series expansion of a true density (in general: orthogonal series estimators), and others. According to Scott and Factor (1981) none of them seems to be better than the others so the authors suggest constructing several estimators in order to eliminate occasional poor ones.

Accuracy measures of p.d.f. estimators

The accuracy of the kernel estimator (7.1) can be expressed in many ways of which the mean square error, *MSE*, and integral mean square error, *IMSE*, are applied.
The mean square error, *MSE*, is an error estimation at x:

$$MSE(x,h) = E[\hat{f}(x) - f(x)]^2 \qquad (7.7)$$

It can be decomposed into two basic components:

$$MSE = \sigma^2(\hat{f}) + bias^2(\hat{f}) \qquad (7.8)$$

where $\sigma^2(\hat{f})$ is a random error component:

$$\sigma^2(\hat{f}) = E[\hat{f}(x) - E\hat{f}(x)]^2 \qquad (7.9)$$

and $bias^2(\hat{f})$ is a systematic error component:

$$bias^2(\hat{f}) = E[E\hat{f}(x) - f(x)]^2 = |E\hat{f}(x) - f(x)|^2 \qquad (7.10)$$

If $h \to 0$ then $E\hat{f}(x) \to f(x)$ so the *bias* tends to zero. However, the random error $\sigma(\hat{f})$ increases then to infinity because the estimator $\hat{f}$ tends to a linear combination of Dirac delta-functions. Thus the choice of the smoothing parameter h (an optimum value of h) should be a compromise between these two errors.

The integral mean square error, *IMSE*, is an estimation of the global error for $\hat{f}$:

$$IMSE = \int E[\hat{f}(x) - f(x)]^2 dx \qquad (7.11)$$

Minimization of the *IMSE* as a function of h is one of the most commonly used techniques for estimation of the smoothing parameter h.

Methods for estimation of smoothing parameter

The choice of h is the most crucial for the performance of any method. If h is too small, the resulting estimated density function $\hat{f}(x)$ is too little smoothed and shows too much noise contained in the sample. And on the contrary: if h is too large, the resulting oversmoothing masks the structure of the true p.d.f. $f(x)$. Unfortunately, the choice of each method is to some extent subjective, and it is upon a researcher to decide which method is to be applied. The situation seems to be similar to the problem of estimating the spectral density function, especially if the data is not very numerous.

We have selected and decided to compare two of the existing methods. The first is a simplification of the *IMSE* minimization method, and the second one is based on the concept of modified (empirical) likelihood function. Anticipating a little, it can be said that the first method is the simplest and most reliable because is simple for calculation and gives one (and only one) h value for every sample. The second method is more time consuming, usually gives more than one h value, and, not infrequently, $h=0$.

The optimum value of the smoothing parameter h can be obtained by minimization of the *IMSE*. According to Scott and Factor (1981), this leads to the following asymptotical optimal choice for h :

$$h = \alpha(K)\,\beta(f)\,n^{-1/5} \qquad (7.12)$$

where $\alpha(K)$ and $\beta(f)$ are factors depending on kernel function K and p.d.f. f, respectively:

$$\alpha(K) = \left[\int K(y)^2 dy\right]^{1/5} \left[\int K(y) y^2 dy\right]^{-2/5} \qquad (7.13)$$

$$\beta(f) = \left[\int f''(x)^2 dx\right]^{-1/5} \qquad (7.14)$$

The unknown function f in the expression $\beta(f)$ is usually replaced with its estimator based on

the chosen kernel function K. The method has good properties, as it was numerically demonstrated that the choice of h based on (7.13) is in the average nearly optimal for even as small samples as $n=25$ (Scott and Factor 1981).

It is possibly to obtain simpler results. It was shown (Adamowski and Feluch 1987, Feluch 1994) that for the parabolic kernel

$$K(y) = \begin{cases} \frac{3}{4\sqrt{5b}}\left[1-\frac{y^2}{5b}\right] & for\ |y| < \sqrt{5b} \\ 0 & for\ |y| \geq \sqrt{5b} \end{cases} \tag{7.15}$$

the smoothing parameter h can be approximated by an expression

$$h \leq \frac{\sum_{i=1}^{n}(2i-n-1)x_i}{n\left[n-\frac{10}{3}\right]\sqrt{5b}} \tag{7.16}$$

Because the value of b does not influence the error of the estimator (7.1), the authors propose to use the value $b=1/5$, which leads to simpler equations for the kernel K

$$K(y) = \begin{cases} \frac{3}{4}(1-y^2) & for\ |y| < 1 \\ 0 & for\ |y| \geq 1 \end{cases} \tag{7.17}$$

and the smoothing parameter h

$$h = \frac{\sum_{i=1}^{n}(2i-n-1)x_i}{n\left[n-\frac{10}{3}\right]} \tag{7.18}$$

The sign of the weak inequality in (7.16) has been replaced in equation (7.18) by the sign of equality. The h value thus obtained is the smallest upper limit for smoothing parameter produced by the method (7.12) of minimizing *IMSE* (7.11).

Another method of obtaining a smoothing parameter estimator is based on the modified (empirical) likelihood function $\hat{L}(h)$ (Scott and Factor 1981, Katkovnik 1985, Silverman 1986):

$$\hat{L}(h) = \prod_{j=1}^{n} \hat{f}^{[j]}(x_j) \tag{7.19}$$

in each case and is simple and fast.where $\hat{f}^{[j]}(x_j)$ is equal to

$$\hat{f}^{[j]}(x_j) = \frac{1}{(n-1)h} \sum_{i=1, i\neq j}^{n} K\left[\frac{x_j - x_i}{h}\right] \tag{7.20}$$

$\hat{f}^{[j]}(x_j)$ is an estimator of the p.d.f. at x_j based on the whole sample excluding point x_j. Combining the last two equations, we get

$$\hat{L}(h) = \prod_{j=1}^{n} \frac{1}{(n-1)h} \sum_{i=1, i\neq j}^{n} K\left[\frac{x_j - x_i}{h}\right] \tag{7.21}$$

The optimum value $\hat{h}$ of h is computed from the condition:

$$\hat{h} = \underset{h\geq 0}{arg\,max} \hat{L}(h) \tag{7.22}$$

The procedure is quite effective even for small n (Katkovnik 1985). However, when kernel (7.17) is used, possible values of h must be greater than $h_{\min}$

$$h_{\min} = \max\left\{\Delta x_2, \min_{i=3,\ldots,n}(\Delta x_i, \Delta x_{i-1}), \Delta x_n\right\}, \qquad \Delta x_i = x_i - x_{i-1} \tag{7.23}$$

otherwise $\hat{L}(h) = 0$. The method is thus insensitive to h values from the interval $(0, h_{\min})$.

Monte Carlo visualization of the $\hat{f}(x)$ estimator quality

Unlike parametric methods of distribution function estimation, nonparametric methods employ local estimation, not global one. The resulting estimator of p.d.f., $\hat{f}(x)$, is basically assigned to that interval Δx of realizations of random variable X which includes the random sample x_i, i=1,2,...,n, $\Delta x \approx x_n - x_1$, not covering thus the whole interval of realizations of X. Extrapolation towards low or high values of X is possible for only a limited left vicinity of x_1 and limited right vicinity of x_n; as far as the kernel and smoothing parameter make it possible. Methods for kernel estimation quality assessing are also different from those for parametric estimation and consist mainly of assessment of the theoretical quality of the smoothing parameter estimator (consistency, bias, etc) and the quality assessed from

simulation experiment, a Monte Carlo simulation. It enables the researcher to observe the interesting aspects of the studied problem and find its pros and contras. The Monte Carlo simulation results, which are presented on subsequent pages, are to illustrate some main features of the kernel estimation method for p.d.f. estimation. Throughout this section, the smoothing parameter h is calculated by equation (7.18) which is the simplest method, giving somewhat overestimated value (with the resulting oversmoothing).

In order to show various aspects of the kernel estimation of a p.d.f., the Monte Carlo simulation was applied to some unimodal and bimodal distributions. We selected those distributions that resembled the shape of empirical event energy or logarithm of energy distributions or possessed features expected to be met in distribution of deflection. In each case a true p.d.f. is assumed to be known, a random sample was taken, and the kernel estimation was used to produce an estimator of $\hat{f}(x)$.

Lognormal unimodal distribution

This two-parameter distribution, defined by the following equation

$$f_{\ln}(x;\mu,\sigma) = \frac{1}{\sigma x\sqrt{2\pi}} \exp\left[-\frac{(\ln x-\mu)^2}{2\sigma^2}\right] \tag{7.24}$$

was used in its standard version ($\mu=0$ and $\sigma=1$) to produce 18 random samples of size n equal to 30, 60, 90, 120, 150 and 180, each size case sampled three times. Results are presented in Fig. 7.1 where also the theoretical p.d.f. is drawn. The maximum for that function is reached at the point $x = \exp(\mu-\sigma^2) = e \approx 2.7$.

Lomnitz (1974) postulated the use of lognormal distribution to model an empirical distribution of earthquake magnitudes. The distribution was also tried to represent logarithm of seismic energy in mining induced seismicity (Lasocki 1989).

Generally, when looking down the Fig. 7.1 along with the increasing sample size n, the expected tendency is visible. The quality (resemblance to the theoretical p.d.f.) of simulated p.d.f.-s seems to increase with increasing n. In certain cases, for small sample sizes, there exist some qualitative differences as, for example, distinctively developed bimodality or shifts of estimated maxima of $\hat{f}(x)$ when compared to the true p.d.f. $f(x)$. As n increases, the differences tend to be smaller: the bimodality is disappearing, locations of the true and estimated maxima are closer one to another, and the shapes of estimated $\hat{f}(x)$ and true p.d.f. $f(x)$ are more consistent, independently to the sample range (e.g. 0 - 60 for the sample

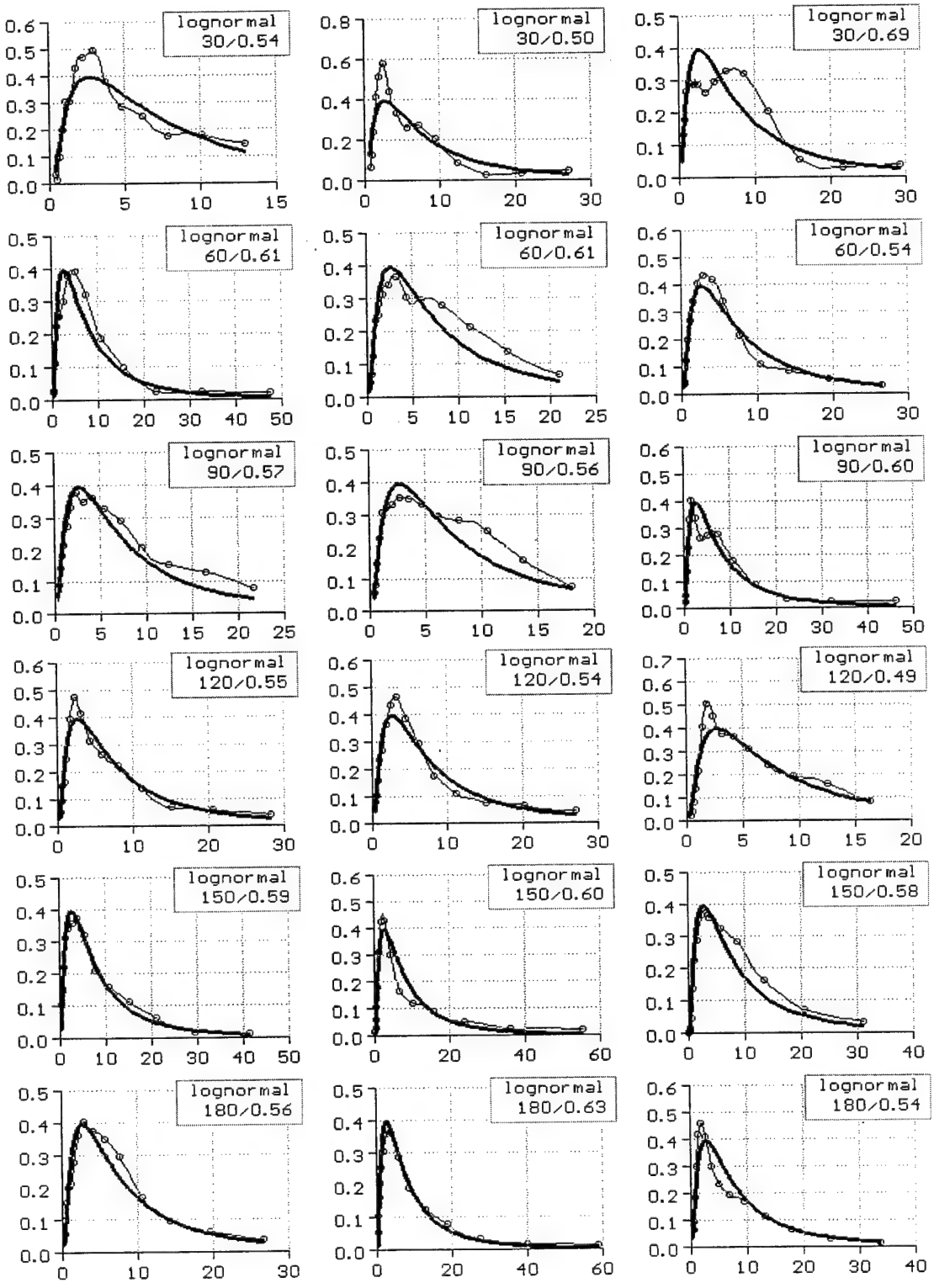

Fig. 7.1. Lognormal distribution p.d.f.-s: theoretical (equation (7.24)), $\mu=0$, $\sigma=1$, (heavy line) and kernel estimated (thin line with circles) for various samples of the same size n (rows) and various sizes (columns); h in the n/h expression is the smoothing parameter calculated by equation (7.18).

180/0.63 or 0 - 30 for 120/0.55 in Fig. 7.1). In each case the estimated function resembled the true p.d.f. at its both tails well. This is the result of the continuous falling to zero of both tails of the theoretical p.d.f. It would be interesting to see how the discontinuity of the true p.d.f. affects its estimator properties. For this purpose the truncated exponential distribution properties are investigated in the next subsection.

Truncated exponential distribution

The one-parameter truncated exponential distribution is defined in the (0,1) interval as follows:

$$f_{te}(x;a) = \begin{cases} \dfrac{a e^{-ax}}{1-e^{-a}} & 0<x<1 \\ 0 & otherwise \end{cases} \tag{7.25}$$

Corrections introduced to the Gutenberg-Richter's relation, that accounted for a deficit of the number of events in the large magnitude range, led to the truncated exponential distribution for earthquake magnitudes (Cosentino et al. 1977). At present, the truncated exponential distribution is the most widely used model for logarithms of energy in strong tremor hazard analyses of induced dynamic failure phenomena (Lasocki 1992a, 1993, Gibowicz and Kijko 1994, Kijko and Funk 1994).

The p.d.f. is not continuous at two points: $x=0$ and $x=1$. This discontinuity causes additional problems in reproducing the true p.d.f. $f(x)$ as the edge effect occurs. Its influence on the estimated p.d.f. can be strong, especially when the jumps at the discontinuity points are large, and can be seen in Fig. 7.2 as the tendency towards smooth transition between zero and non-zero values of an estimated p.d.f. The graphs in Fig. 7.2 shows that this tendency is present in all sampled distributions and it seems that the increase from $n=30$ to $n=180$ does not improve the resemblance of estimates $\hat{f}(x)$ to the true $f(x)$ at the right vicinity of point $x=0$ and the left vicinity of point $x=1$. Multimodality is stronger than for the previous (lognormal) distribution because the edge effect supports strongly the production of additional modes of the estimated p.d.f. This can be seen especially around the left border where the p.d.f. values are about three times greater then for the right one. Central parts of the estimated p.d.f.-s seem to be less affected by the edge effect, which is visible in Fig. 7.2 as decreasing amplitudes of estimated p.d.f. fluctuations around the true p.d.f. as the sample size n increases.

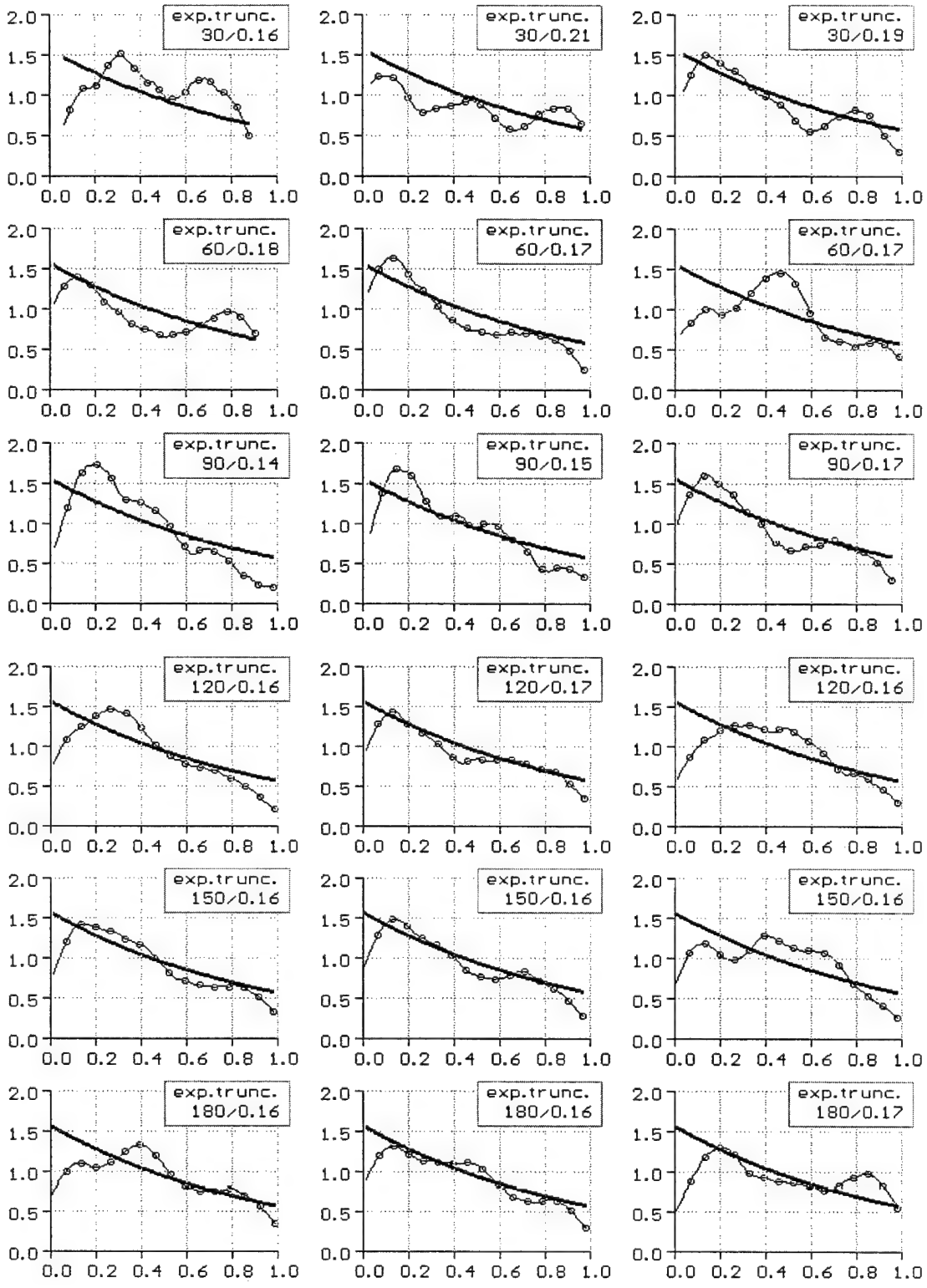

Fig. 7.2. Truncated exponential density functions: theoretical (equation (7.25)), $a=1$, (heavy line) and kernel estimated (thin line with circles) for various samples of the same size n (rows) and various sizes (columns); h in the n/h expression is the smoothing parameter calculated by equation (7.18).

Normal bimodal distribution

Theoretical distributions used in the previous two subsections were unimodal. It can be expected, however, that in reality multimodality is not an exceptional case. The results of numerical experiments presented in this and subsequent sections are to show how bimodality of a theoretical p.d.f. is reflected in its estimated image, $\hat{f}(x)$. The kernel estimation is regarded as the method which is very effective in estimating multimodal p.d.f.-s (Scott and Factor 1981, Katkovnik 1985).

The first bimodal p.d.f. investigated is the normal bimodal p.d.f., $f_{n2}(x;\mu,\sigma)$:

$$f_{n2}(x;\mu_1,\sigma_1,\mu_2,\sigma_2,d) = d\cdot f_n(x;\mu_1,\sigma_1) + (1-d)\cdot f_n(x;\mu_2,\sigma_2) \tag{7.26}$$

which is a mixture of two normal density functions, $f_n(x;\mu_i,\sigma_i)$, $i=1,2$:

$$f_n(x;\mu_i,\sigma_i) = \frac{1}{\sigma_i\sqrt{2\pi}}\exp\left[-\frac{(x-\mu_i)^2}{2\sigma_i^2}\right] \tag{7.27}$$

Parameter d can be interpreted as the probability of taking a random number from population $f_n(x;\mu_1,\sigma_1)$. For the purpose of simulation in all cases a value of 0.85 was adopted for d, as well as $\sigma_1 = \sigma_2 = 1$, and $\mu_1 = 1$. The only varying parameter is μ_2 for which values 2, 4 and 6 were adopted (columns 1, 2 and 3 in Fig. 7.3, respectively). Varying of the μ_2 values increases the distance μ_2-μ_1 between the maxima of the component p.d.f.-s (7.27). The distance of μ_2-$\mu_1 = 1$ (column 1 in Fig. 7.3) is too small to reveal these maxima in the mixture of distributions: the theoretical p.d.f. (7.26) does not show any trace of original bimodality. Out of six cases in column 1, two estimated p.d.f.-s are bimodal. It is interesting that this bimodality seems to some extent to indicate the underlying original maxima.

If the distance μ_2-μ_1 is greater than in the previous case, bimodality begins to be visible in a subtle way (column 2 in Fig. 7.3: μ_2-$\mu_1 = 3$) although, strictly speaking, the resulting theoretical p.d.f. is unimodal, and only a heavy tail occurred on the right. The estimated p.d.f.-s are in most cases bimodal with their main mode near the theoretical one (approximately 1). The second mode is rather loosely related to the second original mode (approximately 4).

Third column in Fig. 7.3 shows the theoretical bimodal p.d.f. for the greatest distance between the maxima: μ_2-$\mu_1 = 5$. The bimodality of the theoretical p.d.f. is clearly visible. The efficiency of the kernel method is in this case very high: the resemblance of the estimated p.d.f.

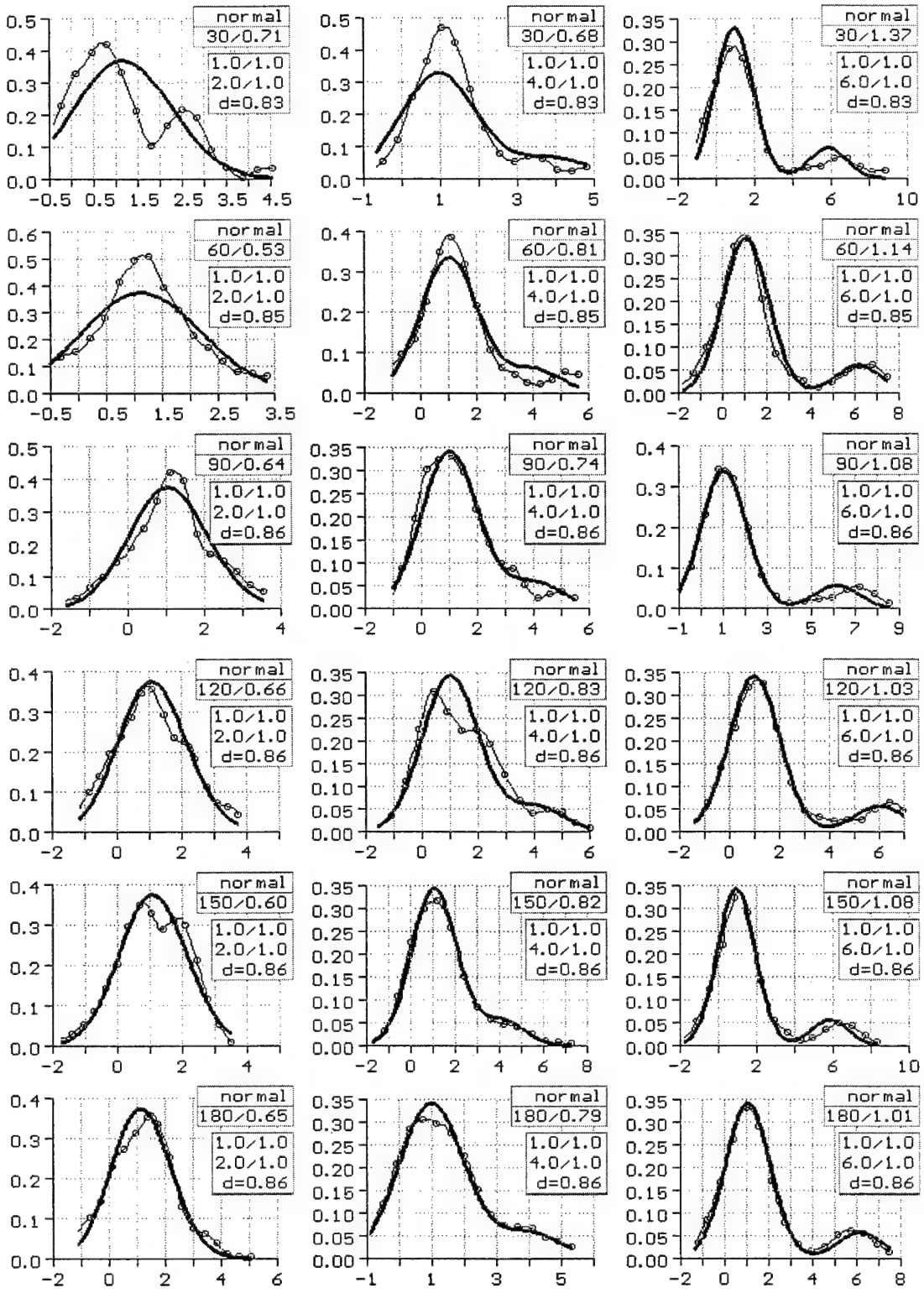

Fig. 7.3. Normal bimodal p.d.f.-s: theoretical (equation (7.26)) (heavy line) with parameters (μ_1,σ_1) and (μ_2,σ_2) and d shown, and kernel estimated (thin line with circles) for samples of the same size (rows) and various sample sizes n (columns); h in the n/h expression is the smoothing parameter calculated by equation (7.18)

to the theoretical one seems to depends weakly on sample size n. Almost all estimated p.d.f.-s are very similar to their theoretical original even in their intensity (especially for $n>60$). As it is expected, the increase in n improves the similarity of the estimated p.d.f.-s to their theoretical original.

Lognormal bimodal distribution

This distribution is a mixture of two lognormal distributions (7.24) with probability d of choosing the distribution with $f_{ln}(x;\ \mu_1,\sigma_1)$ against the second distribution with p.d.f. $f_{ln}(x;\mu_2,\sigma_2)$:

$$f_{ln2}(x;\mu_1,\sigma_1,\mu_2,\sigma_2,d) = d\cdot f_{\ln}(x;\mu_1,\sigma_1) + (1-d)\cdot f_{\ln}(x;\mu_2,\sigma_2) \qquad (7.28)$$

The adopted value of d, 0.8, prefers the first component distribution similarly as for the normal bimodal distribution in the previous section. Parameters μ_1, σ_1 of the first component distribution are constant and their values are 1 and 0.3, respectively, which corresponds to the maximum x-value $x_{max} = \exp(\mu-\sigma^2) \approx 2.5$. Value of the σ_2 parameter for the second component distribution is also constant and equals 0.1, while μ_2 is variable and its value are: 1.5 (first column in Fig. 7.4), 1.7 (second column), and 1.9 (third column). Maxima of that distribution are also variable and their values are 4.4, 5.4, and 6.6, respectively. Overlapping of distributions shifts the maxima only a bit closer to each other.

As in the previous subsection for normal bimodal p.d.f., in almost all cases in Fig. 7.4 the estimated p.d.f.-s mimic main features of the theoretical p.d.f. very well. For as low values of n as 60 (and, of course, for the higher values) the maxima are clearly revealed and their locations are in phase with their theoretical originals. This concerns especially the cases in columns 2 and 3 where the theoretical maxima are more separated than those in column 1. Small distance between original maxima, resulting in large overlapping of component distributions, generates a distinct distortion in their sample images, which can be seen in column 1 where n even as large as 180 does not remove this discrepancy.

In general, it can be stated that the shape reproduction of the theoretical p.d.f. by a sample p.d.f. is very good already for n as low as 60. As expected, the increase in n makes the resemblance of the theoretical to empirical p.d.f.-s larger.

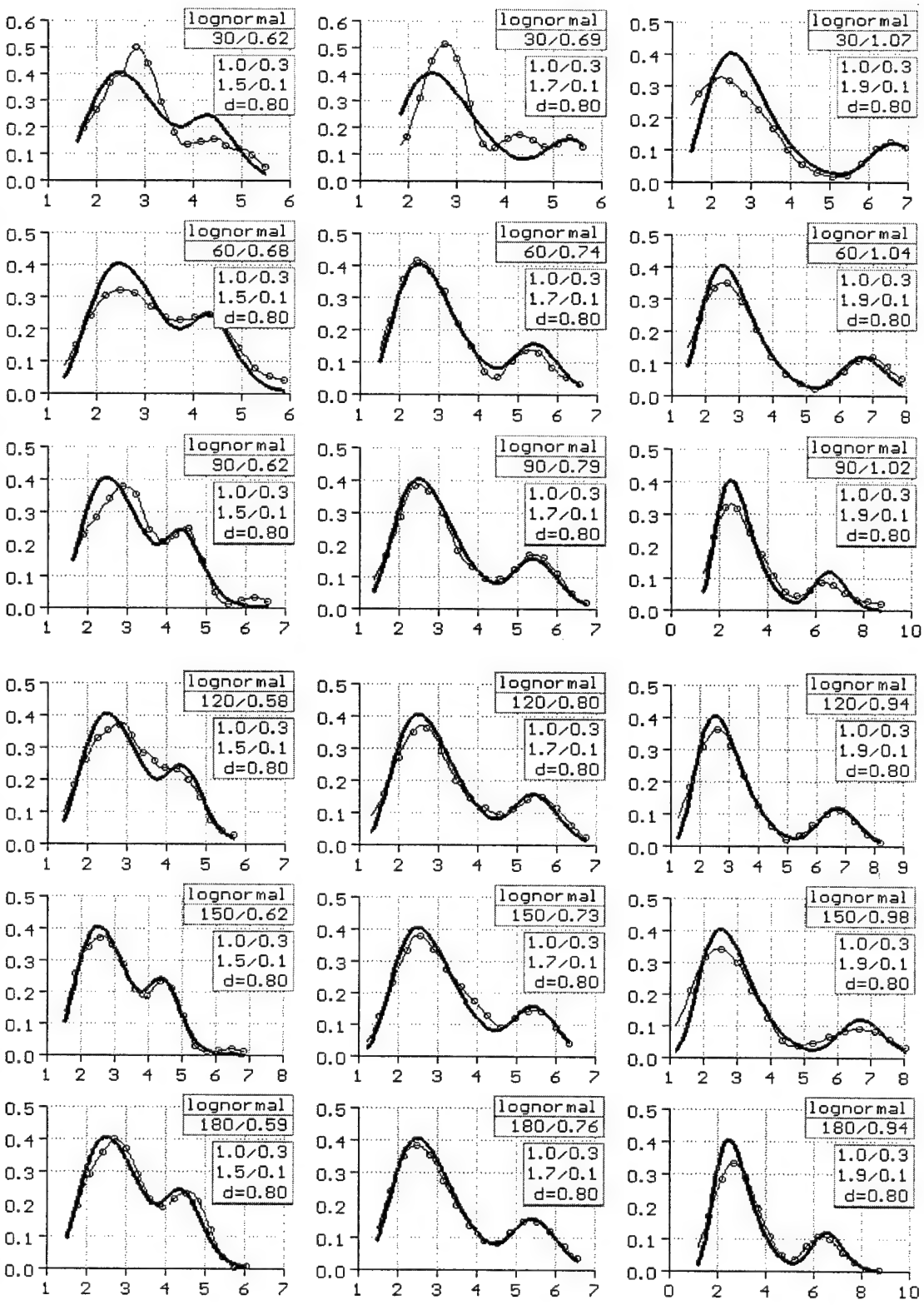

Fig. 7.4. Lognormal bimodal p.d.f.-s: theoretical (equation (7.28)) (heavy line) with parameters $(\mu_1,\sigma_1),(\mu_2,\sigma_2)$, and d shown, and kernel estimated (thin line with circles) for samples of the same size (rows) and various sample sizes n (columns); h in the n/h expression is the smoothing parameter calculated by equation (7.18).

Edge effect case: a sinus bimodal distribution

The truncated exponential distribution already discussed in this section exhibits the strong edge effect which substantially distorts the sampled image of the true p.d.f. There was no reason to expect that the distribution of deflection would smoothly decay at the limits of the variable range. We could, however, mitigate edge effects using the angle identity of deflection determined by (6.1). It was thus important to know how weakening of the sharpness of the jumps in a true p.d.f. would affect estimated p.d.f.-s. For this reason the following distribution defined by a simple p.d.f. was used:

$$f_s(x) = \begin{cases} \frac{1}{a}\left(1 + b\sin(x)\right), & x \in (c, 3\pi - c) \\ 0, & \textit{otherwise} \end{cases} \tag{7.29}$$

where the normalizing constant a is equal to

$$a = 3\pi - 2c + 2b\cos(c) \tag{7.30}$$

For the purposes of the simulation the following parameter values were adopted: $b = 0.8$ (all cases), $c = \pi/2$ (column 1 in Fig. 7.5), $c = \pi/4$ (column 2), and $c = 0$ (column 3). The adopted values of c determines interesting cases showing how the smoothness of the tails of a theoretical p.d.f. enables the estimator to reproduce its original. If there is no falling tail then the peaks occur in estimated p.d.f. tails that are shifted towards the center part of the interval of realizations. A slightly falling tail (column 2) makes that shift smaller and the greater interval of the center part of the theoretical p.d.f. is better reproduced. In column 3, locations of maxima of estimated p.d.f.-s are placed almost at the same x-values as the theoretical maxima.

Comparison of two methods of estimation of the smoothing parameter h

Two methods: the modified (empirical) likelihood criterion method (7.22) (or the cross-validation method) and the simplest method (7.18) based on minimization of the *IMSE* of the theoretical p.d.f. $f(x)$ are compared in this section. Based on the real data sets of deflections and logarithms of energy of tremors, the comparison is to show how both methods work and give some additional justification for choosing of the method (7.18).

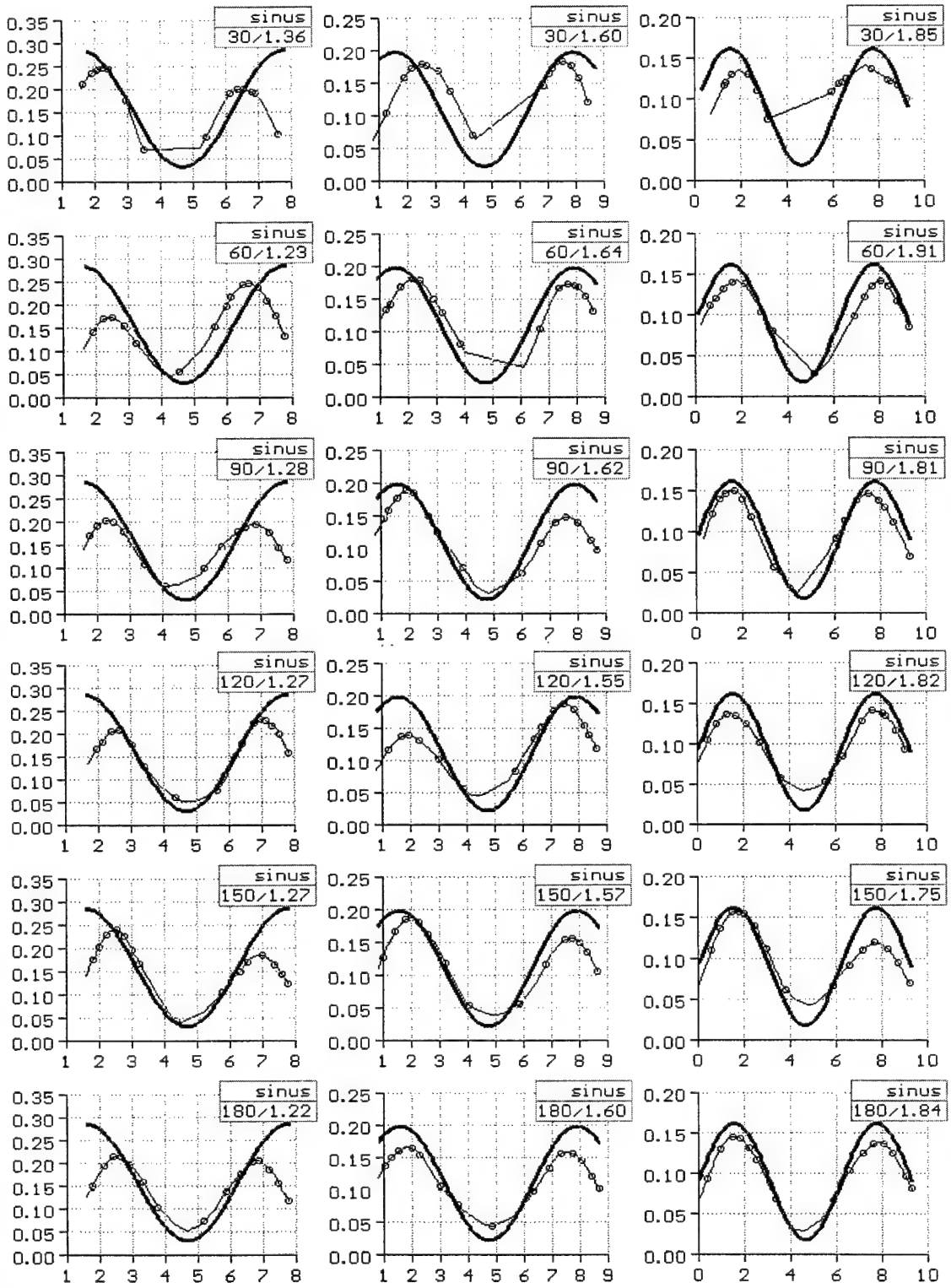

Fig. 7.5. Sinus bimodal p.d.f.-s: theoretical (equation (7.29)) (heavy line) with parameters $b=0.8$ (all cases), $c=\pi/4$, $\pi/2$ and 0 for columns 1,2 and 3 respectively, and kernel estimated (thin line with circles) for samples of the same size (rows) and various sample sizes n (columns); h in the n/h expression is the smoothing parameter calculated by equation (7.18).

The data sets for the study were selected so that they represented the variety of empirical distribution shapes of both logarithm of energy and deflection. The sample notation used in this section is given in Table 7.1.

Table 7.1. Studied data sets

Data set name	Variable	Origin of the data
501_CEN	deflection	events from norther part of C region at level 501
SW_E5	deflection	events of energy $\geq 10^5$J from SW region at level 501
SW_45	deflection	events of energy $\geq 3.2 \cdot 10^4$J from SW region at level 501
416_LOGE.SW	logarithm of energy	events from SW region at level 416
504_LOGE.NW	logarithm of energy	events from NW region at level 504
510_LOGE.NEA	logarithm of energy	events from NE region at level 510

The modified likelihood criterion method (7.22) has been investigated very extensively for various kernels, various sample sizes and various distribution functions (Katkovnik 1985, Scott and Terrel 1987). For purposes of this paper, two conclusions can be interesting: (i) this procedure has turned out to be quite effective even for small sample sizes, and (ii) discontinuous p.d.f.-s are reproduced worse than the continuous ones. Katkovnik (1985) investigated also the quality of the nearest-neighbor method. If unimodal distributions are taken into considerations, the method is comparable to the modified likelihood criterion method. However, when the theoretical p.d.f. is bimodal, the nearest-neighbor method quality is much worse.

Figures 7.6 and 7.7 present the results of optimization of the smoothing parameter h by the modified likelihood criterion method (left column in both Figures). There are also given nonparametric p.d.f.-s and cumulative distribution functions (cdf's) calculated using the optimized value of h, $h2$, and, as comparison, the same functions employing the smoothing parameter value $h1$ calculated by equation (7.18).

All $lnL(h)$ functions are multimodal, with the number of modes varying from three to five. It is possibly that shorter optimization steps would reveal more modes. To further calculation the values maximizing the $lnL(h)$ function within the investigated interval were chosen. They are indicated as $h2$ values in Figures 7.6 and 7.7. Also sample data are shown (right columns

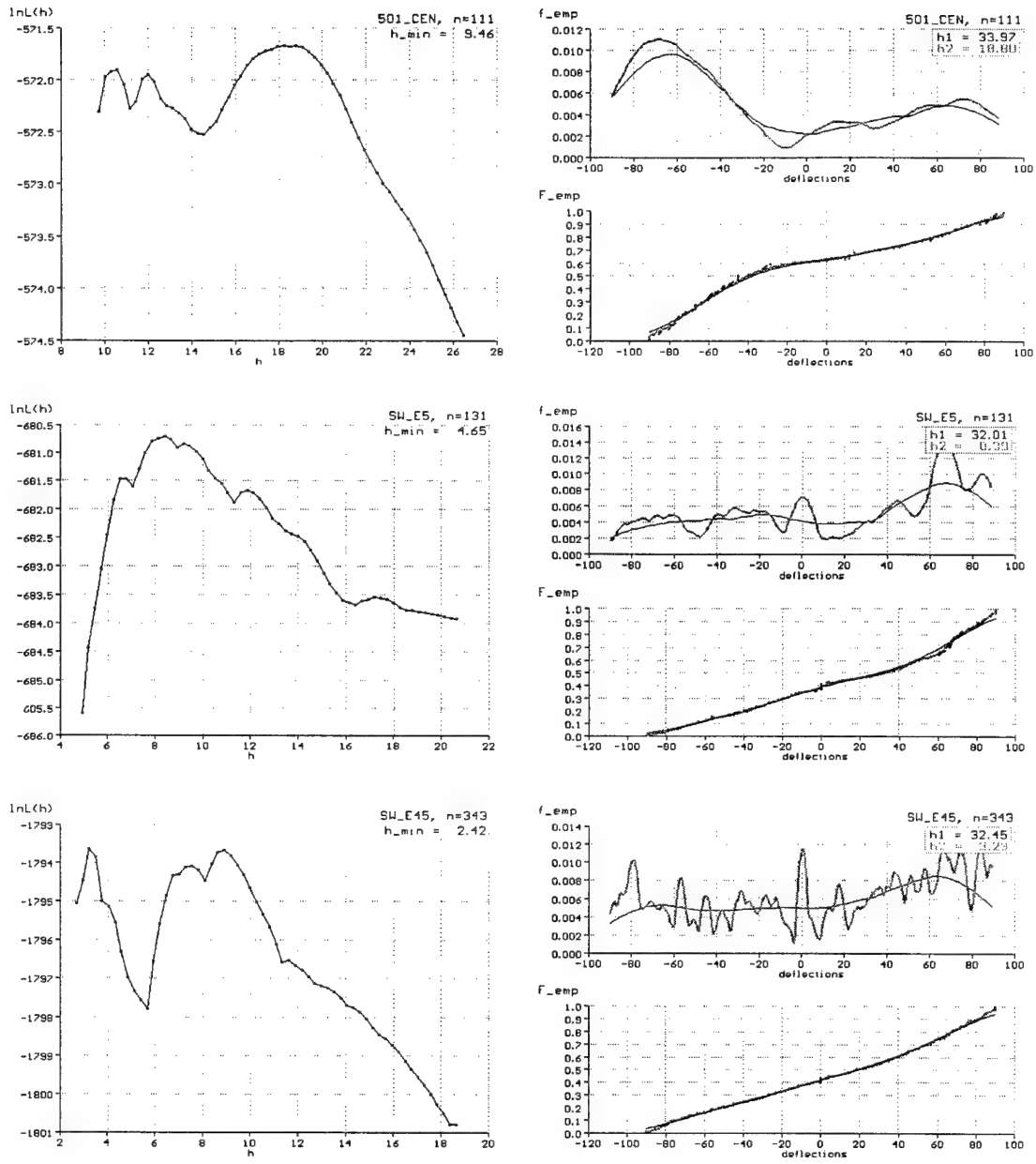

Fig. 7.6. The modified likelihood criterion method optimization of the smoothing parameter h for three real data sets of deflections. $lnl(h)$ is the logarithm of the empirical likelihood function (7.21), n denotes sample size, h_min is the lower boundary value for optimized h calculated by equation (7.23), $h1$ and $h2$ are the values of the h calculated by equation (7.18), and taken as the h-value for the largest maximum of $lnl(h)$, respectively. Symbols *f_emp* and *F_emp* denote the estimated probability density function and the cumulative distribution function, respectively. Scattered points in the *F_emp* plots are the sample data.

in Figs. 7.6 and 7.7, the *F_emp* plot) in the form of the classical empirical distribution function.

All optimized values for the defection p.d.f. smoothing parameter ($h2$ in Fig. 7.6) are smaller than the corresponding simplest method values $h1$ (for the sake of clarity, the values

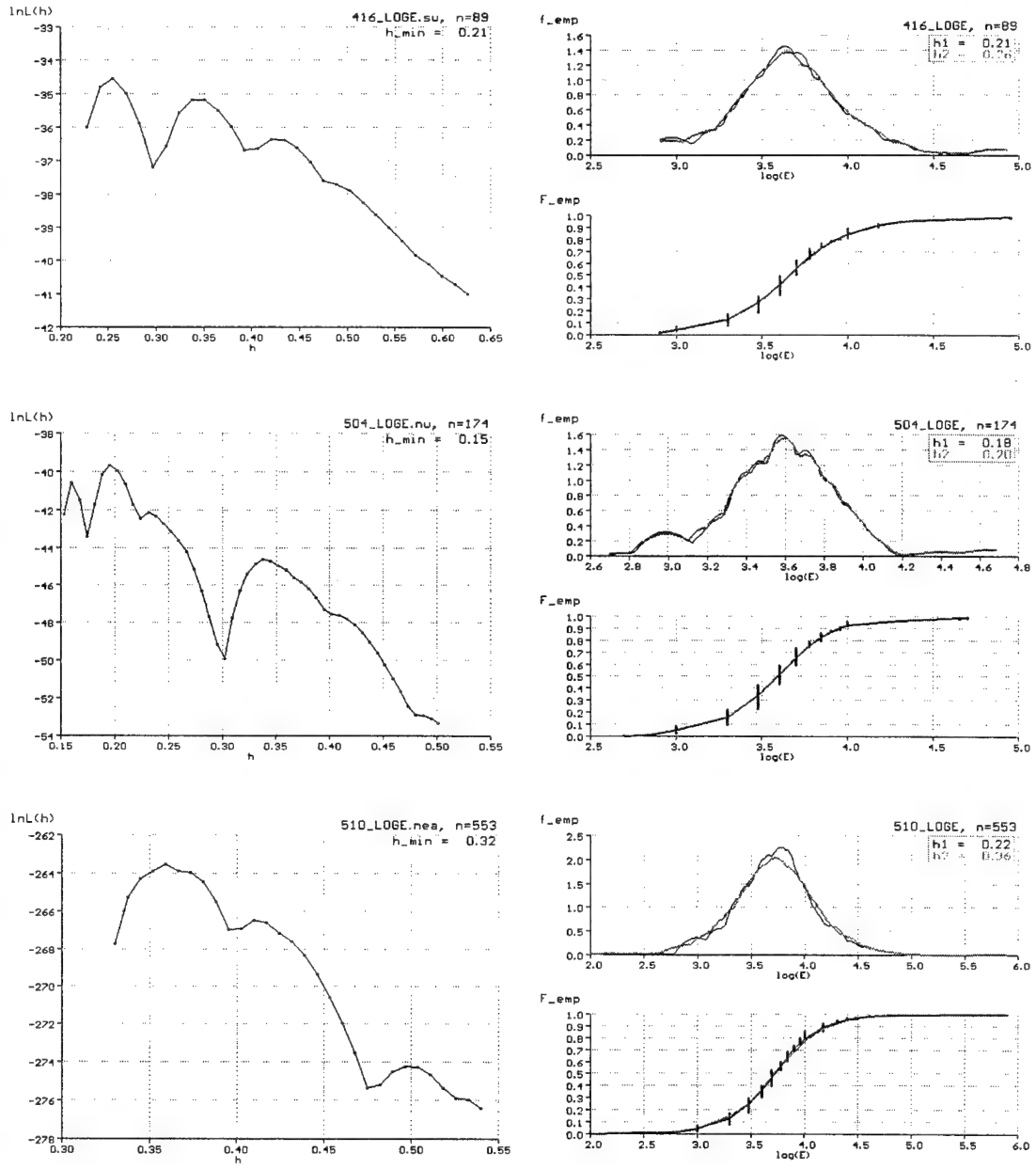

Fig. 7.7. The modified likelihood criterion method optimization of the smoothing parameter h for three real data sets of logarithms of energy. *lnl*(h) is the logarithm of empirical likelihood function (7.21), n denotes sample size, *h_min* is the lower boundary value for optimized h calculated by equation (7.23), $h1$ and $h2$ are the values of the h calculated by equation (7.18), and taken as the h-value for the largest maximum of *lnl*(h), respectively. Symbols *f_emp* and *F_emp* denote the estimated probability density function and the cumulative distribution function, respectively. Vertical heavy lines in *F_emp* plots are the sample data.

of *lnL*(h) for higher values of h are not shown in Figure), which implies that using $h2$ values will discover more multimodal structure of the estimated p.d.f., $\hat{f}(x)$, than it would happen if the $h1$ values were used. The consequences can be very different: from almost negligible, as for the 501_CEN data set, to those introducing great changes, as it is for the SW_E45 data

set. The intermediate case is shown for the SW_E5 data set.

For the first case (501_CEN), the $h2$ value is approximately a half of $h1$. Such a difference does not make substantial variations to the estimated p.d.f., although revealing some additional rather flat modes.

The optimized h, $h2$ (equal to 8.39), for the SW_E5 data set is smaller than that of 501_CEN and is about one fourth of $h1$ (32.01). The resulting p.d.f. has so many modes (many of them are very subtle) that it could be expected that some of them do not reflect the underlying population and are an effect of sample randomness. The same effect, in more developed version, can be seen for the SW_45 data set. It seems that the p.d.f. using $h2$ = 3.23 reveals much more noise than the amount of population information that is hidden by the p.d.f. using $h1$ = 32.45. All those relations between $h1$ and $h2$ do not seem to substantially affect the cdf's - all of them are little sensitive to the changes in the smoothing parameter values.

For energy logarithms, $log(E)$, Fig. 7.7, the general situation is different than that for deflections. The left boundary, h_min, of the range of optimized values of h is in all cases greater than $h1$, so the smoothness produced by the modified likelihood criterion method (7.22) is greater than if $h1$ is used. However, all $h2$ values are not very different from $h1$ values, and the resulting p.d.f.-s are very similar.

Conclusions

1. Properties of the nonparametric kernel estimation method of probability density function were investigated in order to recognize the possibility of its application to objective reproduction of deflection probability density functions based on empirical data. The nonparametric kernel estimation method, a novel and innovative approach in studies of structure of seismic catalogs, is designed for direct estimation of an unknown true probability function of a random variable X given only a random sample x_i, $i=1,2,\ldots,n$.

2. Monte Carlo experiments with variety of both unimodal and multimodal probability distributions, and investigations carried out on real (empirical) sets of deflections and logarithms of energy of seismic events from the Wujek mine, made it possible to select a method of estimation of the smoothing parameter the choice of which is crucial for the performance of the kernel method for actual data. The investigation results show that when application purposes of the nonparametric kernel estimation method are taken into consideration, the most suitable estimation method of that parameter is the method of

minimization of the integral square error. The selected estimation method of the smoothing parameter oversmoothes to some extent the resulting probability density function estimator. For that reason, in analysis of real data not only distinct modes of this estimator should be traced but also minor inflexions distorting the smooth course of the estimated p.d.f. should be considered. However, the chosen method of smoothing parameter estimation ensures that the nonparametric kernel estimation method is independent of the user and its oversmoothing protects against occurrence of artefacts on the resulting p.d.f.

3. Further on carried out experiments showed that for samples of sizes of 50 - 60 the nonparametric kernel estimation method well reproduces both the number of modes of true probability distributions and the locations of these modes. An interesting feature of the nonparametric kernel estimation method is the fact that sometimes an estimated p.d.f. enables better identification of distribution modality than the course (plot) of the true p.d.f.

4. When the true p.d.f. does not tend to zero at the variability interval limits of a random variable, the nonparametric kernel estimation method produces an edge effect. This makes estimated p.d.f.-s smaller than the true p.d.f.-s near the limits of the variability interval and may generate false modes near these limits. The effect does not affect the central part of the estimated p.d.f. Because we expect that the nonparametric kernel method for deflections will be endangered by the edge effect, in estimation of deflection distributions we will use the angle identity of deflection (6.1), estimate p.d.f.-s several times for cyclically transformed deflection values, and glue their central parts.

5. In future, the nonparametric kernel estimation method can be used for estimation of distributions of energy or logarithm of energy of the seismic events based on empirical data. However, because of the recently applied methods of evaluation of seismic energy, empirical energy distributions behave as discrete ones. Further studies are needed to distinguish the modes which are produced by the repeatability of some energy values as the consequence of energy evaluation methods from real modes which are the result of the multimodality of energy distribution.

8. Deflections. Identification of modes of distribution.

The nonparametric kernel estimation of probability density function of deflections was applied to all data sets given in Table 6.1 in Section 6.

It was shown in Section 7, that when the actual probability distribution does not tend to zero at limits of the variability range of the random variable the nonparametric kernel estimation of the p.d.f. introduces some boundary errors or edge effects. To eliminate them from the estimated p.d.f.-s we make use of the angle identity of deflection (6.1). For each data set the deflections were shifted four times, each time of 30° , so that the same data covered the ranges $(-90^\circ, 90^\circ)$, $(-60^\circ, 120^\circ)$, $(-30^\circ, 150^\circ)$ and $(0^\circ, 180^\circ)$ respectively. Next, the p.d.f. was evaluated for each of the four ranges. The final form of the p.d.f. was obtained by gluing central parts of these four estimates. Finally, the resultant p.d.f. was re-transformed to the $(-90^\circ, 90^\circ)$ range.

The shape of the unimodal distribution should be smooth. Every distortion of the p.d.f. like high order discontinuous inflexions, folds etc. usually represent summarised effects of two or more peaks. Our Monte-Carlo simulations and the real data studies of the p.d.f. kernel estimation method for multimodal distributions point out that the estimates particularly well reproduce locations of maxima and inflexions caused by the superposition of peaks. The smoothing parameter, which we accept, smoothes, however, the final p.d.f. form. Therefore, besides the distinct peaks of the estimates, the minor effects should also be traced and interpreted.

As mentioned, it is expected that plane structures (linear on the horizontal plane), like old workings edges, faults and other weak zones have a particular significance for the seismic event generation. Therefore, we tried to correlate the dominant and secondary trends identified in the distributions of deflections with the directions of such plane structures picked from the mine maps.

The results of the deflection analysis for the particular mine parts are given below.

The series recorded in C part, at the coal level 416

The estimated p.d.f.-s of deflection for the seismic events recorded in C part, at the level 416 (data sets 1, 2, 3) are shown in Figure 8.1. In all distributions the main mode has the maximum located at the same place, about 2°. This direction perfectly agrees with the direction of front advance of all active longwalls in this mine region (see: Appendices 1 and 2). The main mode of the deflection distribution for the series of events of energy from 10^4J, has the complex structure and the secondary peak at some -17° can be seen. This secondary mode can also be traced for the series with threshold $3.2x10^3$J. No mine structure can be correlated with the direction of -17°. The small peak is visible in the distribution for strong event series (threshold 10^4J), at some -72°. This direction can be correlated with the strike direction of Klodnicki fault or with the direction of the edge of gob in slab 2 of the coal layer 416. Minor distortions, however present in all distributions, are identified at some -30° or -35° and at some 47°. While the first direction cannot be correlated with any mine structure, the second one agrees with the direction of the small fault, of some 2 m throw, located leftside the seismically active area.

The series recorded in SW part, at the coal level 416

This is the first case of "strange", that is not justified by active excavations, seismicity. Similar seismic cluster of unknown origin was observed in this part, at the level 507. It was speculated that these clusters could be side results of the tremor generation processes, that took place in this part, at the level 501. The estimated p.d.f. of deflections for the seismic cluster from the level 416 is given in Figure 8.2. Two distinct modes of the distribution are located at some -86° and -47°. The first one and also little jumps at some -68° and -62° correlate with the strike directions of Klodnicki fault, which enclose the region from the south and bends in this area (see: Appendices 1, 2). The other one (-47°) cannot be correlated with any mine structure. This mode is, however, also present in distributions of deflections for seismic series recorded in the same part of the mine, at the levels 501 and 507. The location of the small but distinct distortion, at about 26°, agrees roughly with the average of strke directions of Arkona (13m throw) and the other secondary (4 meter throw) faults. These faults unite in this region, and the seismically active area was located at this corner. Finally the distortion around -29° cannot be linked to any mine structure.

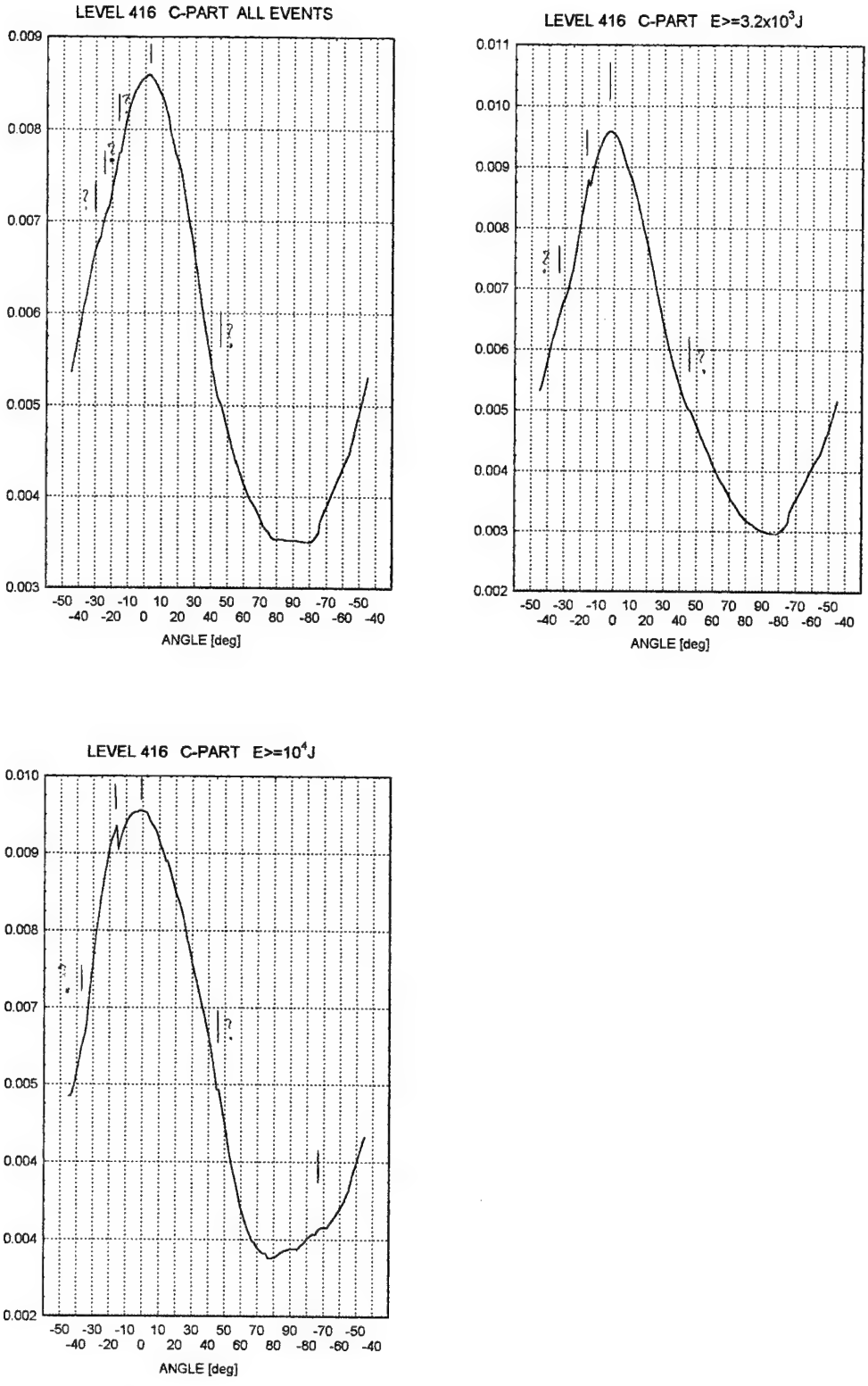

Figure 8.1 Probability distribution functions of deflection of events recorded in C region, at the level 416

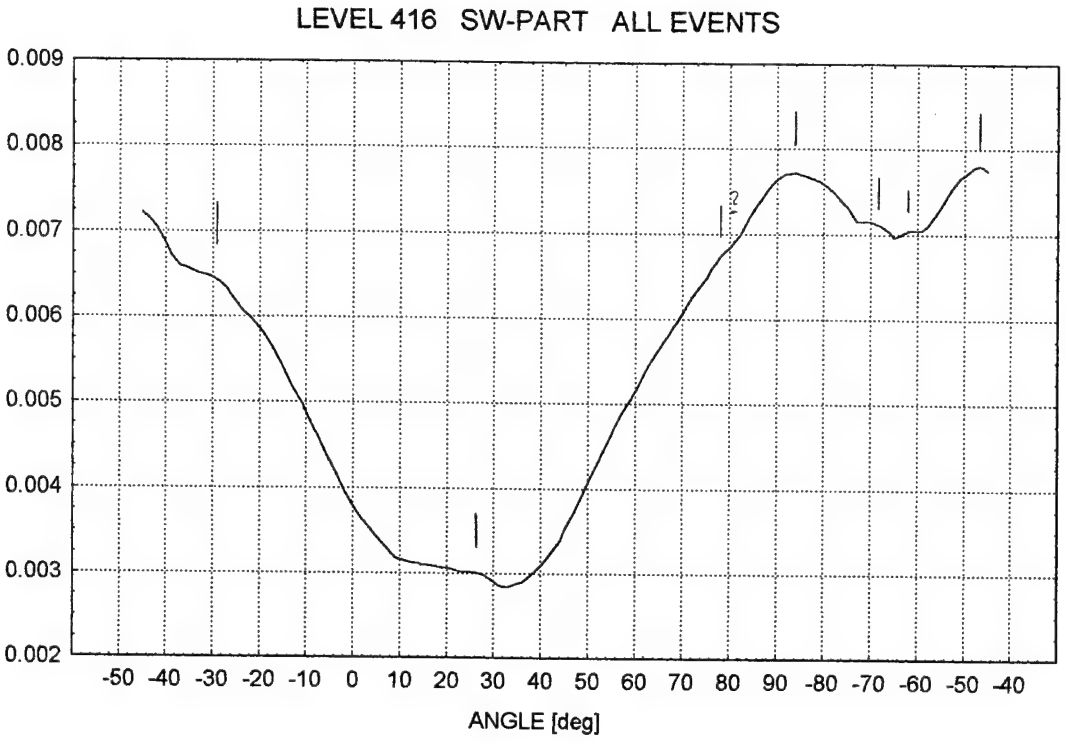

Figure 8.2 Probability distribution function of deflection of events recorded in SW region, at the level 416

The series recorded in SW part, at the coal level 501

The estimated p.d.f.-s of deflections for the seismic series recorded in SW part, at the level 501 (data sets 5, 6, 7, 8) are shown in Figure 8.3. The identified modes and their possible correlations with mine structures are as follows:

i) 52°. The maximum of the main peak for set 5, splits for set 6, is hardly visible for set 7 and practically disappears for set 8. No structure matches this direction. It is likely that this maximum value of the main mode of distribution for all recorded events is incidentally caused by summing up poorly separated mode components;

ii) some 67° to 77°. The distortion in the distribution for set 5, can be clearly identified as a component of the main mode for set 6 and becomes the main peak maximum for sets 7 and 8. The direction perfectly agrees with the strike direction of Arkona fault of some 20m throw and with the front advance directions of the majority of active longwalls in this area (see: Appendices 3, 4, 5). The increasing significance of this direction for the seismic series from which small events were removed evidences the particular role played by faults in generating strong tremors;

iii) -22°. The second distinct mode for set 8. It is also visible in the distribution for set 7 but its presence in the distribution for sets 6 and 5 can only be guessed. This is the strike direction of all longwalls worked in the area. The open question remains why this direction is important only for the strong event series;

iv) some -5° or -8°. Appear as distortions in sets 5 and 6 curves and as a distinct maximum in set 7 curve. It is not present in the distribution for set 8. No simple geometrical explanation can be given for this mode;

v) some 22° to 27°. The distortions of the p.d.f. estimates at these angles are observed for all samples. The direction agrees with the strike direction of the second fault (4.5m throw) in the area;

vi) some minor effects appear here and there at -70° or -80° and at -40° or -45°.

One can note that the dominant direction of the series rotated of as much as 20° after small events were removed from the sample. Besides changing location of maximum, the main peak of the p.d.f.-s of deflections became narrower while increasing the energy threshold.

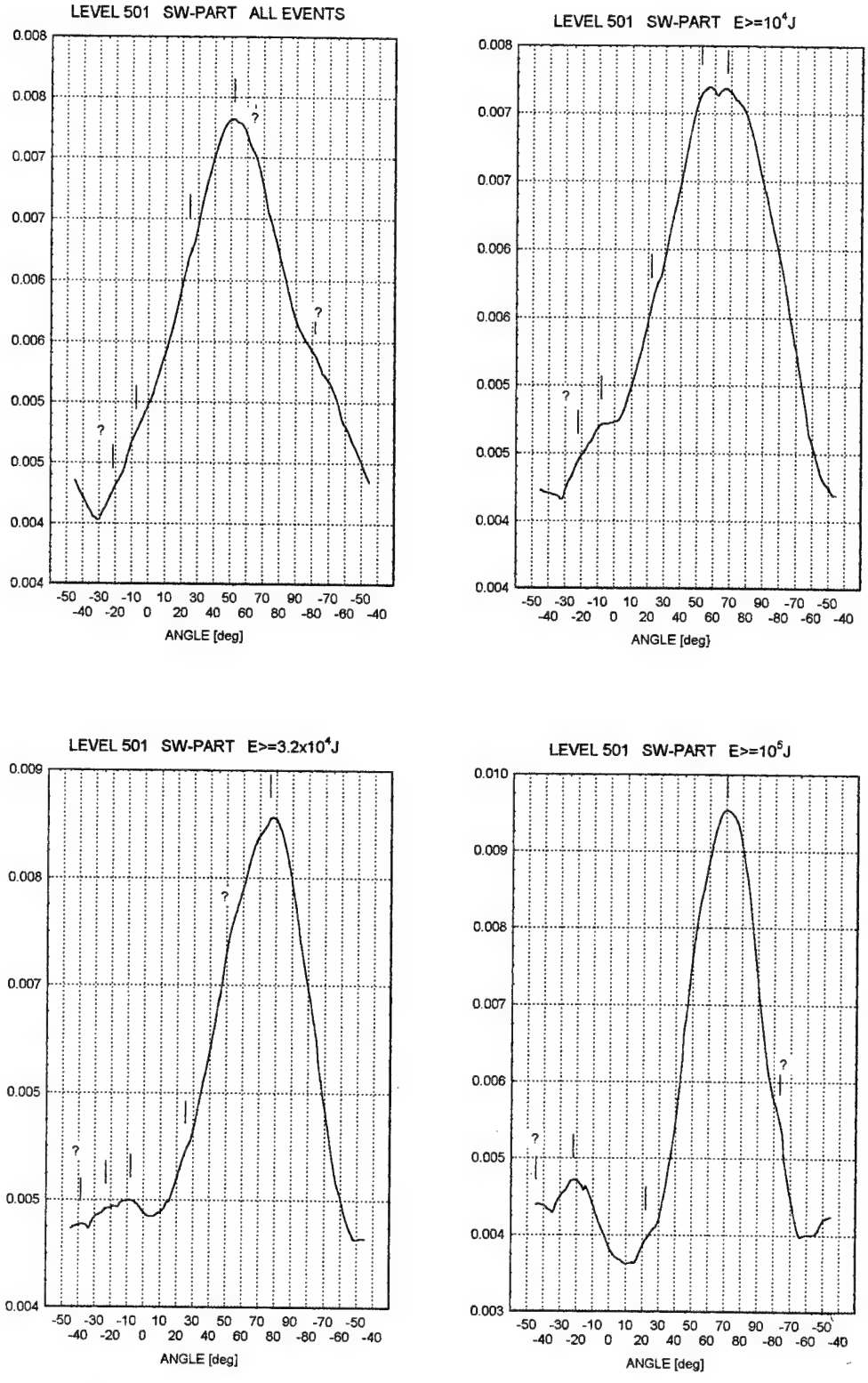

Figure 8.3 Probability distribution functions of deflection of events recorded in SW region, at the level 501

Moreover, the large tremor series have also the distinct secondary trend which is not visible in the distribution for the series comprising all recorded events.

The series recorded in the southern part of C region, at the coal level 501

The estimated p.d.f.-s of deflections for to the data sets 9, 10, 11, 12 are shown respectively in Figure 8.4. One may see the main mode of the distribution for the series of all recorded events (set 9) located in the range from 80° to -60°. the mode narrows and shifts its maximum from -82° to $+81^{\circ}$ after the threshold of 10^4J is applied and uncovers a complex subtle structure in the range from -75° to -50°. These two new components again unite after increasing the threshold of the next half of order (set 11). Finally, for the series comprising the strongest events (set 12) the main mode of the distribution of deflections is narrow and regular, with maximum at 90° . 90° is the strike direction of all active longwalls in C part, at this coal level (see: Appendices 3, 4, 5).

Other distortions of the set 9 curve are visible at some 15° and from 0° to -20° . The are not displayed in the p.d.f. for set 10 except a slight trace at some 15° but they reappear in the distribution for set 11. Finally the distinct and complex secondary mode is formed in the range from -20° to 20° for the series of strong events (set 12). This mode can be correlated with the front movement directions of all longwalls and the direction of old gob edges, in the area.

The series recorded in the northern part of C region, at the coal level 501

Set 13 is the other "strange" case among induced seismicity clusters from Wujek mine. As mentioned previously, no miming works were carried on in this part of the mine during the period under study. The estimated p.d.f. of deflections for this series of seismic events is shown in Figure 8.5. The main mode is wide with maximum at some -70° . This mode could be eventually correlated with the closest edge of old gobs in slab 3 of this coal layer (see: Appendix 3). Minor distortions of the p.d.f. curve are seen at some -55°, $+46^{\circ}$ and $+15^{\circ}$ respectively. No mine structures can be related to these directions.

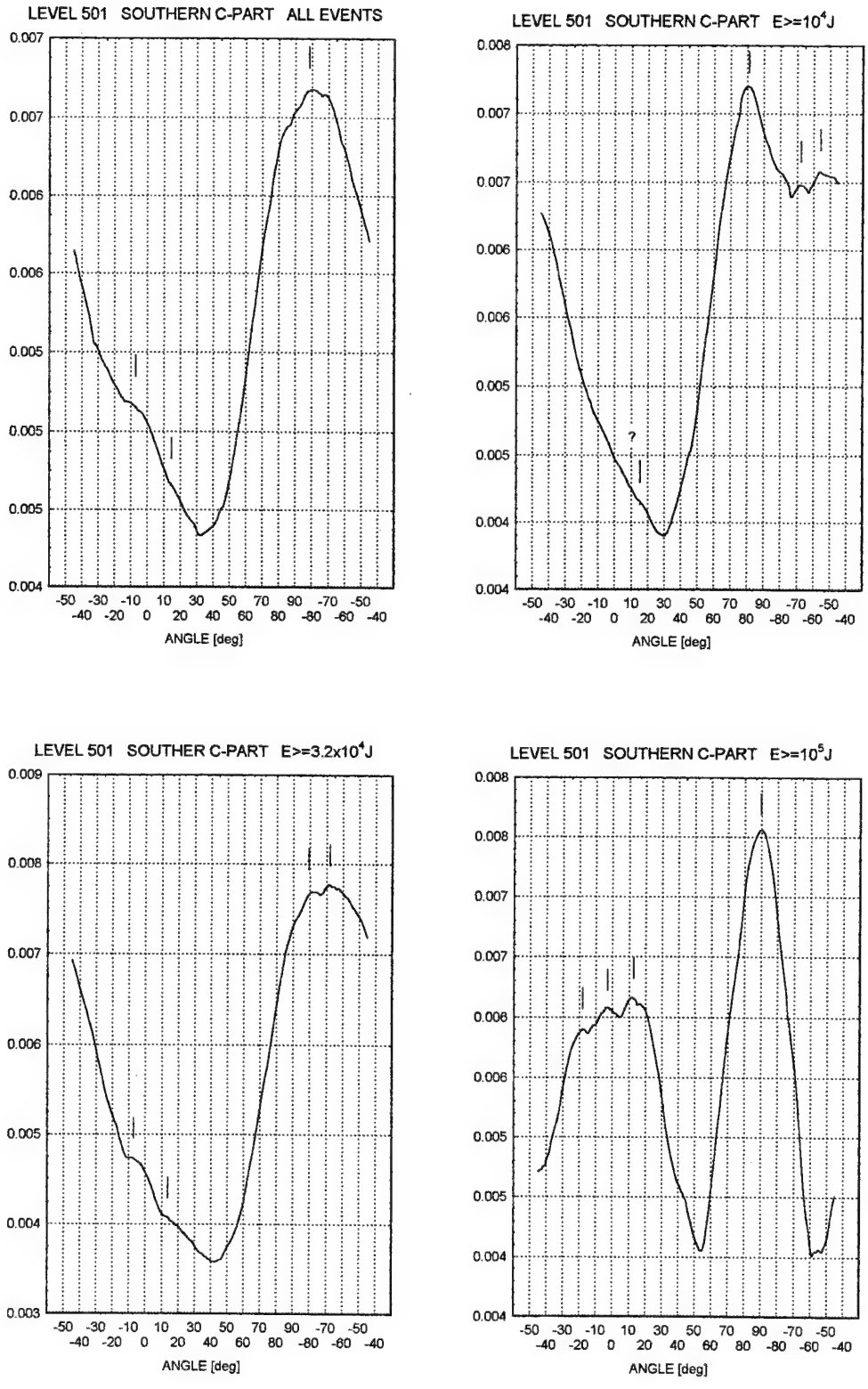

Figure 8.4 Probability distribution functions of deflection of events recorded in the southern part of C region, at the level 501

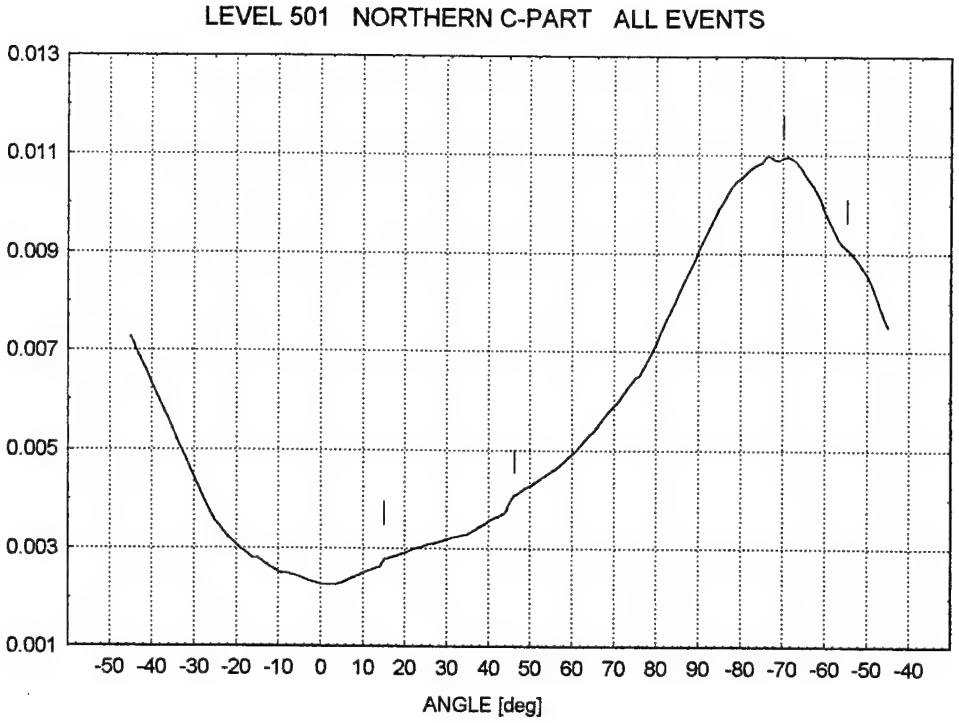

Figure 8.5 Probability distribution function of deflection of events recorded in the northern part of C region, at the level 501

The series recorded in C part, at the coal level 504

The estimated p.d.f.-s of deflections for the seismic series recorded in C part, at the level 504 (data sets 14, 15, 16) are shown in Figure 8.6. Besides the main mode with maximum at about 1°or -5°, present in all curves, one can observe development of the second, wide mode at some 55°or 60° with the increase the energy threshold value applied to the data. For the set comprising the strongest event this second mode is nearly as big as the main one. The main mode direction matches the direction of advance of all active longwalls in this part of the mine (see: Appendix 6). The second mode direction agrees with the strike direction of the fault of some 2 m throw which crosses the area of excavations. The figure gives the clear evidence of fault influence on generating of strong events.

There are other distortions of the deflection p.d.f.-s at some -18° or -20° , 35° or 40° and the most distinct one between -65° and -75°. The last direction corresponds to the strike direction of the Klodnicki fault, that encloses the area from the south. For the other directions no clear link to mine structures can be found.

The series recorded in NW part, at the coal level 507

The estimated p.d.f.-s of deflection for the data sets 17, 18, 19 are shown in Figure 8.7. The main mode, with maximum located at some -80°, becomes wider and displayes a complex multicomponent structure after the prescribed energy thresholds are applied to the data. One can see the second peak in the distribution of deflections for the strongest event series at 75°. The -80° direction is the direction advance of the active longwalls in this area (see: Appendix 7). The 75° direction matches the strike direction of the nearby Arkona fault (15-25 m throw in this area). Again the influence of the fault becomes visible when only strong events are taken into account. The slight jump, located at 4° by the global minimum of distribution for the strong event series, correlates with the strike direction of the small fault wing (1.8 meter throw) that crosses the area of excavation. The distortion noticed in the same curve at some 53° cannot be linked to mine structures.

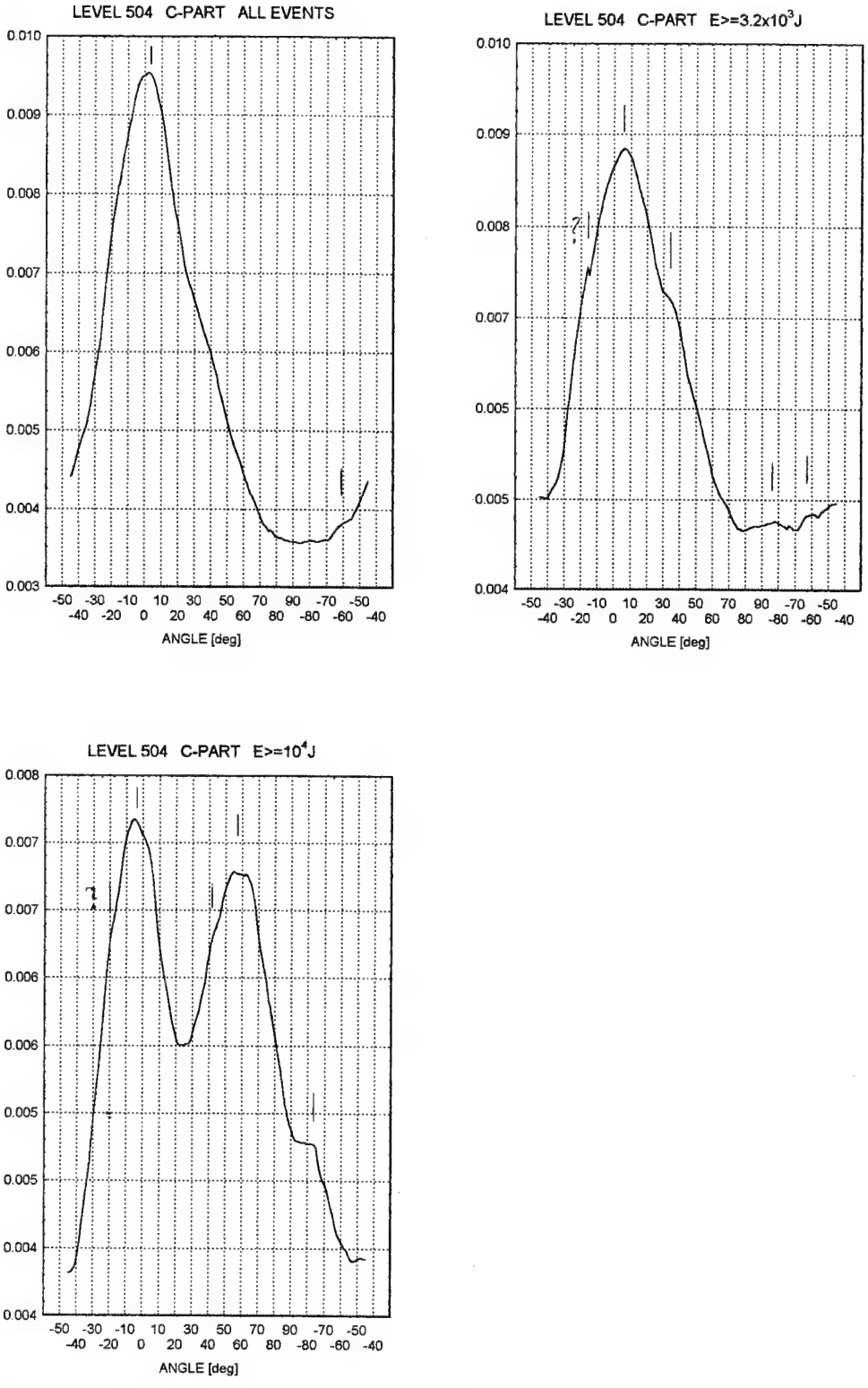

Figure 8.6 Probability distribution functions of deflection for events recorded in C region, at the level 504

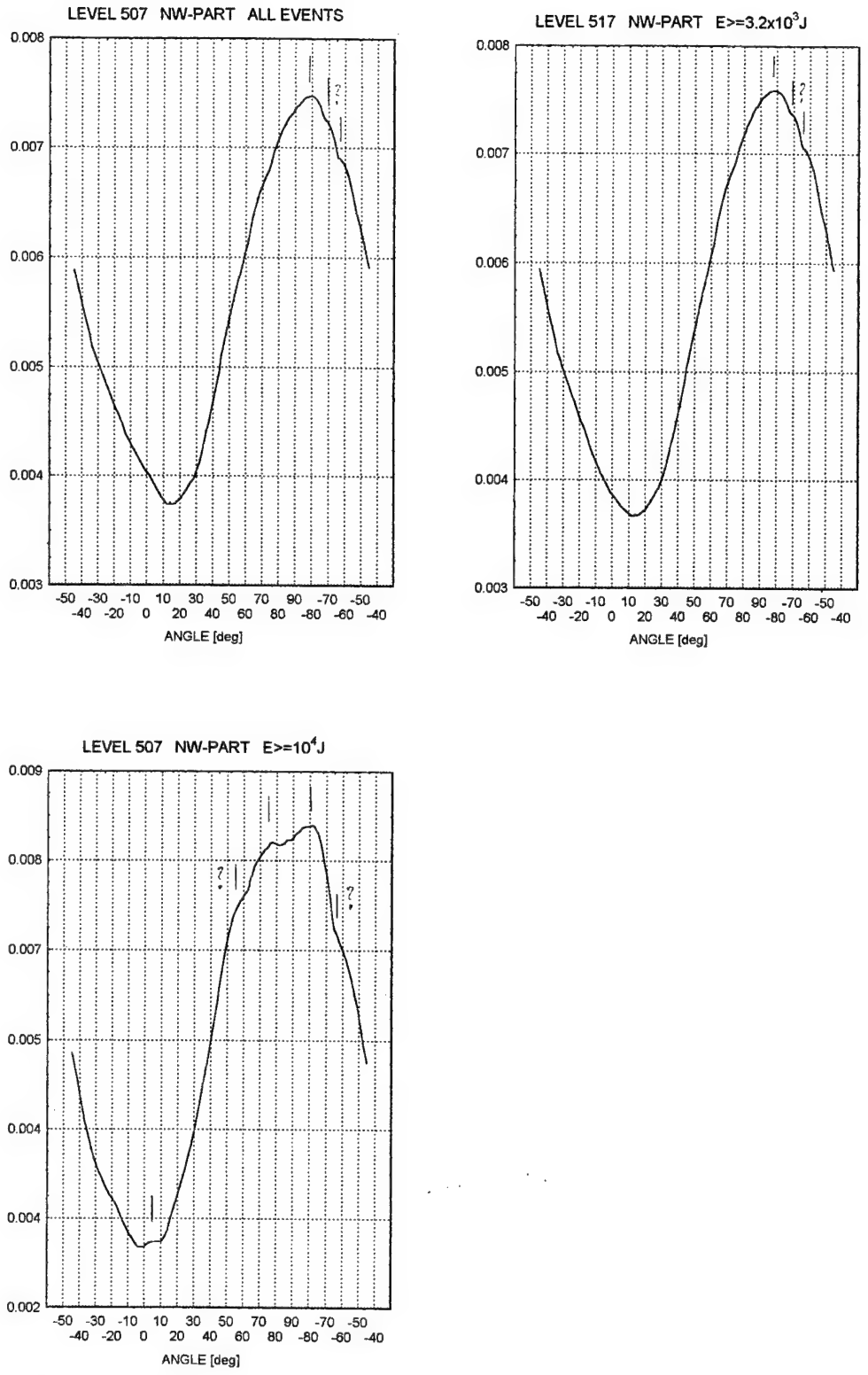

Figure 8.7 Probability distribution functions of deflection for events recorded in NW region, at the level 507

The series recorded in SW part, at the coal level 507

Here we have the next example of the seismic cluster that occurred in the area where no mining works were carried on. As mentioned, the similar effect was observed in the same part of the mine, at the level 416. The estimated p.d.f. of deflections for this cluster (set 20) is presented in Figure 8.8. The main mode of the distribution has comlex shape and is located between -48° and -38° . There is no structural explanation for this direction. However, the same direction modes have been also found for events recorded in the same region, at the level 416 (the main mode) and at the level 501 (the minor effect). The other identified distortions are:

i) The flat well separated peak at some 14°. The direction agrees with the strike direction of the small fault (3-4m throw) located rightside of the area (see: Appendix 7);

ii) Some 74°. This direction matches the strike direction of Arkona fault, located leftside of the area. It also agrees with the dominant trend of the seismic series recorded in this area, at the level 501;

iii) possibly about -73°. No mine structure can be correlated with this eventual mode.

The series recorded in NW part, at the coal level 510

The estimated p.d.f.-s of deflections for the seismic series recorded in NW part, at the level 510 (data sets 21, 22, 23) are presented in Figure 8.9. The case turns down eventual suspitions that the rising complexity of the distributions of deflections with the increase of the value of energy threshold value could be caused by the decrease of sample sizes. Unlike in the majority of cases, here the shape of the estimated p.d.f. of the seismic series composed of strong events (set 23) is less complex than that for the series comprising all recorded events (set 21). The main mode of the distribution for the series of all events has the maximum located somewhere between -85° and -65°. For the strong event series the maximum of the main mode of distribution is identified at some -75° or -68°. This direction agrees with the direction of front advance of the active longwalls (see: Appendices 8, 9). Neither the peak at about -25° nor the peak at some 5°, that are identified for the all event series distribution and that gradually disapear after the prescribed thresholds are applied, can be linked to the mine structures. Two other distortions appear in the distribution for the series of events $\geq 10^4$J, at some 52° and possibly at about 20°. The first one cannot be correlated with any mine structure, but it also appeared, as

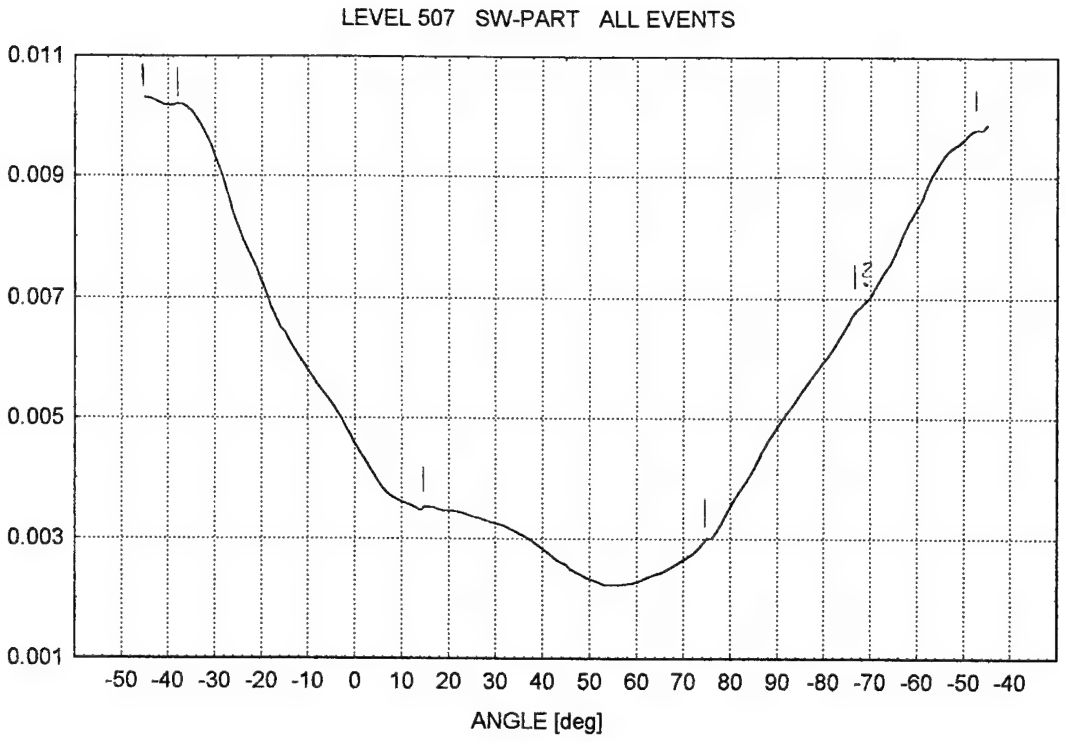

Figure 8.8 Probability distribution function of deflection for events recorded in SW region, at the level 507

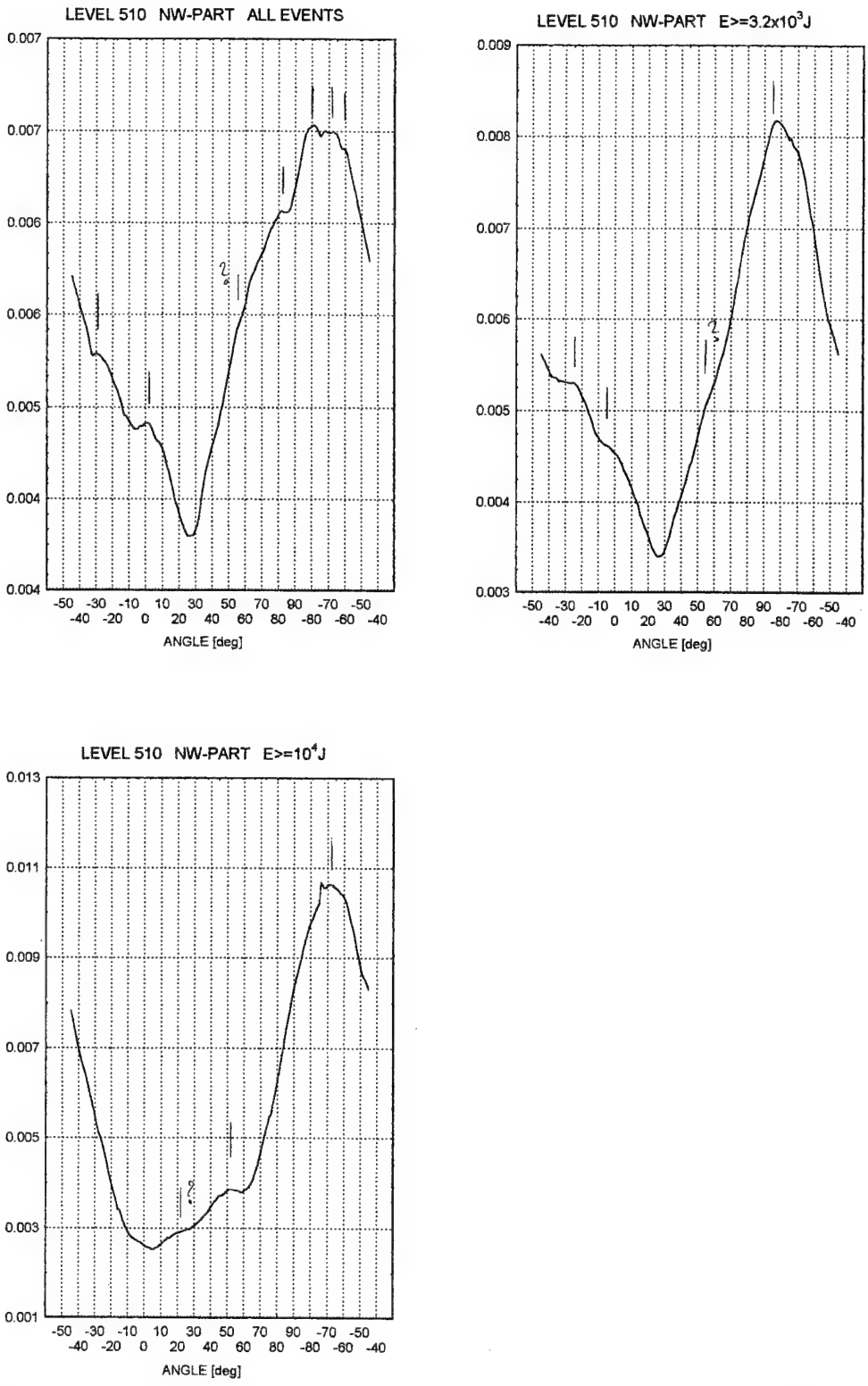

Figure 8.9 Probability distribution functions of deflection for events recorded in NW region, at the level 510

the slight distortion, for strong event sequence recorded in the same part of the mine, at the level 507. The second one could be eventually related to the small fault adjoining the area of excavation from the right hand side.

The series recorded in the western part of NE region, at the coal level 510

The last case of "strange" cluster of seismicity. In this case the number of events and the energy distribution of events allow also to study the series from which small events were removed. The estimated p.d.f.-s of deflections for these series (data sets 24, 25, 26) are shown in Figure 8.10. The shapes of the p.d.f.-s, particularily the locations of the global minimum significantly differ between the distributions for the all event series and for the strong event series. The main mode maximum follows, more or less, the same direction about -80°or -85° for all curves. This direction can be correlated with the direction of the closest gob edge located south from the seismically active area (see: Appendices 8, 9). The other peaks, identified at -27° , -47° and -85° in the distributions for sets 24 and 25; at -9° in the distribution for set 24, and at 25°, 61° and 85° in the distribution for set 26 cannot be correlated with mine structures.

The series recorded in SE part, at the coal level 510

The last considered case deals with the seismic cluster located in SE part of the level 510. This is the only analysed cluster that occurred in SE part of the mine. The estimated p.d.f.-s of deflections are shown in Figure 8.11. The main mode is located similarily in all distributions. Its maximum, at some 45° to 50°, perfectly agrees with the advance direction of the longwalls IA, IIA and of the longwall IIIA in its first part, in slab 2, with the old works edge in slab 1 and with the strike direction of Wojciech fault (see: Appendices 8, 9). The longwall IIIA was bend in its second part. One can see in Figure 8.11 a slow development of the secondary mode at some -5°, 5° after the thersholds are applied to the data. This secondary mode direction matches the advance direction of the second part of longwall IIIA and the advance directions of all langwalls in slab 1 of the level. The small distortions appearing here and there in the distributions in the range between -35°and -55° could be roughly correlated with the strike direction of the lonwalls in slab 2. The small distinct peak at - 73° in the estimated p.d.f. of

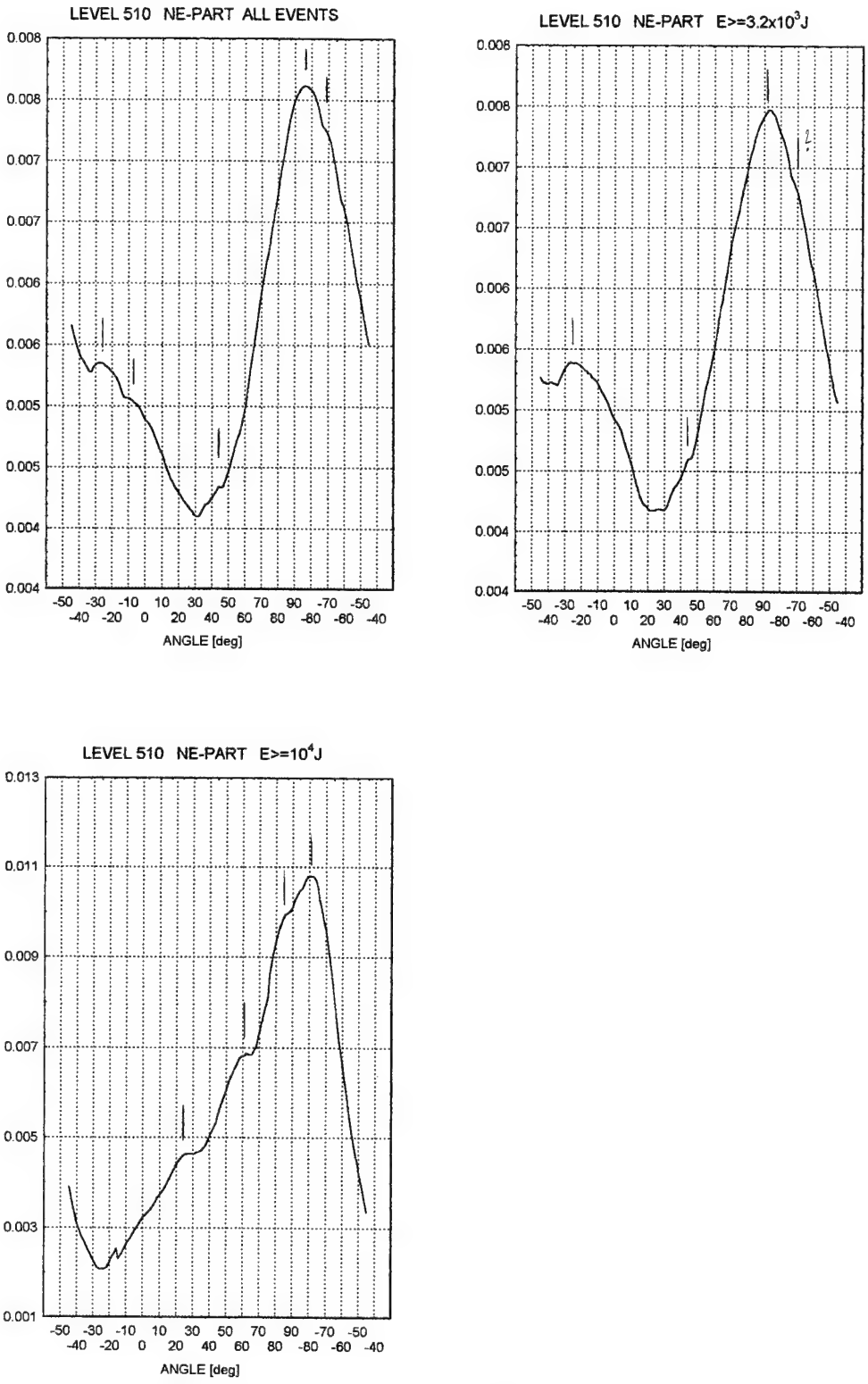

Figure 8.10 Probability distribution functions of deflection for events recorded in the western part of NE region, at the level 510

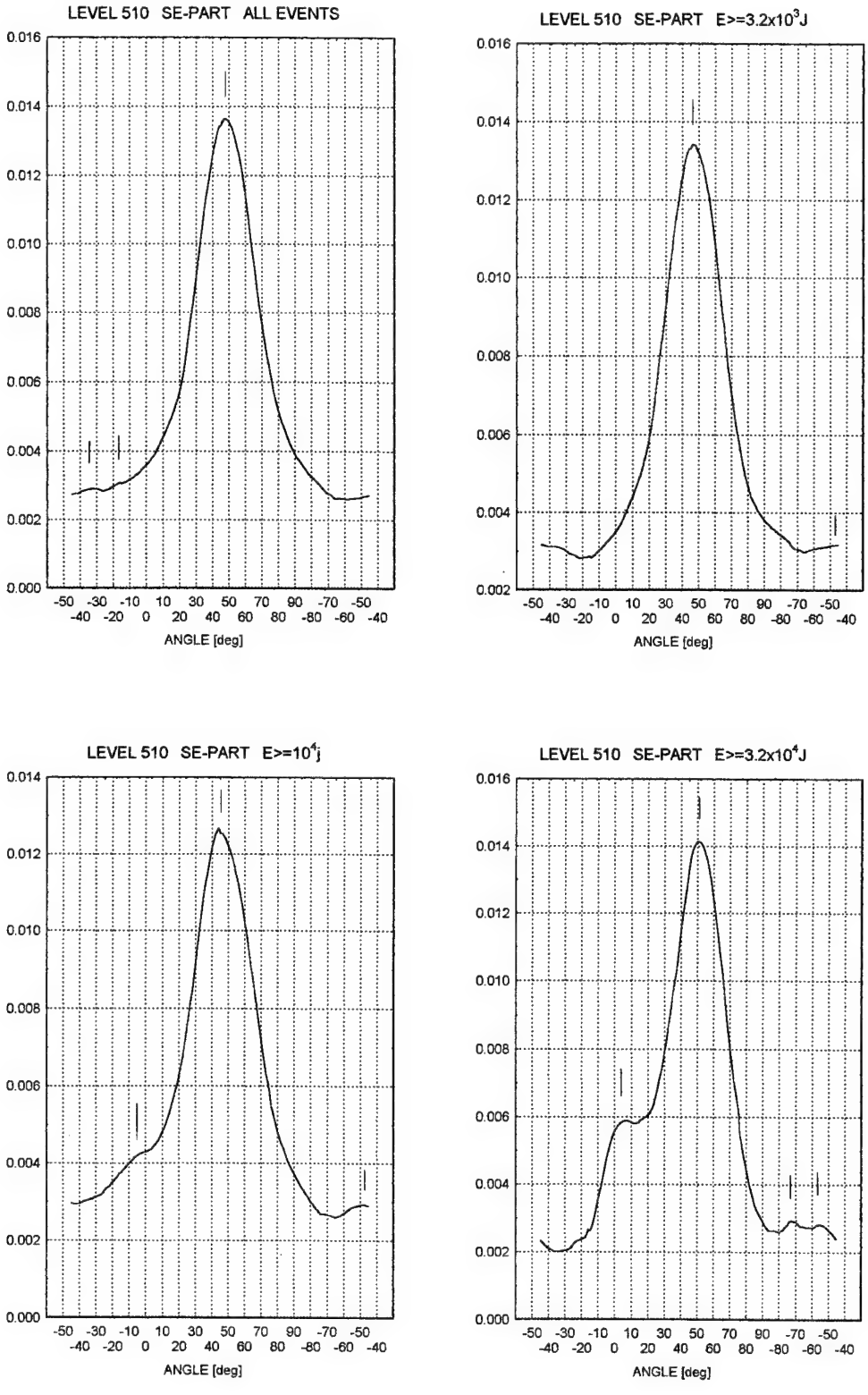

Figure 8.11 Probability distribution functions of deflection for events recorded in SE region, at the level 510

deflections of events $\geq 3.2 \times 10^4$J agrees in direction with the direction of the Klodnicki fault strike in this area.

Discussion

Within the variety of considered cases it is not easy to find common rules governing the processes of the seismic events generation at the identified dominant directions. Seismic series from each part of the mine have their own dominant directions and the own ways in which the dominant directions change when different thresholds are applied to the data. Certainly at least one distinct mode of the distributions of deflections appeares in all cases. The main mode usually becomes narrower with the increase of the value of threshold. The maximum of the main mode is usually located at, more or less, the same place for all seismic series associated with the same area of the mine, regardless the threshold applied. There are, however, two cases where the locations of the global maximum of deflection distributions differ strongly between the distributions for all events and for strong events. Both cases were noted for the seismic clusters associated with the level 501, the most seismically active and the most complex level from the mining point of view.

The number of visible modes in the distributions of deflections for the series of strong events is, in general, greater than that in the distributions for all event series. One could suspect that the new modes found in the distributions for the strong event series are artefacts, caused by the drop of the sample sizes after applying the thresholds. There are, however, cases for which the proportion of the numbers of modes for the all event series and for the strong event ones is reversed (e.g., the seismic series from NW part, at the level 510). Thus we think that this general feature is indirectly resulted by the decreasing complexity of the series with the rise of the threshold. In the series comprising all events recorded in the area small events outnumber large ones. The dominant trends of the small event deflections change in time because of variations of the mining process. Thus in such series from long time periods these varying trends construct a sort of random noise which is added to the constant components of the distribution of deflections. The structure of the distribution is usually so dominated by this random noise that the secondary modes are hidden. The tendecy to narrow the main peak after small events are removed from the sample and the presence, in some cases, of uninterpretable directions for the

series of all events, which rotate, split and match characteristic directions of mine geometry after the threshold is applied, support this reasoning.

In all but one considered cases of seismic activity occurring in the areas of active excavations the locations of the main modes of distributions of deflections agree with the advance directions of longwalls. The agreement is usually better for the distributions for the strong event series than for those for the all event sets. There is one case for which the longwall faces in two slabs of the same area were advancing in different directions (SE part at the coal level 510). In this case the distribution of deflection for the strong event series displayes two dominant trends that respectively match the advance directions.

For the seismically active areas of mining works at the level 501 the distributions of deflections display dominant trends corresponding with the strike directions of the longwalls. The feature is not found for the seismic series from other levels.

The distinct secondary directions of the seismic series recorded in the areas of mining works usually correspond with the strike directions of the faults located close to the areas. This correspondence is better for the strong event series than for the small event ones evidencing the importance of faults in the strong event generation processes. Sometimes the secondary mode directions correlate with the positions of edges of old works. There are, however, modes of the distributions of deflections, which cannot be linked neither with any tectonic nor with any mine structures.

For the seismic clusters that appeared apart from the mine work areas the dominant directions, found in the distributions of deflections, usually correlate with the strike directions of the faults, if the faults are present in the area, and sometimes with the directions of closest edges of old works. Again, however, one can see modes of the distributions, which cannot be explained by the locations of mine structures. Such the interesting cases concern the seismic clusters associated with SW parts of the levels 416 and 507. For both cases, the main modes are located at the same angles. Moreover, the same angle is assigned by the secondary mode of distribution of deflections for the series recorded in this area at the level 501, however, no mine structure justify importance of this angle.

Conclusions

1. Directional structure of the seismic series is assessed by tracing the dominant and secondary directions in the probability density functions of deflections, estimated by the nonparametric kernel estimation method.

2. The results of the analysis of variuos seismic clusters from Wujek coal mine show that the epicentre distribution of seismic events there is not random. The dominant directions of the distribution are significantly different for the studied sets of events that have occurred in different areas of the mine.

3. Furthermore, the dominant trends in the same set of events become different when various energy thresholds are considered. Several secondary trends are also observed in the distributions. This confirms that the generation of events is controlled by various generating processes and that mining-induced seismicity is a multimodal phenomenon.

4. It is possible, by careful inspection of the distributions of deflections, to identify generating processes of seismicity responsible for particular modes of the distribution.

5. In some cases, after complementing the results of the analysis of deflections with information from other sources, for instance from mine maps, it is also possible to conclude about factors that controll these processes.

6. The dominant trends of the seismic series from Wujek coal mine usually correlate with the directions of front advance of working faces.

7. Some of the secondary trends can be associated with known geological, tectonic and mining features, whereas the others are not directly connected with the known mine structures.

8. The study evidences, in particular, that faults have a significant role for the strong seismic event generation. Their presence in or in vicinity of the seismically active areas changes the distributions of deflections.

9. The analysis of deflection forms a basis for separating, from the seismic series, events generated by indovidual processes. These will be the events connected with particular modes of the distribution of deflections.

10. The dominant trends considered here are based on bilateral movements of seismic events. Their possible migration (for which unilateral movements must be considered), a well-studied phenomen from natural earthquakes (e.g. Gedney et al. 1980, Meyer et al. 1985, King

and Ma 1988, Yoshida 1988, Rydelek et al. 1990, Loo et al. 1992), is another highly interesting subject awaiting future studies. Correlations of the dominant trends with source mechanism and source parameters are also needed for better understanding of the multimodal character of seismic events induced by mining.

9. Separating of events generated by the single process

The analysis of deflections presented in Sections 6, 7, 8 can be used to separate, from the seismic series, events generated by the processes related to particular modes of the distribution of deflections. Here one example of such the separation is presented.

The seismic series recorded in C part, at the level 504 was considered. The analysis of deflection of the series showed apparent development of the second dominant trend in the distribution of deflections after increasing energy threshold was applied to the data (see: Figure 8.6). This trend was linked to the small fault that crossed the seismically active area. The other dominant trend matched the direction of front advance of all mine longwalls that were worked in the studied area.

The separation procedure starts form assigning the interval of deflections which contributed to the trend of interest. In this case, on the basis of the estimated p.d.f. of deflections for the series of events of energy $\geq 10^4$J, the interval [45°, 75°] was accepted. A value of deflection is evaluated from locations of epicenters of two consecutive events. Linking it with one of these events is artificial and can only be used to study serial properties of deflections. In the separation of events presented here we mark both events of each pair in the studied series of events, which have deflection values in the specified interval. According to our reasoning given in previous section the marked events are likely to be outcomes of the same identified generating process. It was interesting, however not unexpectable, that the marked events form, in some cases sequences of more than two events.

The spatial distribution of all seismic events recorded in the studied area of the mine is presented in Figure 9.1. Positions of the separated events are shown by crosses. The strike of the fault, which could be the reason of the considered dominant trend of the series, is approximately sketched with the broken line. The full line shows boundaries of the excavations worked during the period selected for our study. The longwalls were moving towards the north. The separated events locate on lines more or less parallel to the strike of the fault. It is interesting that they are not placed at the fault but are distanced, in average, more than 100m in the northernmost part of the area. Similar behavior of distributions of sources were noticed for other series of events

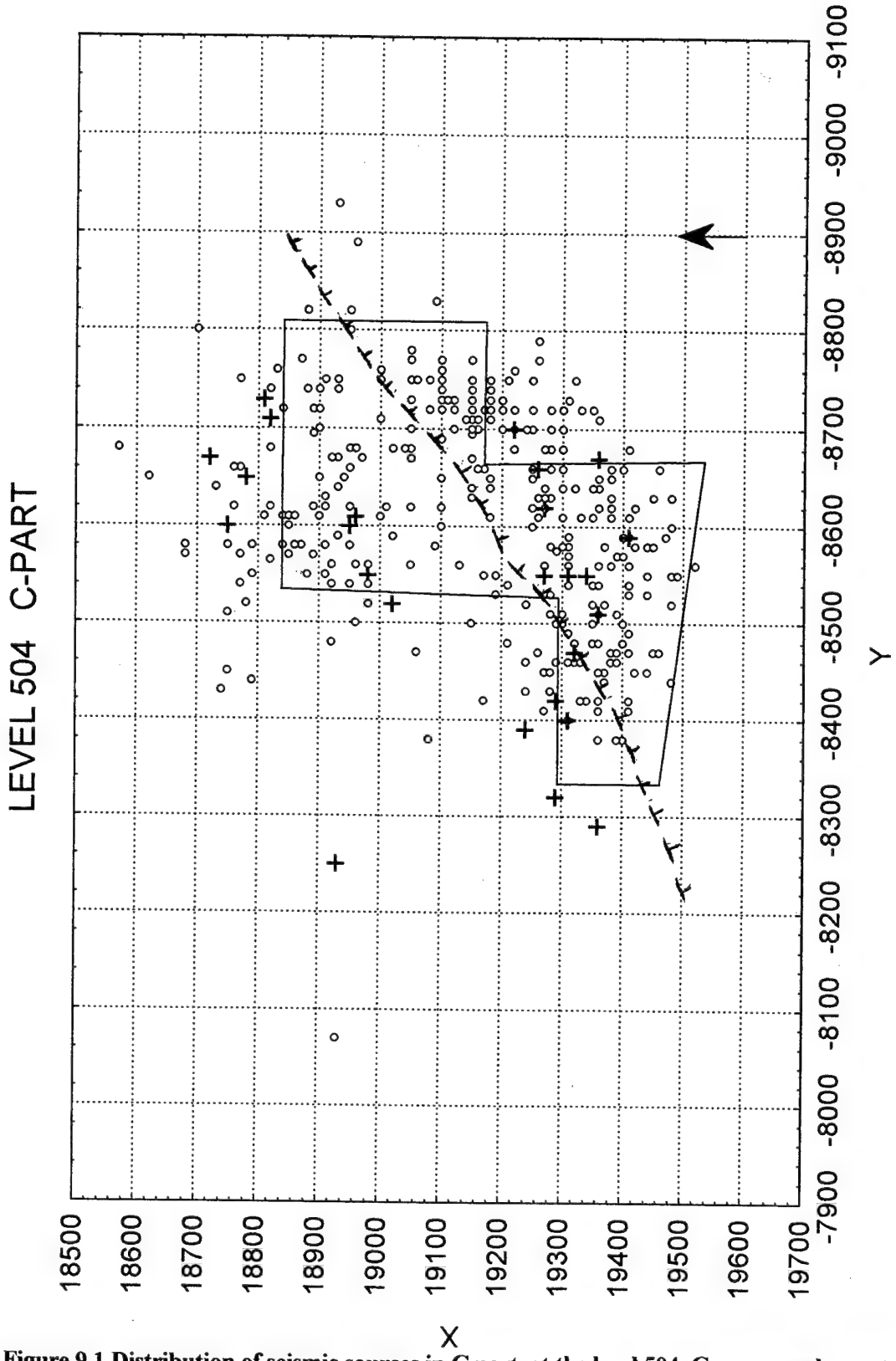

Figure 9.1 Distribution of seismic sources in C part, at the level 504. Crosses mark events separated by the analysis of deflections. Boundaries of active excavations are sketched with full line and the arrow marks the direction of front movements. Broken line marks approximately the strike of the fault.

determined as related to faults. In some cases they were located on more than one lines parallel to the strikes of the faults on the same fault wings.

10. Conclusions

1. Selected statistical methods are proposed to investigate complexity of the series of seismic events with the aim to identify different event generating processes. The pseudo-multivariate approach, that is the repeated analysis of one parameter distributions for the subsets of the seismic catalog, extracted according to conditions put on the other parameters of events, is used.

2. The seismic catalog from Wujek coal mine, Upper Silesian Coal Basin, Poland satisfied initial requirements concerning size, quality, variability and completeness of the database. Altogether 14297 seismic events were analyzed. Inspection of the catalog evidences completeness of the database and allows to recognize qualitatively its features, important for its future division into more homogeneous subseries.

3. The descriptive statistics studies show that the induced seismicity is a complex, multimodal, both time and space dependent phenomenon. The event rate and the energy distribution of events are time varying due to time changes of mining.

4. Moreover, the descriptive statistics studies show that the multimodality of the seismic series is reflected in the distribution of event energy. At least two classes of generating processes have been identified. The one comprises time-varying, controlled by mining works processes, responsible for occurrence of, in general, small events. The other one comprises processes weakly dependent on time, giving rise to strong events. The processes from the first class are predominantly dependent upon the coal layer and stope characteristics. The second class processes depend more upon joint influence of structures in the environment of excavations than upon the excavations themselves.

5. The maximum energy value statistics method complemented with testing procedures assessing differences in the empirical distributions of maxima turns out to be a valuable tool in the detailed studies of the multimodal structure of seismic series. The results of the maximum value analysis prove that the energy distribution of seismic events is multimodal in both the mine-wide scale as well as for particular clusters of seismicity. The method enables to single out individual modes of the event energy distributions and to estimate their limiting values. However, the extreme value statistics method is an indirect

way to identify processes of seismic event generation and it is not possible, on the basis of this method, to separate, from the seismic series, events generated by the specific identified processes.

6. A new method is proposed to study nonrandom character of the spatial distribution of seismic series. The method is based on deflection of straight line connecting epicenters of every two consecutive events, measured from the N-S direction.

7. The efficiency an the conditions of applicability of the nonparametric kernel estimation method of probability density function for reproducing of deflection probability functions, based on empirical data, have been investigated. The nonparametric kernel estimation method, a novel and innovative approach in studies of structure of seismic catalog, is an objective, user-independent technique which can be used for deflection series of sizes from 50-60. The method well reproduces both the number of modes of true probability distributions and the locations of these modes.

8. In future the nonparametric kernel estimation can be also used for estimation of energy or logarithm of energy of the seismic events, based on empirical data. Further studies are needed to account for distortions of the estimated probability density function of energy introduced by the repeatability of some energy values.

9. The application of the analysis of deflection with the use of the nonparametric kernel estimation of the probability distribution function to the data from Wujek coal mine shows that the epicenter distribution of seismic events there is not random. The dominant directions of the distribution are significantly different for the studied subsets of events that occurred in different areas of the mine. Furthermore, the dominant trend, in the same subset of events, become different when various energy thresholds are considered. Several secondary trend are also observed in the distributions.

10. The main trend and the secondary trends as well, found in the estimated probability density functions of deflections are supposed to identify different processes of seismic event generation.

11. In some cases, after complementing the results of the analysis of deflection with information from other sources, it is possible to conclude about factors that control these identified processes. Some of the dominant and secondary trends in the distributions of

deflections can be associated with known geologic, tectonic and mining feature, whereas the others are not directly connected with the known mine structures.

12. The analysis of deflection is a direct method to study the seismic catalog and allows to separate, from the seismic series, events originated by the generation processes identified in the distribution of deflections.

13. The statistical analysis of seismic series reveals information about properties of seismic event parameters that is contained in the data. Its integration, whenever possible, with other kinds of seismic event analysis, e.g. source mechanism and source parameters studies, would increase certainty of identification of event generating processes and of separation of events generated by individual processes.

References:

Adamowski K.and W. Feluch 1987. The comparison of parametric and nonparametric methods of flood frequency estimation. *Wiad. IMGW* 31(2-3): 67-78 (in Polish)

Anderberg M.R. 1973. *Cluster Analysis of Applications.* New York, London: Accademic Press

Box G.E.P., W.G. Hunter, J.S. Hunter 1987. *Statistics for Experimenters.* New York: John Wiley and Sons, Inc.

Cosentino P., V. Ficarra and D. Luzio 1977. Truncated exponential frequency-magnitude relationship in earthquake statistics. *Bull. Seismol. Soc. Am.* 67: 1615-1623

Cosentino P., L. De Luca, D. Luzio and S. Lasocki S. 1996. Fractal analysis as an approach to seismic hazard estimation. *Proc. 4th Int. Symp. on Rockbursts and Seismicity in Mines - Kraków, Poland.* Rotterdam: A.A. Balkema (in print)

Davis S.D. and C. Frohlich 1991. Single-link cluster analysis, synthetic earthquake catalogs, and aftershock identification. *Geophys. J. Int.* 104: 289-306

Dessokey M.M. 1984. Statistical models of the seismic hazard analysis for mining tremors and natural earthquakes. *Publs. Inst. Geophys. Pol. Acad. Sci.* A-5(174): 1-80

Epstein B. and C. Lomnitz 1966. A model for occurrence of large earthquakes. *Nature* 211: 954-956

Feluch W. 1994. *Selected Methods of Kernel Estimation of Probability Density Function and Regression in Hydrology.* Warsaw: Publ. House of the Warsaw Univ.of Techn. (in Polish)

Frohlich C. and S.D. Davis 1986. Single-link cluster analysis as a potential tool for evaluating spatial and temporal properties of earthquake catalogs. *EOS* 67: 1119

Gan Z. J. and C.C. Tung 1983. Extreme value distribution of earthquake magnitude. *Phys. Earth Planet. Int.* 32: 325-330

Gardner J.K. and L. Knopoff 1974. Is the sequence of earthquakes in southern California, with aftershocks removed, Poissonian? *Bull. Seismol. Soc. Am.* 64: 1363-1367

Gedney L., S. Estes & N.N. Biswas 1980. Earthquake migration in the Fairbanks, Alaska, seismic zone. *Bull. Seism. Soc. Am.* 70: 223-241

Gibowicz S.J. 1990. The mechanism of seismic events induced by mining. *Proc. 2nd Int. Symp. on Rockbursts and Seismicity in Mines - Minneapolis, USA.* Rotterdam: A.A. Balkema: 3-27

Gibowicz S.J. and A. Kijko 1994. *An Introduction to Mining Seismology.* San Diego, London: Academic Press

Grasso J.R. 1993. Triggering of self organized system: Implications for the state of the uppermost crust. *Proc. 3rd Int. Symp. on Rockbursts and Seismicity in Mines - Kingstone, Canada*: 187-104. Rotterdam: A.A. Balkema

Gumbel E.J. 1962. *Statistics of Extremes.* New York: Columbia University Press

Hollander M. and D.A. Wolfe 1973. *Nonparametric Statistical Methods.* New York: John Wiley and Sons, Inc.

Idziak A., G. Sagan and W.M. Zuberek 1991. An analysis of energy distributions of shocks from the Upper Silesian Coal Basin. *Publs. Inst. Geophys. Pol. Acad. Sci.* M-15(235): 163-182 (in Polish)

Idziak A. and W.M. Zuberek 1995. Fractal analysis of mining induced seismicity in the Upper Silesian Coal Basin. *Proc. Int. Conf. on Mechanics of Jointed and Faulted Rock - Vienna, Austria*. Rotterdam: A.A. Balkema

Johnson N.L. and S. Kotz 1970. *Continuous Univariate Distributions - 1.* Boston: Houghton Mifflin Company

Johnston J.C. and H.H. Einstein 1990. A survey of mining associated rockbursts. *Proc. 2nd Int. Symp. on Rockbursts and Seismicity in Mines - Minneapolis, USA.* Rotterdam: A.A. Balkema: 121-128

Katkovnik W.J. 1985. *Nonparametric Identification and Data Smoothing. Local Approximation Method.* Moscow: Nauka (in Russian)

Kijko A. 1982. A modified form of the first Gumbel distribution model for the occurrence of large earthquakes. *Acta Geophys. Pol.* 30: 333-340

Kijko A. and M.A. Sellevoll 1981. Triple exponential distribution, a modified model for the occurrence of large earthquakes. *Bull. Seism. Soc. Am.* 71: 2097-2101

Kijko A., B. Drzezla and T. Stankiewicz 1987. Bimodal character of the distribution of extreme seismic events in Polish mines. *Acta Geophys. Pol.* 35: 157-166

Kijko A., C.W. Funk and A.v.Z. Brink 1993. Identification of anomalous patterns in time-dependent mine seismicity. *Proc. 3rd Int. Symp. on Rockbursts and Seismicity in Mines - Kingstone, Canada.* Rotterdam: A.A. Balkema: 205-210

Kijko A. and C.W. Funk 1994. The assessment of seismic hazard in mines. *JSAIMM:* 179-185

King C.-Y. and Z. Ma 1988. Migration of historical earthquakes in California. *Pure Appl. Geophys.* 127: 627-639

Kushnir N.J., N.H. Al-Saigh and D.P. Ashwin 1984. Induced seismicity generated by longwall coal mining in the North Staffordshire Coal-field, U.K. *Proc. 1st Int. Symp. on Rockbursts and Seismicity in Mines - Johannesburg, RSA.* Johannesburg: SAIMM: 153-160

Lasocki S. 1988. The distribution of energy of mining shocks recorded in an exploitation region. *Zesz. Nauk. AGH 1240, s Mining* 141: 131-140 (in Polish)

Lasocki S. 1989. Some estimates of rockburst danger in underground coal mines from energy distribution of MA events. *Proc. 4th Conf. on AE/MA in Geologic Structures and Materials. - Pennsylvania, USA.* Clausthal: Trans Tech Publs.: 617-633

Lasocki S. 1992. Non-Poissonian structure of mining induced seismicity. *Acta Montana* 84: 51-58

Lasocki S. 1992a. Truncated Pareto distribution used in the statistical analysis of rockburst hazard. *Acta Montana* s.A 2(88): 121-132

Lasocki S. 1993. Statistical prediction of strong mine events. *Acta Geophys. Pol.* 41: 197-234

Lasocki S. 1993a. Weibull distribution as a model for sequence of tremors induced by mining. *Acta Geophys. Pol.* 41: 101-111

Lasocki S. and Z. Mortimer 1996. Variations of MS source distribution geometry before a strong tremor occurrence in mines. *Proc. 6th Conf. on Acoustic Emission/Microseismic Activity in Geologic Structures and Materials - Pennsylvania, USA.* Clausthal: Trans Tech Publs (in print)

Lasocki S., S. Weglarczyk and S.J. Gibowicz 1996. A new method to estimate directional character of mining-induced seismicity: application to the data from Wujek coal mine, Poland. *Proc. 4th Int. Symp. on Rockbursts and Seismicity in Mines*, Rotterdam: A.A. Balkema (in print)

Lomnitz C. 1974. *Global Tectonics and Earthquake Risk.* Amsterdam: Elsevier

Loo H.-Y., X.-L. Gao, J.-X. Sun et al. 1992. Three-dimensional numerical modeling of earthquake migration along a northwestern Pacific subduction slab. *Geophys. Res. Lett.*19: 313-316

McGarr A. 1984. Some applications of seismic source mechanism studies to assesing underground hazard. *Proc. 1st Int. Symp. on Rockbursts and Seismicity in Mines - Johannseburg, RSA*. Johannesburg: SAIMM: 199-208

Meyer K., R. Olsson & O. Kulhanek 1985. High-velocity migration of large earthquakes along the Azores-Iran plate boundary. *Pure Appl. Geophys.* 122: 831-847

Morrison D.M., G. Swan, C.H. Scholz 1993. Chaotic behaviour and mining-induced seismicity. *Proc. 3rd Int. Symp. on Rockbursts and Seismicity in Mines - Kingstone, Canada.* Rotterdam: A.A. Balkema: 233-237

Nordquist J.M. 1945. Theory of largest values applied to earthquake magnitudes. *Trans. Am. Geophys. Union* 26: 29-31

Parzen E. 1962. On estimation of probability density function and mode. *Annals of Mathematical Statistics* 33: 1065-1076

Rosenblatt M. 1956. Remarks on nonparametric estimates of a density function. *Annals of Mathematical Statistics* 27: 832-835

Rydelek P.A., L. Knopoff & C.-Y. King 1990. Comment on "Migration of historical earthquakes in California" by C.-Y. King and Z. Ma. *Pure Appl. Geophys.* 133: 547-551

Scott D.W. and L.E. Factor 1981. Monte Carlo study of three data-based nonparametric density estimators. *J. Am. Stat. Assoc.* 76(373): 9-15

Scott D.W. and L.E. Terrel 1987. Biased and unbiased cross-validation in density estimation. *J. Am. Stat. Assoc.* 82(400): 1131-1146

Silverman B.W. 1986. *Density Estimation for Statistics and Data Analysis.* Monographs on Statistics and Applied Probability. London, New York: Chapman and Hall

Smalley R.Jr., J.L. Chatelain, D. Turcotte and R. Prevot 1987. A fractal approach to the clustering of earthquakes: application to the seismicity of the New Hebrides. *Bull. Seismol. Soc. Am.* 77: 1368-1381

Teper L., A. Idziak, G. Sagan and W.M. Zuberek 1992. New approach to the studies of the relations between tectinics and mining tremors occurrence on example of the Upper Silesian Coal Basin (Poland). *Acta Montana* s. A 2(88): 161-177

Xie H. and W.G. Pariseau 1992. Fractal character and mechanics of rock bursts. *Proc. 33- rd U.S. Symp. on Rock. Mech. - Santa Fe, USA*. Rotterdam: A.A. Balkema

Yegulalp T.M. and J.T. Kuo 1974. Statistical prediction of occurrence of maximum magnitude earthquakes. *Bull. Seismol. Soc. Am.* 64: 393-414

Yoshida A. 1988. Migration of seismic activity along intraplate seismci belts in the Japanese Islands. *Tectonophysics* 145: 87-99

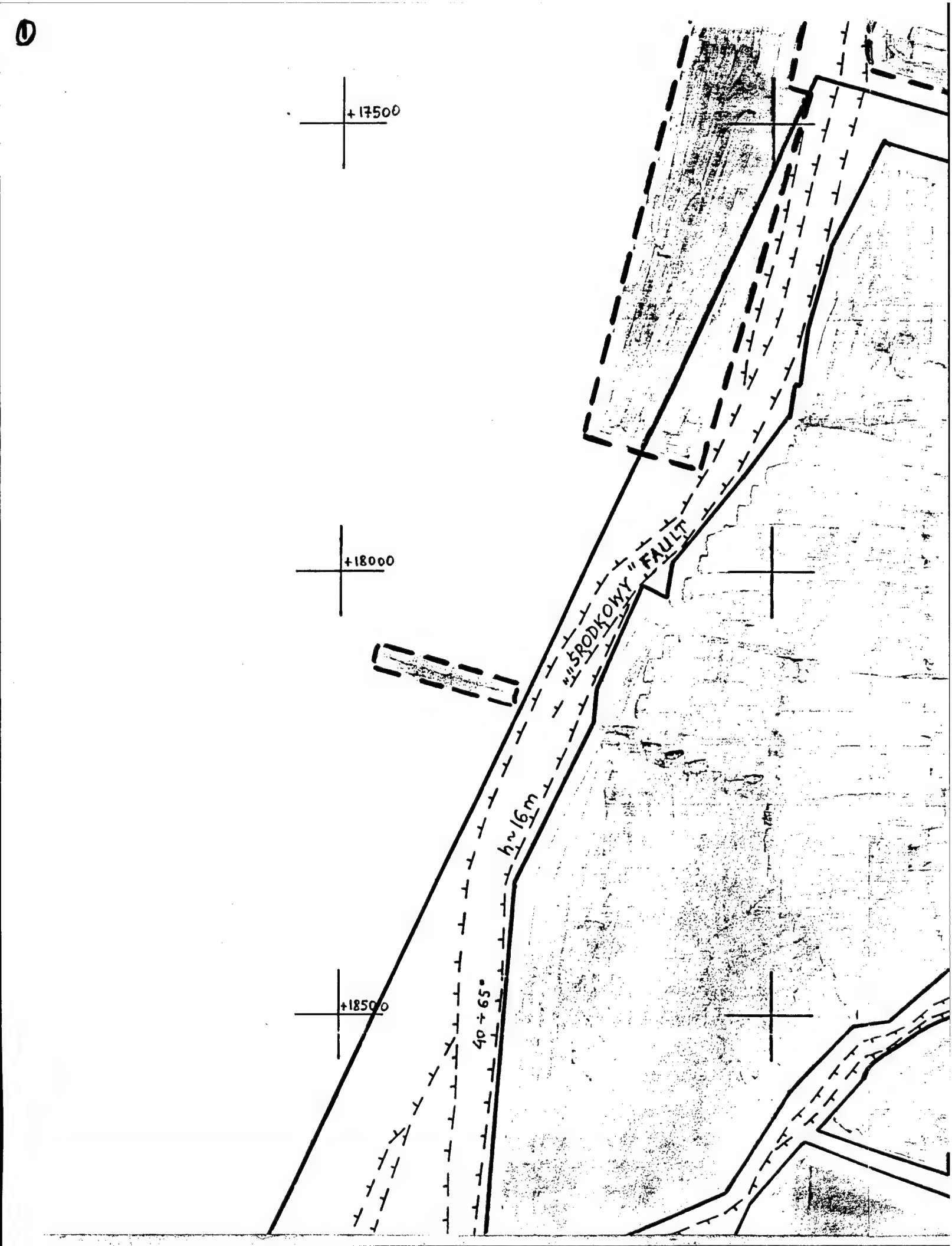
+17500
+18000
+18500
"ŚRODKOWY" FAULT
h≈16m
40÷65°

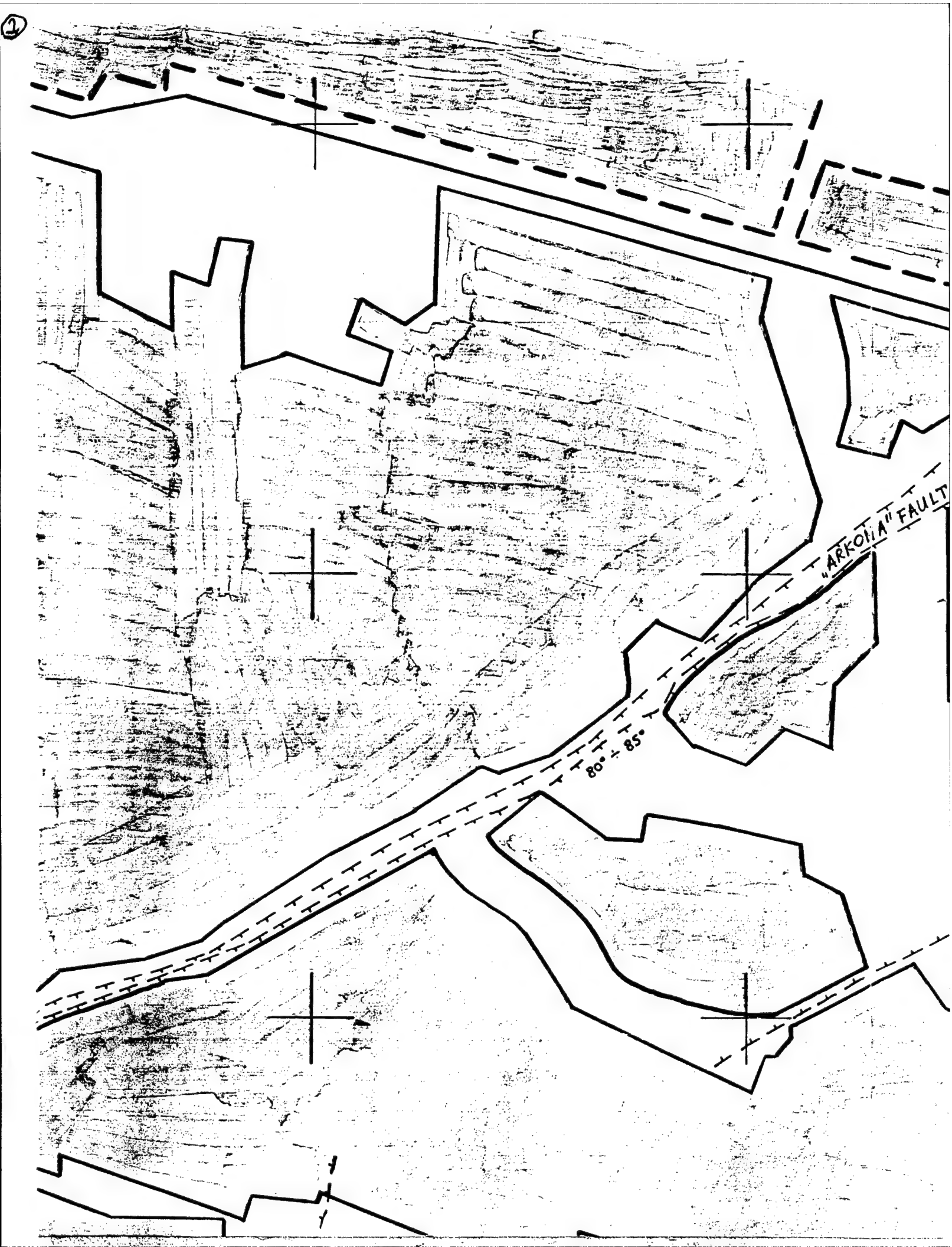
"ARKONA" FAULT
80° ± 85°

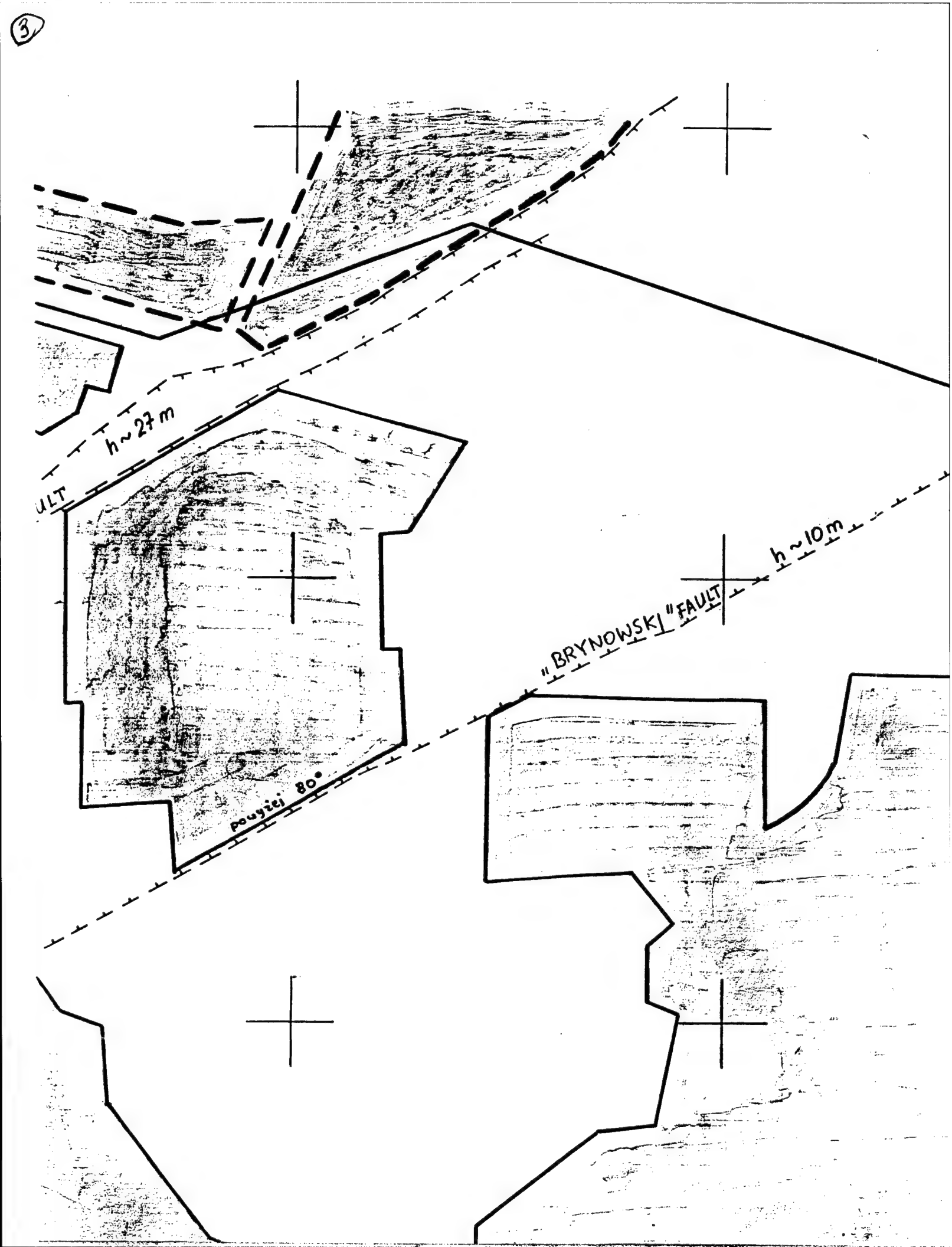
3
h~27 m
ULT
h~10m
"BRYNOWSKI" FAULT
powyżej 80°

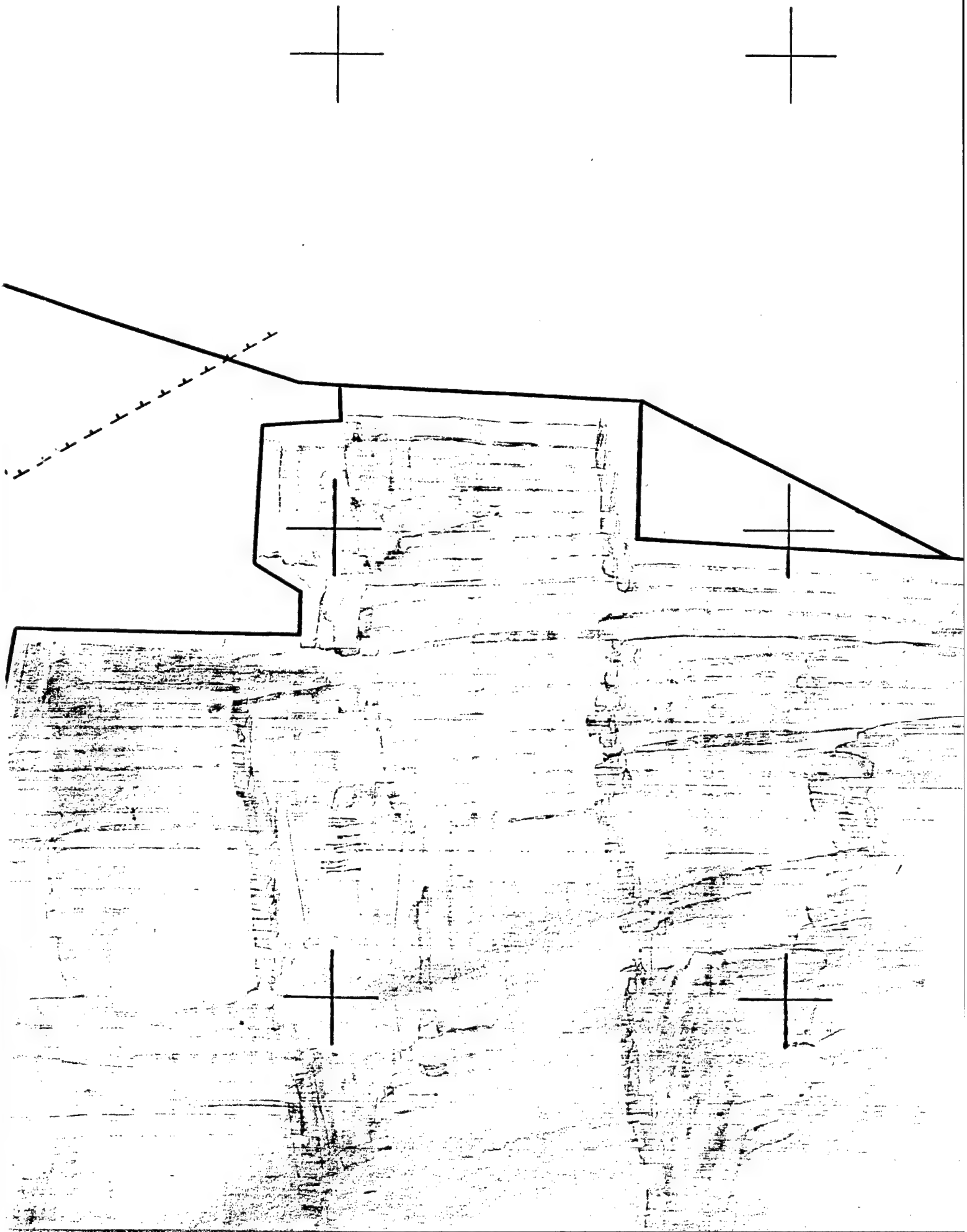

(5)

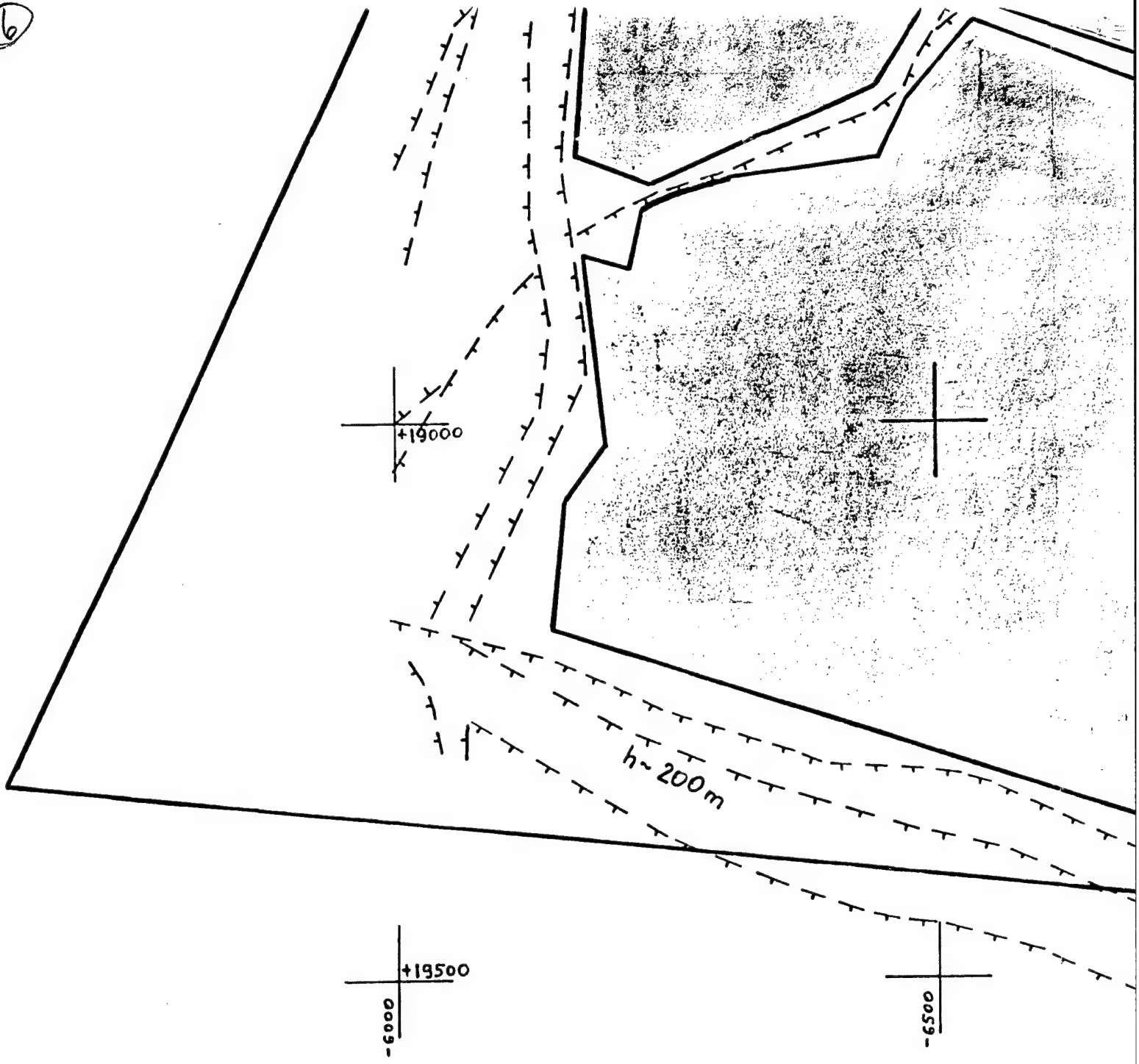
6
+19000
h~200m
+19500
6000
6550

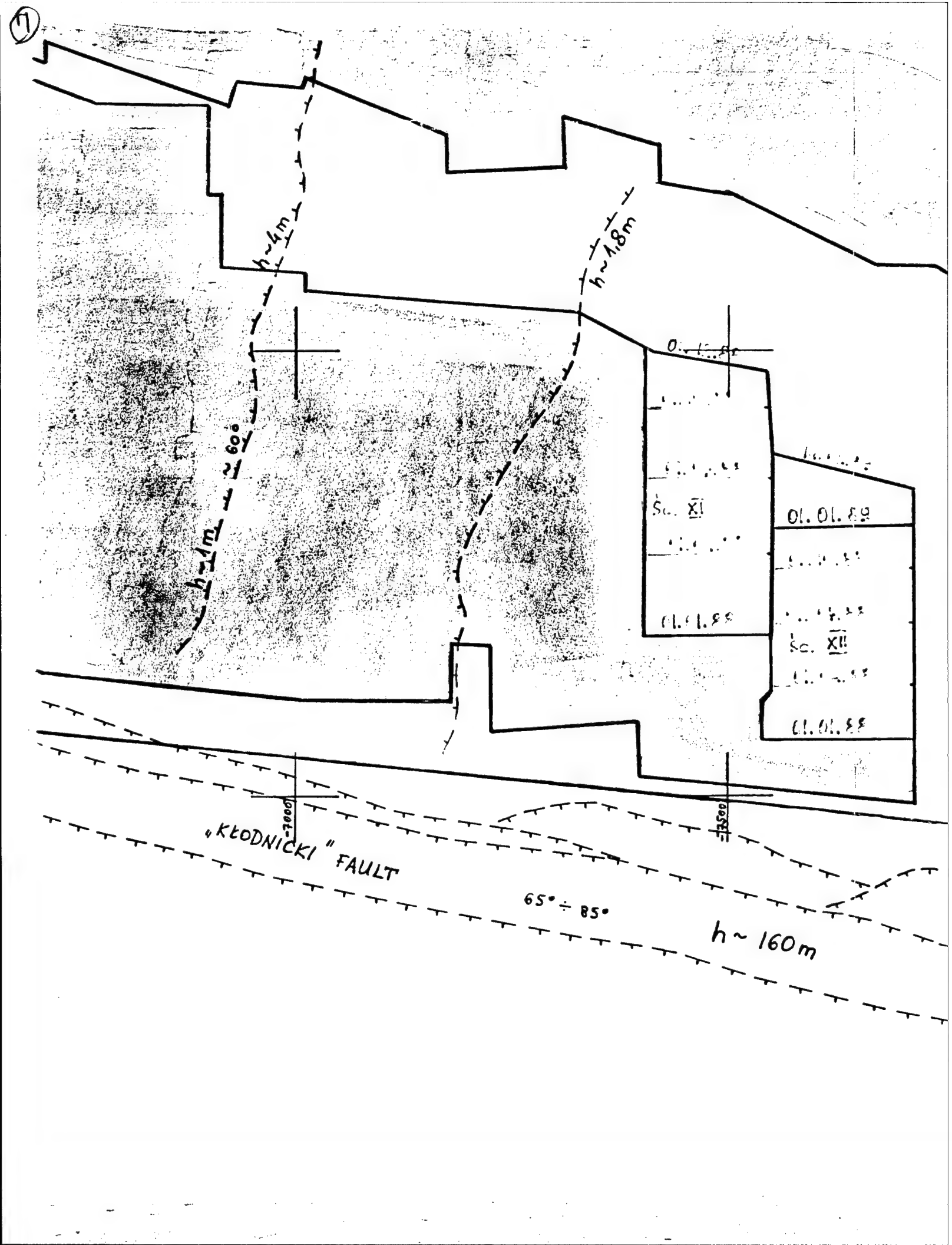
h~4m
h~1,8m
h~1m
~60°
Sc. XI
Sc. XII
-7000
-13500
„KŁODNICKI" FAULT
65° ÷ 85°
h ~ 160m

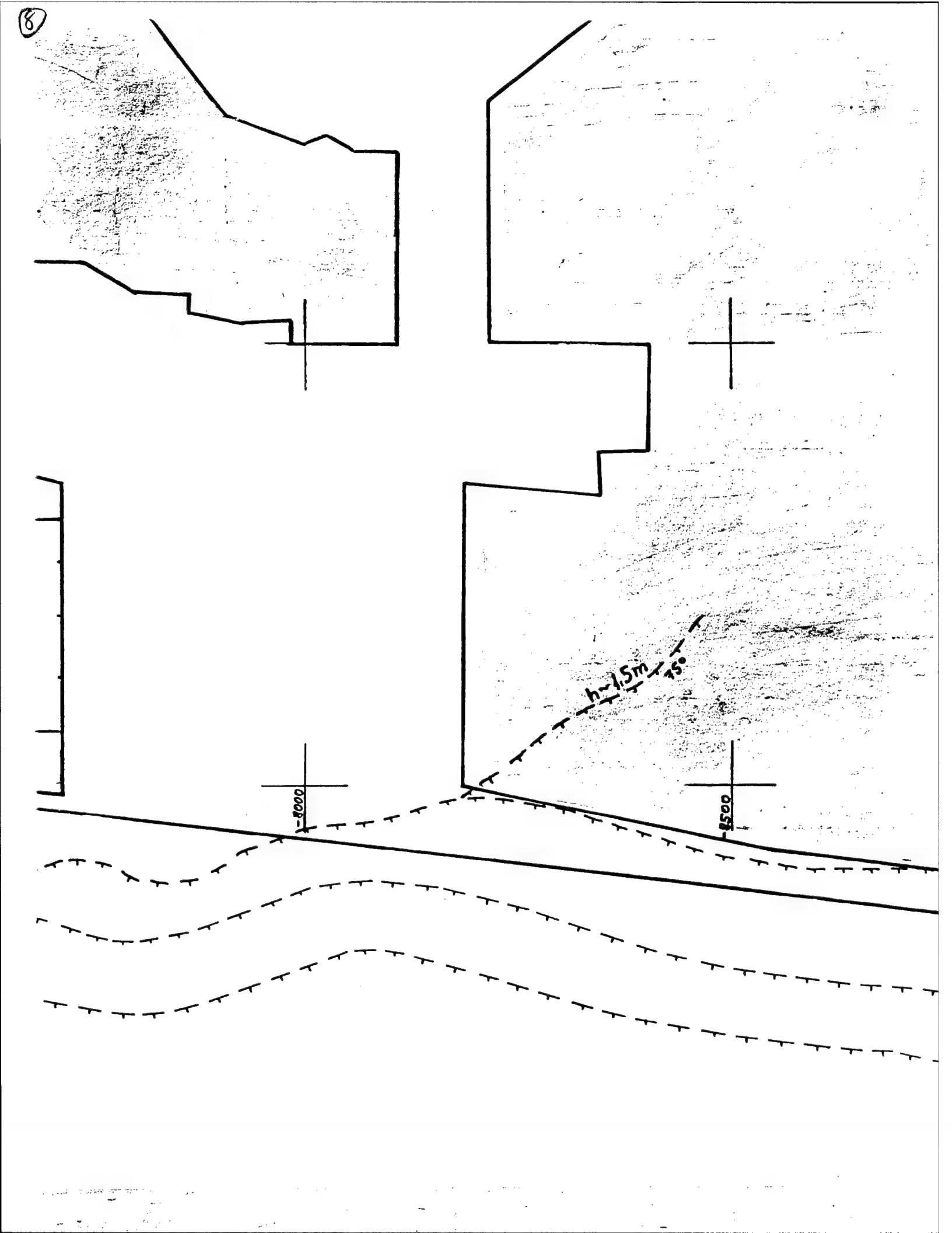
8
h=1.5m
45°
-8000
-8500

(9)

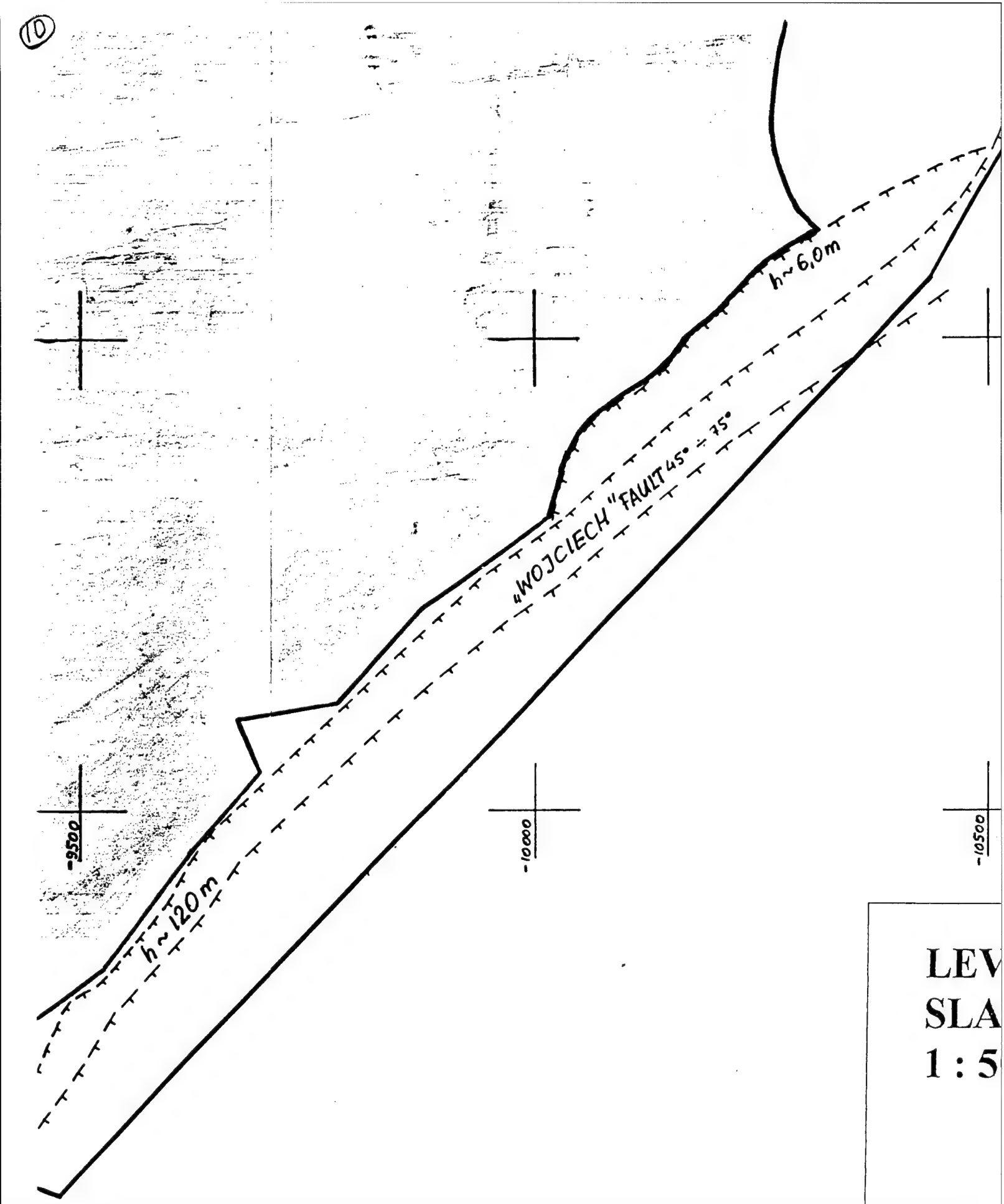

LEV
SLA
1 : 5

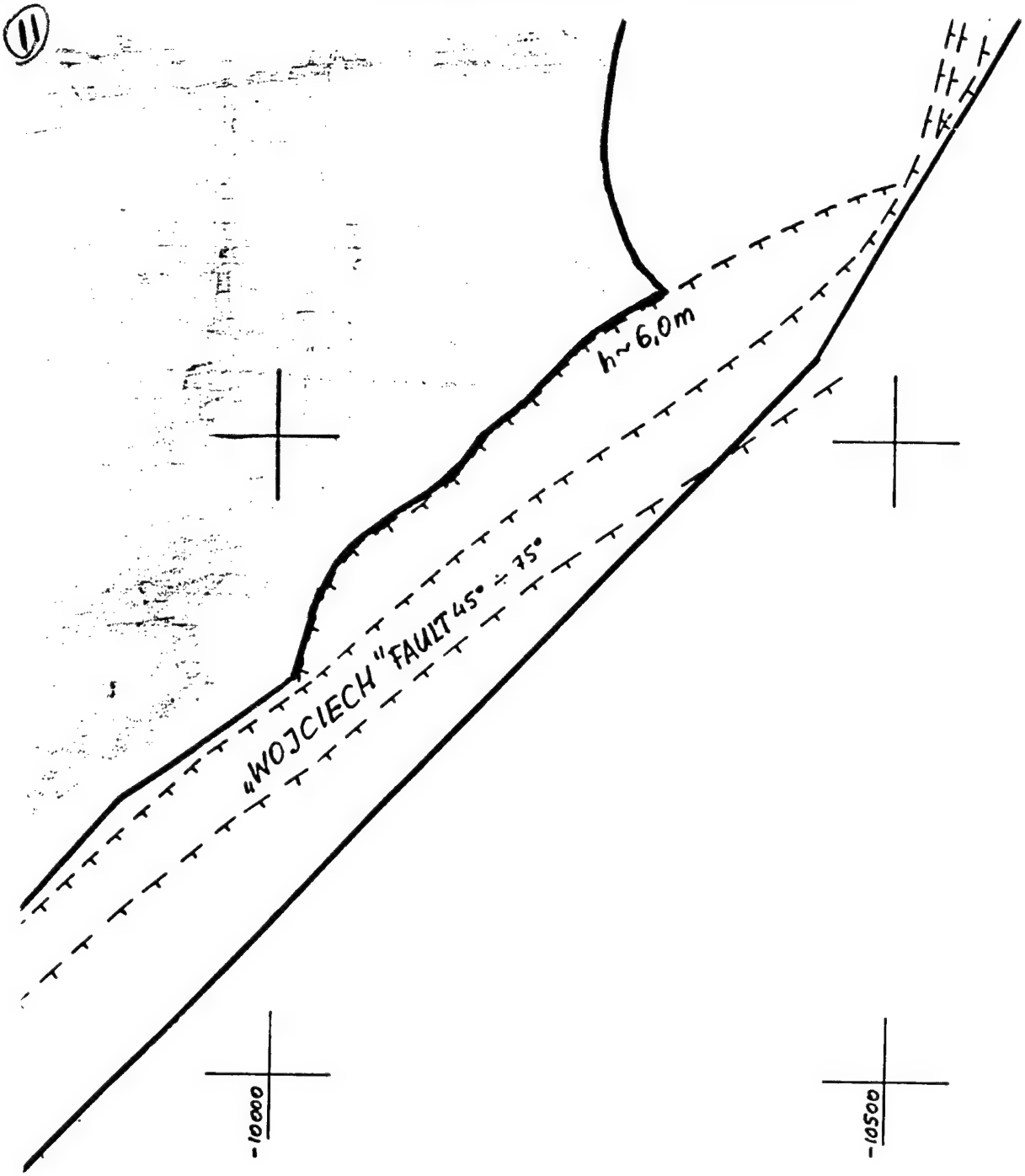

LEVEL 416
SLAB 1
1 : 5000

APPENDIX 1

①

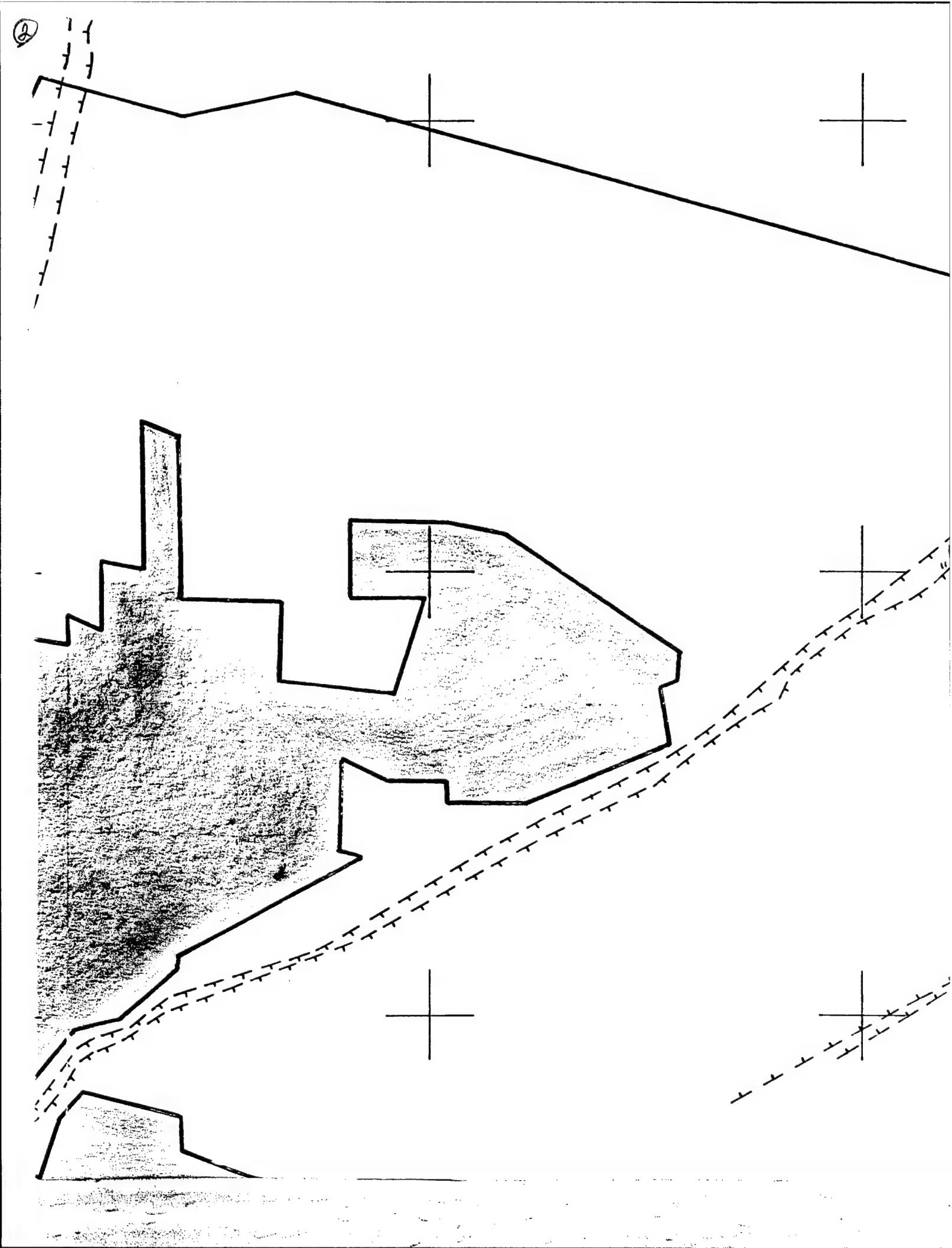

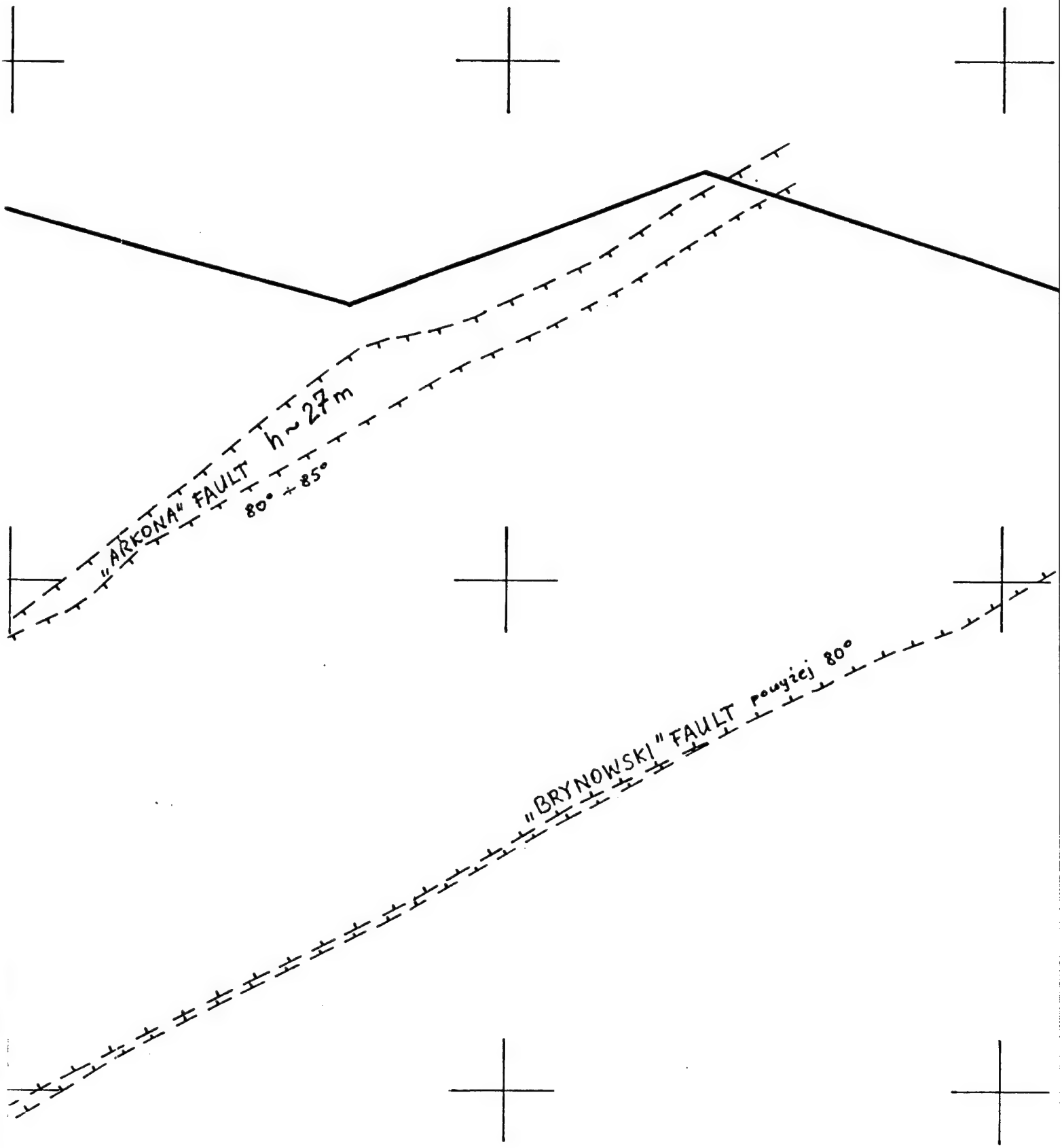
"ARKONA" FAULT h~27m
80° ÷ 85°
"BRYNOWSKI" FAULT powyżej 80°

(4)

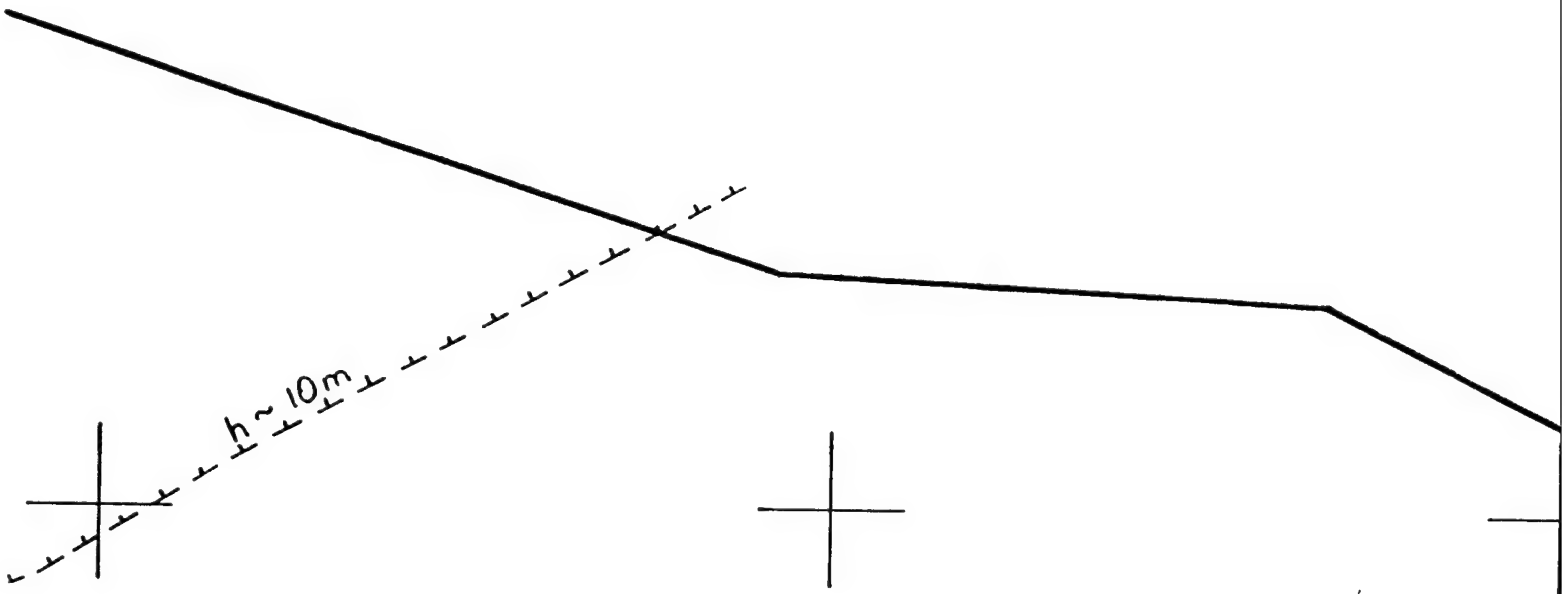

(5)

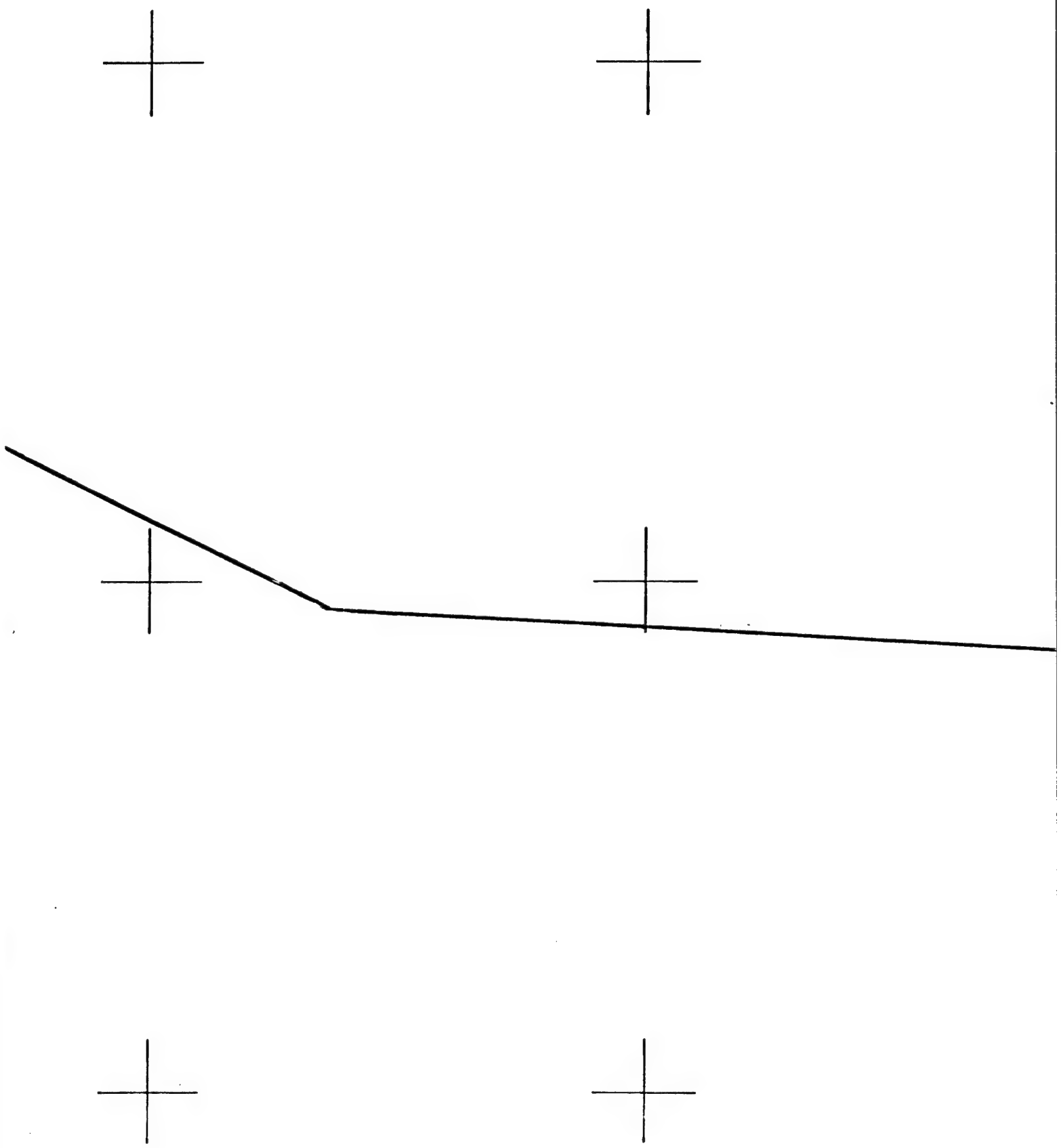

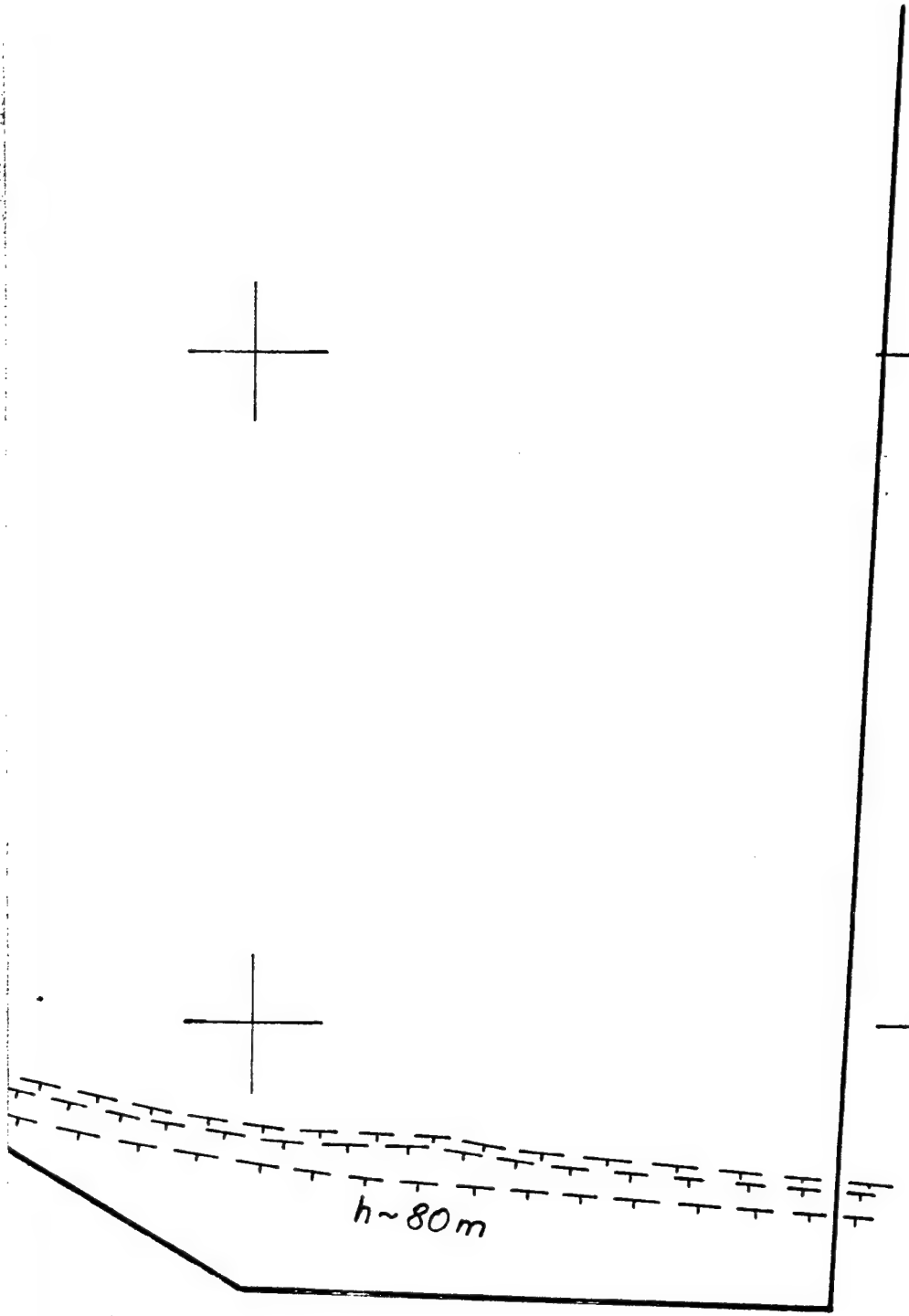
h~80m

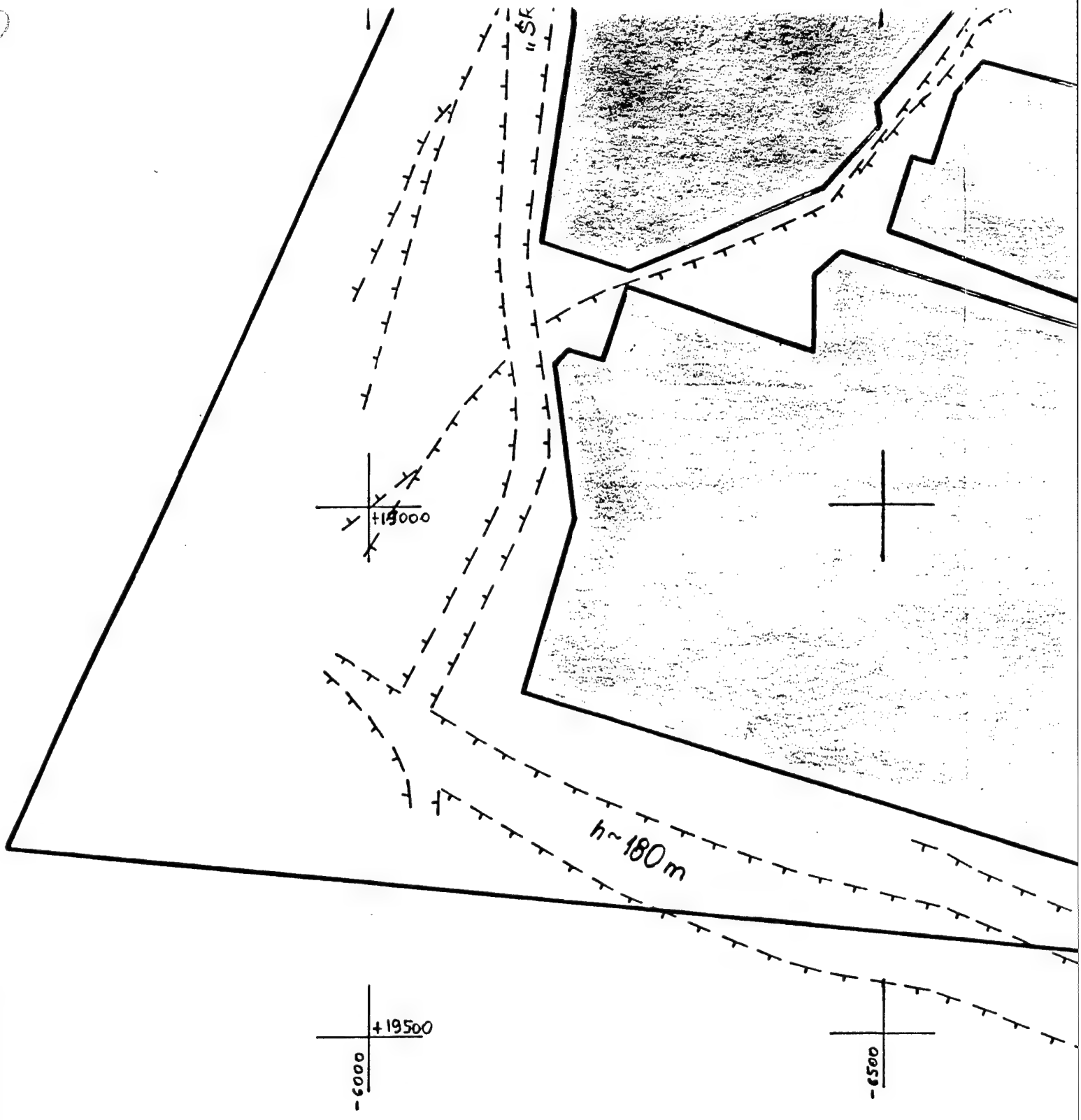
SK
+19000
h~180m
+19500
-6000
-6500

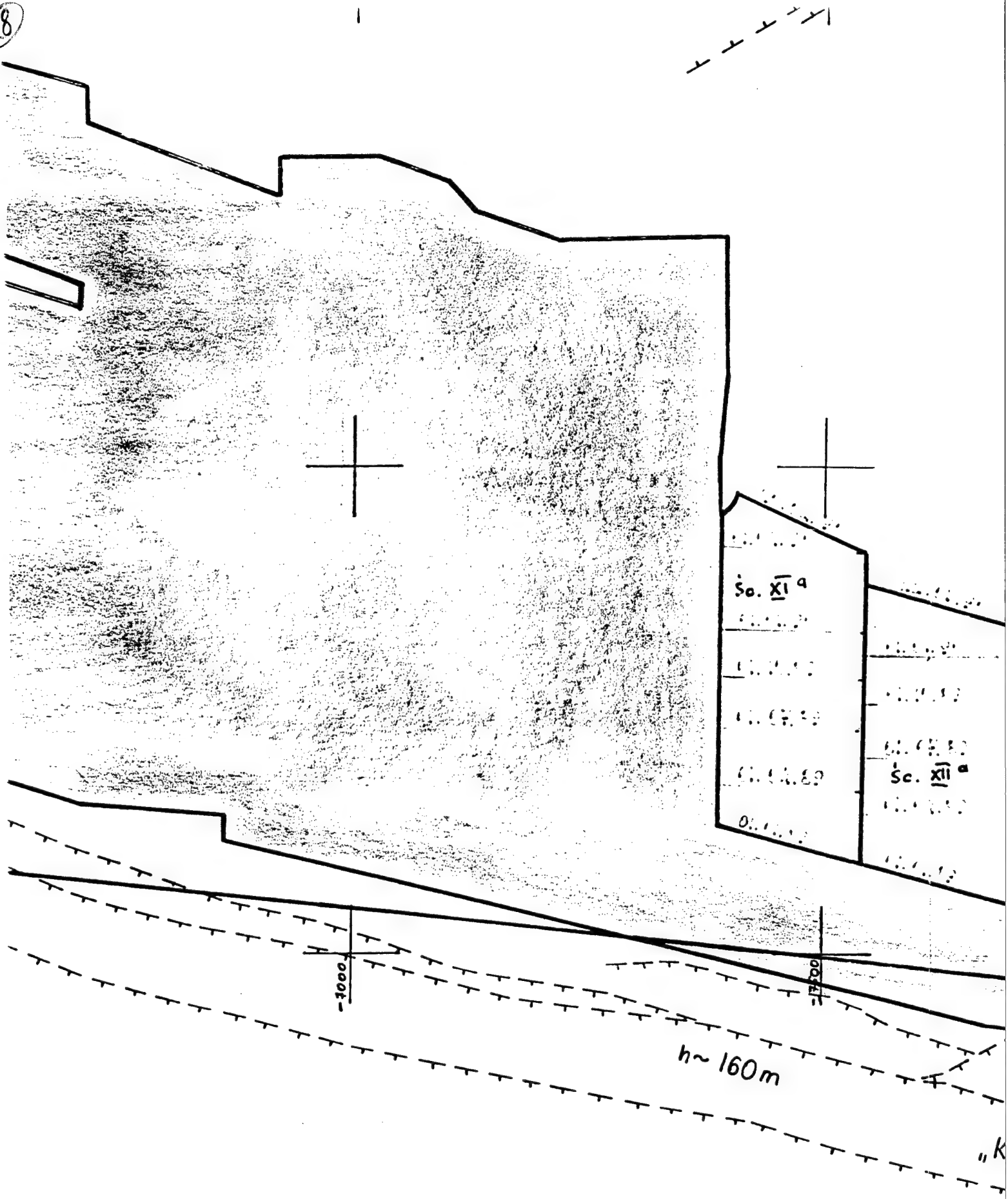
So. XI a
Sc. XII a
-3000
-3200
h~ 160m

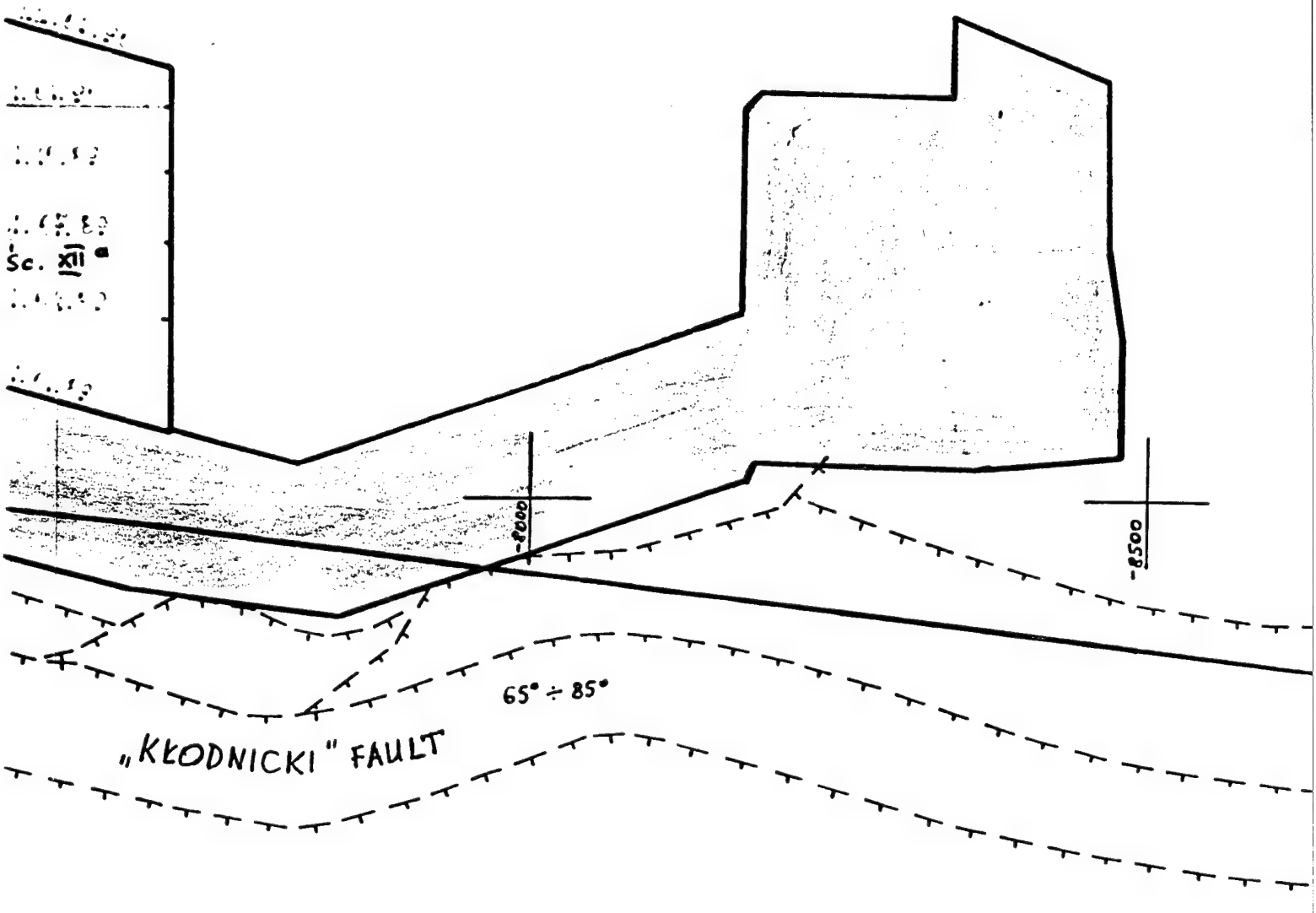
Sc. XII
-8000
-8500
65° ÷ 85°
„KŁODNICKI" FAULT

(10)

-9000

-9500

h ~ 120 m

(11)

LEV
SLA
1 : 5

(12)

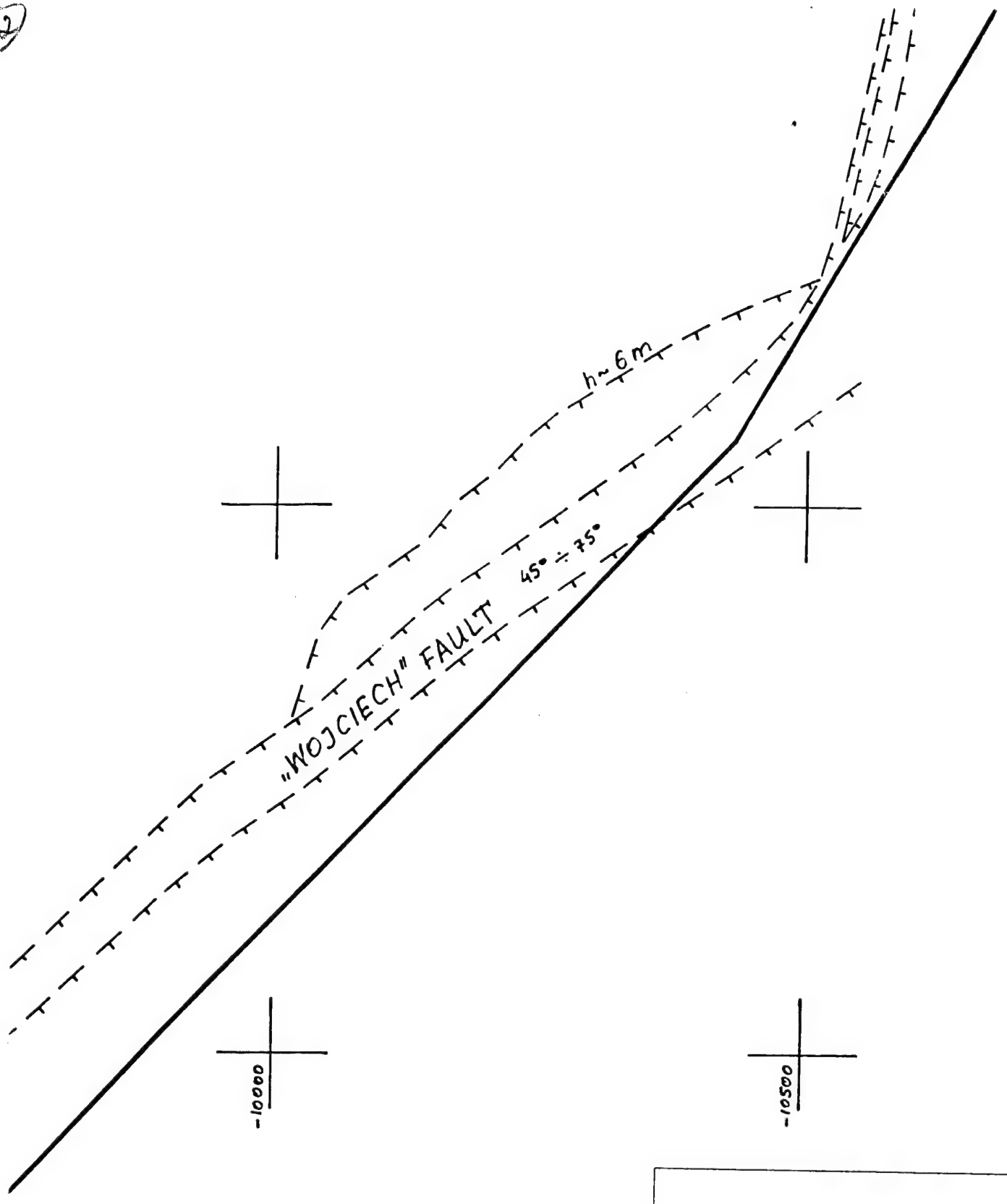

LEVEL 416
SLAB 2
1 : 5000

APPENDIX 2

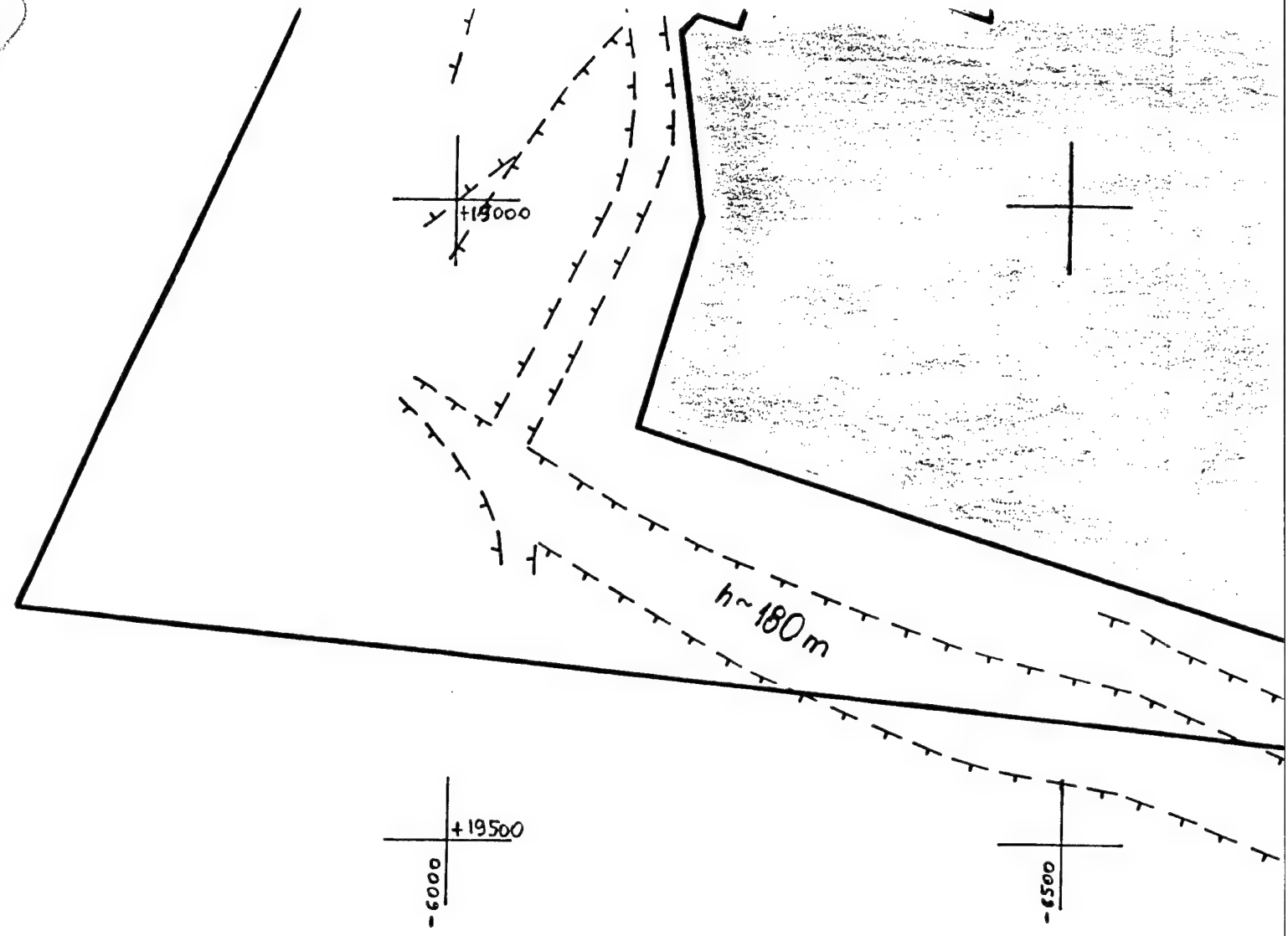
+18000
h~180m
+19500
-6000
-6500

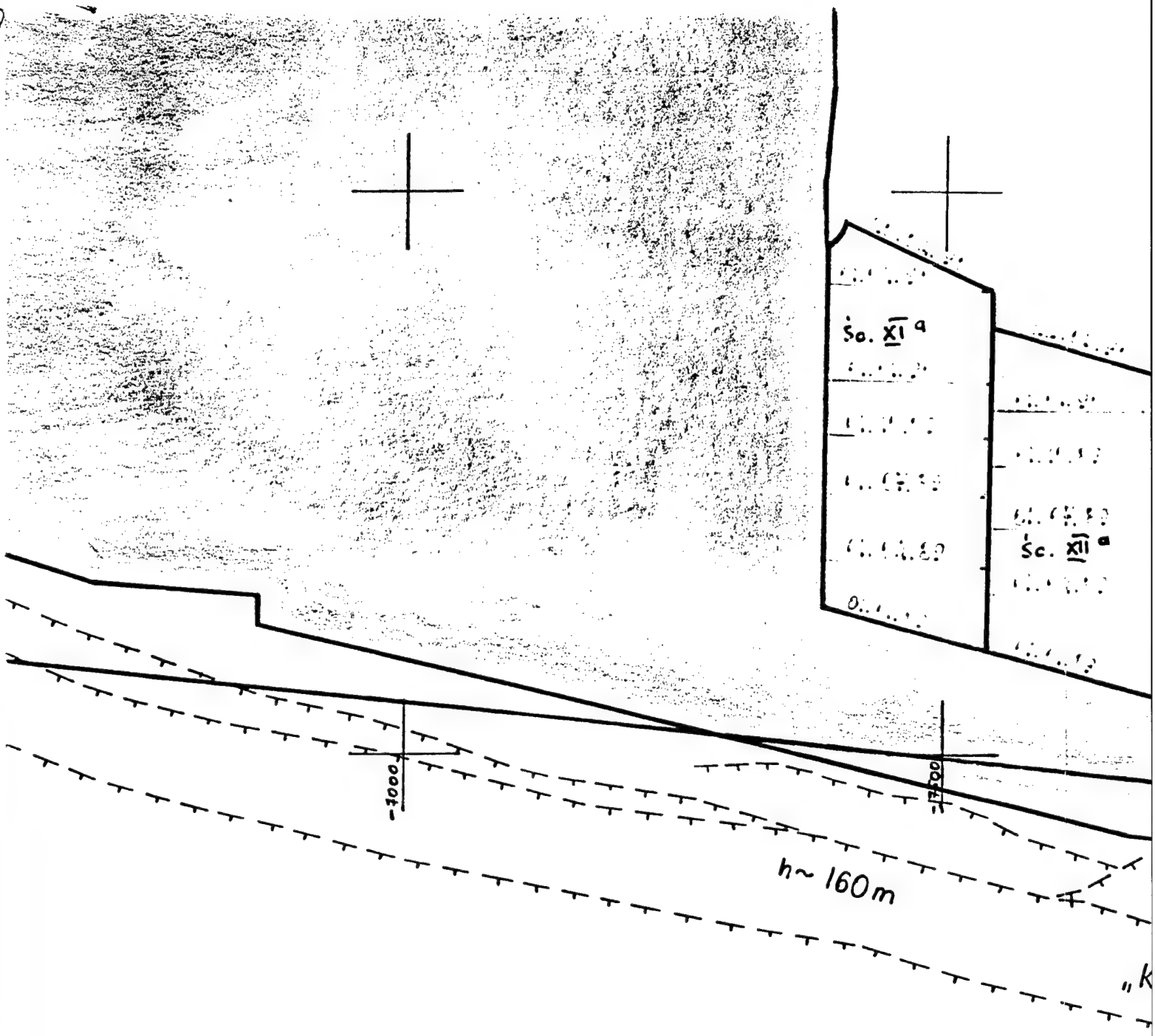
Sa. XI a
Sc. XI a
-3000
-3500
h~ 160m

15

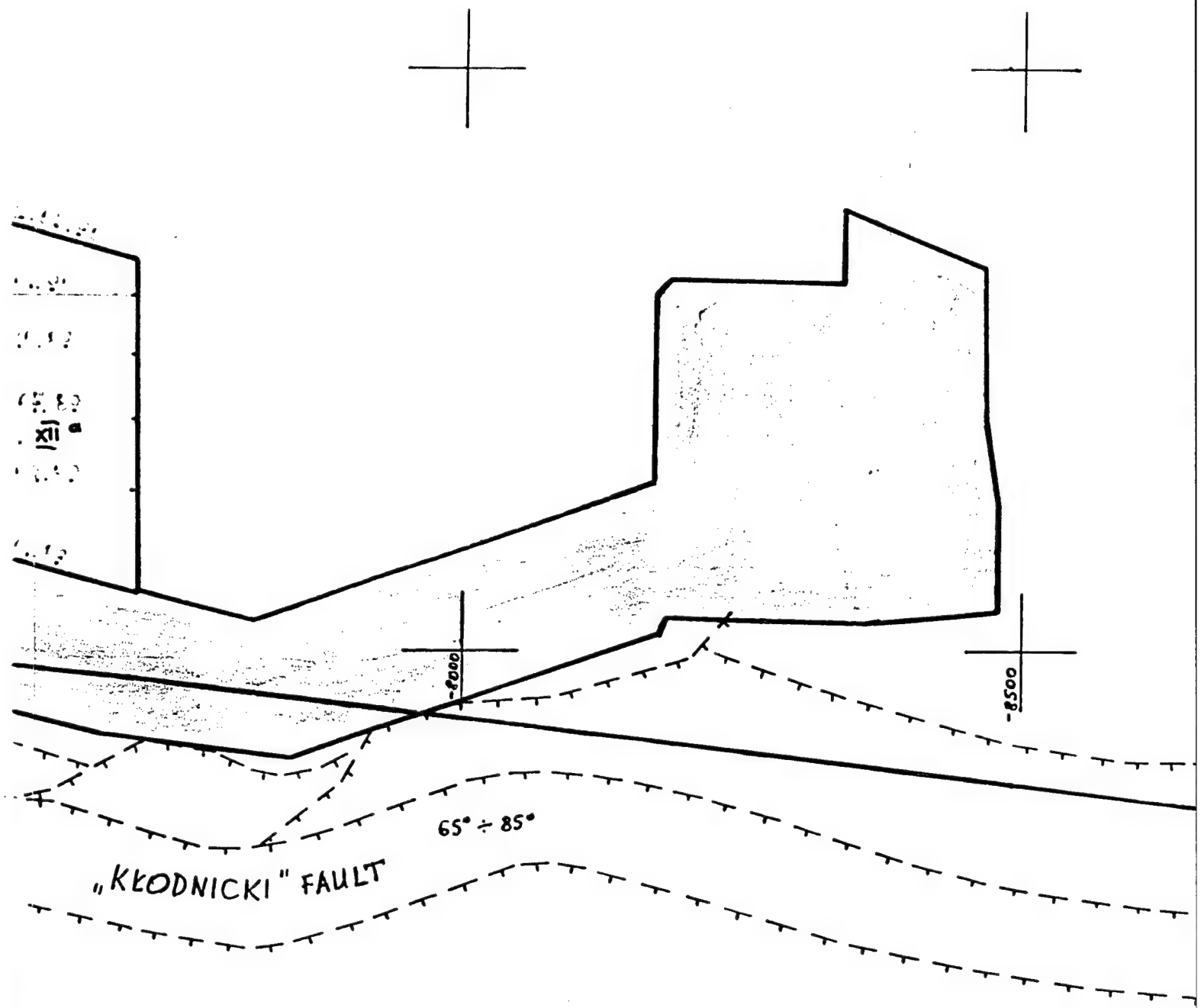

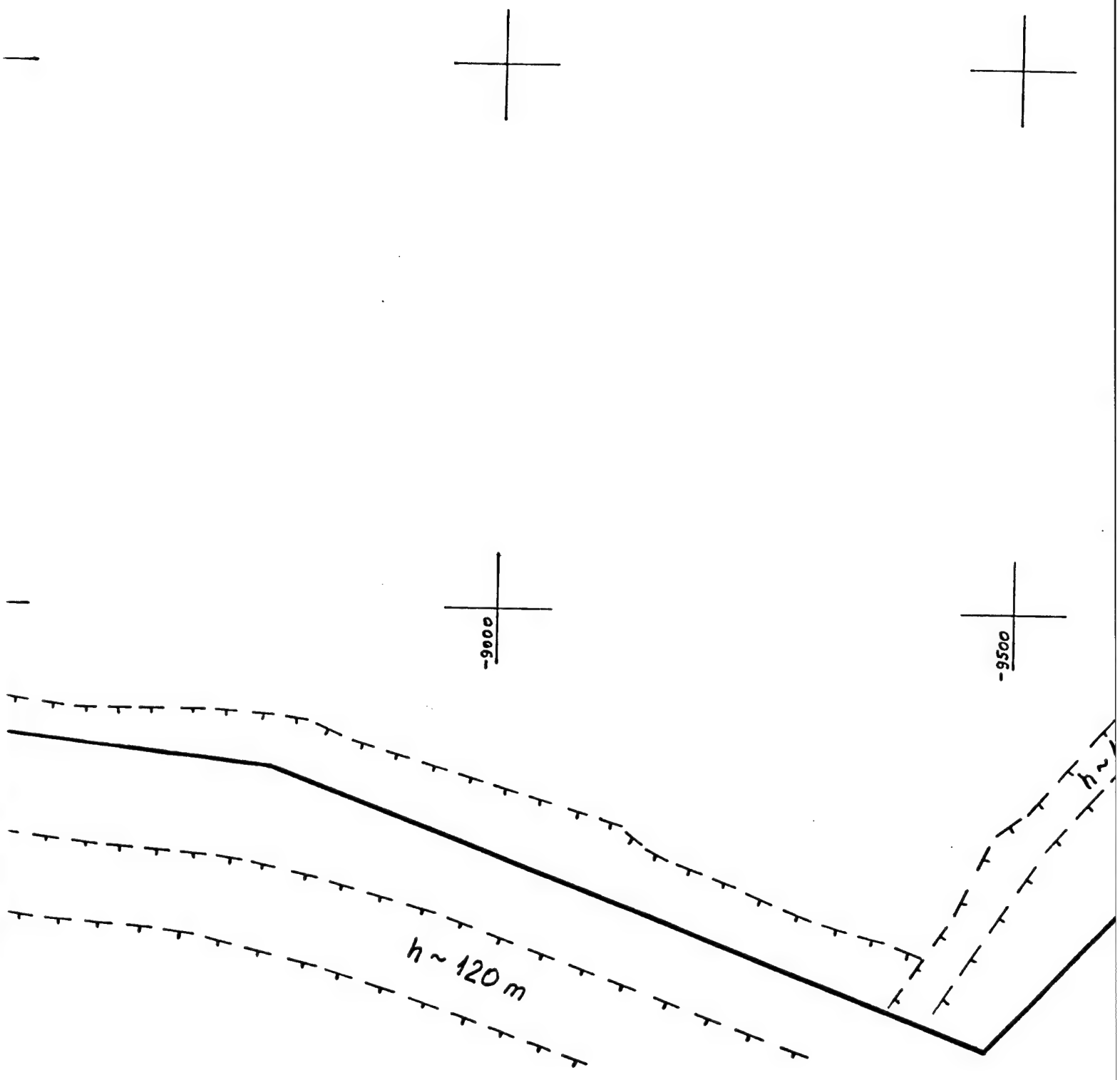
-9000
-9500
h ~ 120 m

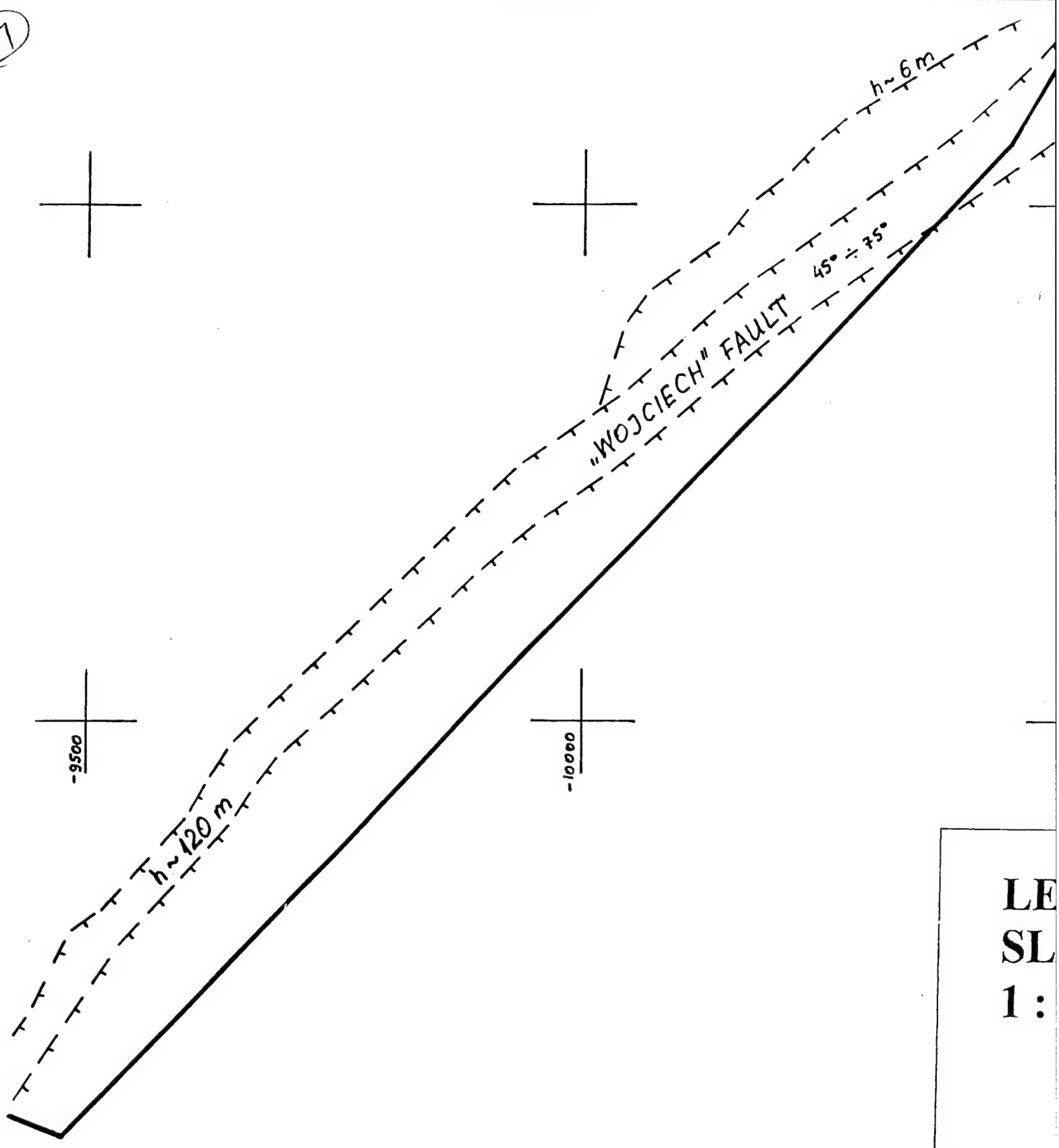

LE
SL
1 :

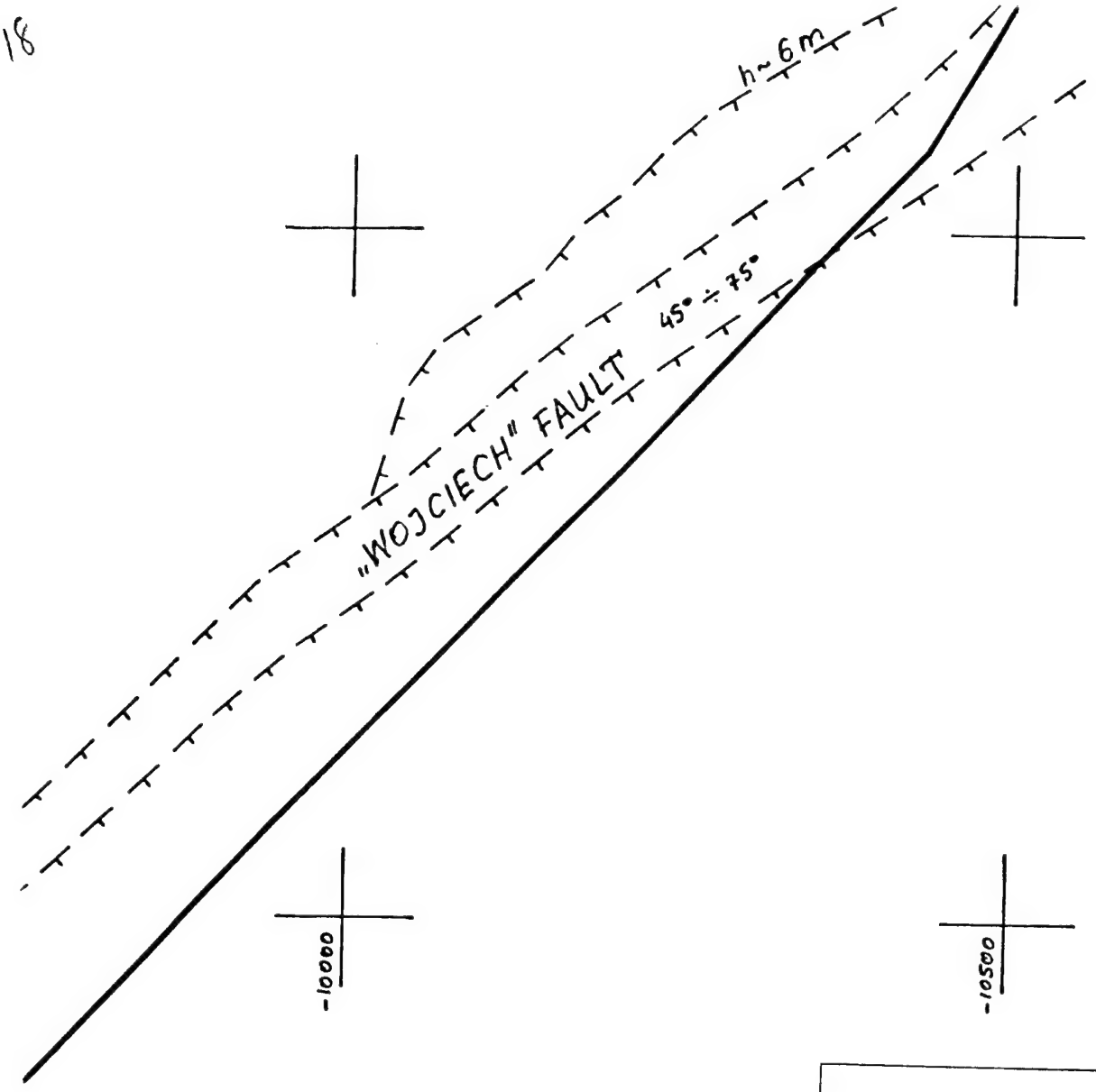

LEVEL 416
SLAB 2
1 : 5000

APPENDIX 2

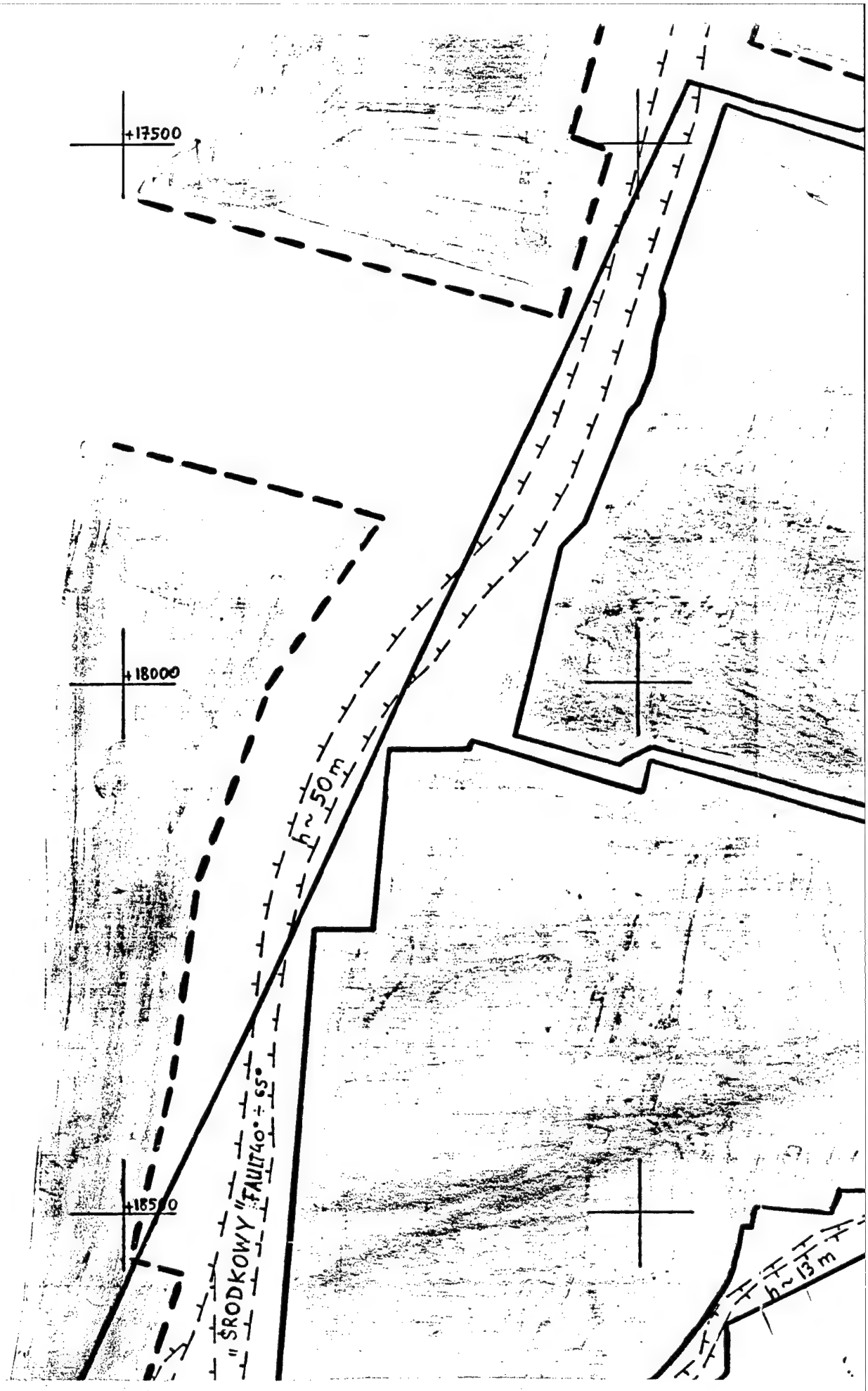
+17500
+18000
+18500
h~50m
"ŚRODKOWY" FAULT 40÷65°
h~13m


(2)
h~1,7m
h~3m
h~14m
h~5m
h~0,5m
h~1m
13m
Sc. I

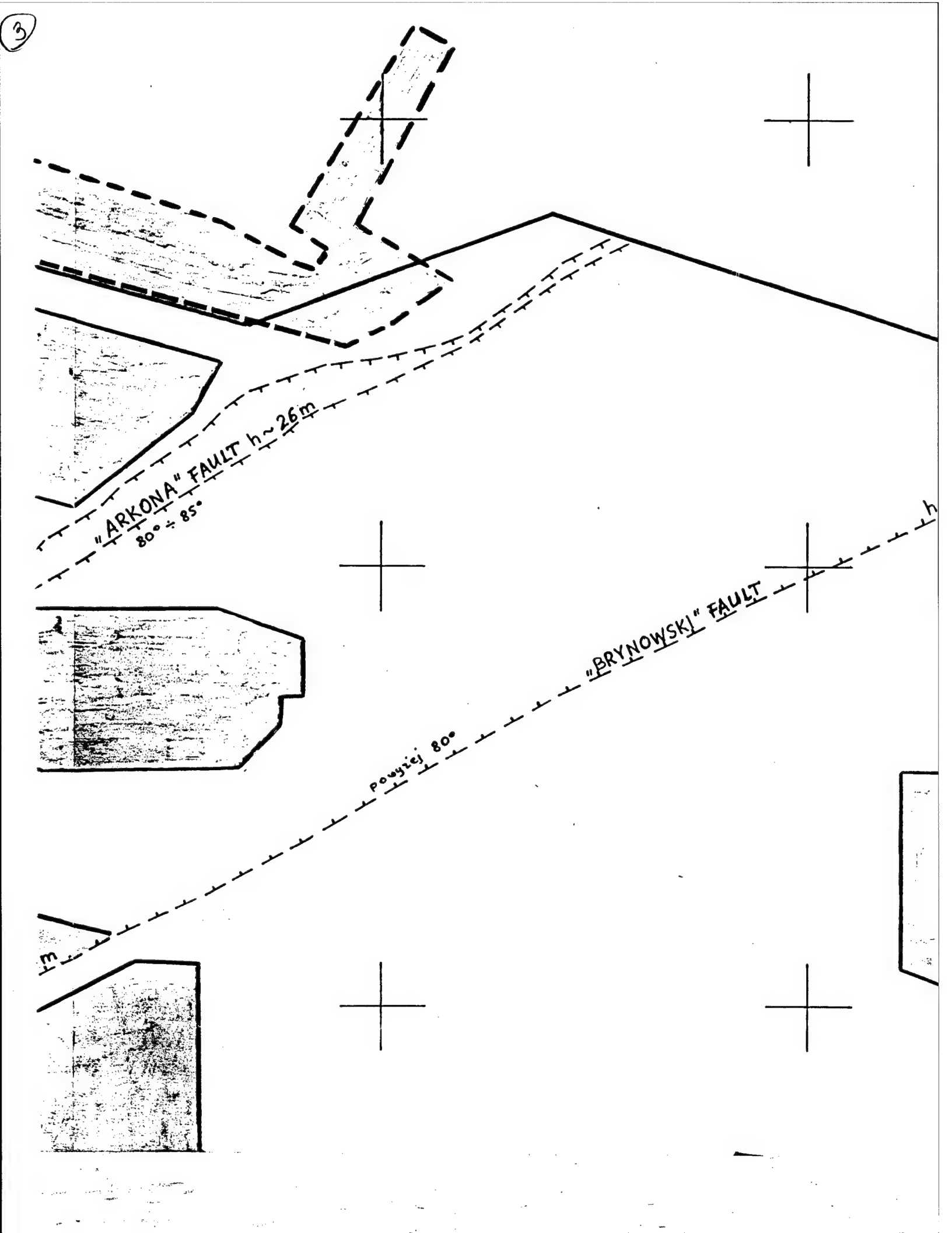
3
"ARKONA" FAULT h~26m
80° ÷ 85°
"BRYNOWSKI" FAULT
powyżej 80°

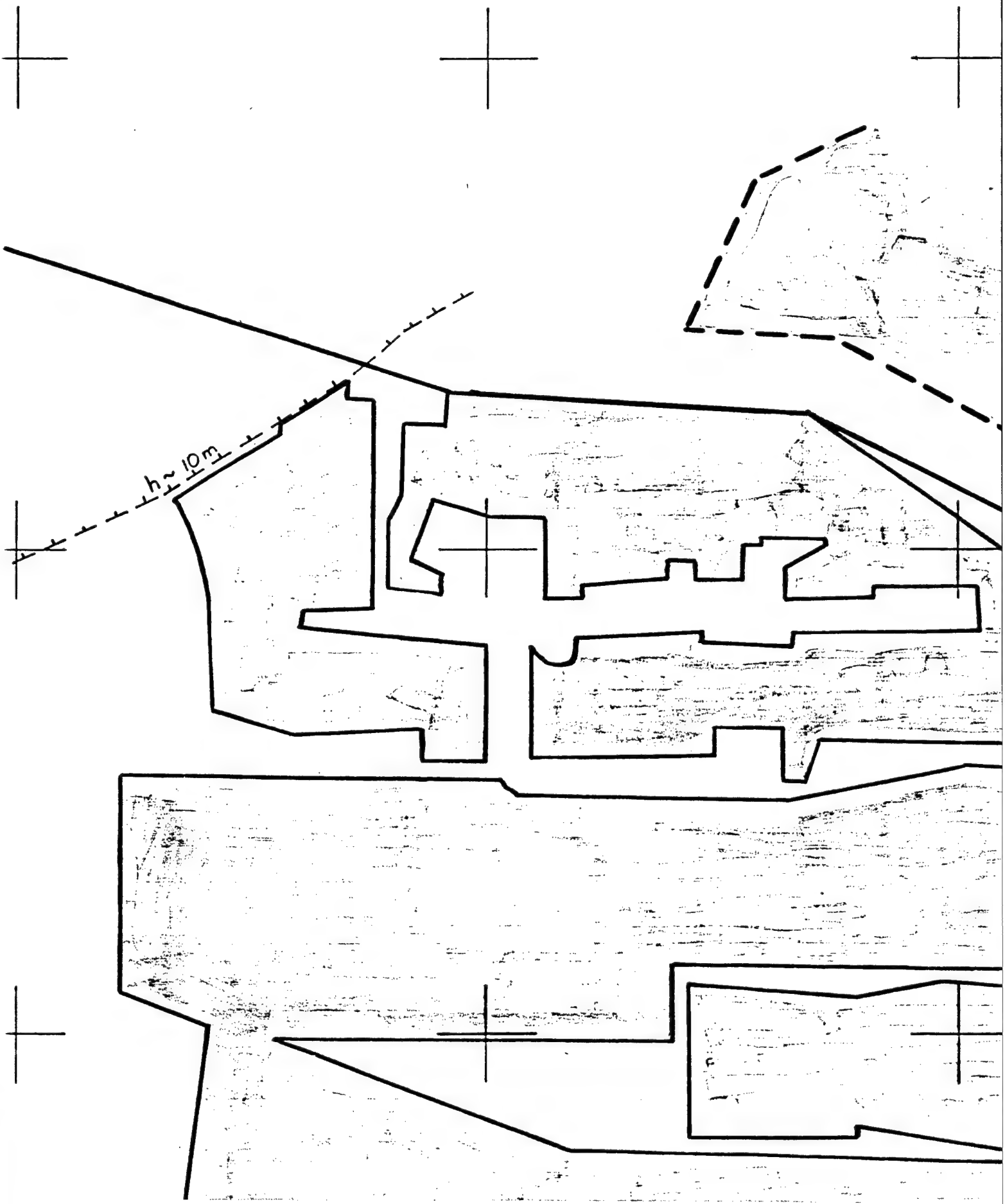
h ~ 10m

(5)

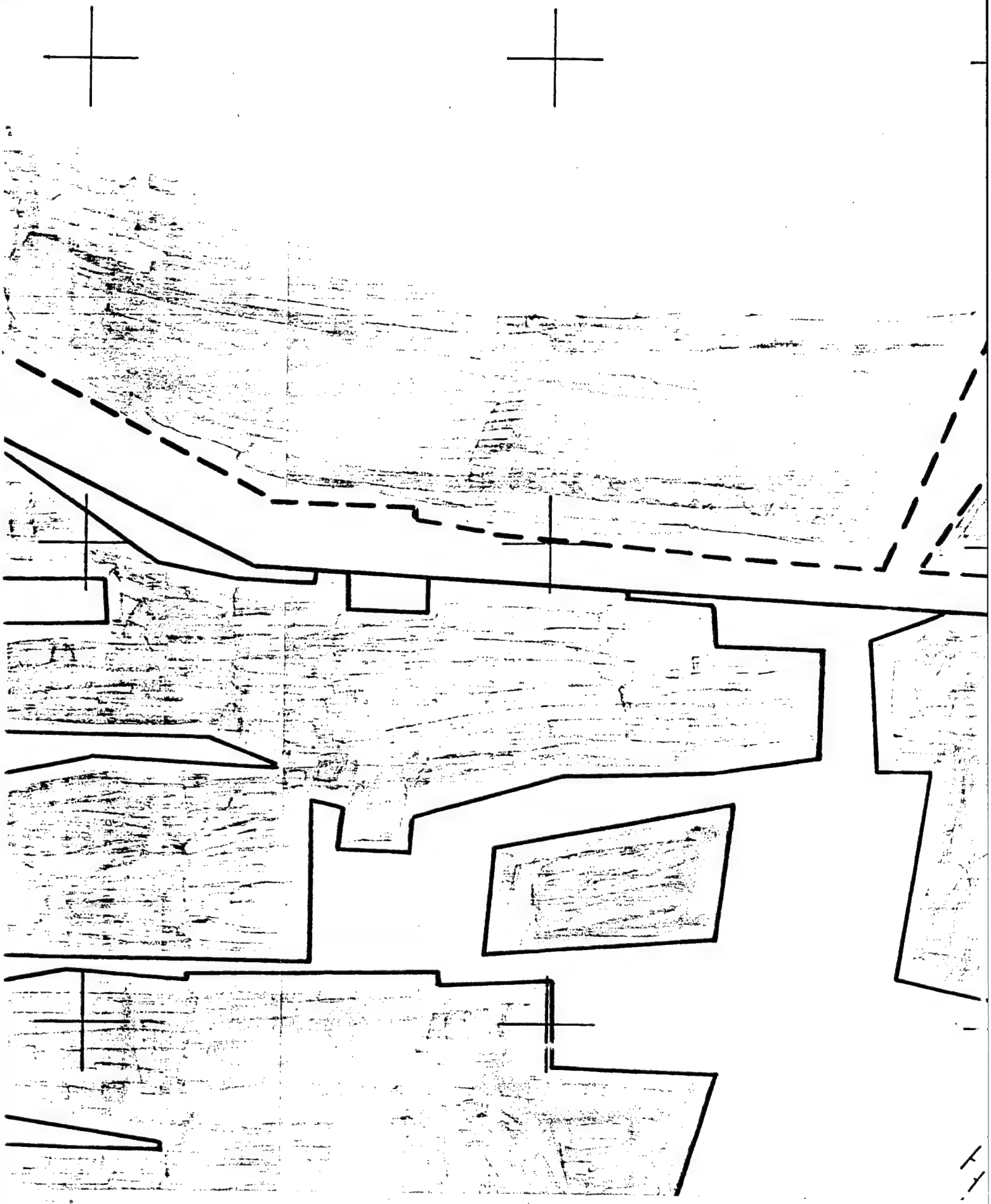

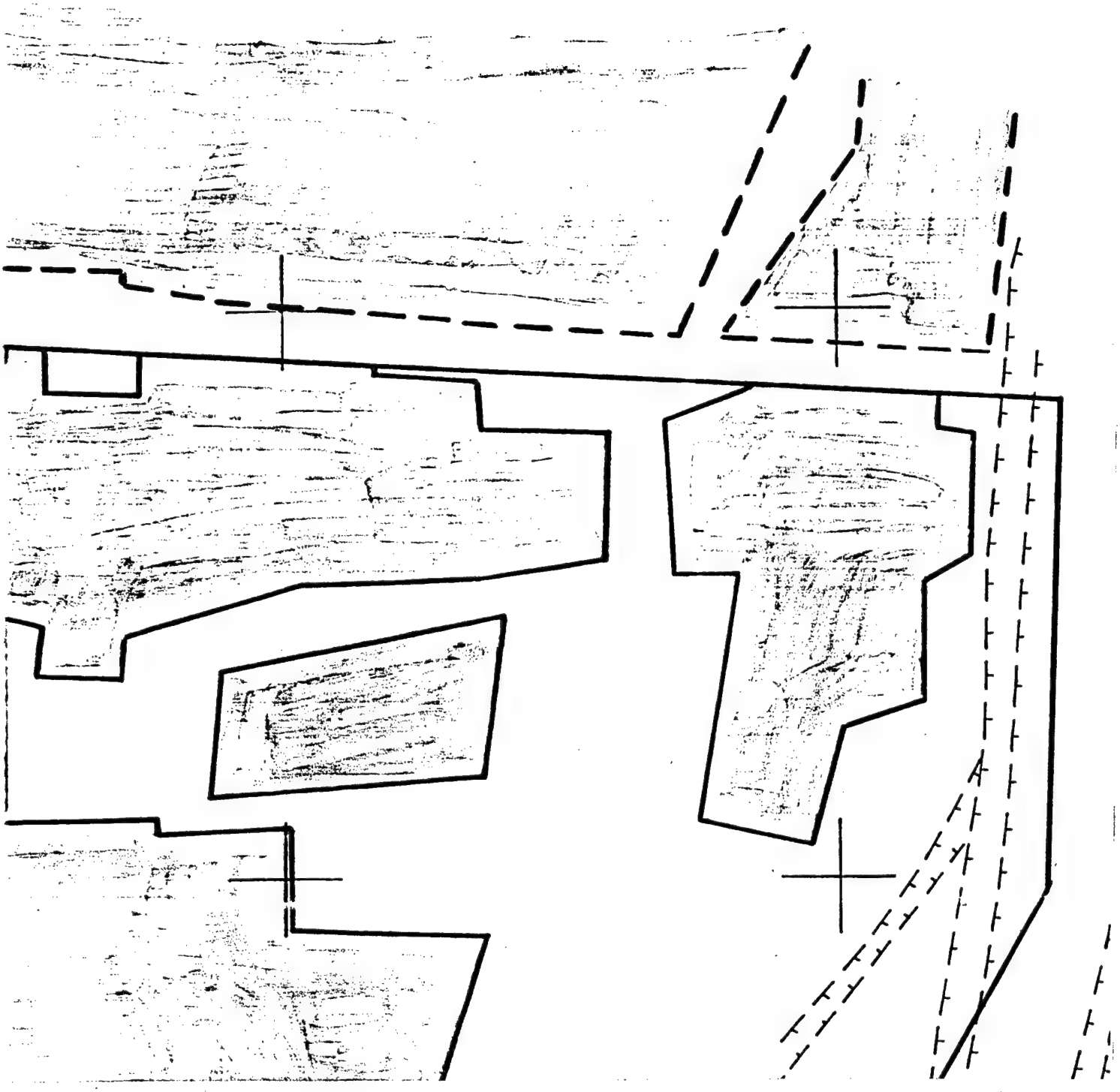

(7)

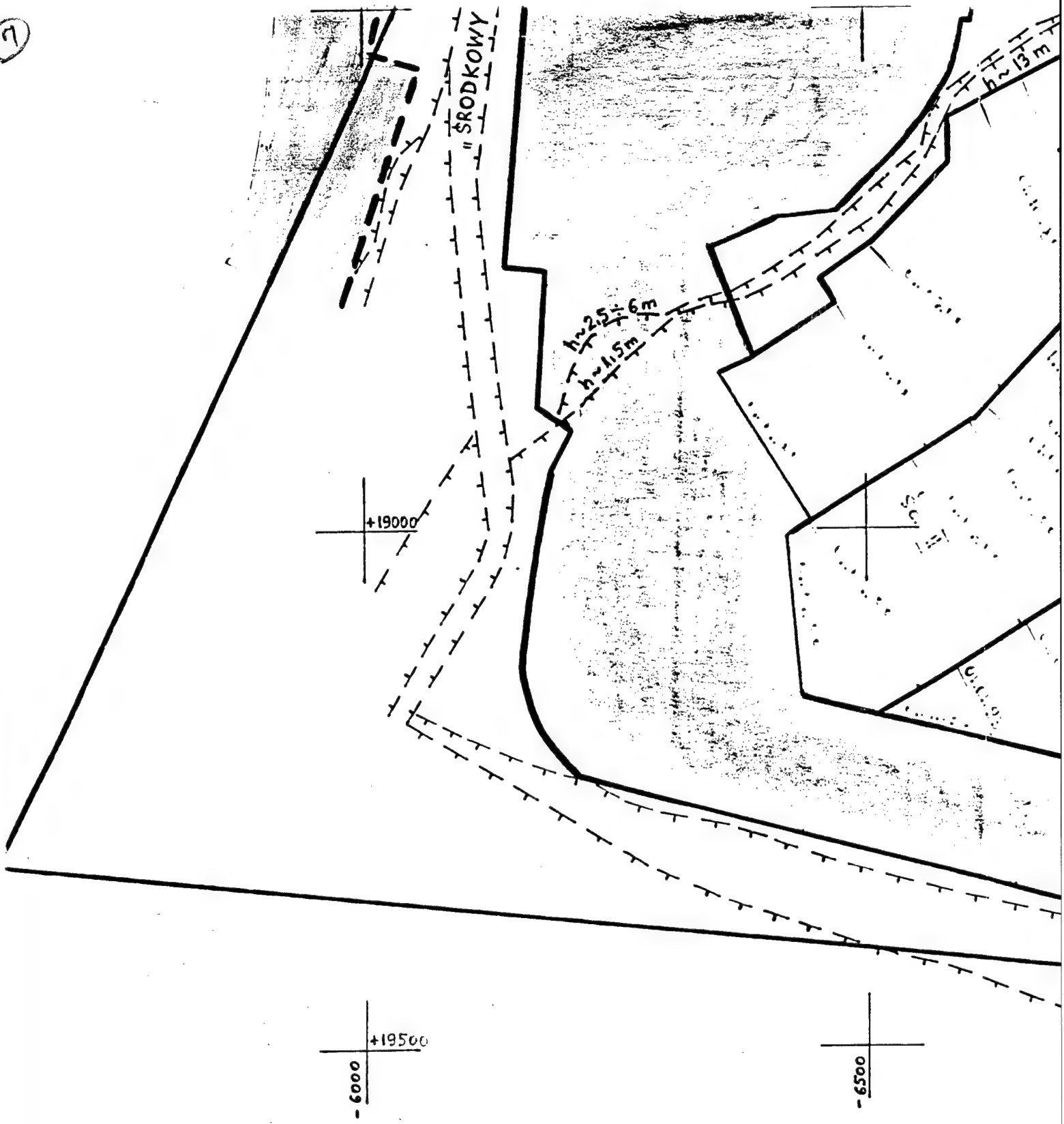

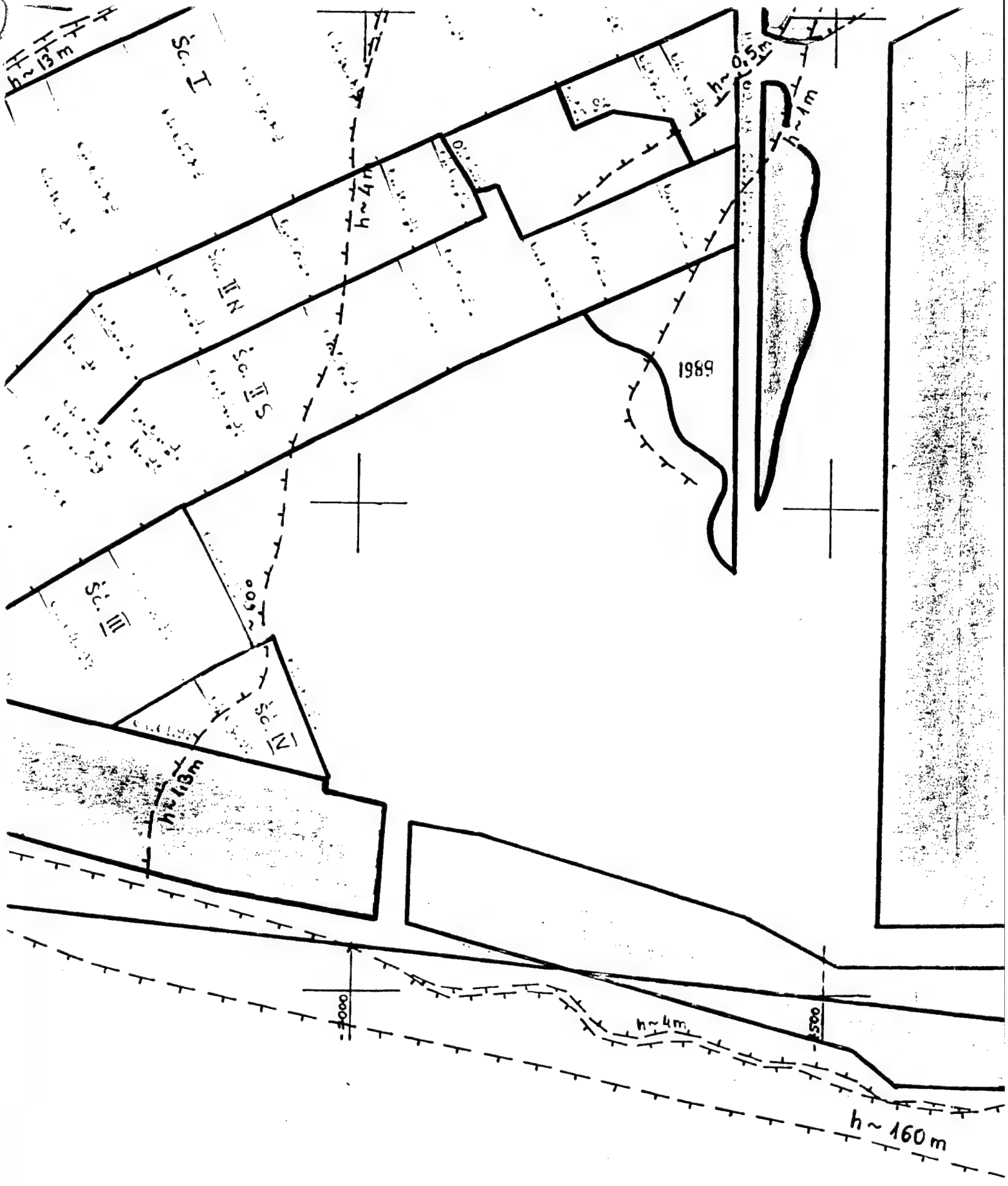
8
h~13m
Sc. I
h~0,5m
h~1m
h~4m
Sc. II N
Sc. II S
1989
Sc. III
Sc. IV
h~1,3m
-1000
h~4m
-500
h~160m

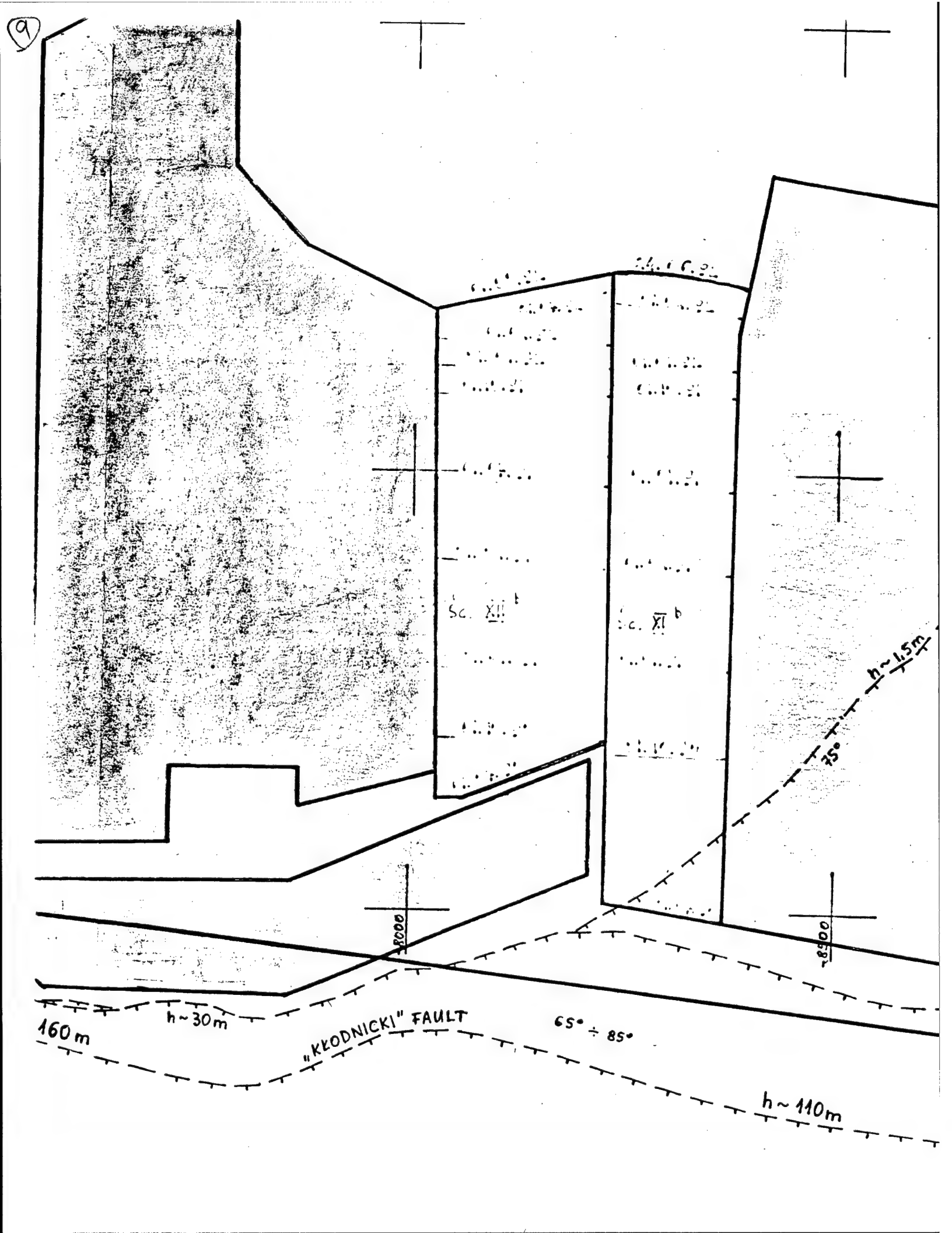
9
Sc. XII b
Sc. XI b
h~1,5m
75°
-8000
-8900
h~30m
160 m
"KŁODNICKI" FAULT
65° ÷ 85°
h~110m

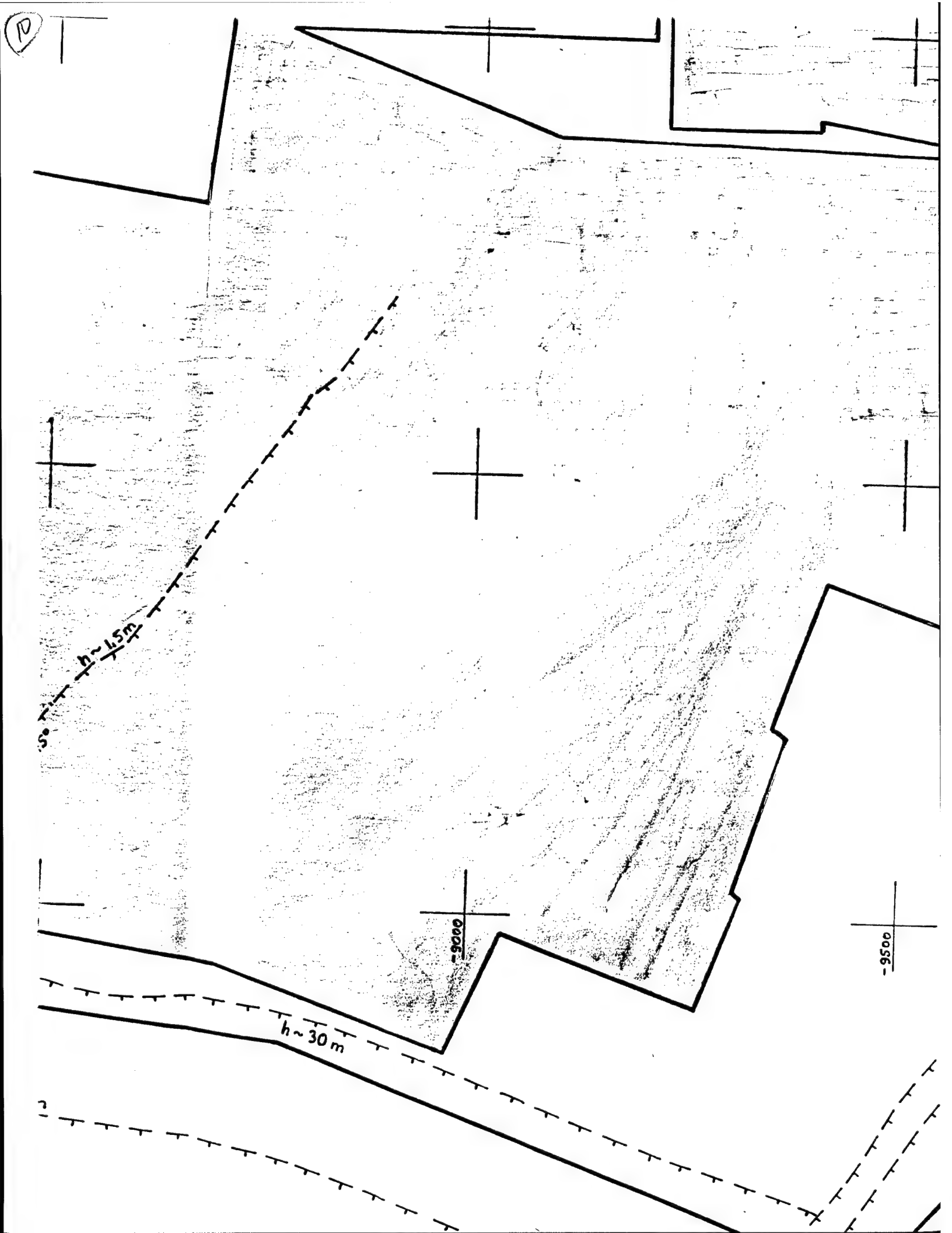
h~1.5m
-9000
-9500
h~30m

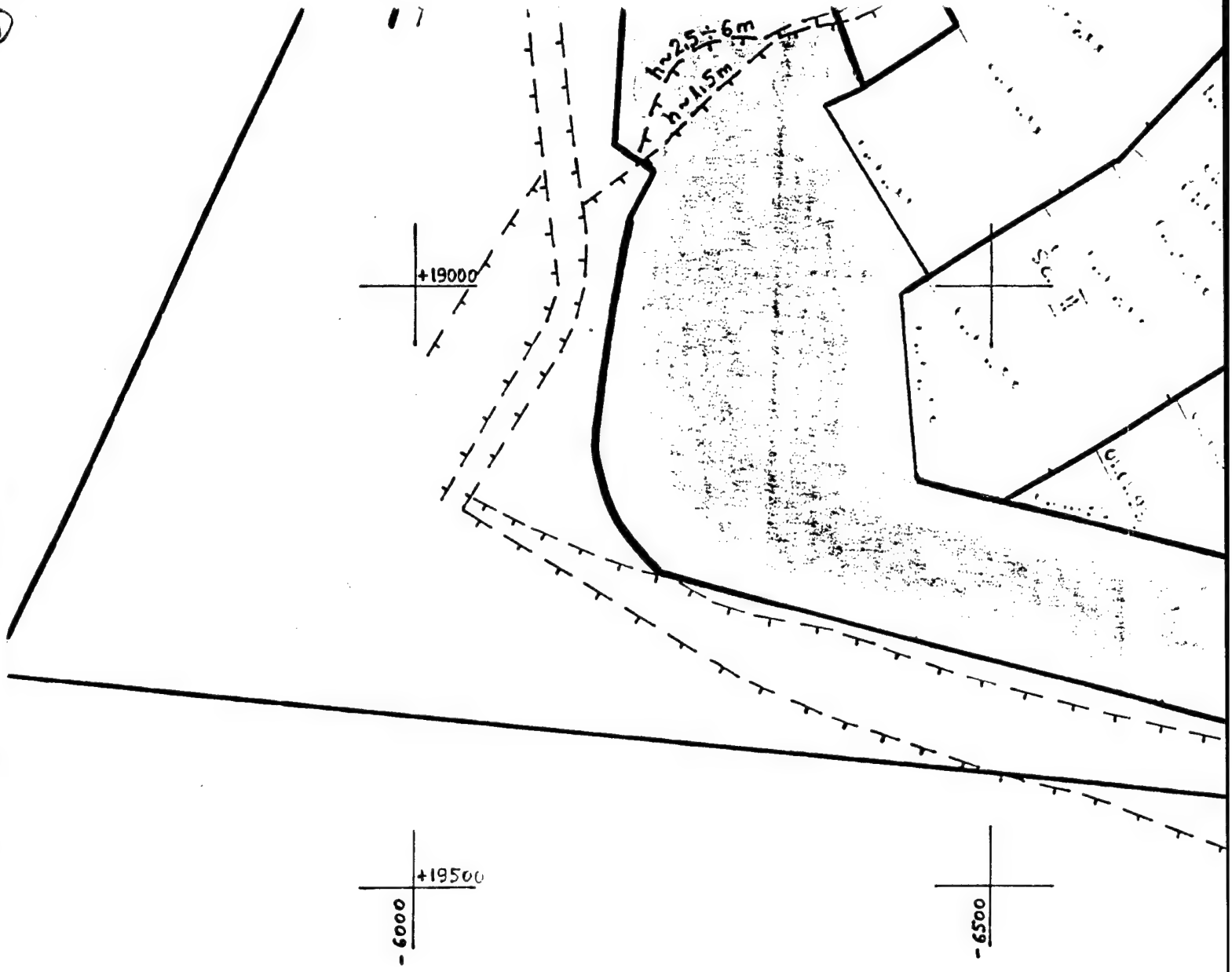
①
h~2.5÷6m
h~1.5m
+19000
+19500
-6000
-6500

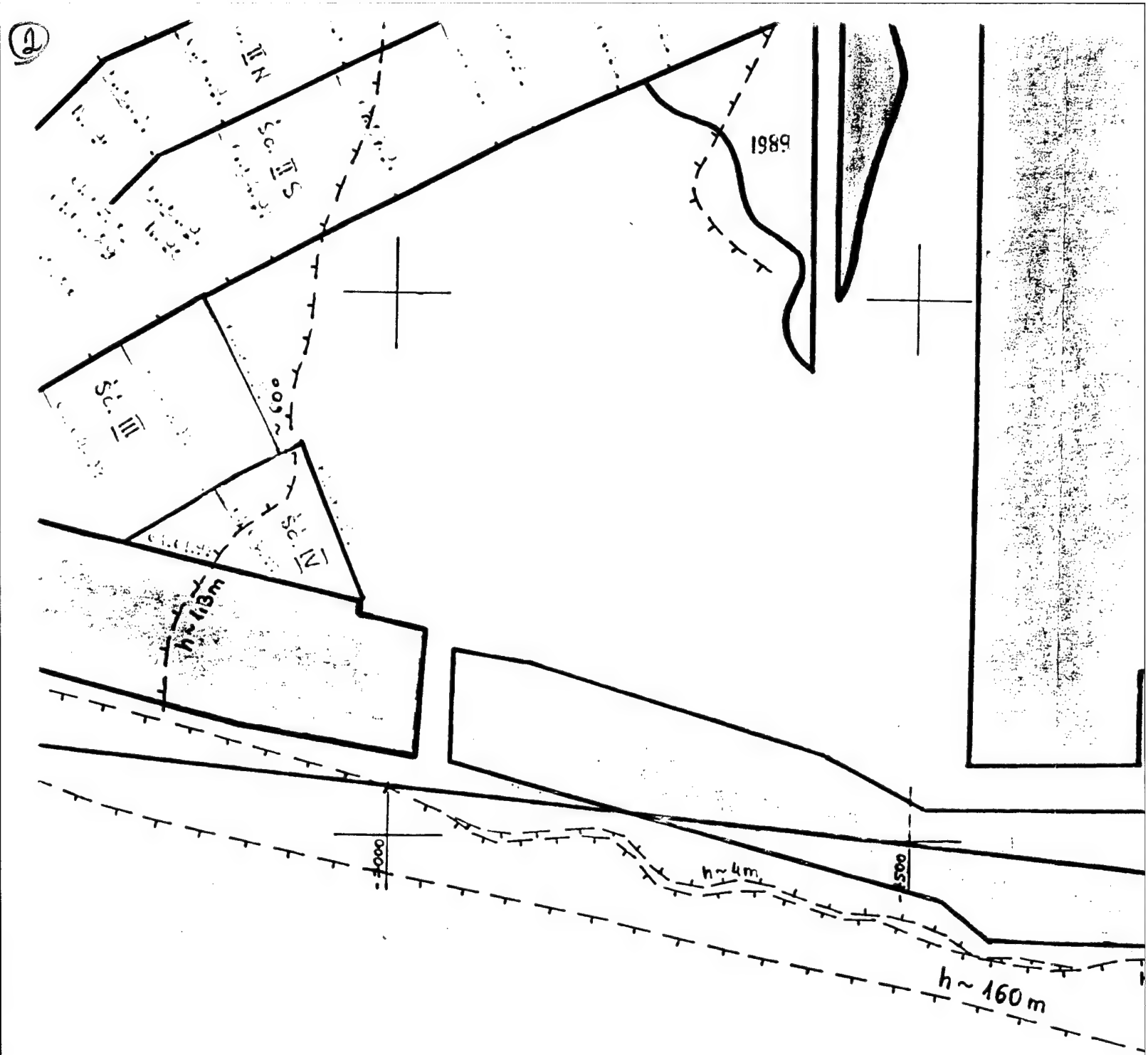
1
Sc. II N
Sc. II S
1989
Sc. III
Sc. IV
h~1,3m
h~4m
h~160m

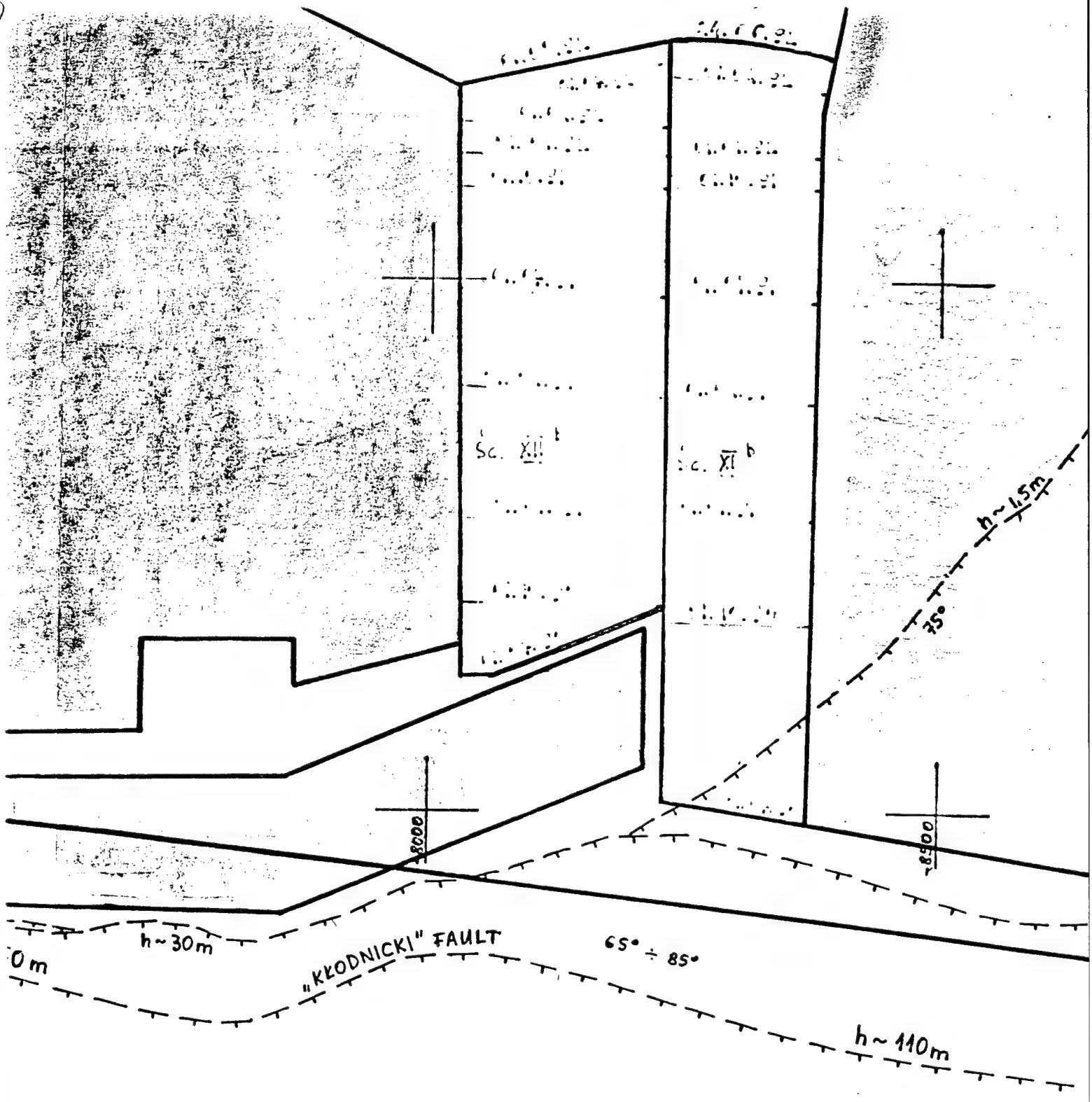
Sc. XII b
Sc. XI b
-8000
-8500
h~1.5m
35°
h~30m
"KŁODNICKI" FAULT
65° ÷ 85°
h~110m

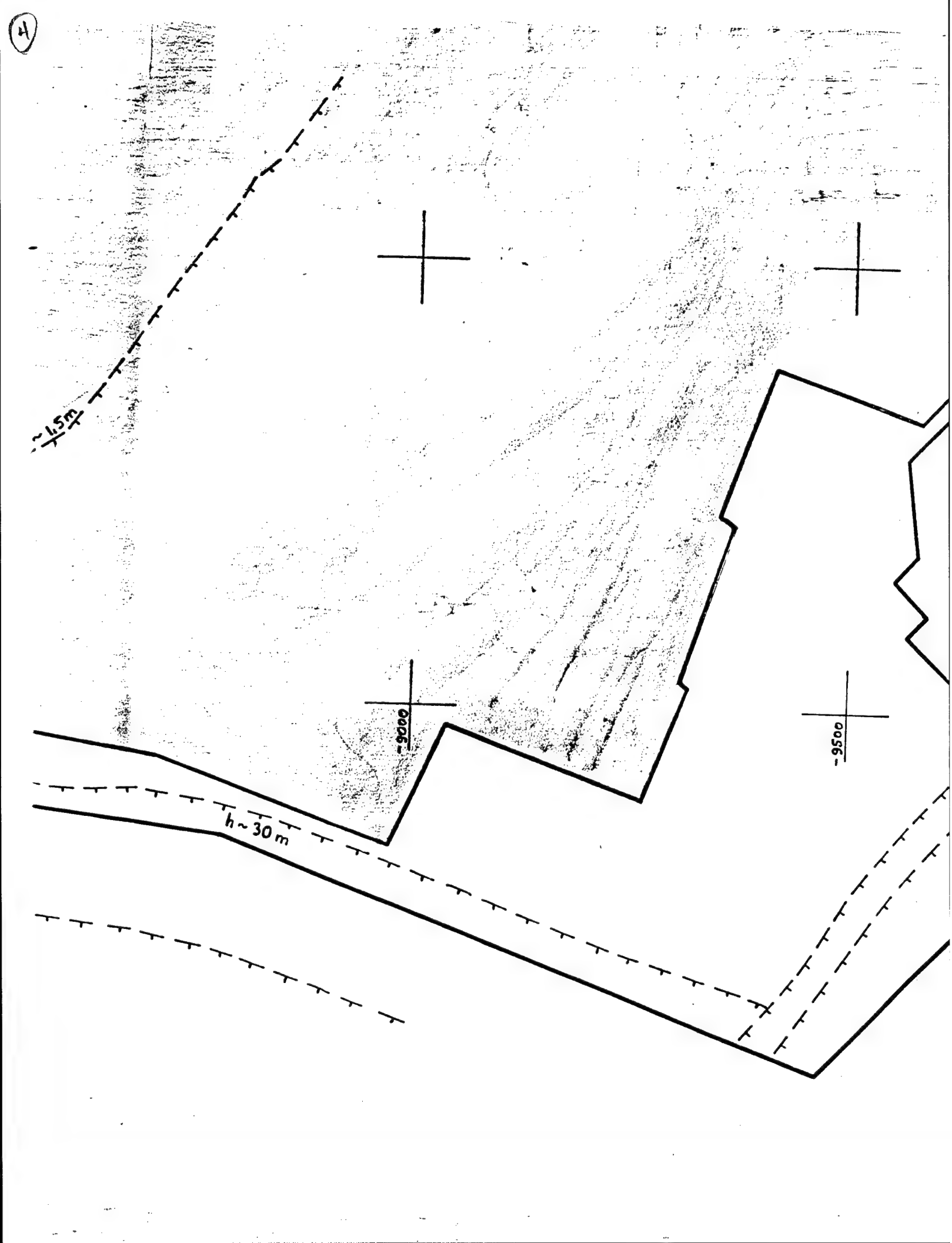
4
~1,5m
-9000
-9500
h ~ 30 m

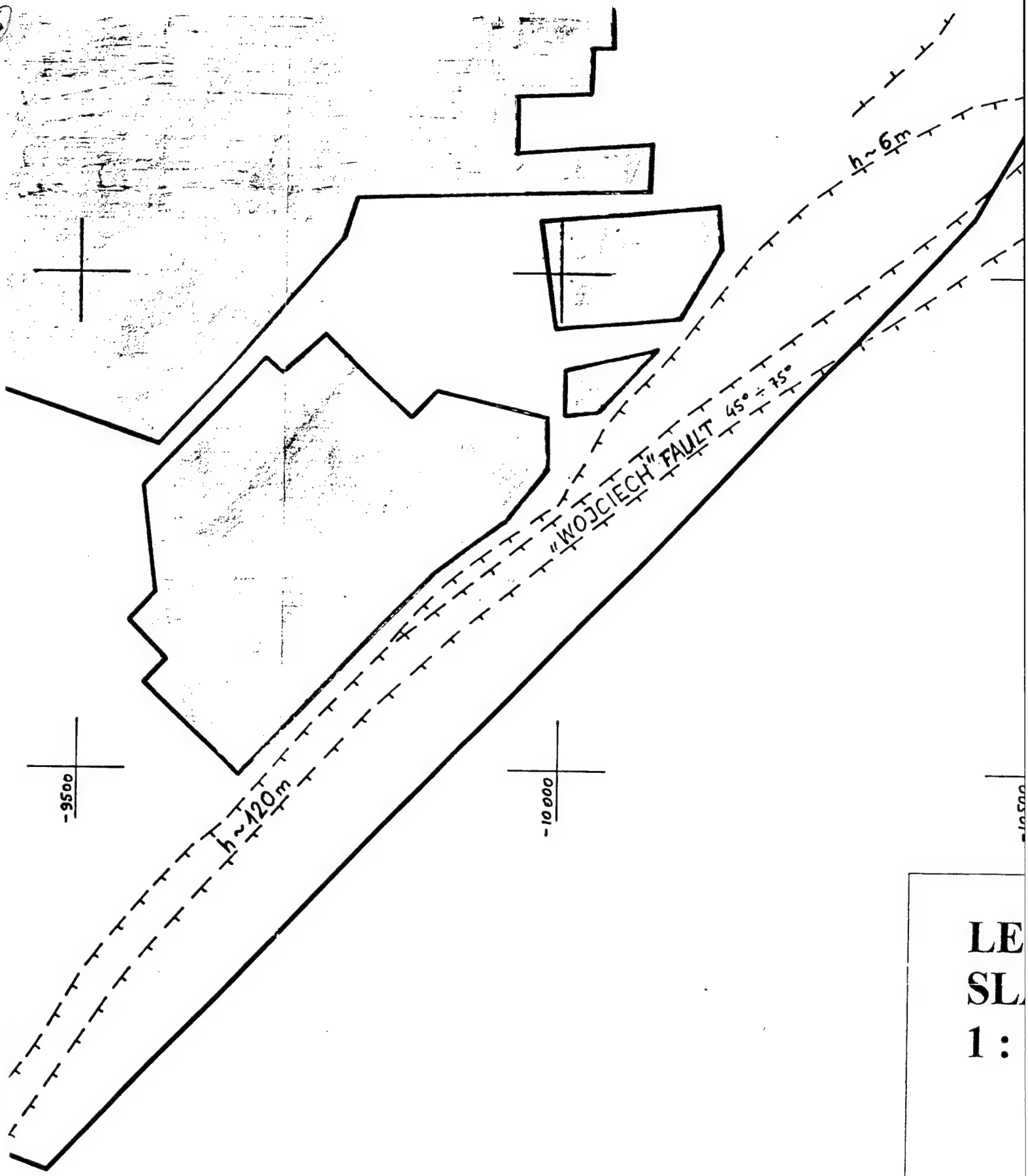

LE
SL
1 :

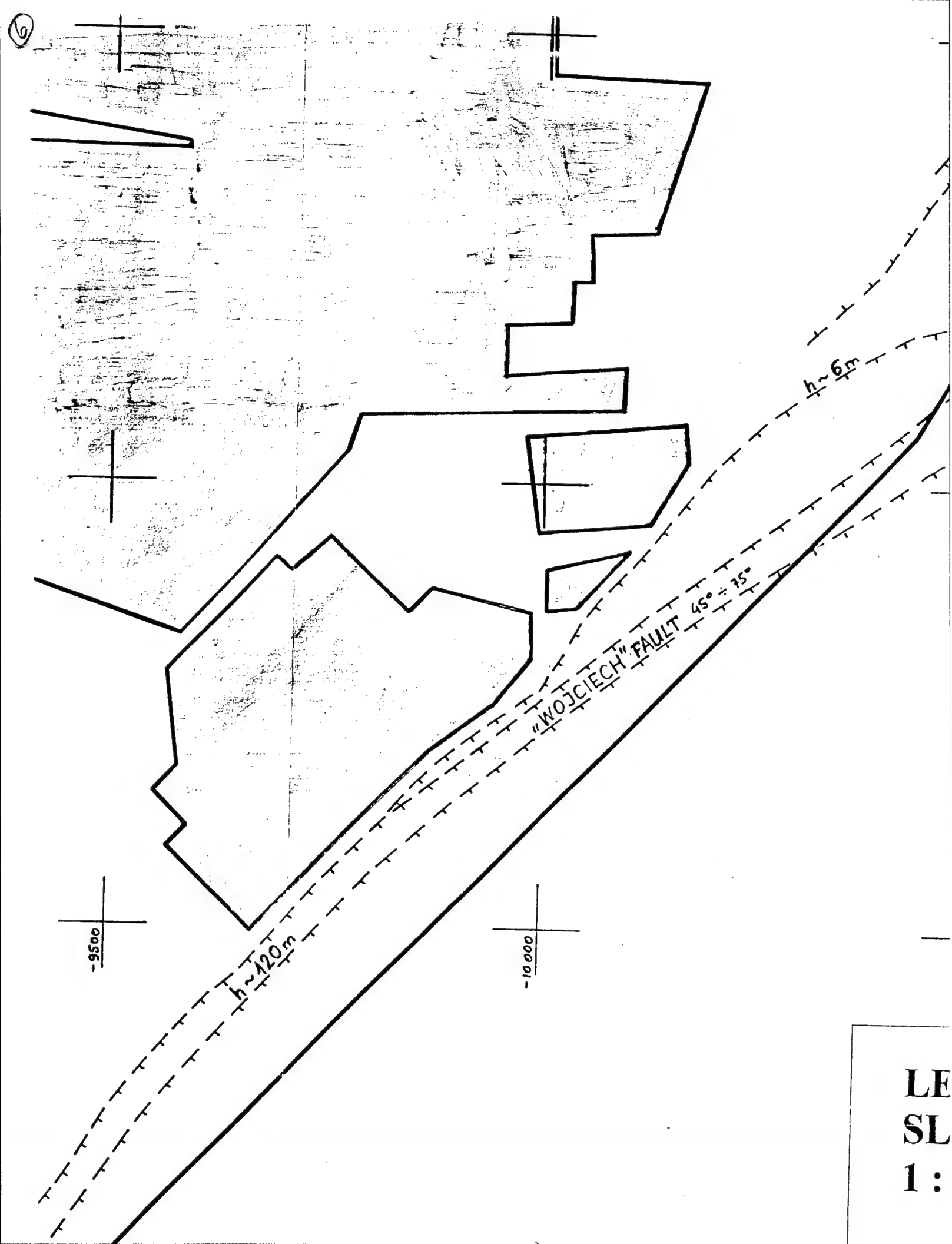

LE
SL
1 :

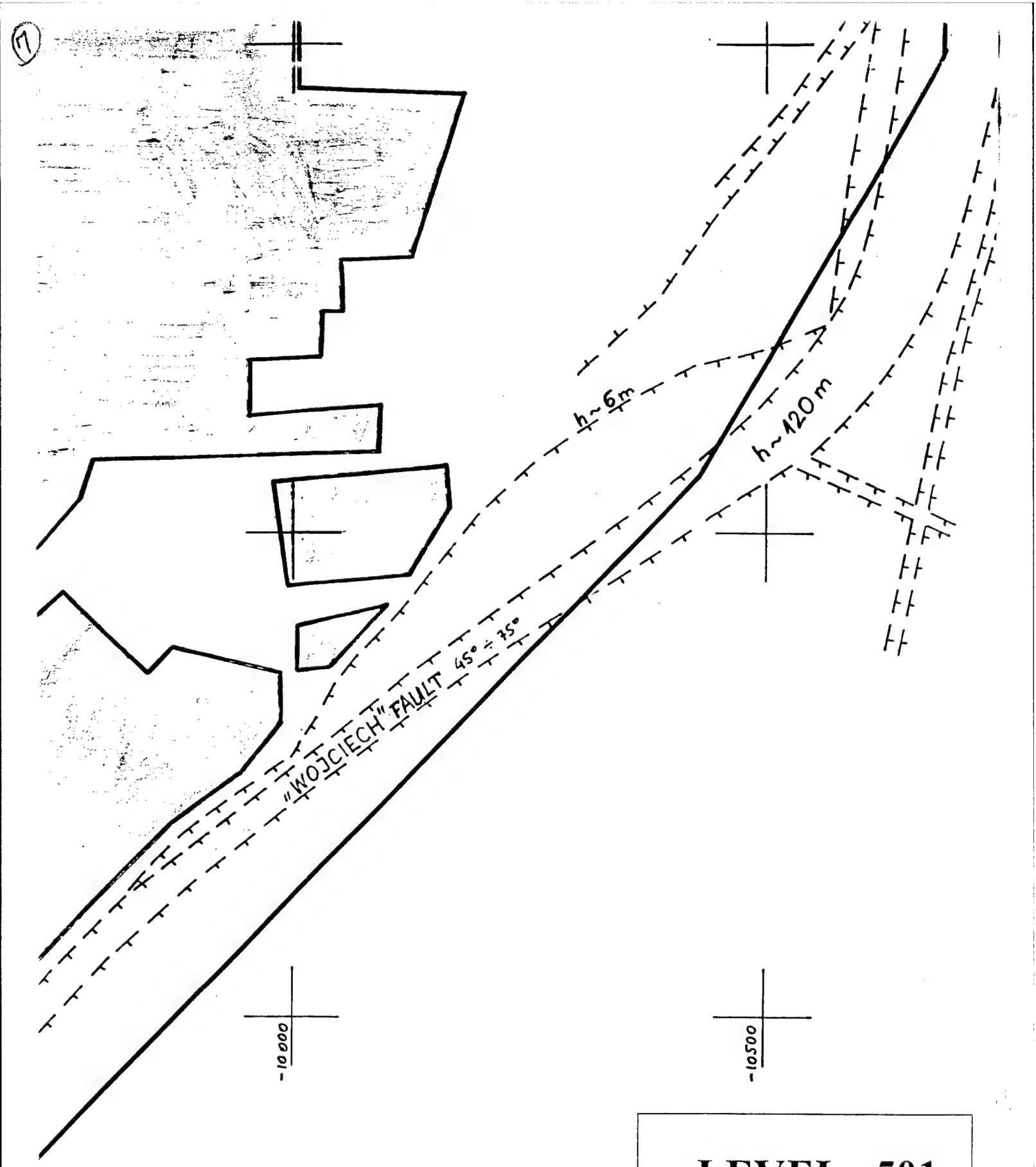

LEVEL 501
SLAB 3
1 : 5000

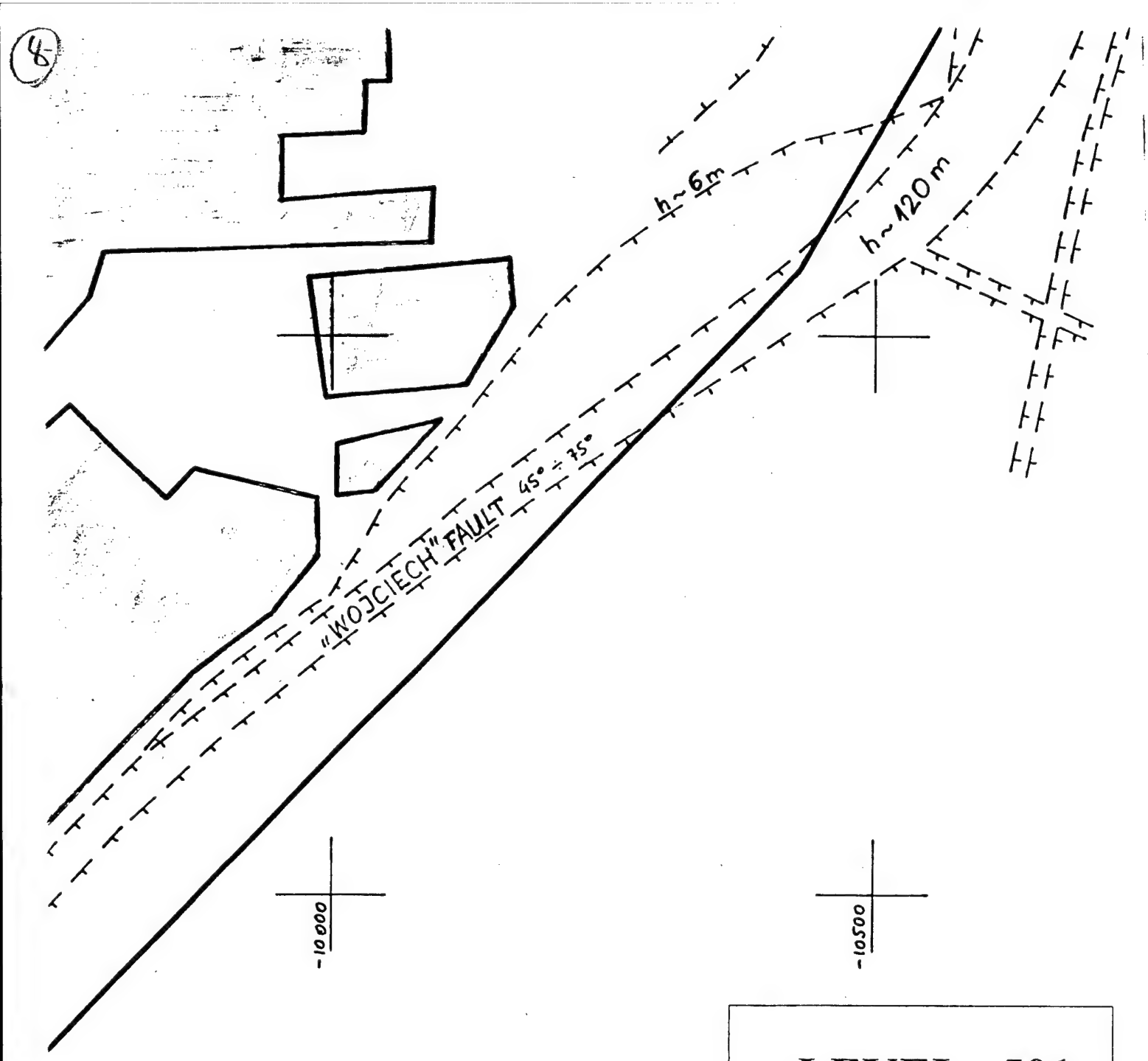

LEVEL 501
SLAB 3
1 : 5000

APPENDIX 3

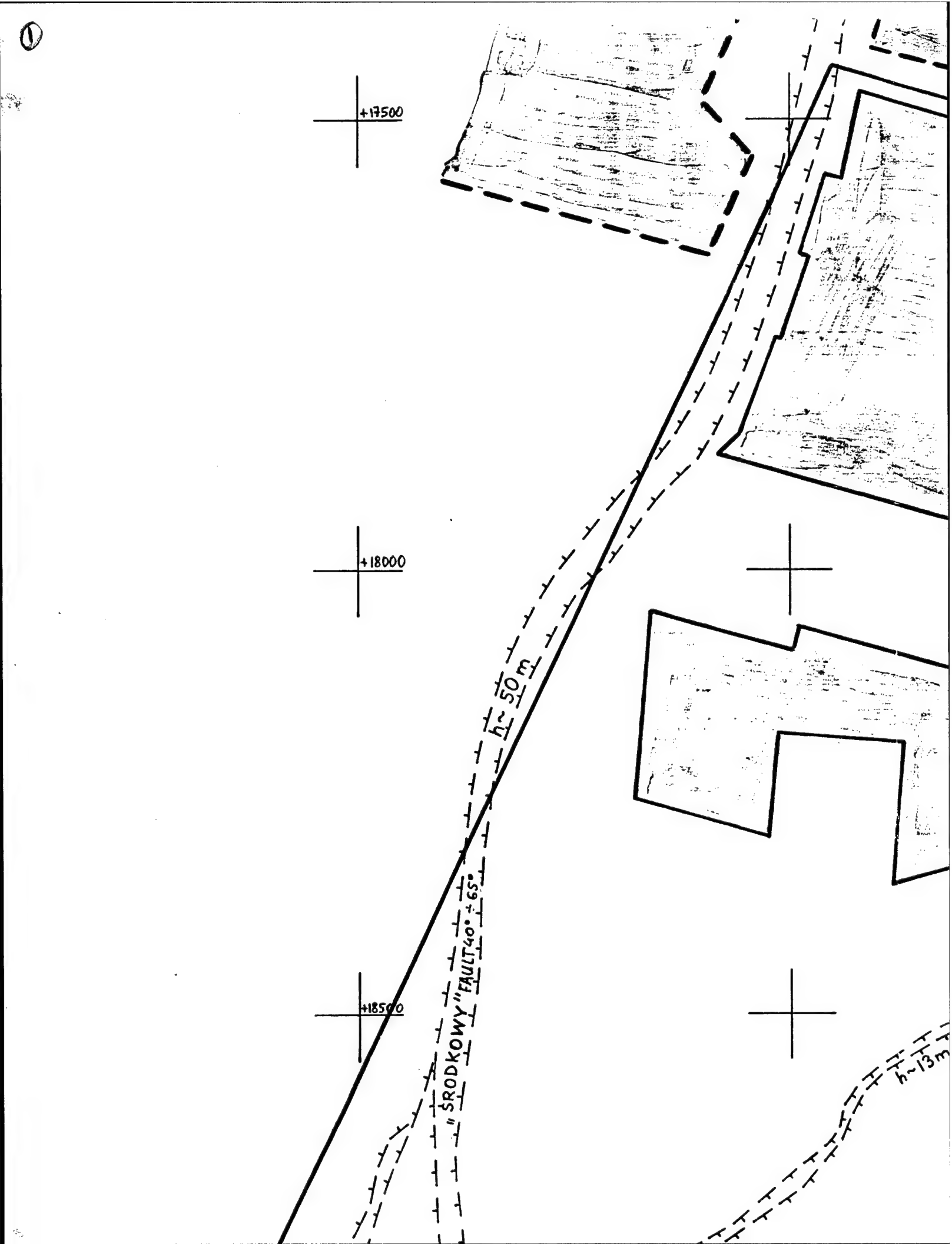
+17500
+18000
+18500
h~50m
"ŚRODKOWY" FAULT 40°÷65°
h~13m

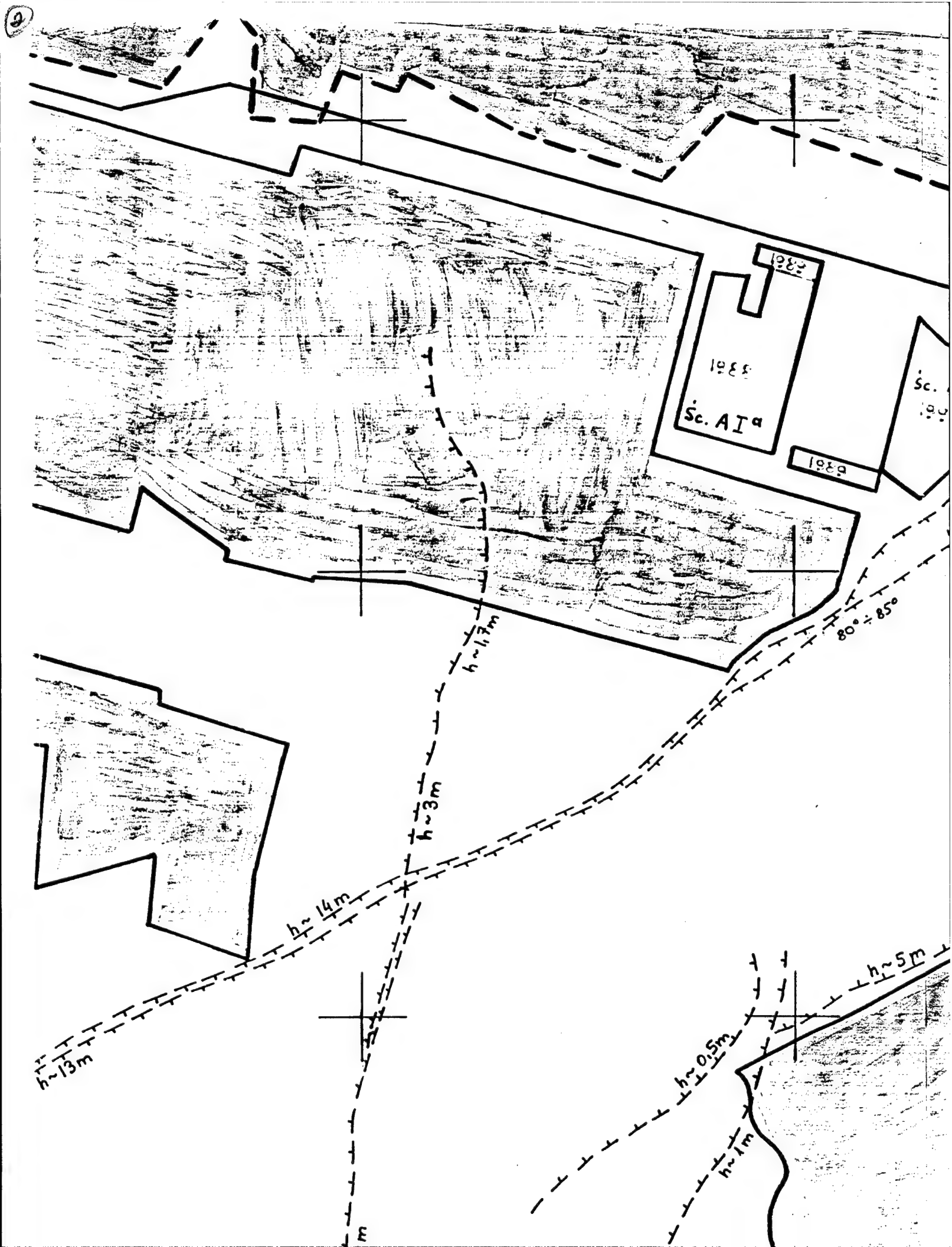
Sc. AI a
80° ÷ 85°
h~13m
h~14m
h~3m
h~17m
h~13m
h~0,5m
h~5m
h~1m

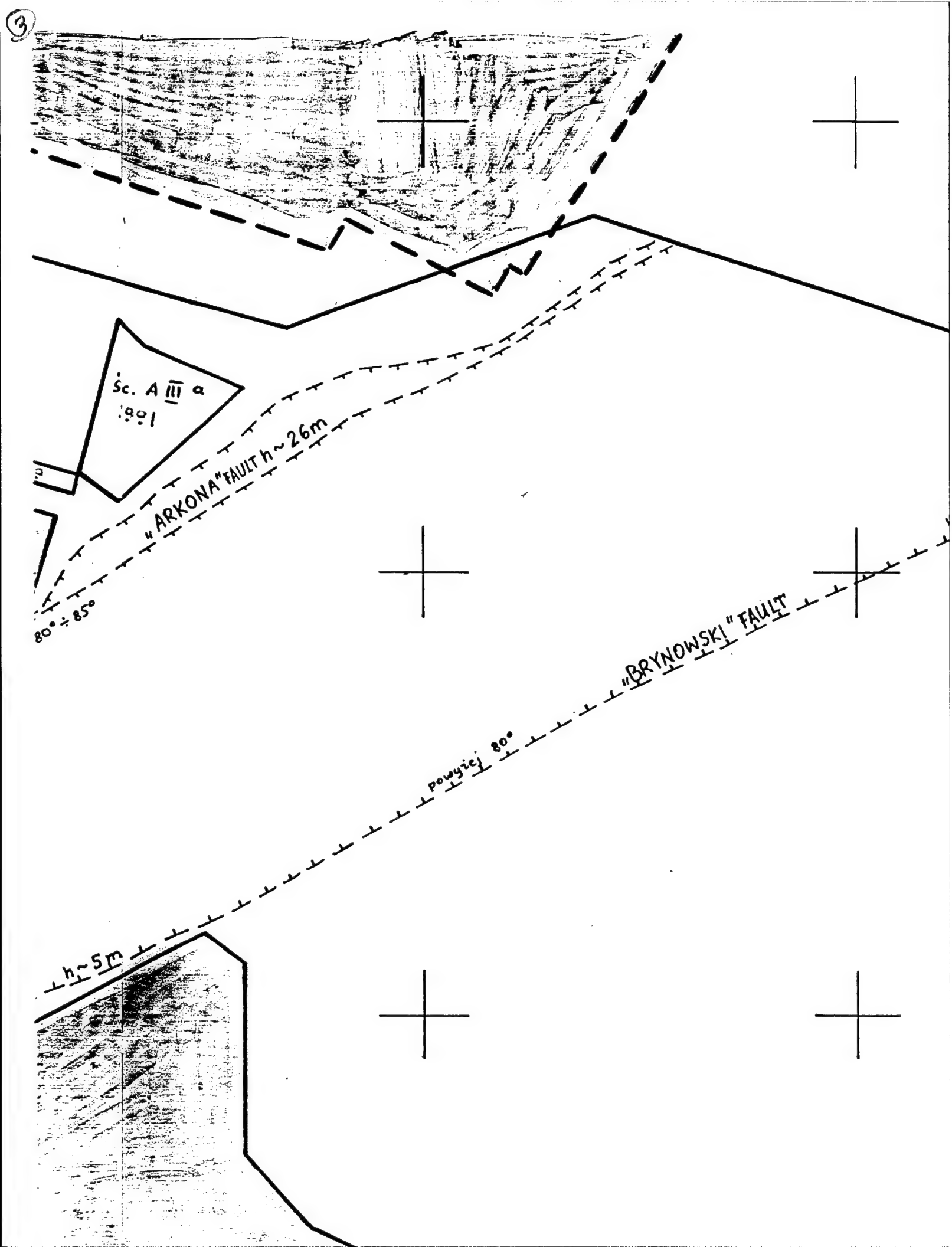
3
Sc. A III a
1981
"ARKONA" FAULT h~26m
80° ÷ 85°
"BRYNOWSKI" FAULT
powyżej 80°
h~5m

(4)

(5)

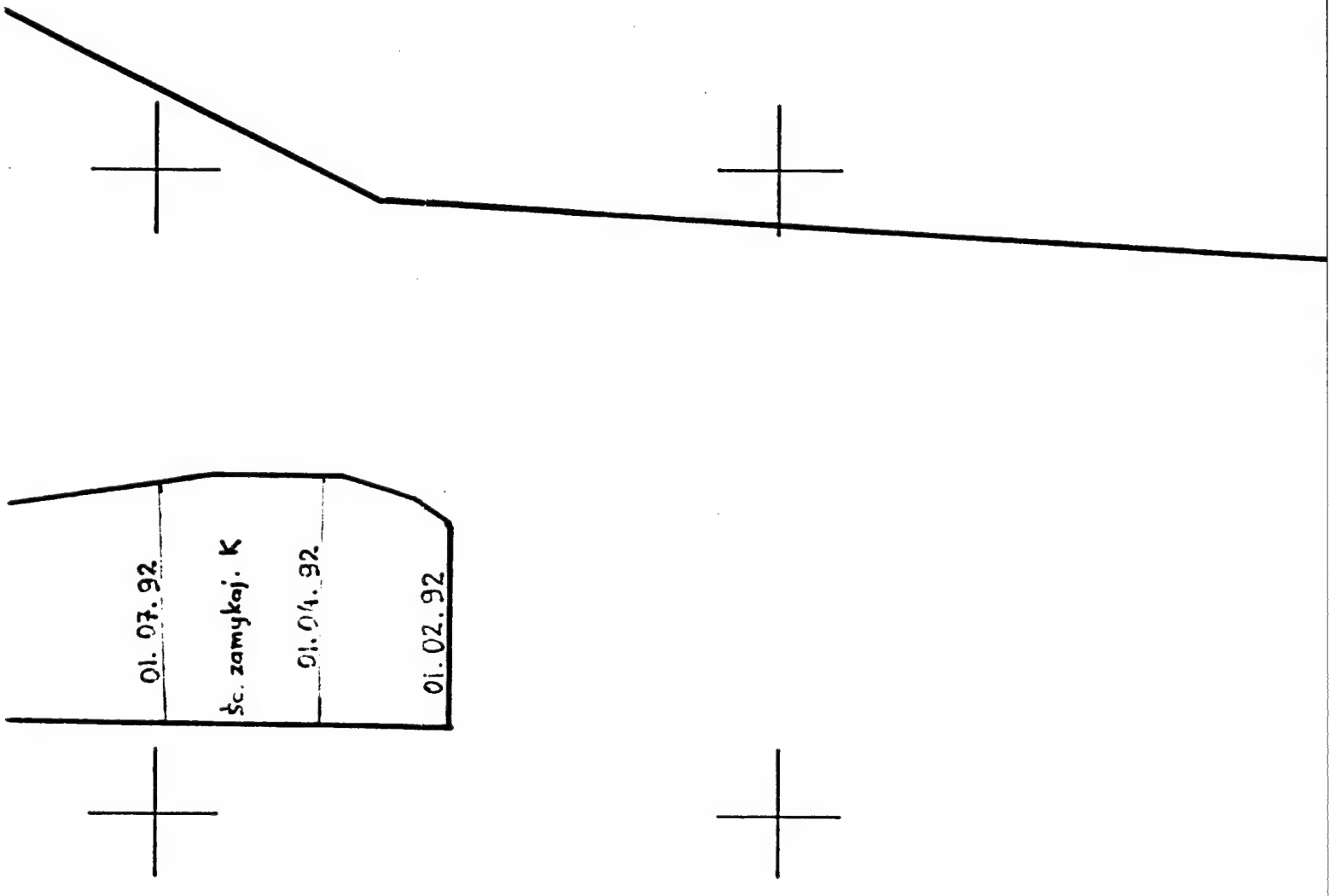

Wyeksploatowano na 2 warstwy

(b)

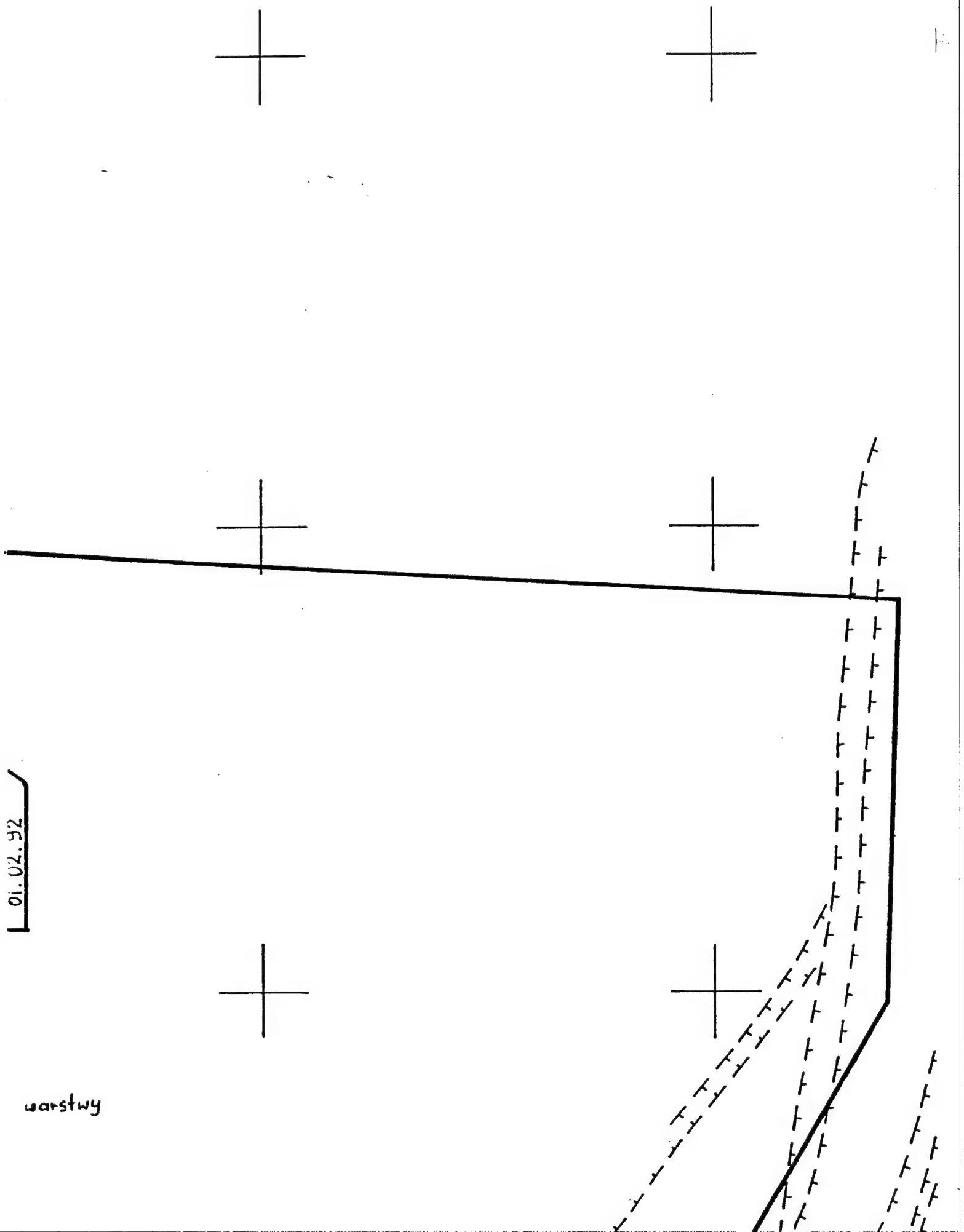

warstwy

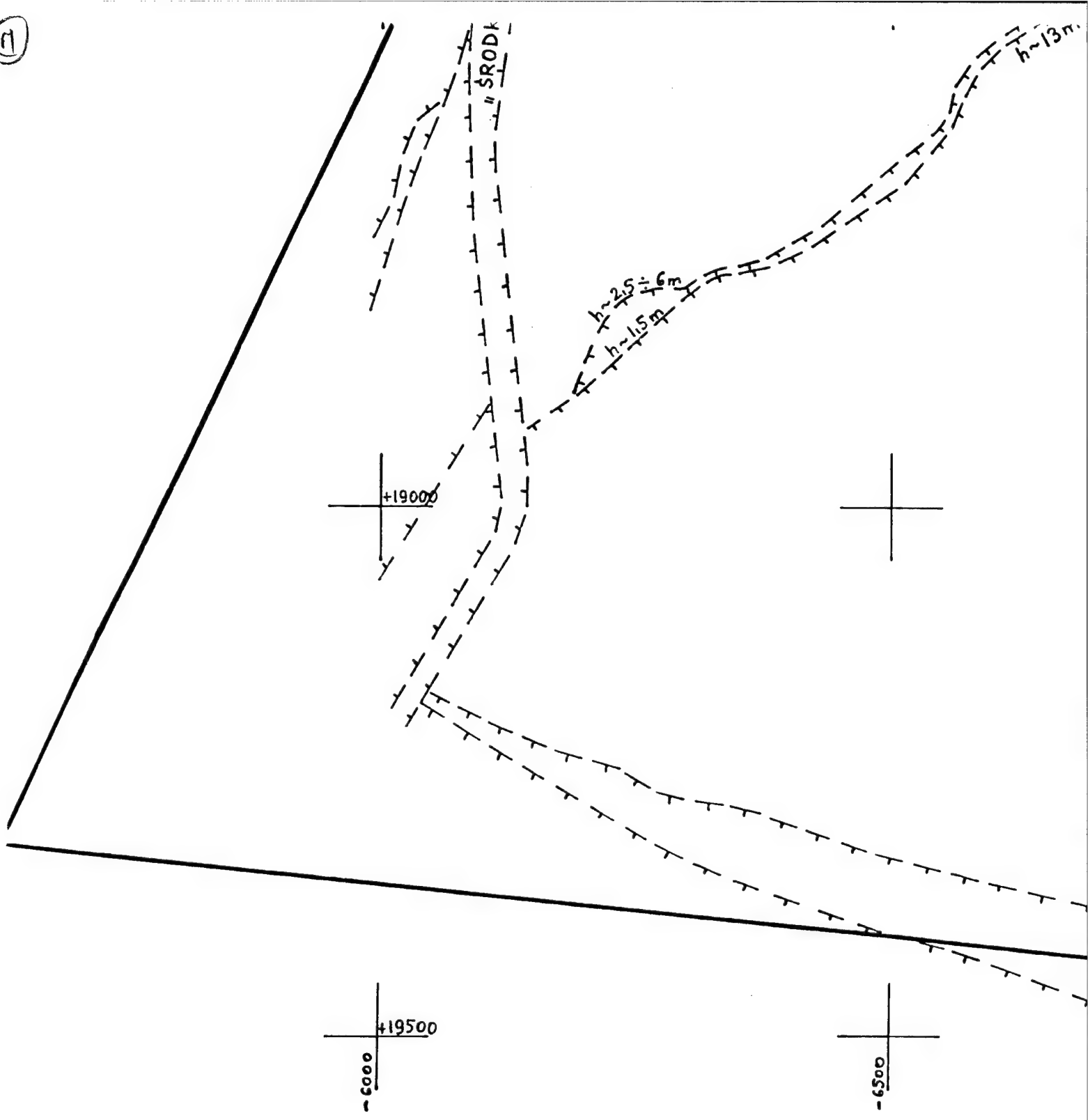
(1)
ŚRODK
h~13m
h~2,5÷6m
h~1,5m
+19000
+19500
-6000
-6500

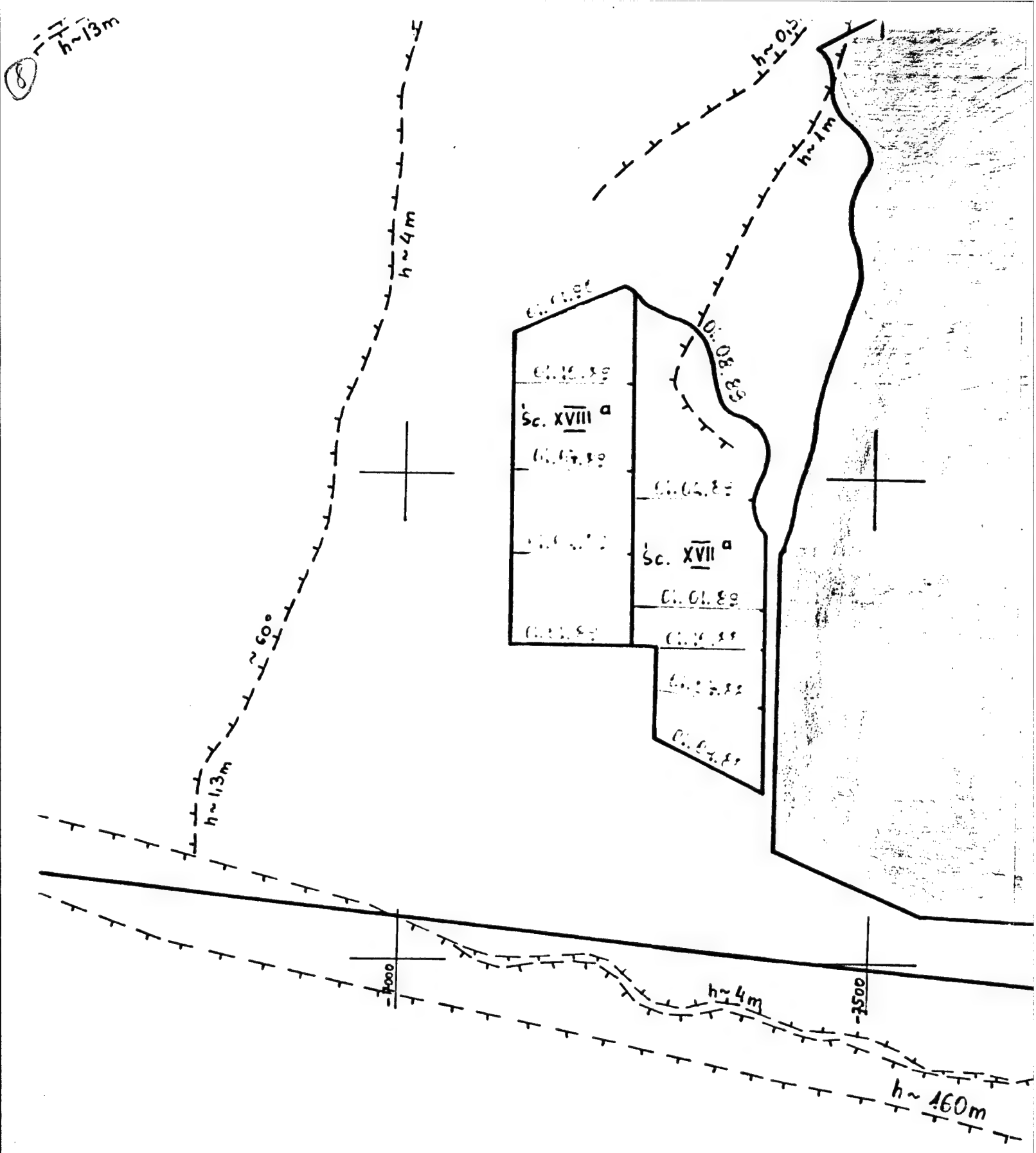
h~13m
h~0,5
h~1m
h~4m
h~1,3m
~60°
Sc. XVIII a
Sc. XVII a
-1000
-1500
h~4m
h~160m

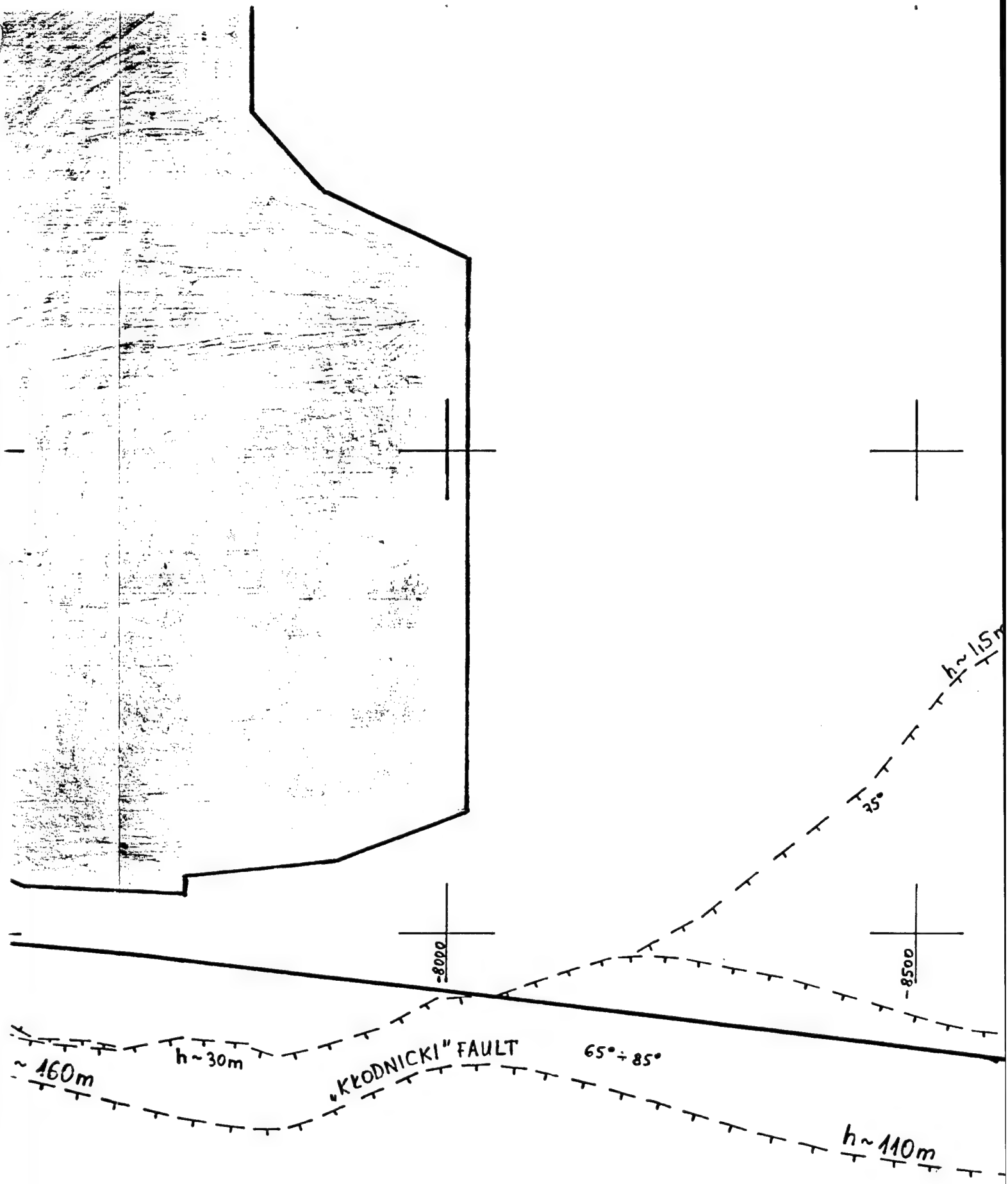
-8000
-8500
h~115m
25°
h~30m
~160m
„KŁODNICKI" FAULT
65°÷85°
h~110m

(10)

Wyeksp

h~15m

-3000

-9500

h~30m

)m

(11)

wyeksploatowano na 2 warstwy

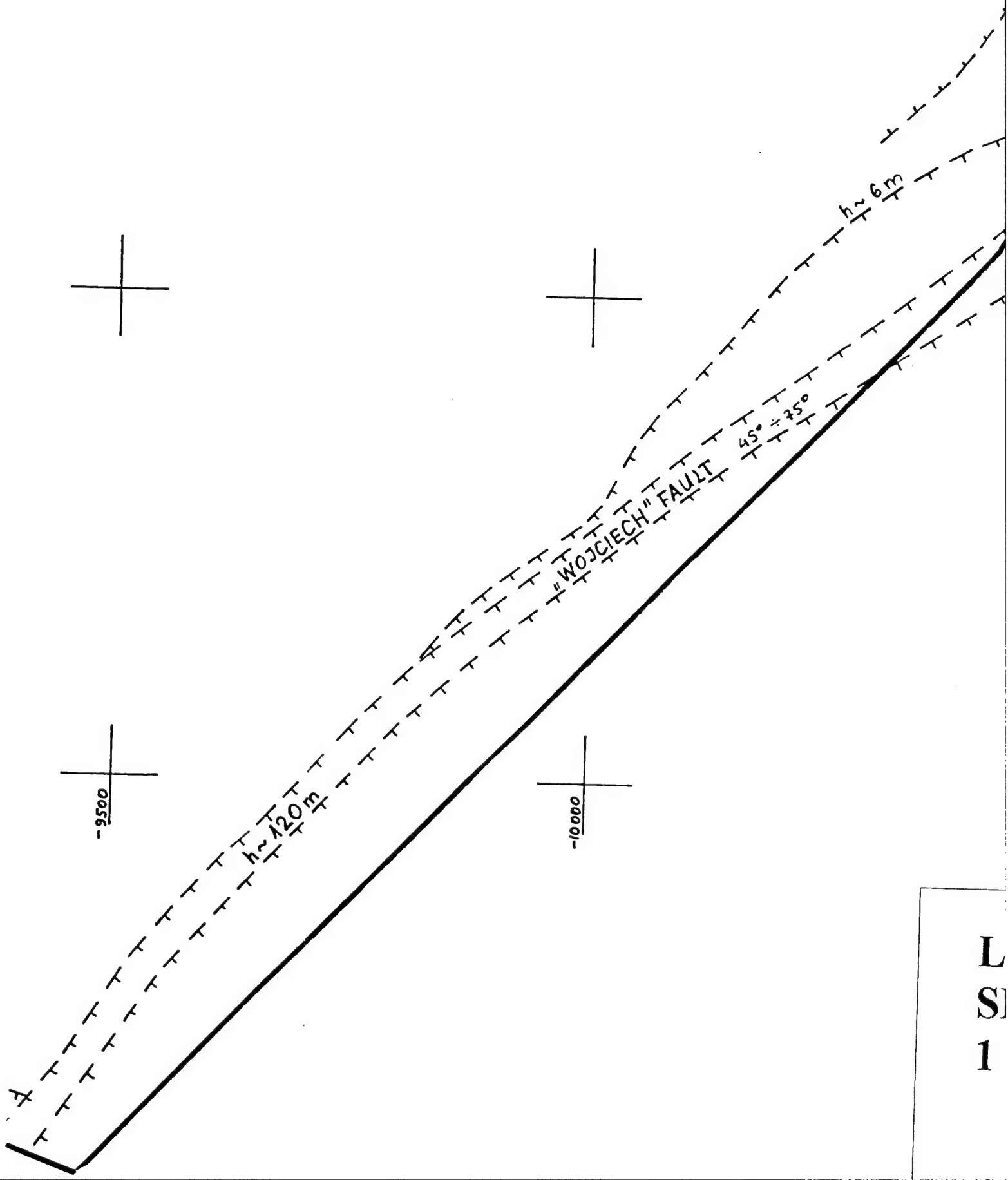

(12)

sarstwy

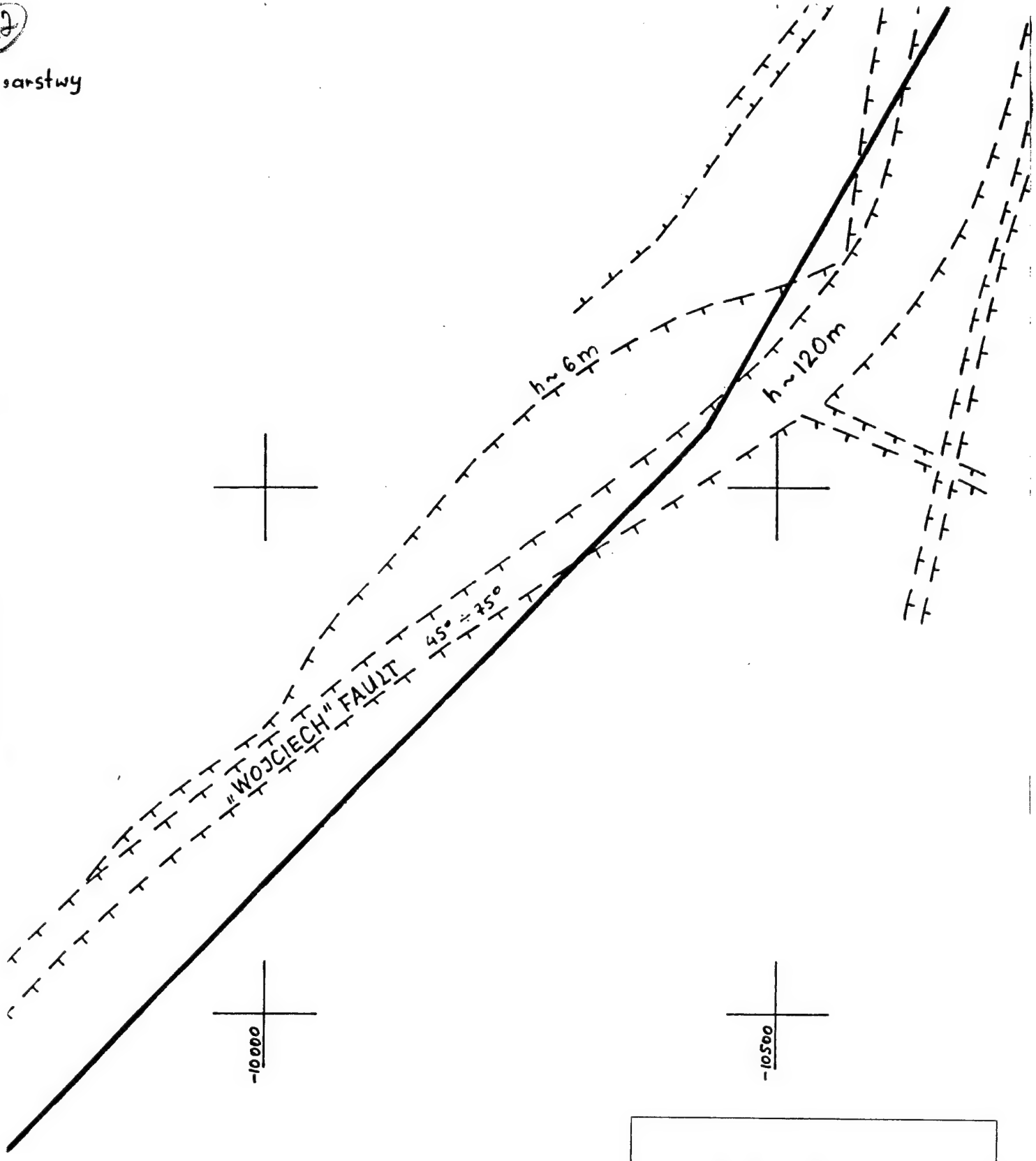

LEVEL 501
SLAB 2
1 : 5000

APPENDIX 4

(13)

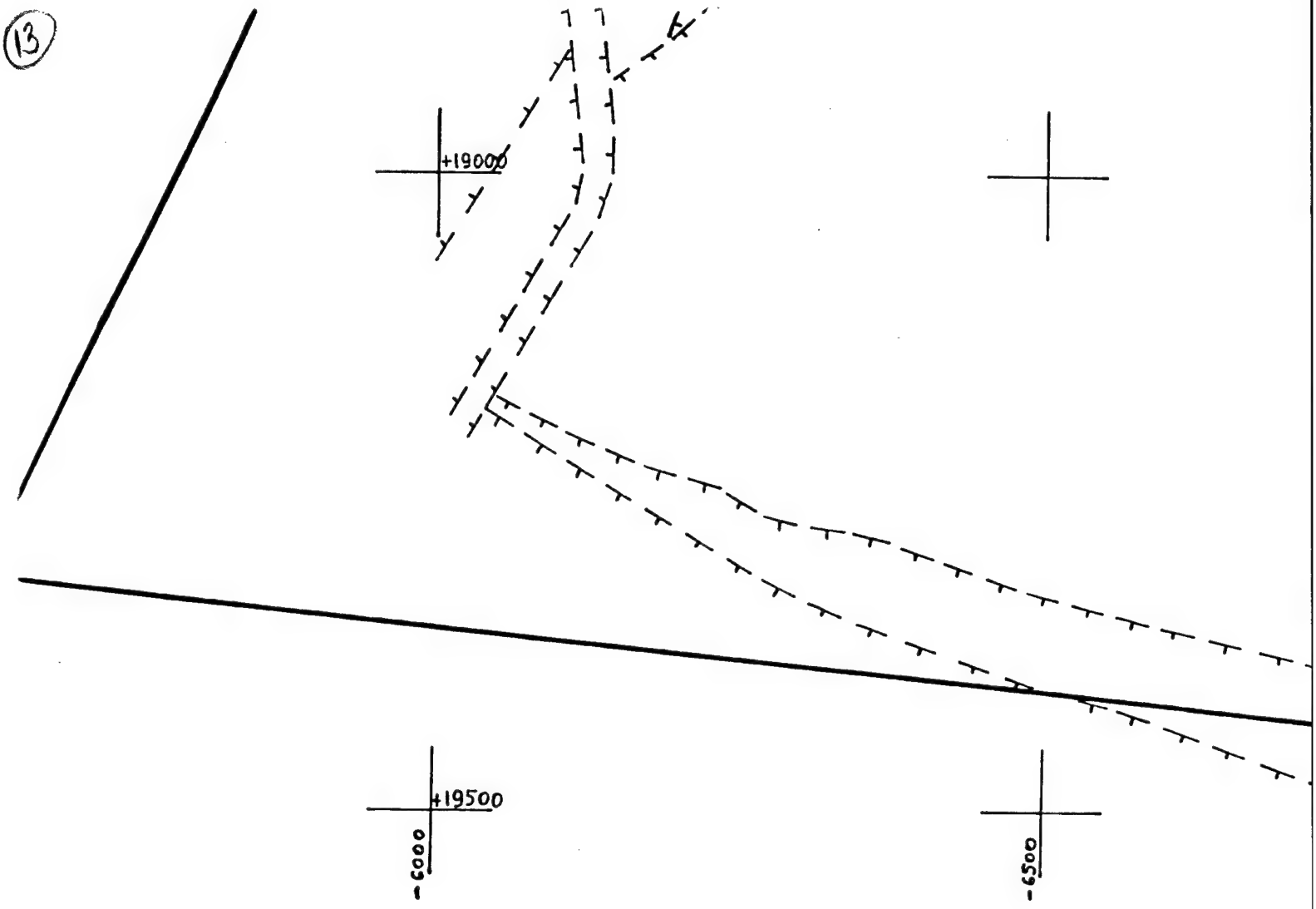

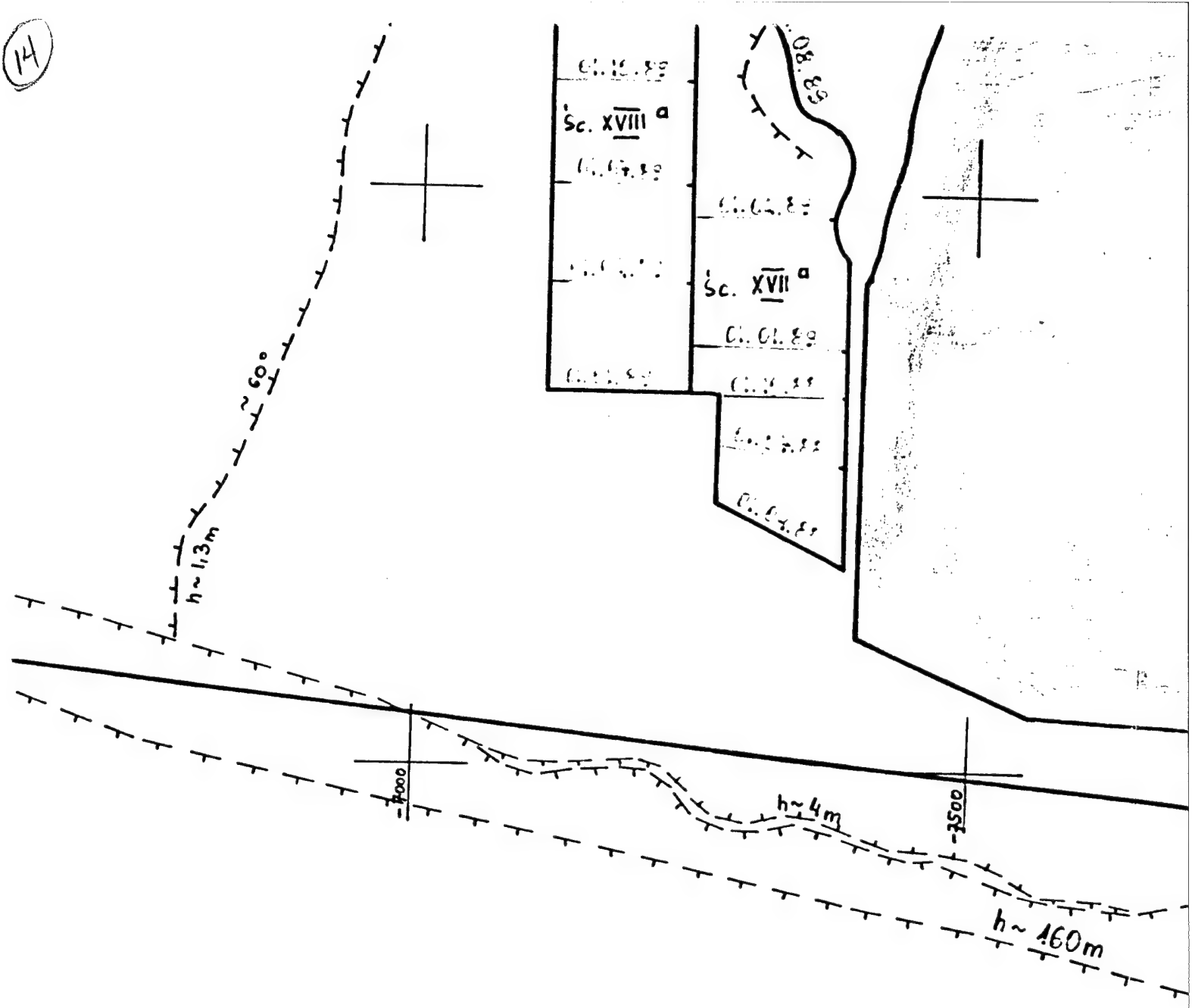
Sc. XVIII a
Sc. XVII a
~60°
h~113m
-3000
-3500
h~4m
h~160m

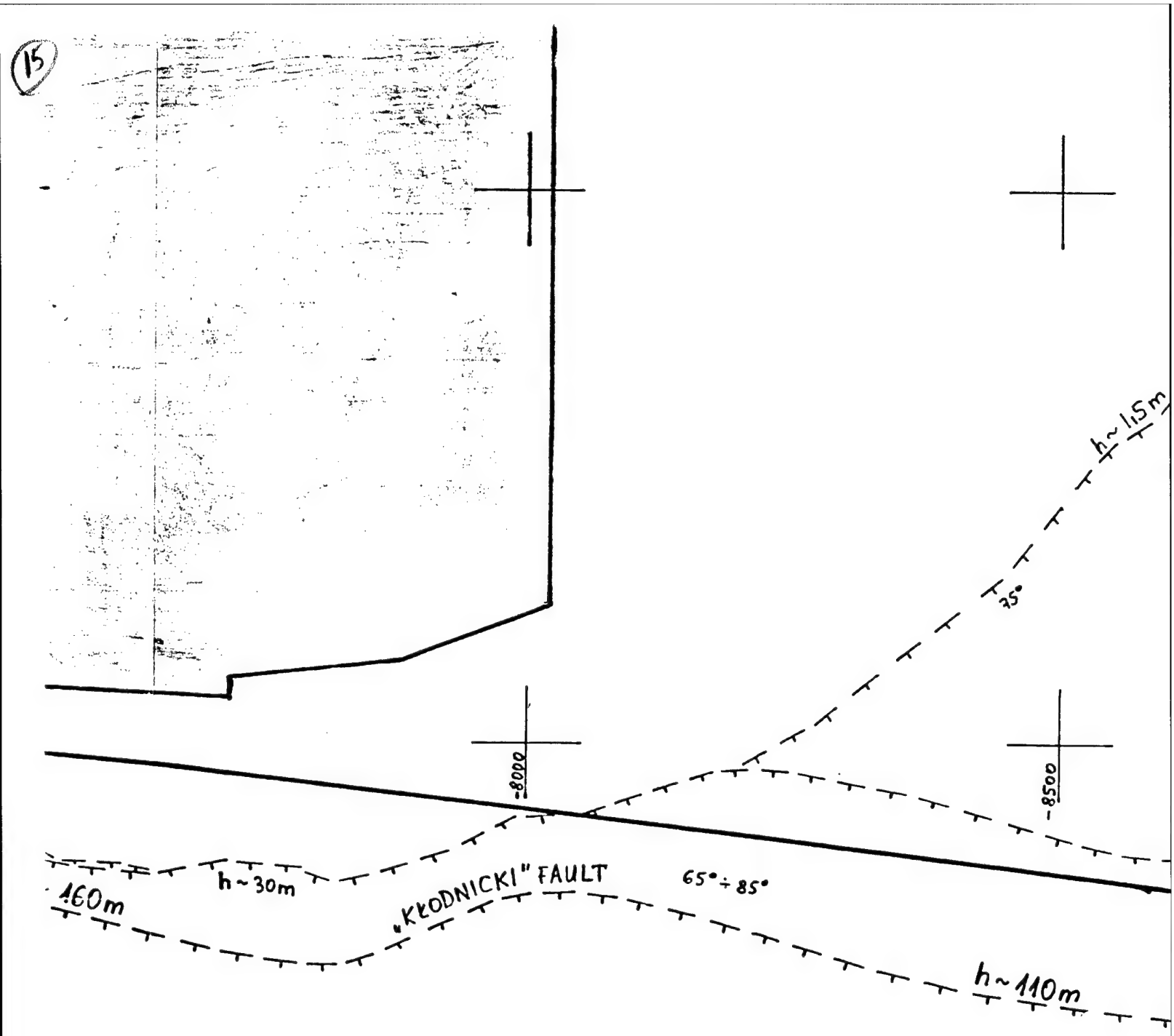
15
h~1.5m
25°
-8000
-8500
h~30m
160m
„KŁODNICKI" FAULT
65°÷85°
h~110m

16

17

h~6m

"WOJCIECH" FAULT 45° ÷ 75°

h~120m

-9500

-10000

LE
SL
1 :

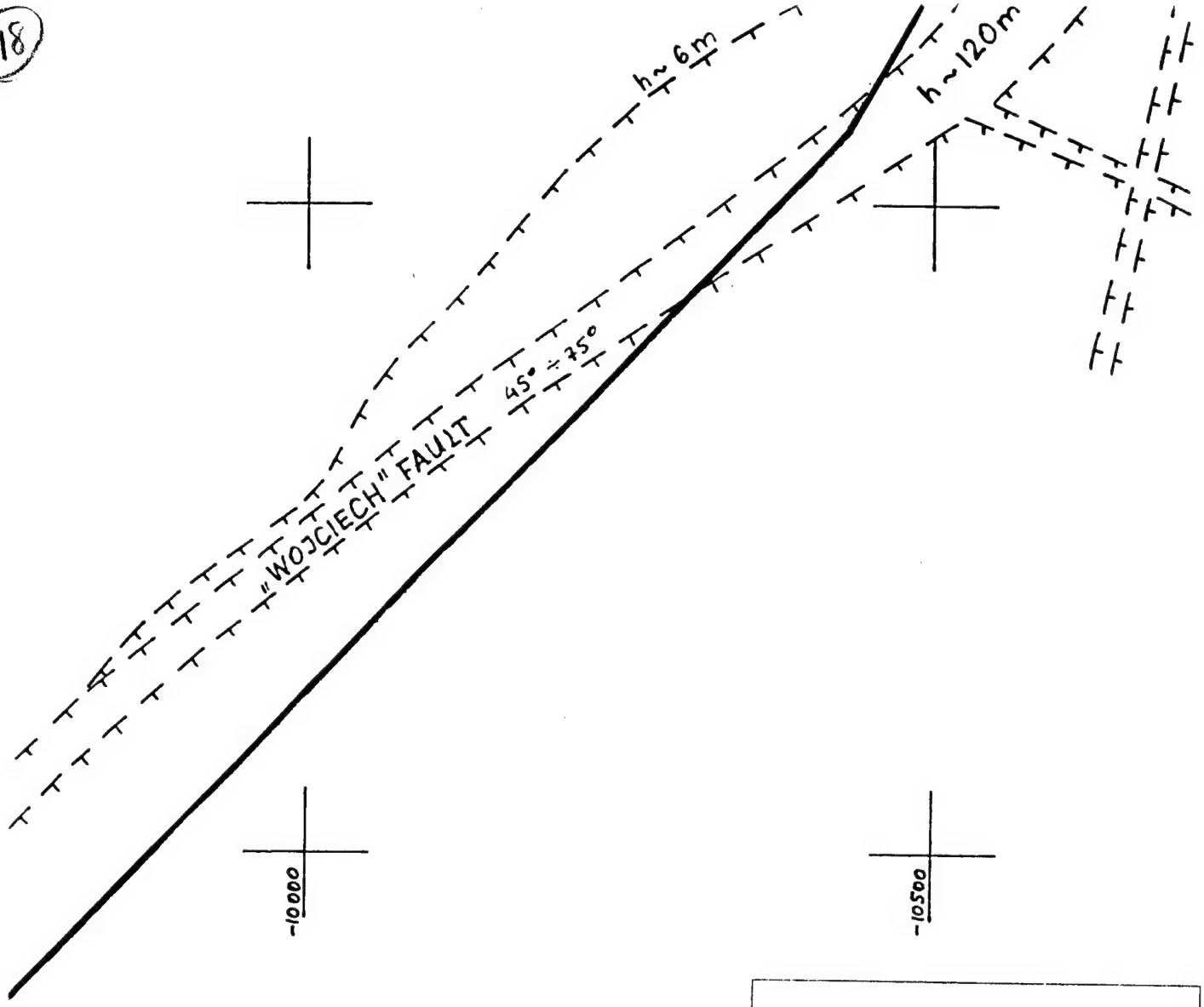

LEVEL 501
SLAB 2
1 : 5000

APPENDIX 4

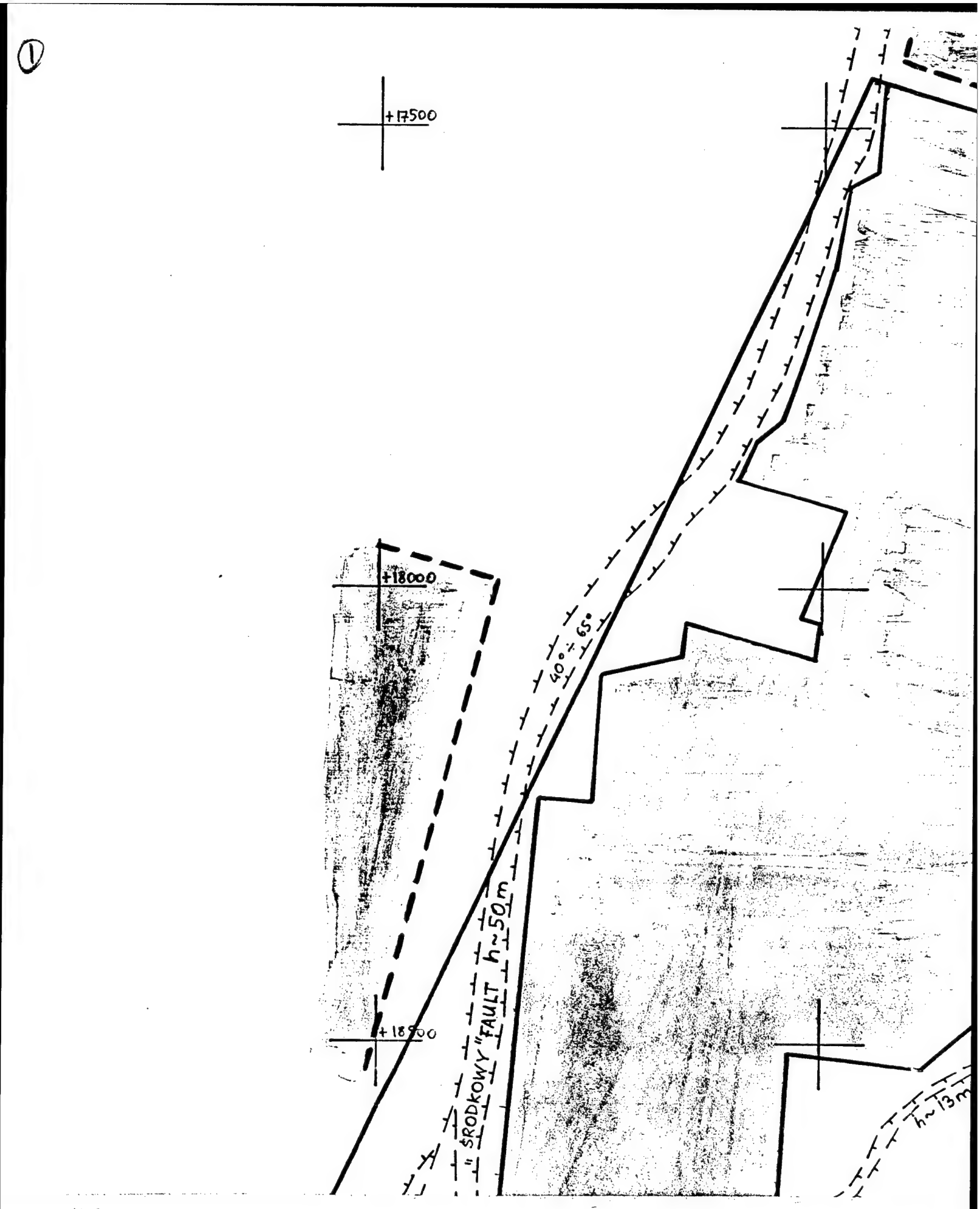
+17500
+18000
+18500
40° ÷ 65°
"ŚRODKOWY" FAULT h~50m
h~13m

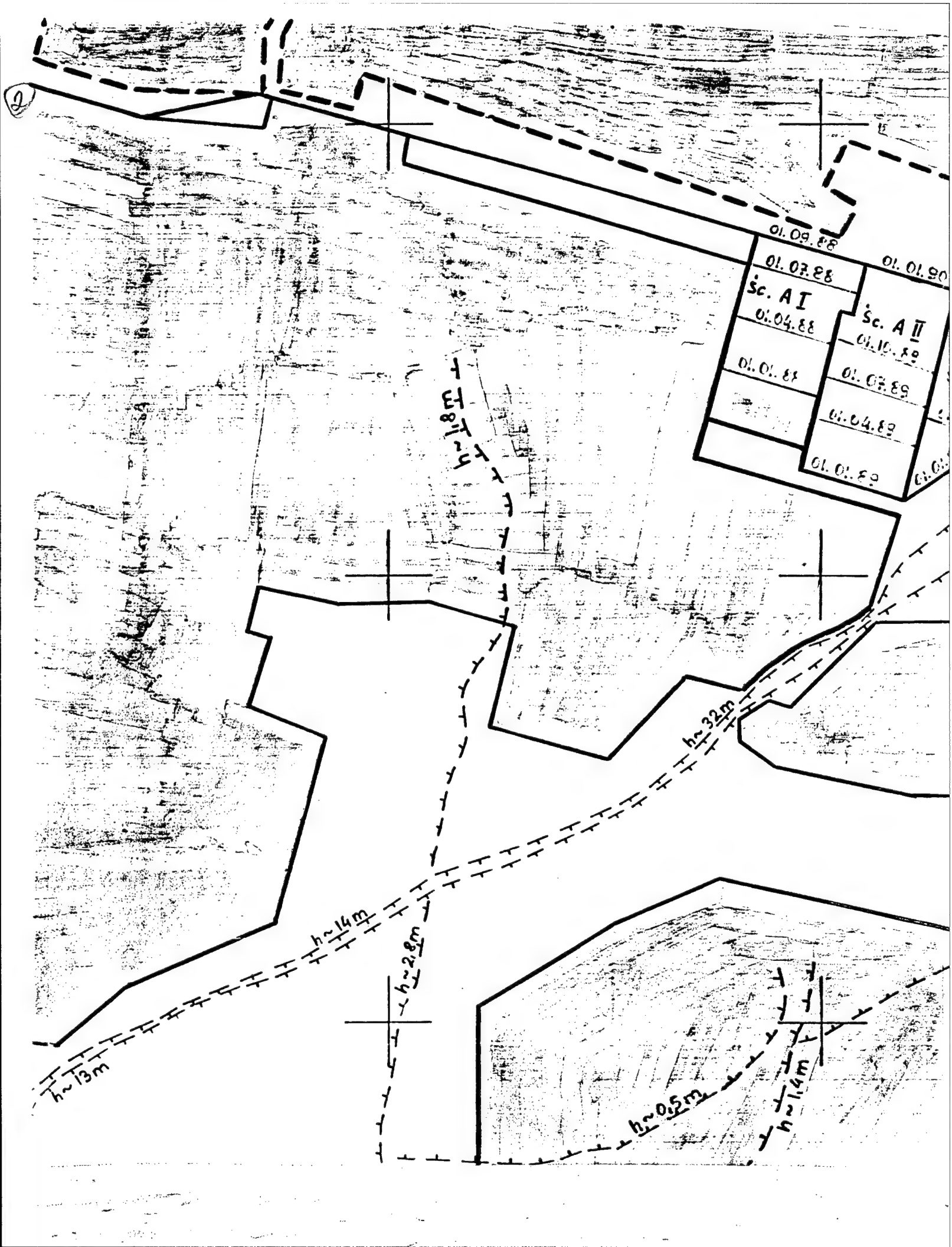
2
01.09.88
01.07.88
01.01.90
Sc. A I
01.04.88
Sc. A II
01.10.89
01.01.89
01.07.89
01.04.89
01.01.89
h~18m
h~32m
h~14m
h~2,8m
h~13m
h~0,5m
h~1,4m

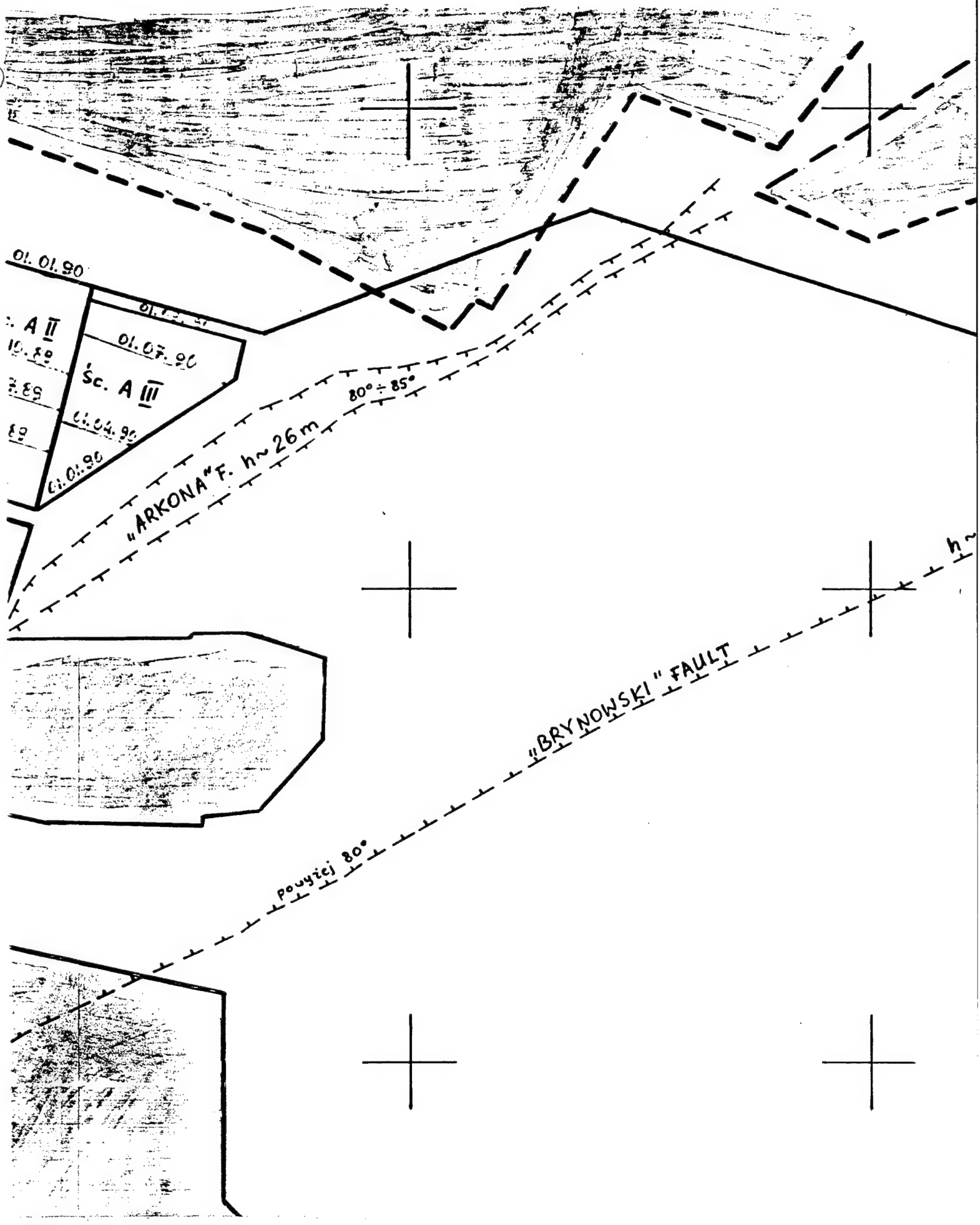
(3)
01. 01. 90
Sc. A III
01. 07. 90
01. 04. 90
01. 01. 90
80° ÷ 85°
"ARKONA" F. h~26m
"BRYNOWSKI" FAULT
Powyżej 80°

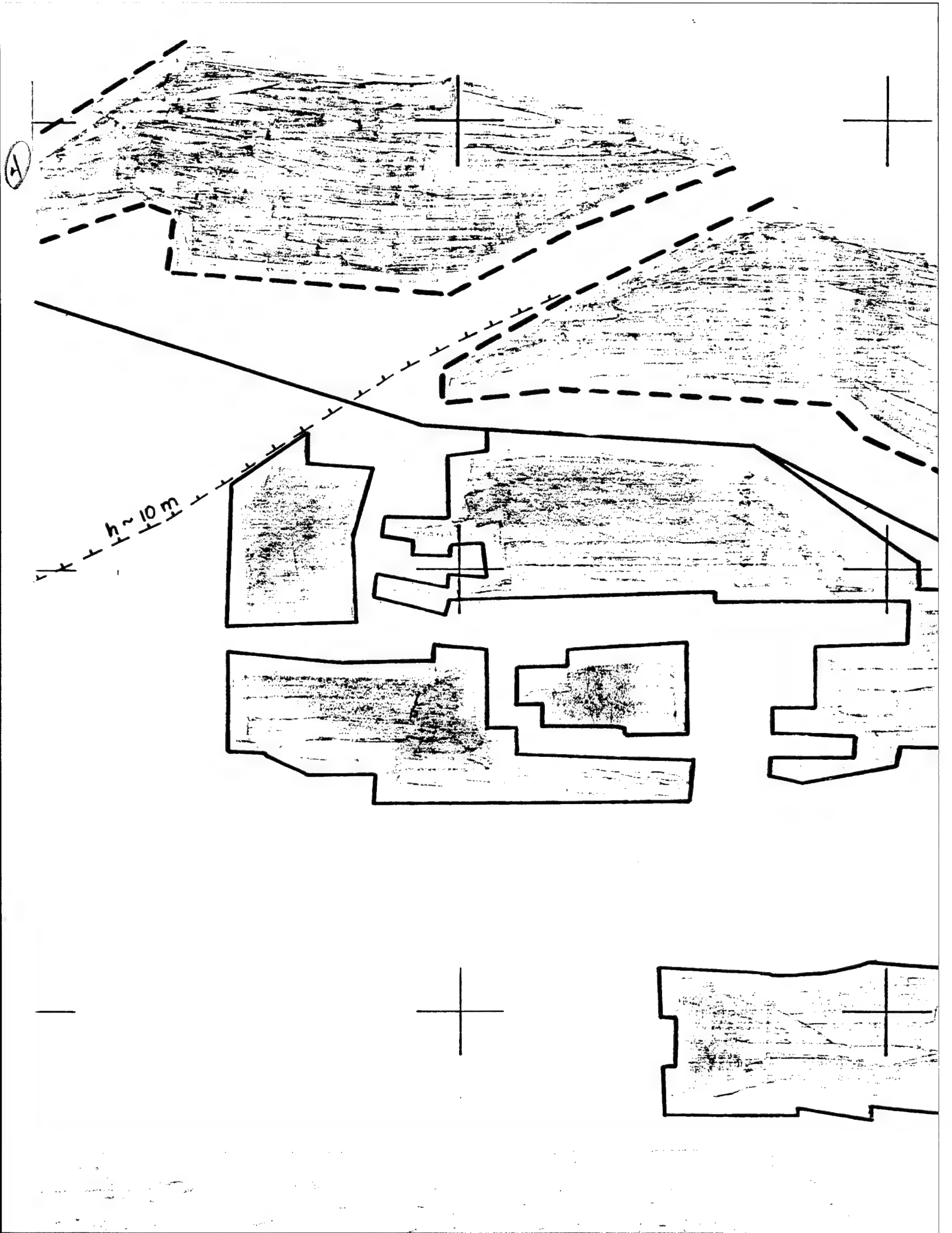
h~10m

(5)

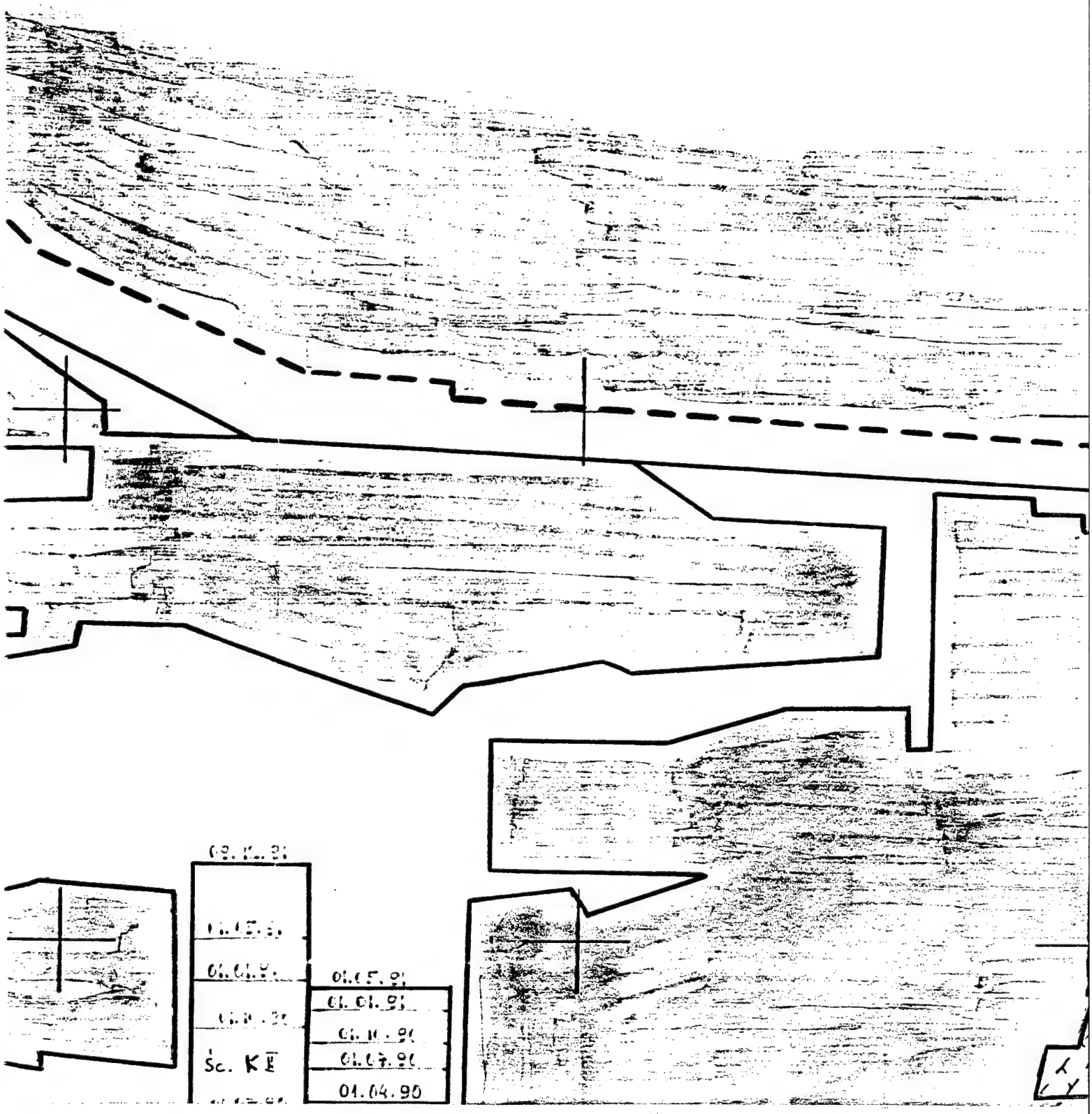

(16)

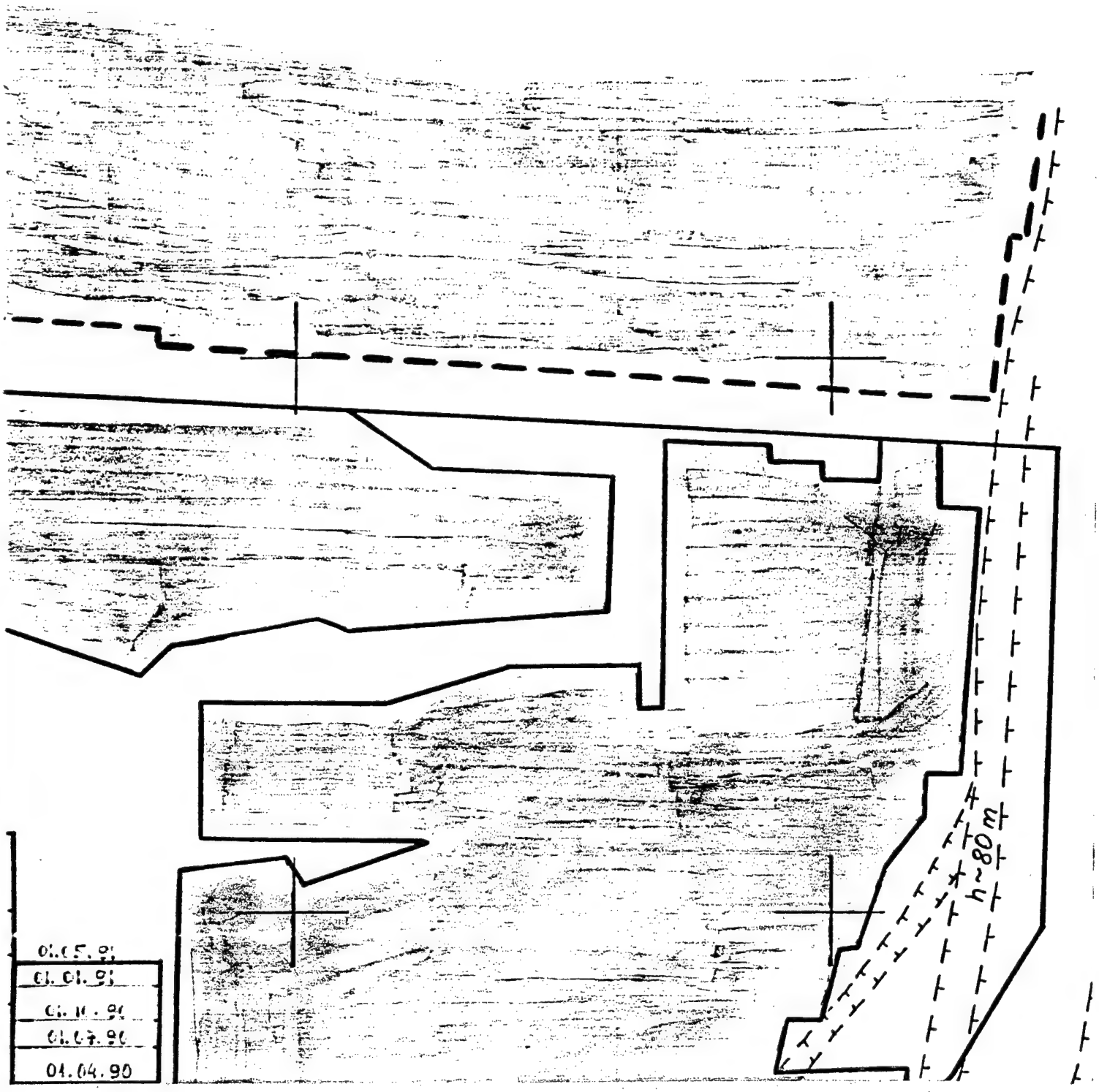

(7)

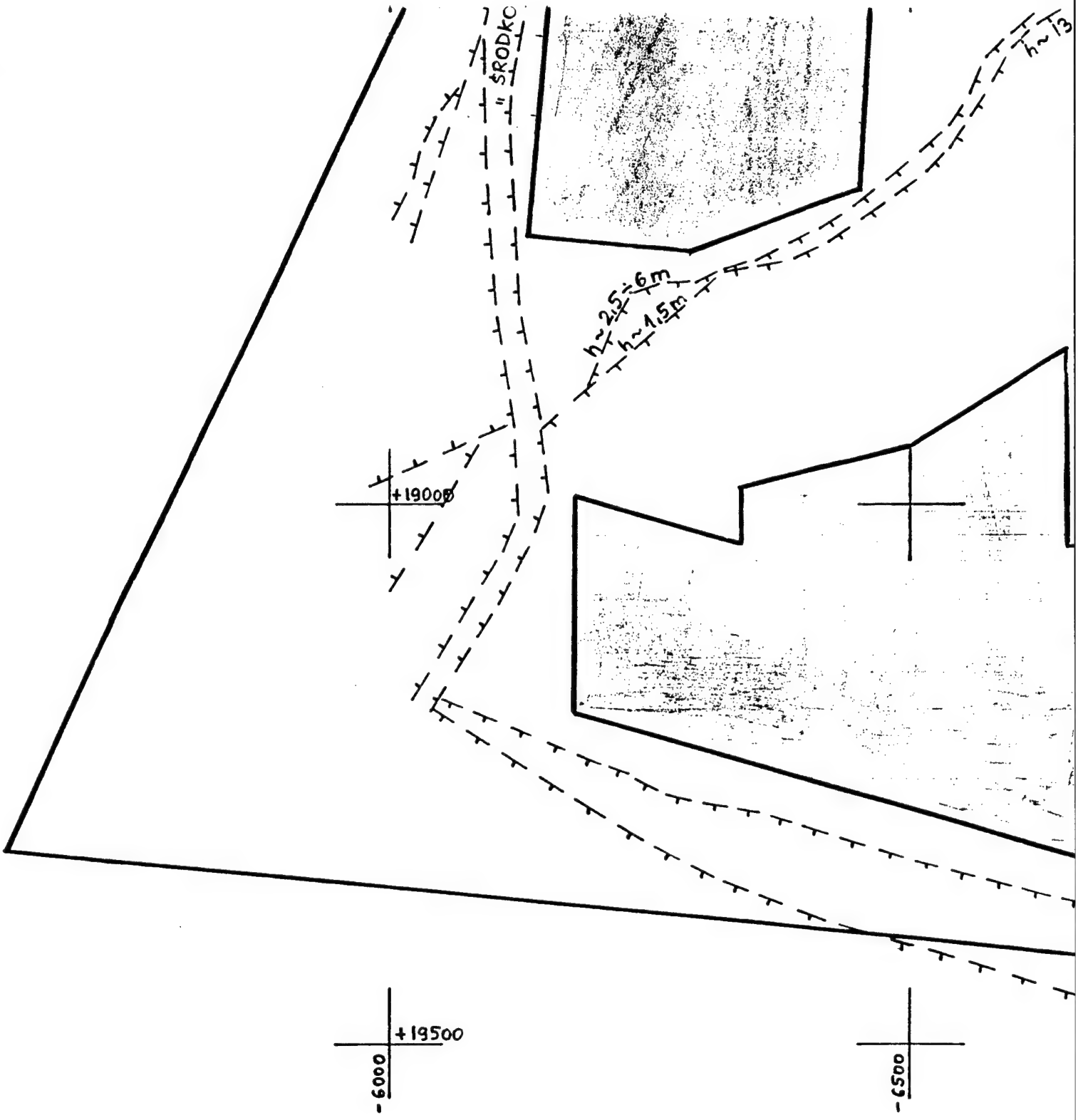

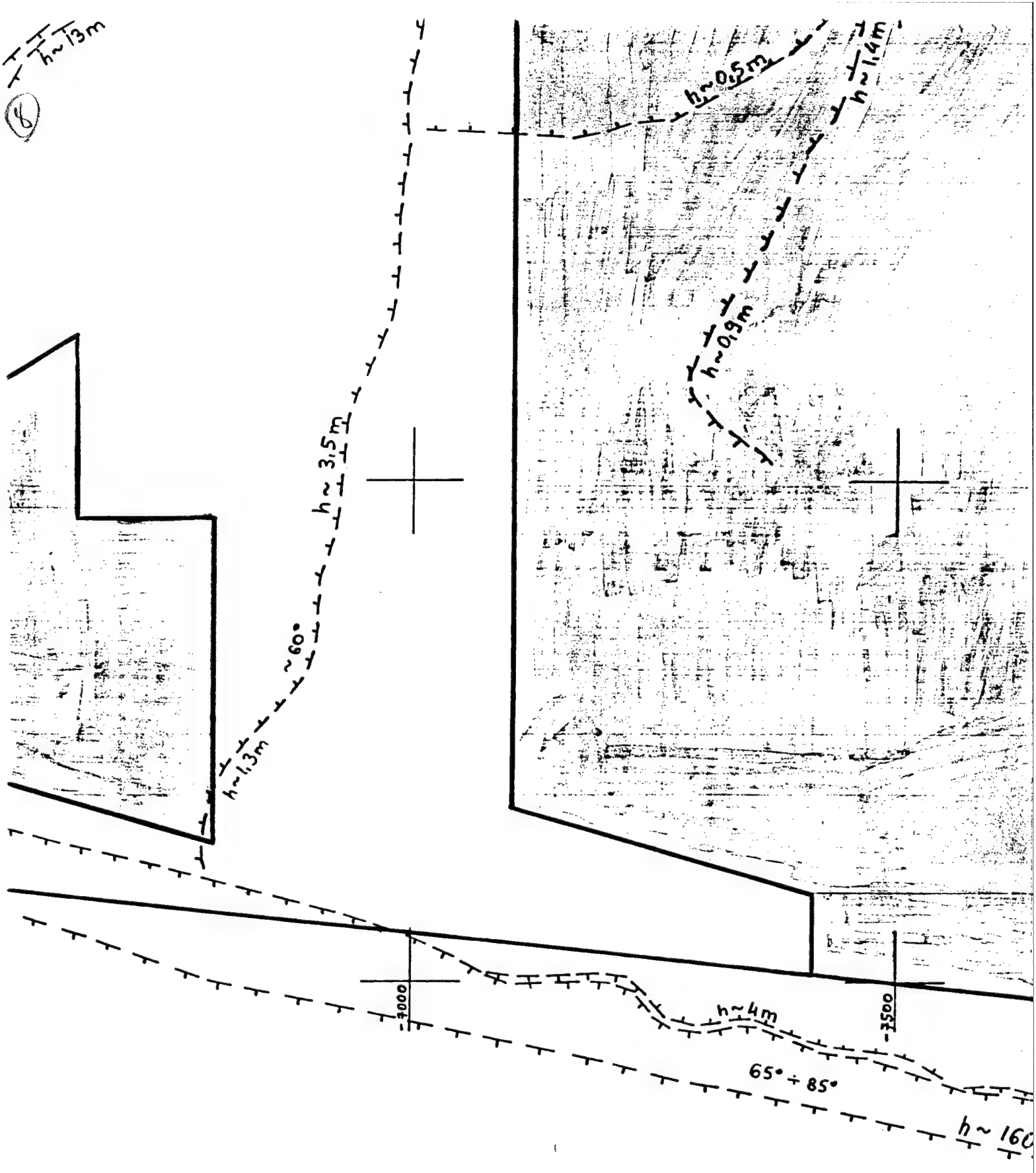
h~13m
(8)
h~0,5m
h~1,4m
h~0,9m
h~3,5m
~60°
h~1,3m
-3000
-3500
h~4m
65° ÷ 85°
h~160

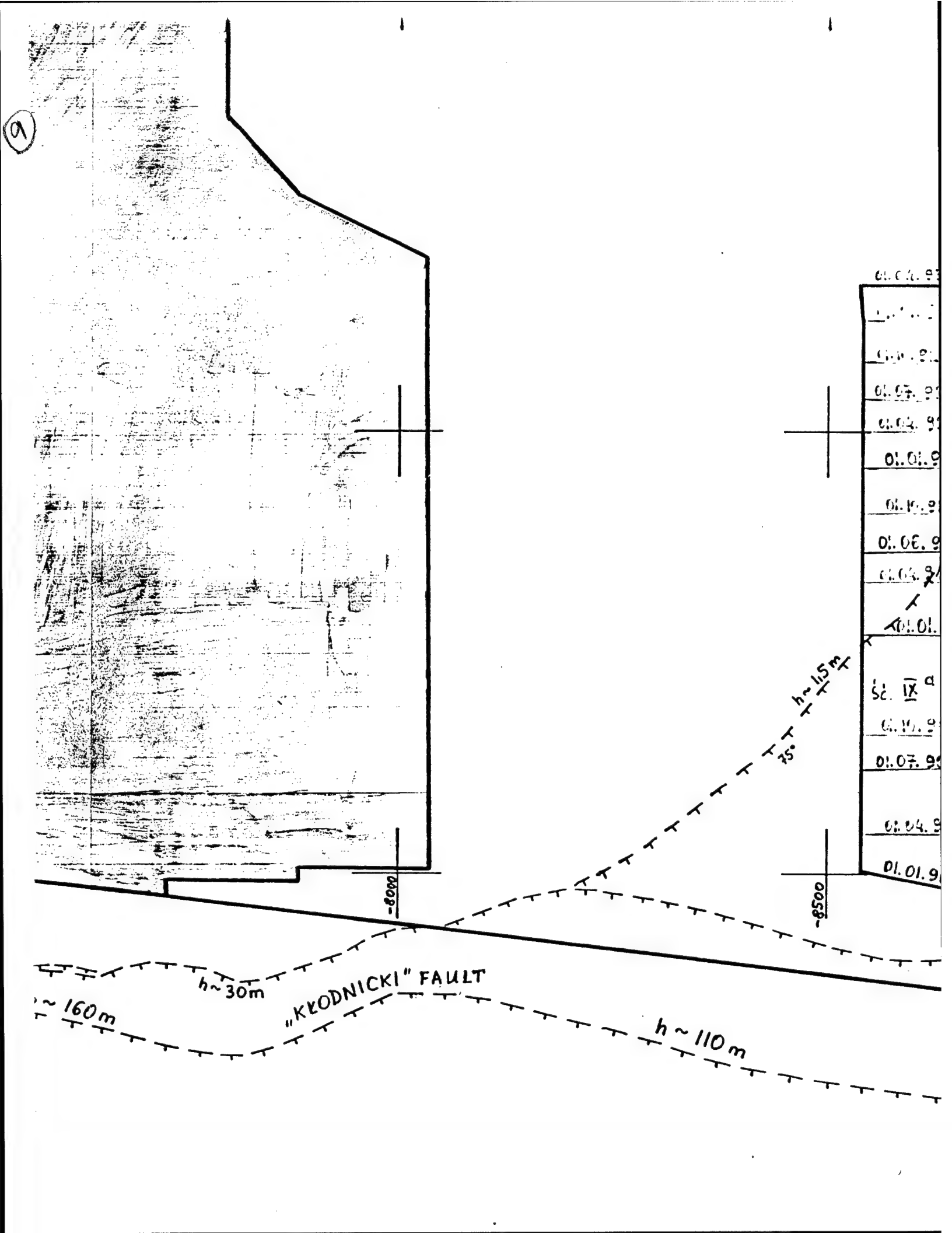
(9)
-8000
-8500
h~115m
25°
h~30m
~160m
"KŁODNICKI" FAULT
h~110m

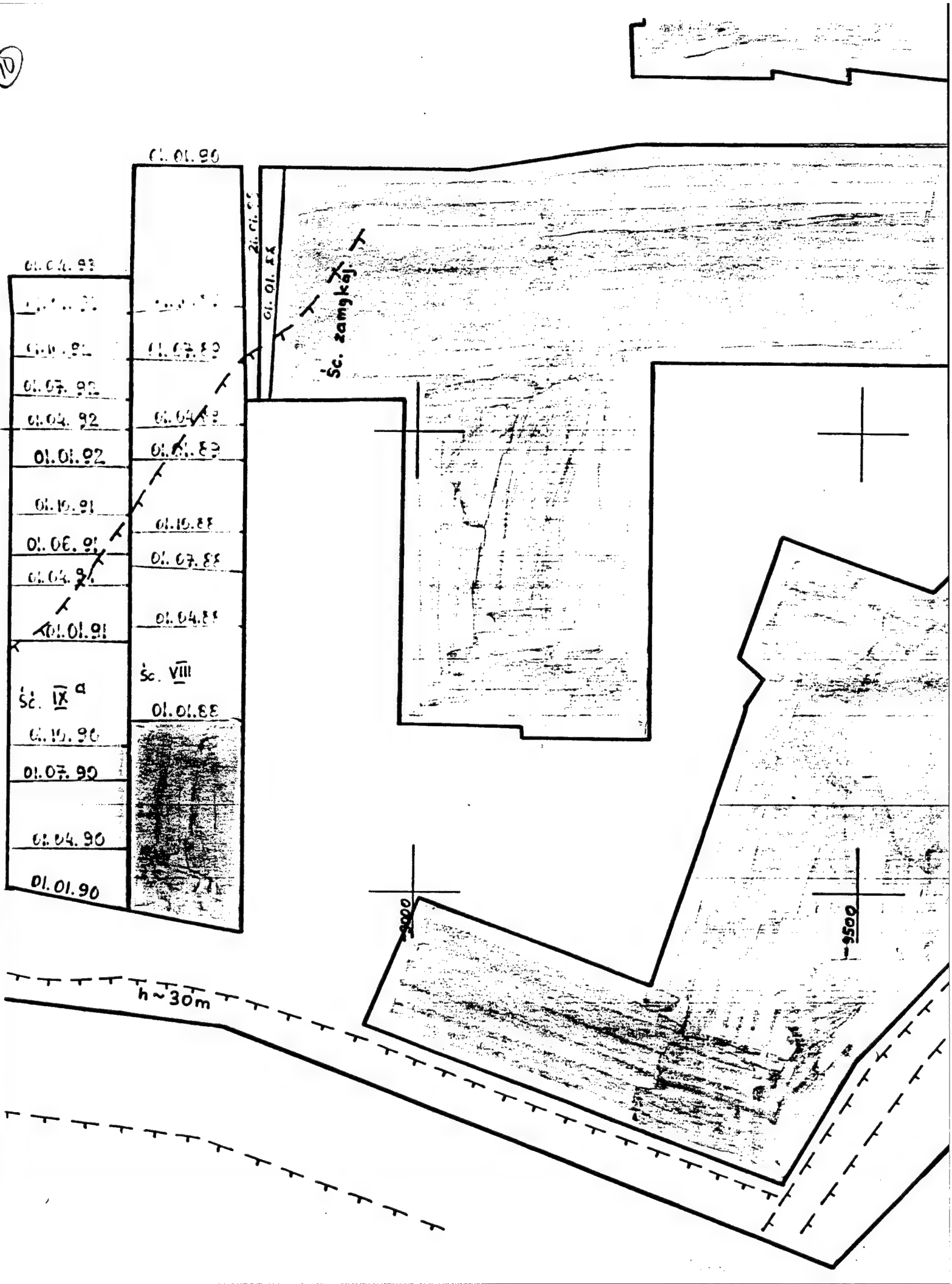
01.01.90
01.04.92
01.07.89
01.04.92
01.01.92
01.10.91
01.06.91
01.04.91
01.01.91
01.10.88
01.07.88
01.04.88
Sc. VIII
01.01.88
Sc. IX a
01.10.90
01.07.90
01.04.90
01.01.90
Sc. zamykal.
h ~30m
3000
3950

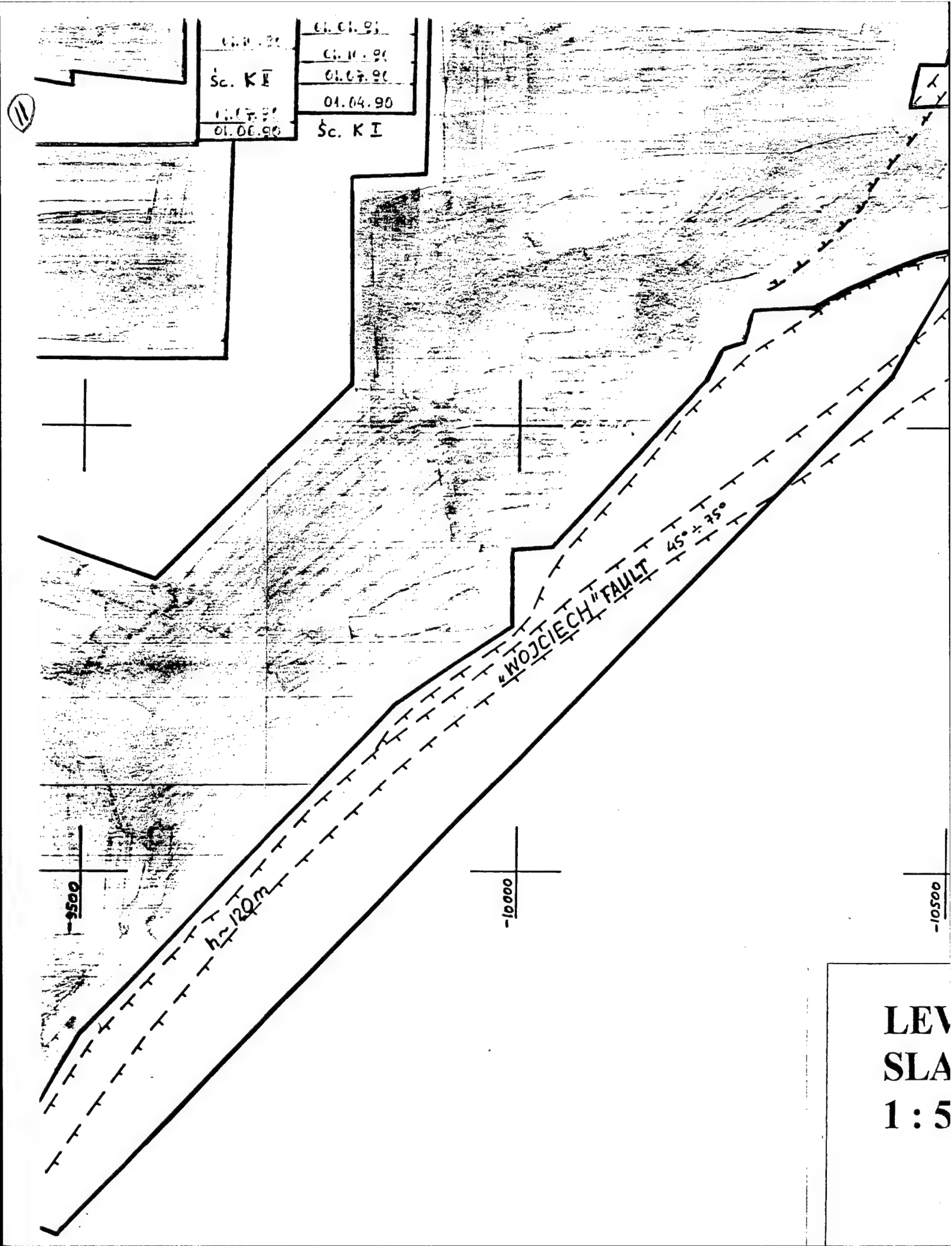
Sc. K II
01.06.90
01.04.90
Sc. K I
„WOJCIECH" FAULT
45° ÷ 75°
h~120m
-9500
-10000
-10500

LEV
SLA
1 : 5

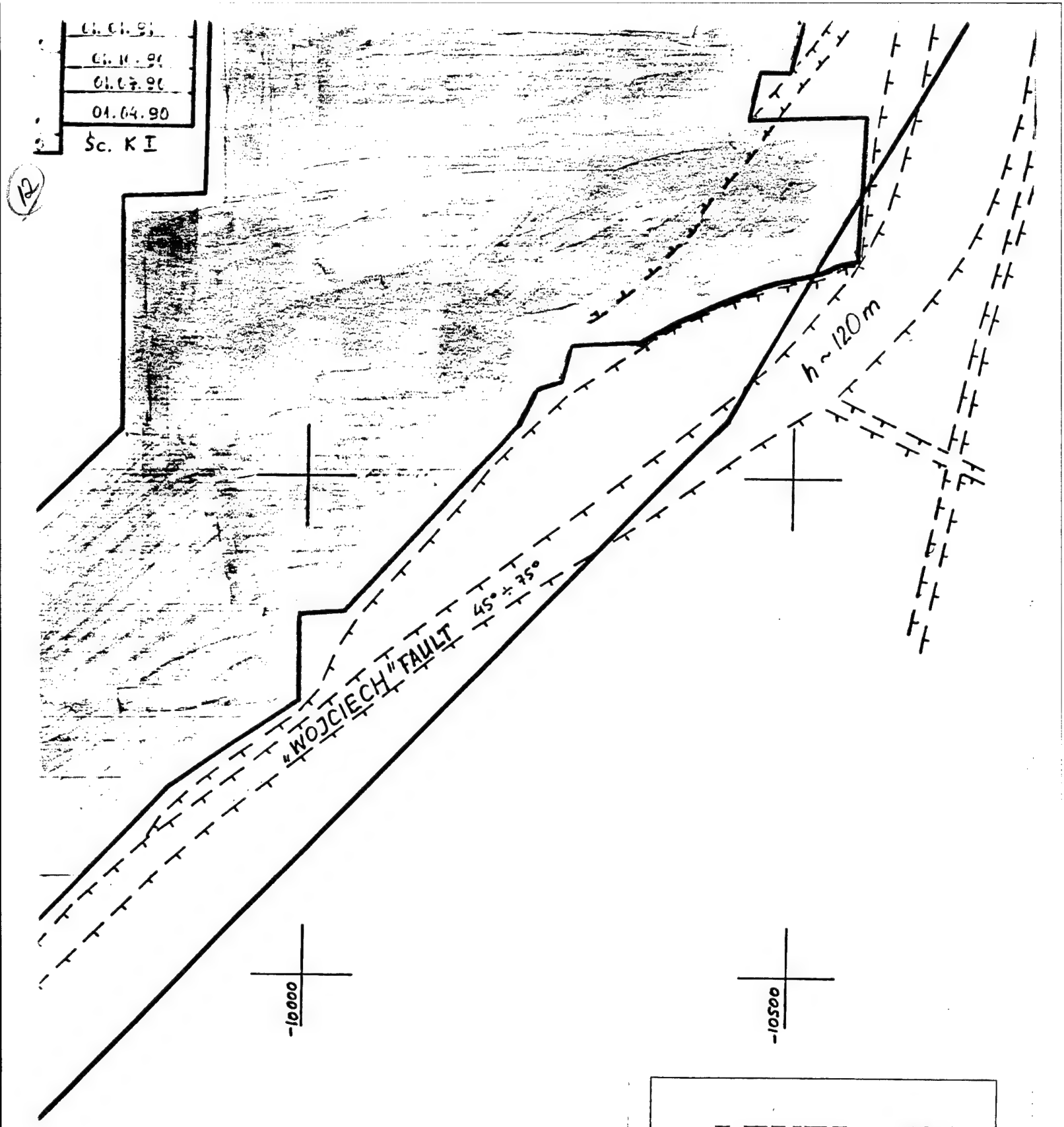

LEVEL 501
SLAB 1
1 : 5000

APPENDIX 5

13

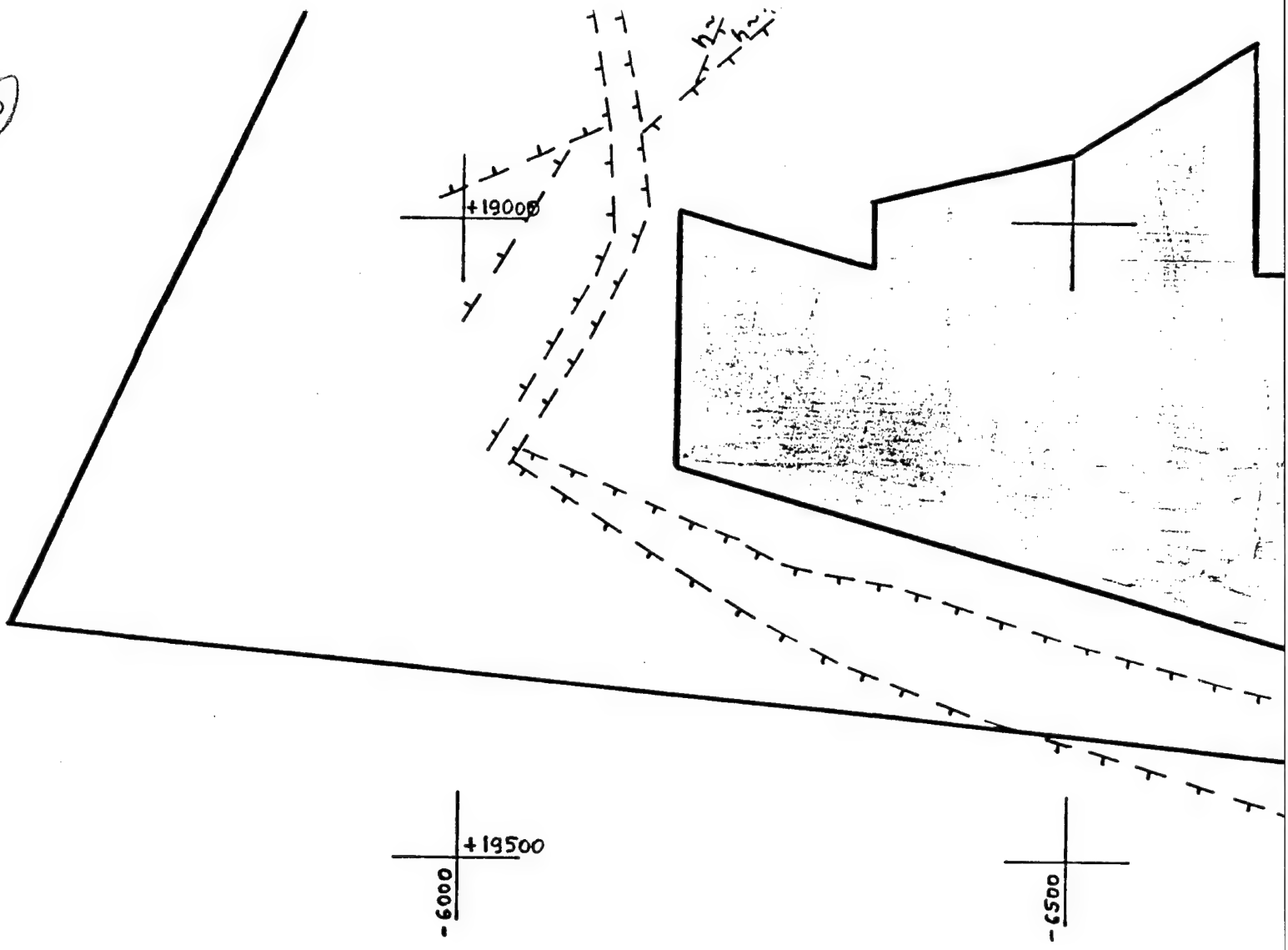

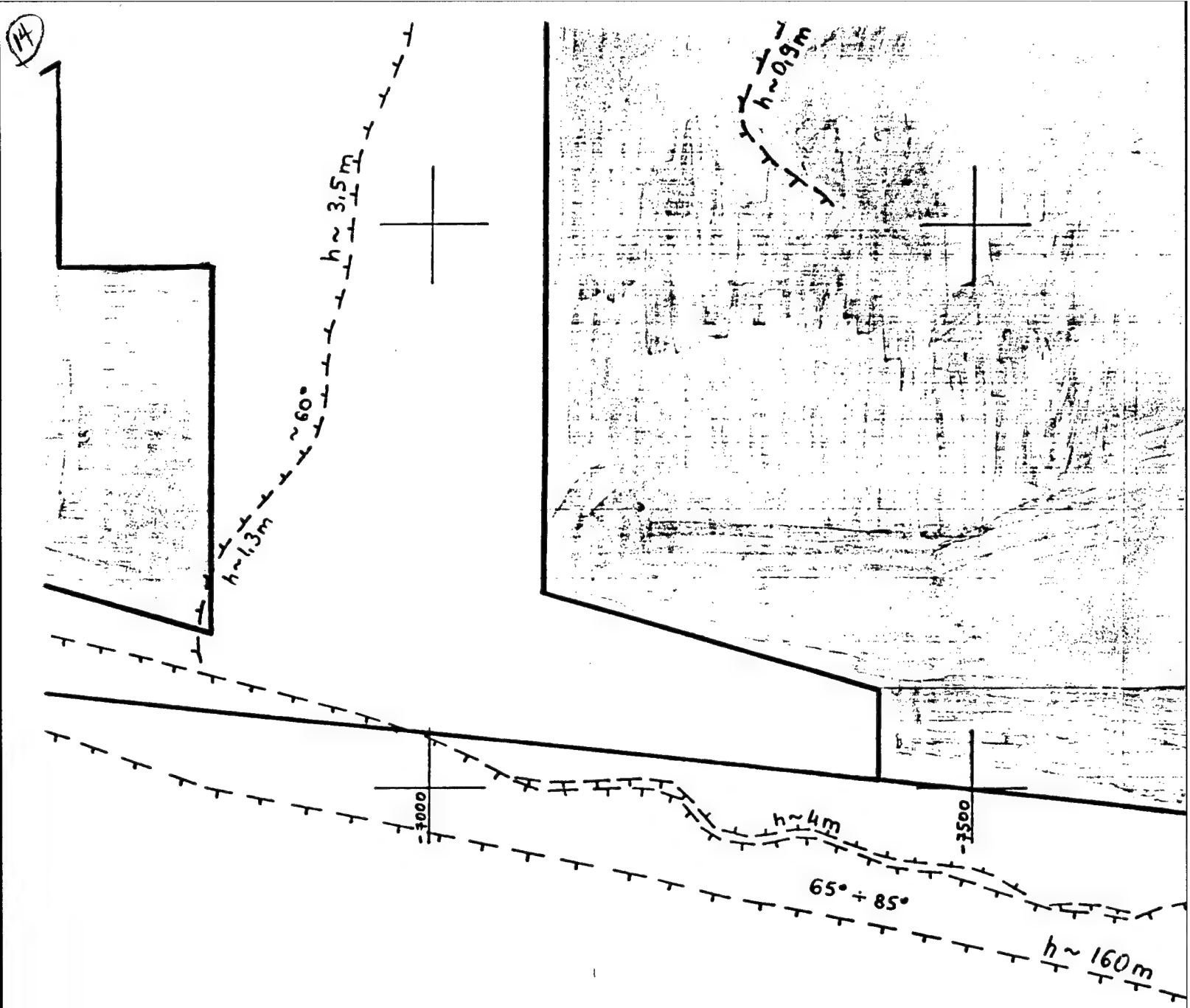
14
h~3,5m
~60°
h~1,3m
h~0,9m
-3000
-3500
h~4m
65° ÷ 85°
h~160m

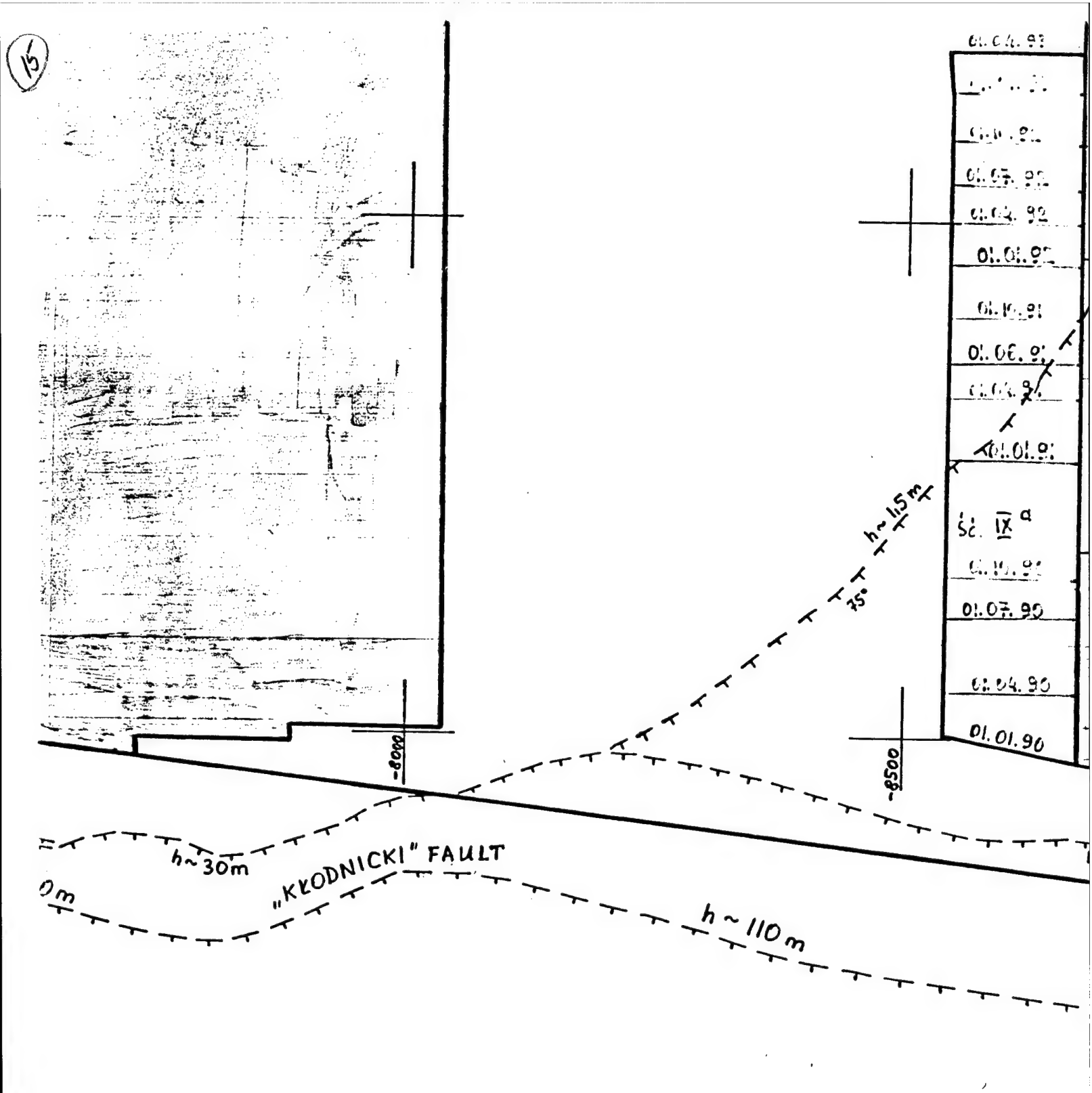
15
01.04.93
01.07.92
01.01.92
01.06.91
01.01.91
Sz. IX a
01.07.90
01.04.90
01.01.90
-8000
-8500
h~15m
75°
h~30m
"KŁODNICKI" FAULT
h~110m

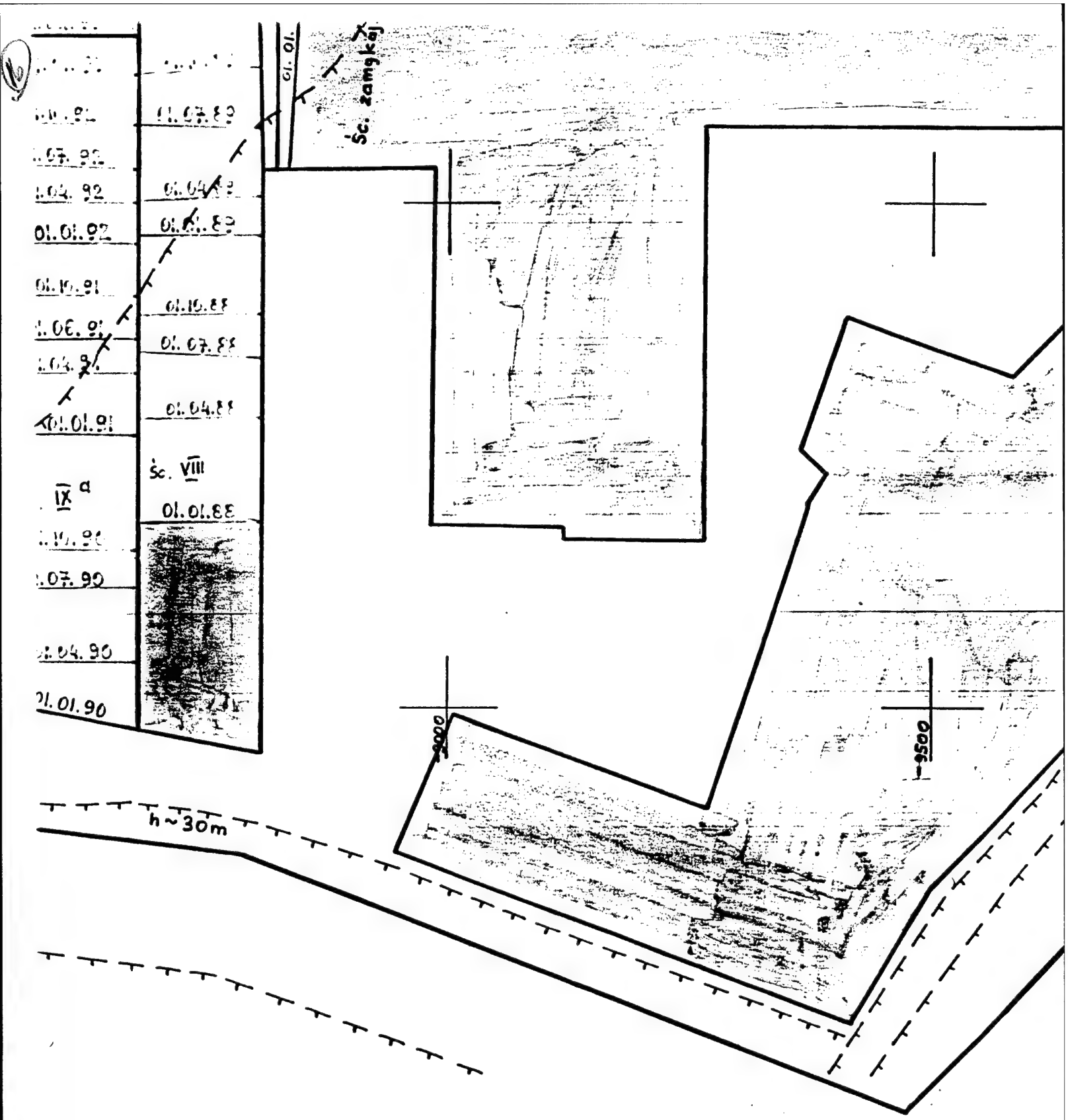
Ść. zamkaj
01.01.
11.07.89
01.04.92
01.01.92
01.10.91
01.07.88
01.04.88
01.01.91
Ść. VIII
IX a
01.01.88
01.07.90
01.04.90
01.01.90
h ~ 30m

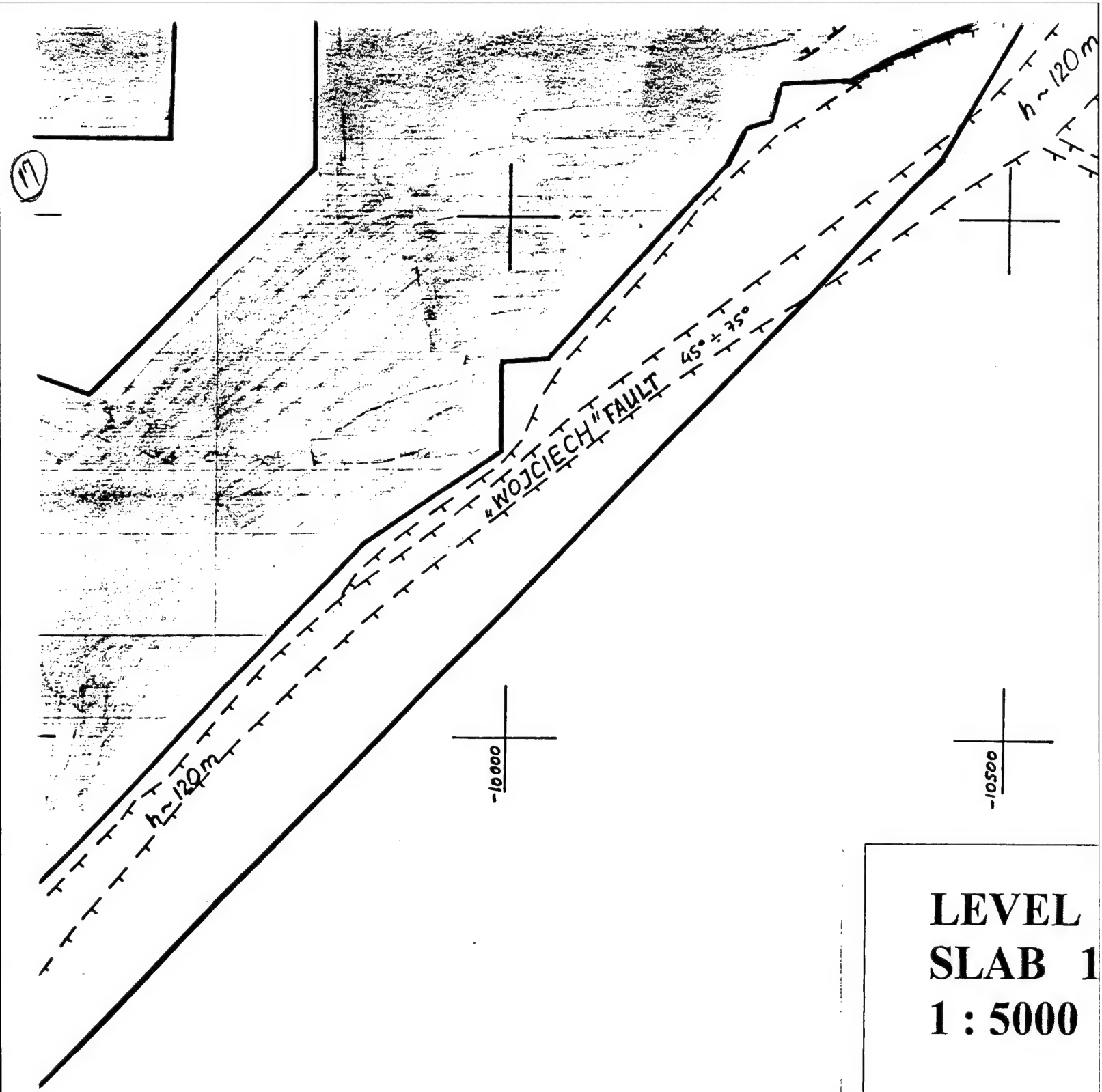

LEVEL
SLAB 1
1 : 5000

APPEN

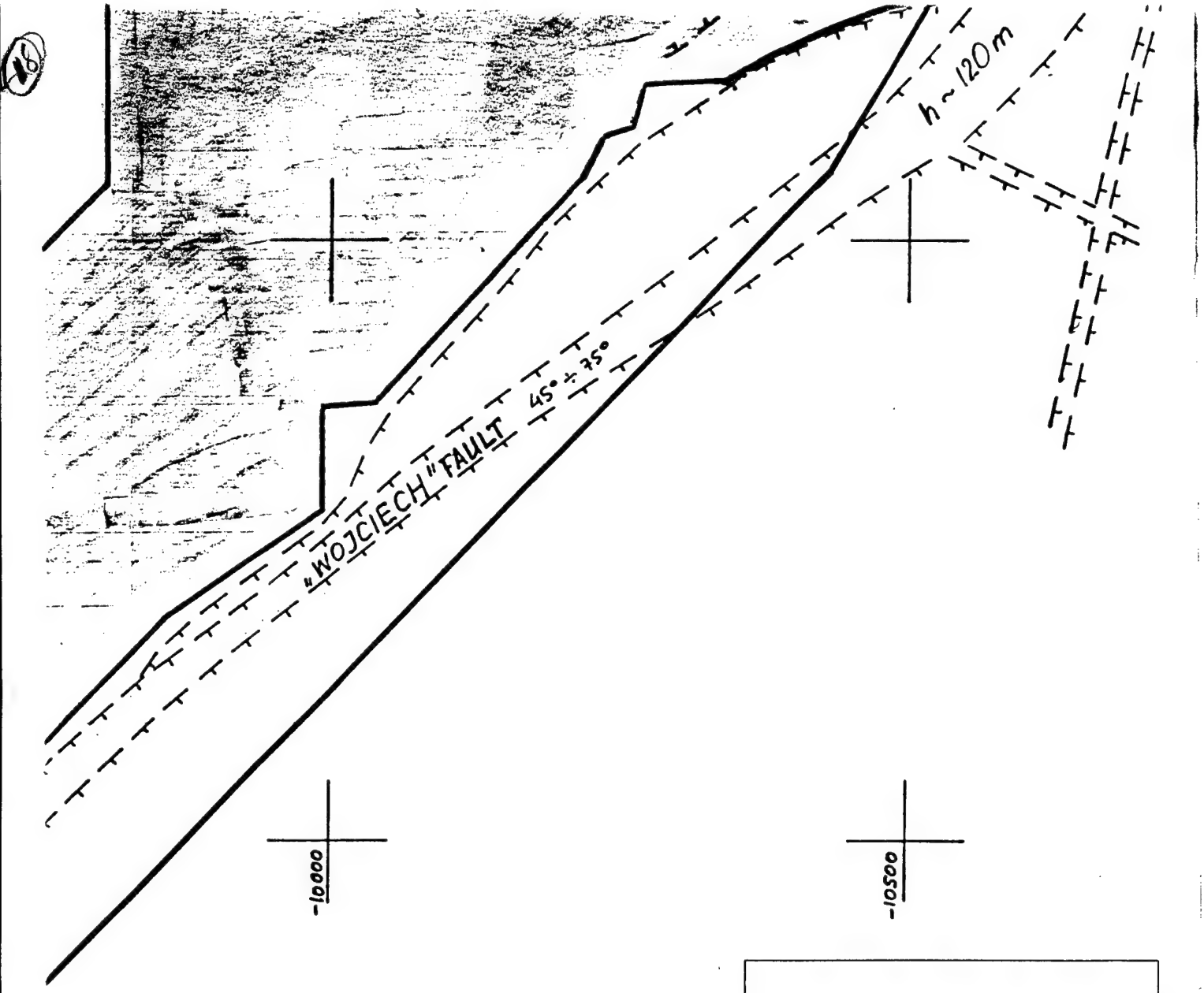

LEVEL 501
SLAB 1
1 : 5000

APPENDIX 5

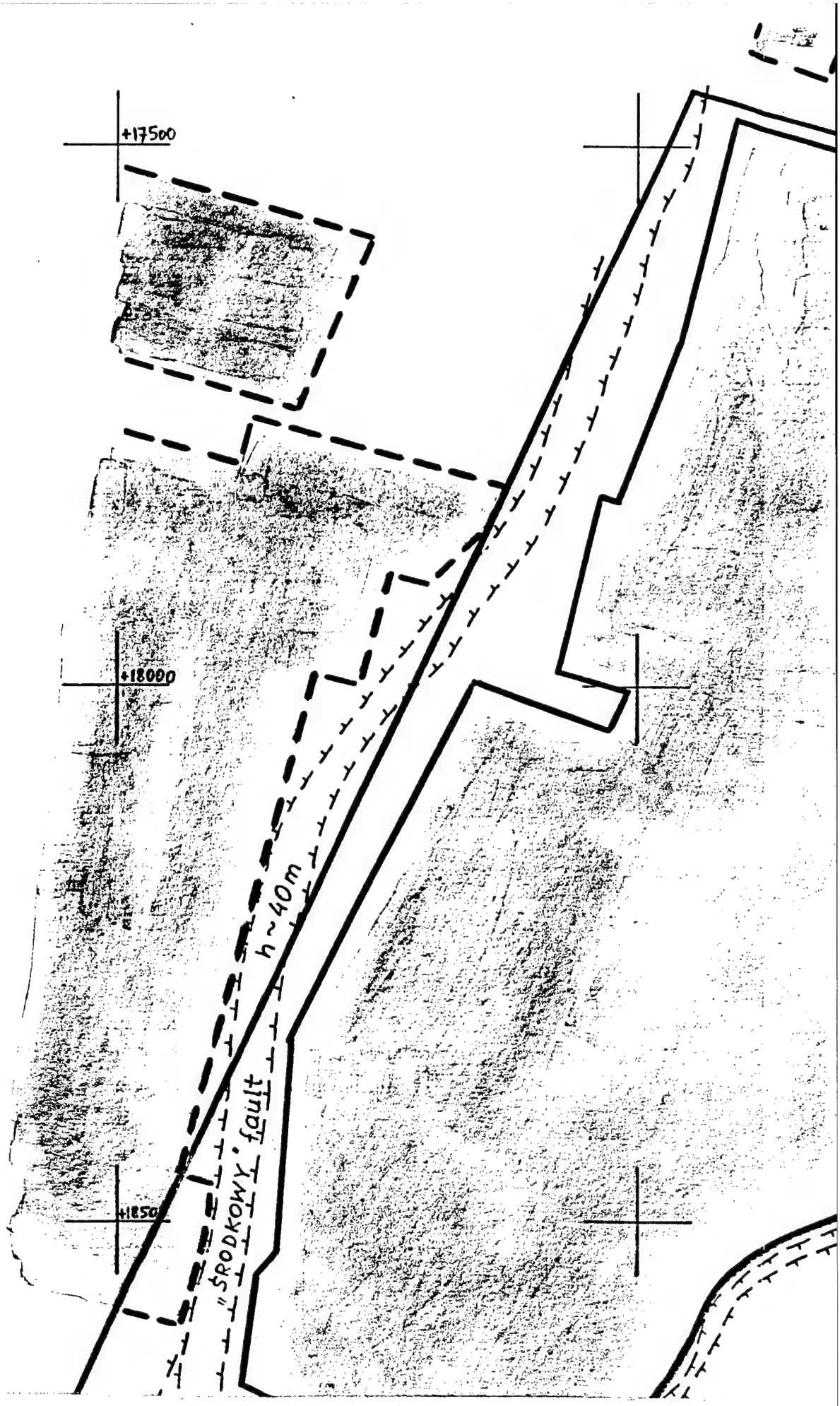
+17500
+18000
+18500
"Środkowy" fault
h~40m

(2)

Sc. IV

Sc. V

Sc. VII

h~2,4m

80°-85°

h~6m

h~0,6m

h~1,4m

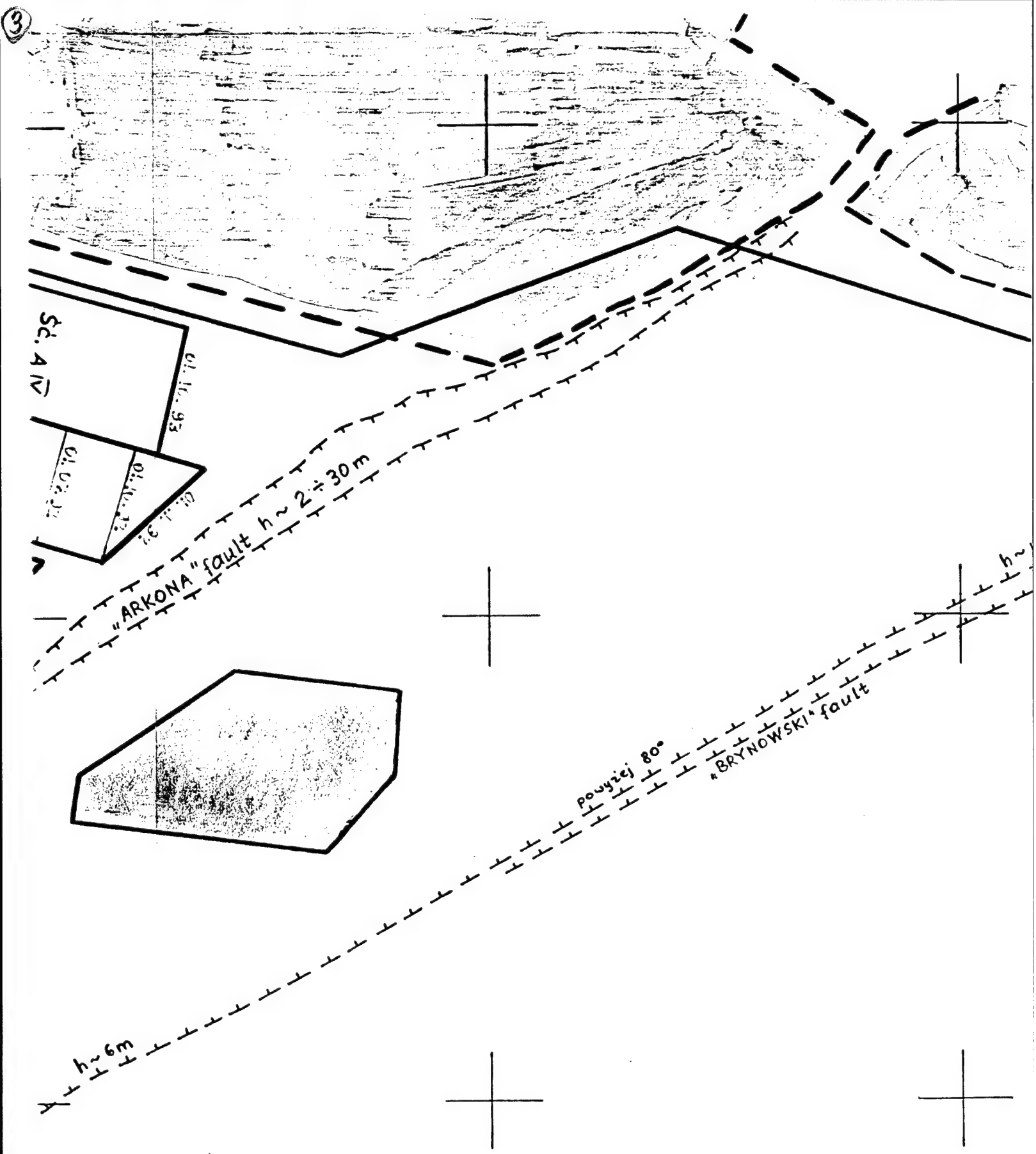
(3)
Sc. 4 IV
"ARKONA" fault h ~ 2 ÷ 30 m
powyżej 80°
„BRYNOWSKI" fault
h ~ 6m

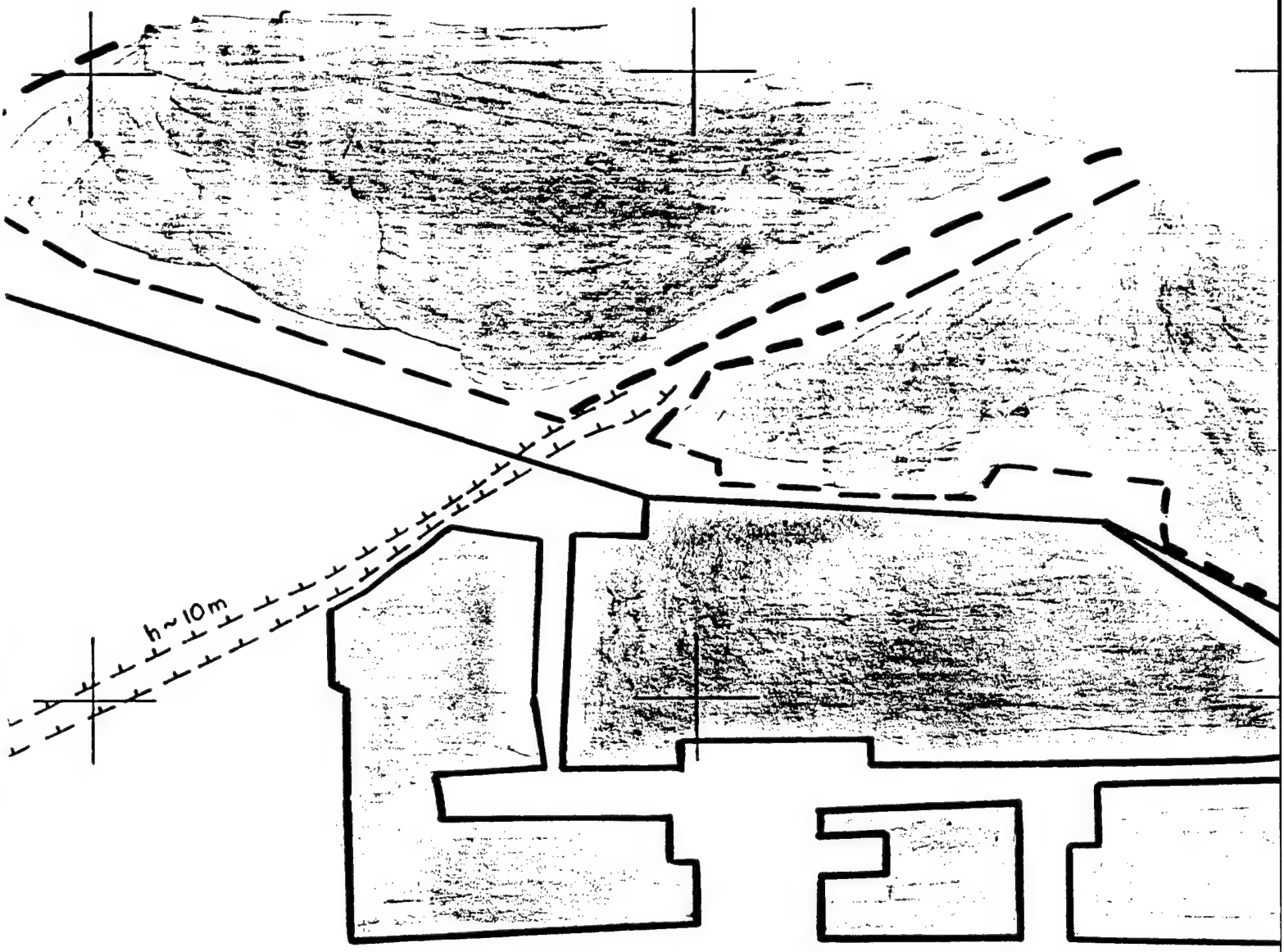
h~10m

(5)

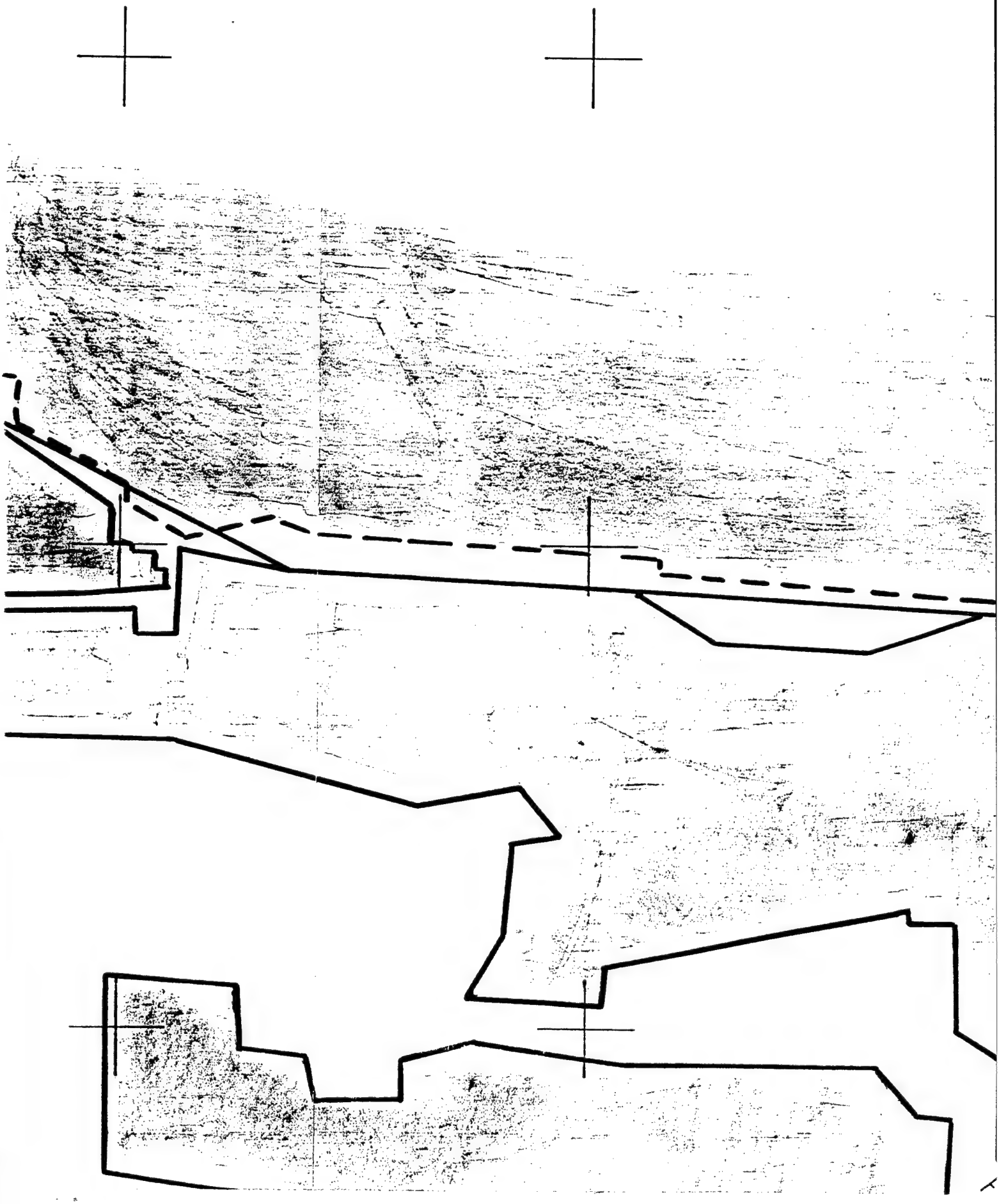

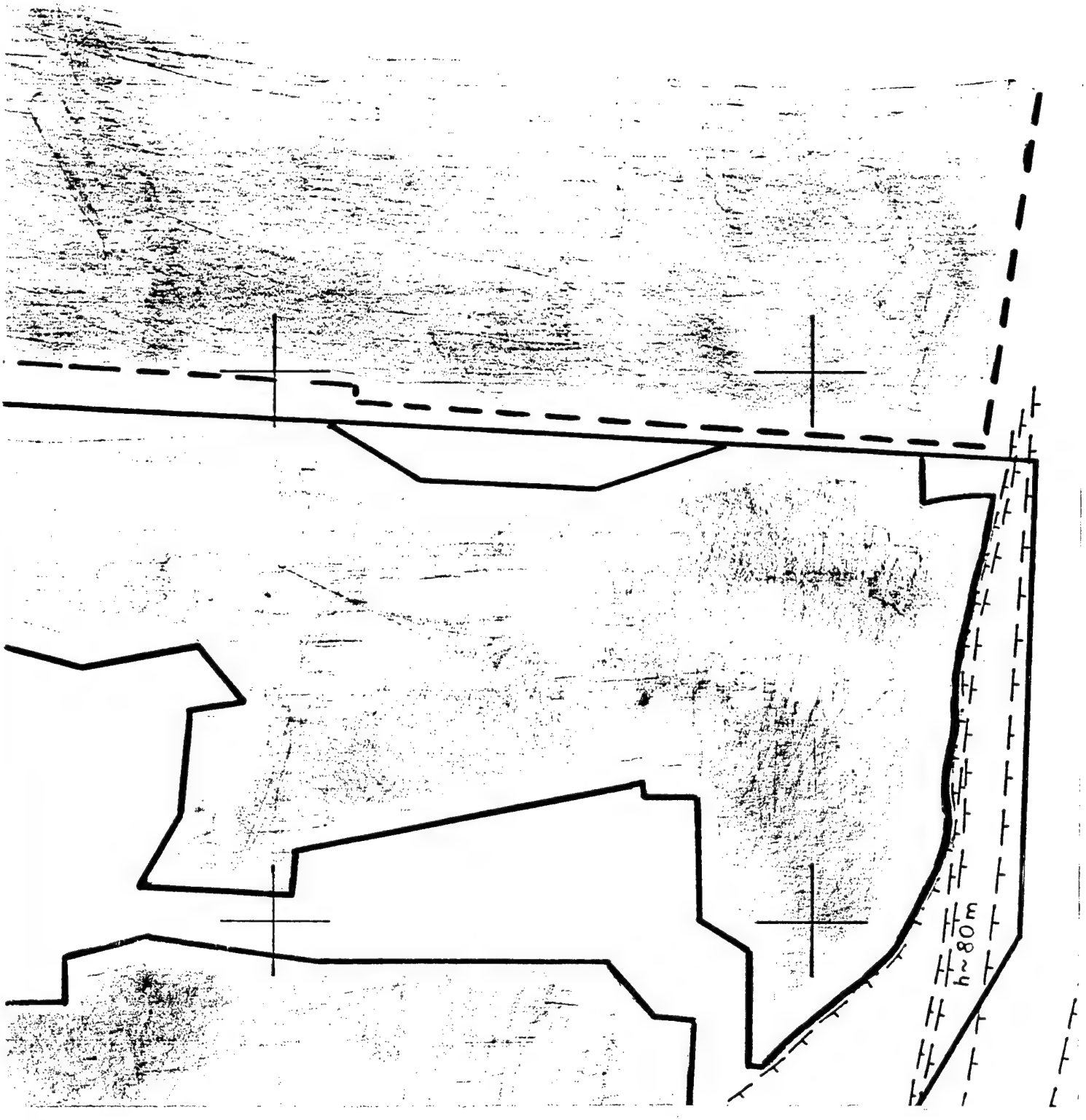

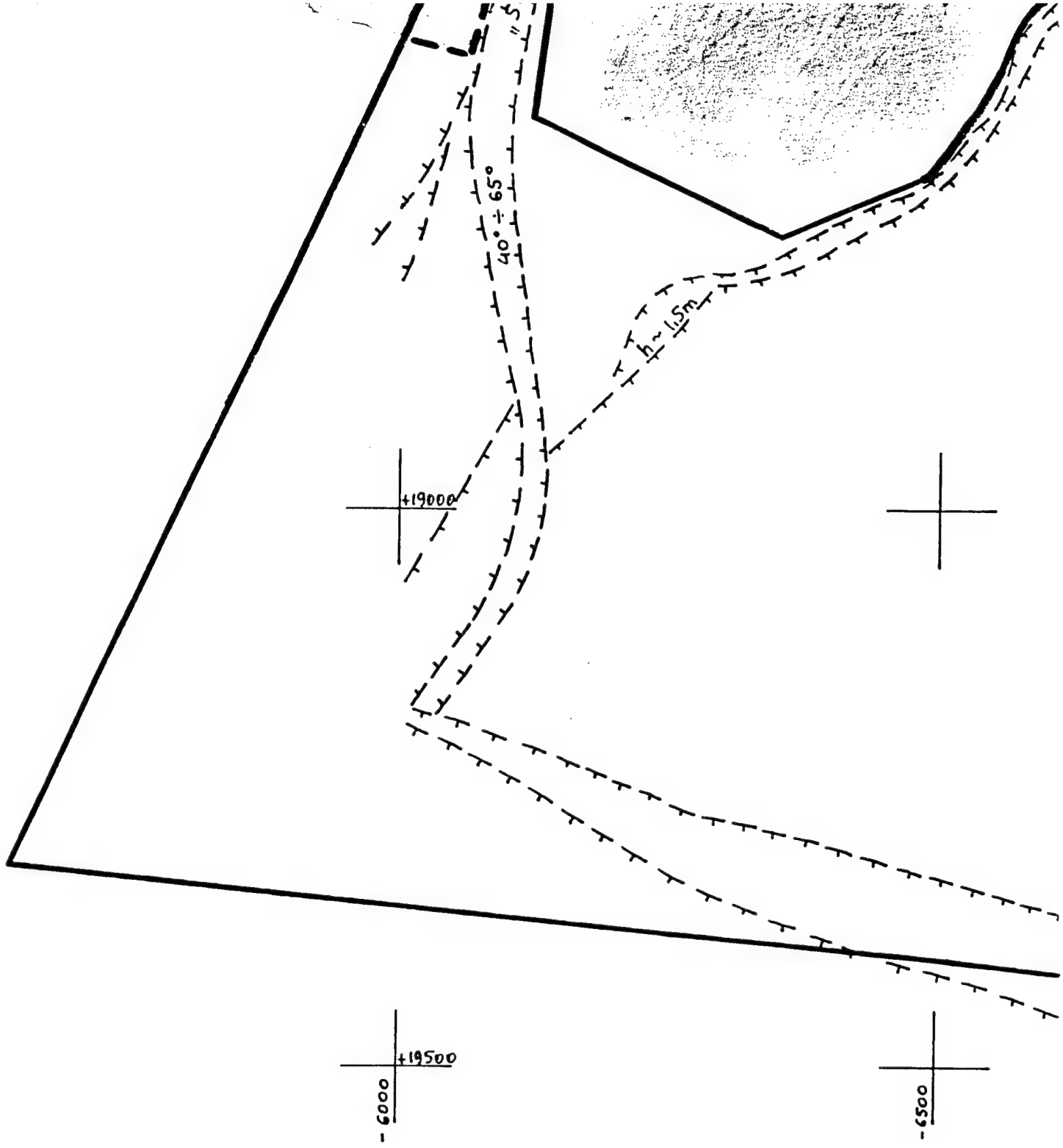
40°÷65°
h~1.5m
+19000
+19500
-6000
-6500

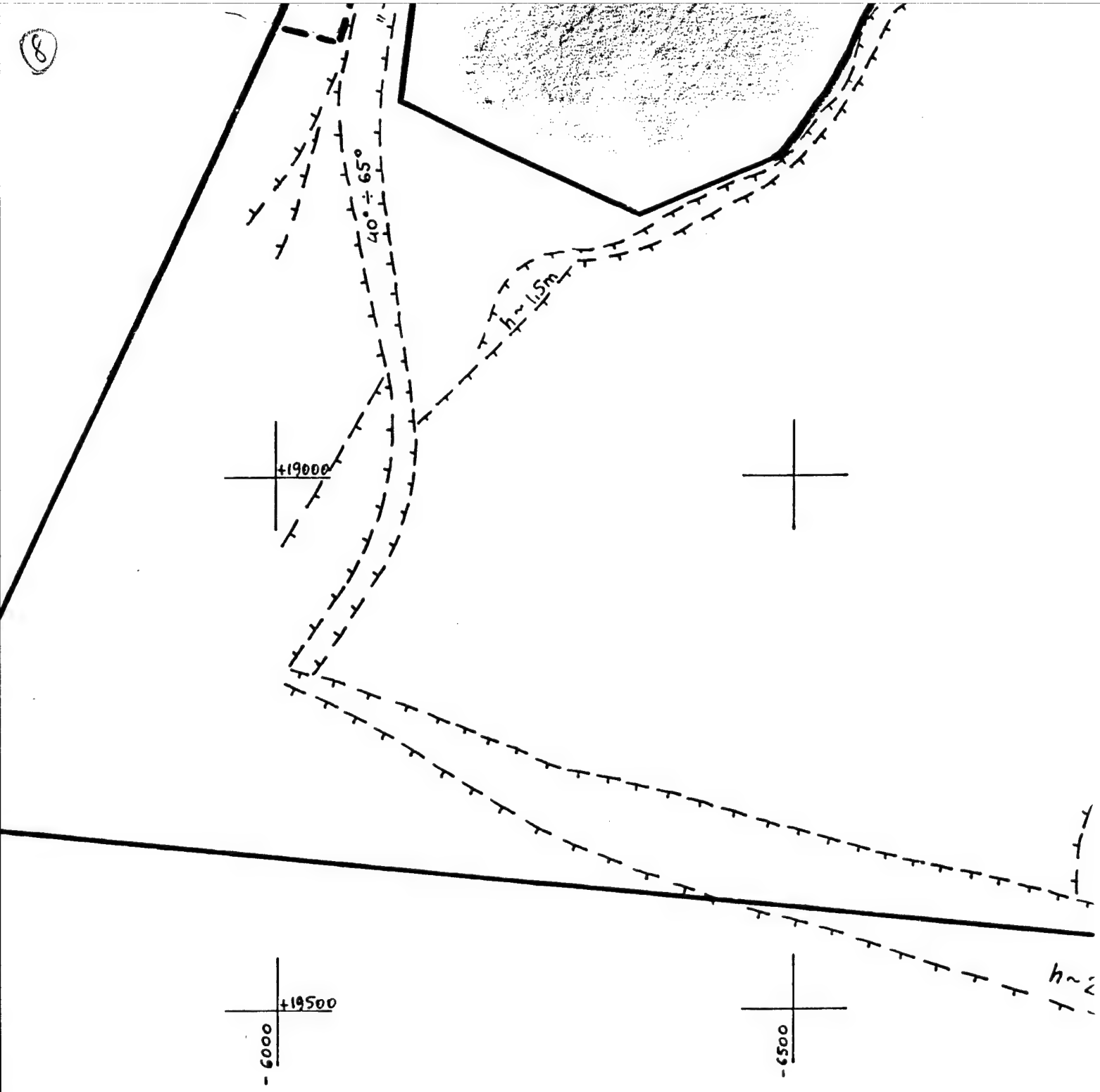
(8)
40÷65°
h~1.5m
+19000
+19500
-6000
-6500

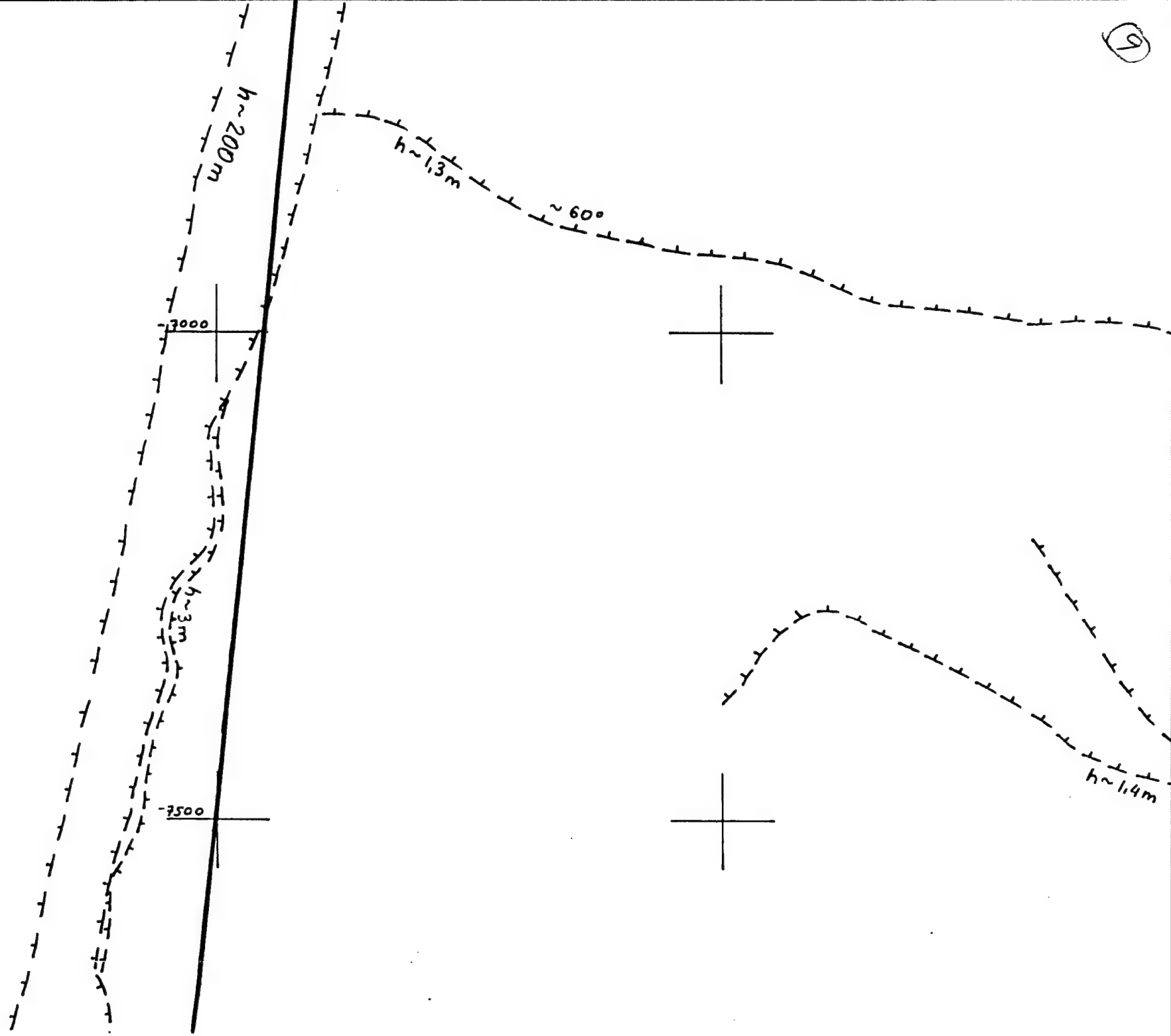
h~200m
h~1,3m
~60°
-3000
h~4
-7500
h~1,4m

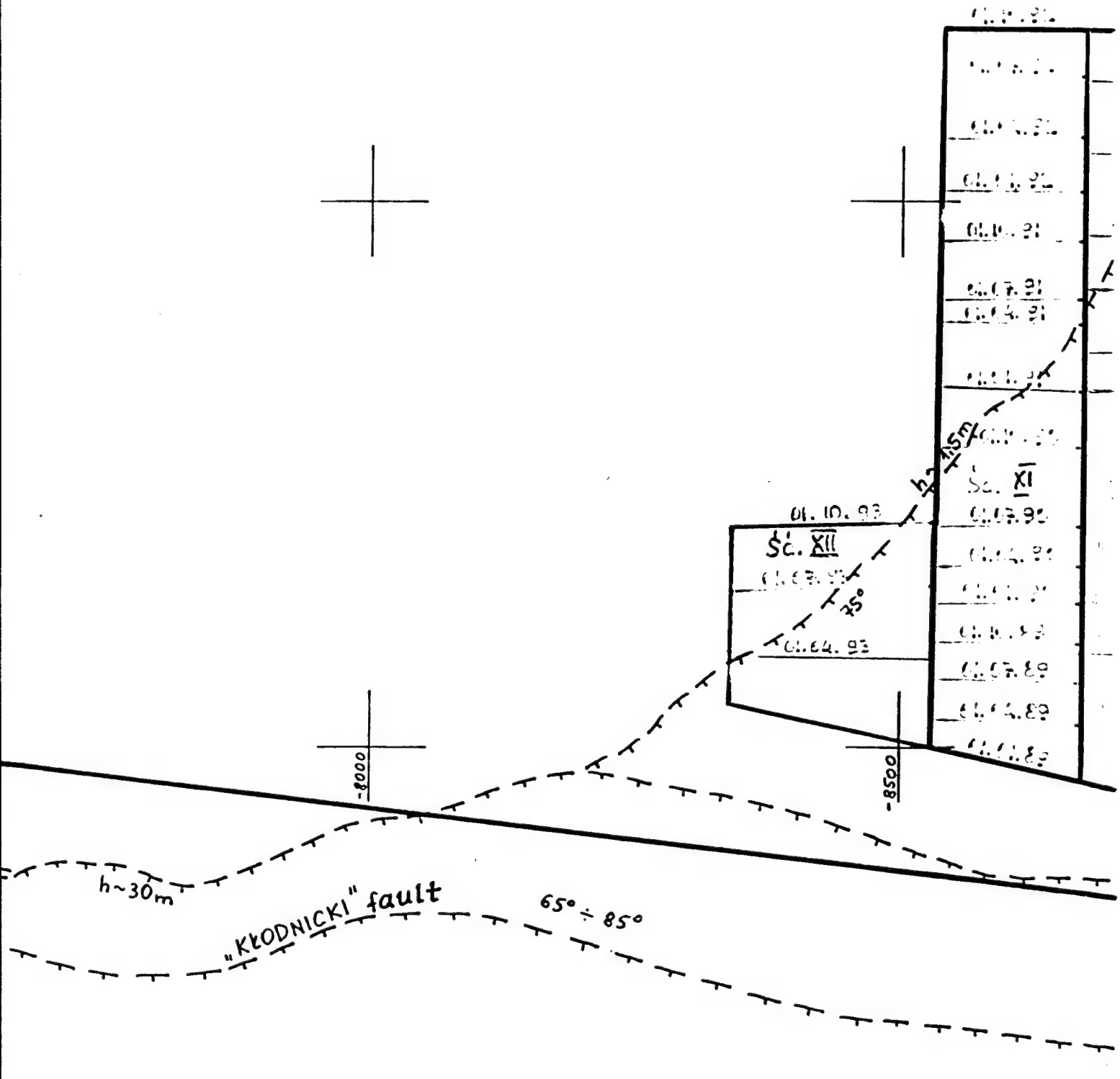
01. 10. 93
Sc. XII
01. 10. 93
Sc. XI
h=45m
25°
-8000
-8500
h~30m
"KŁODNICKI" fault
65° ÷ 85°

(11)

Sc. X

-9000

-9500

h~30m

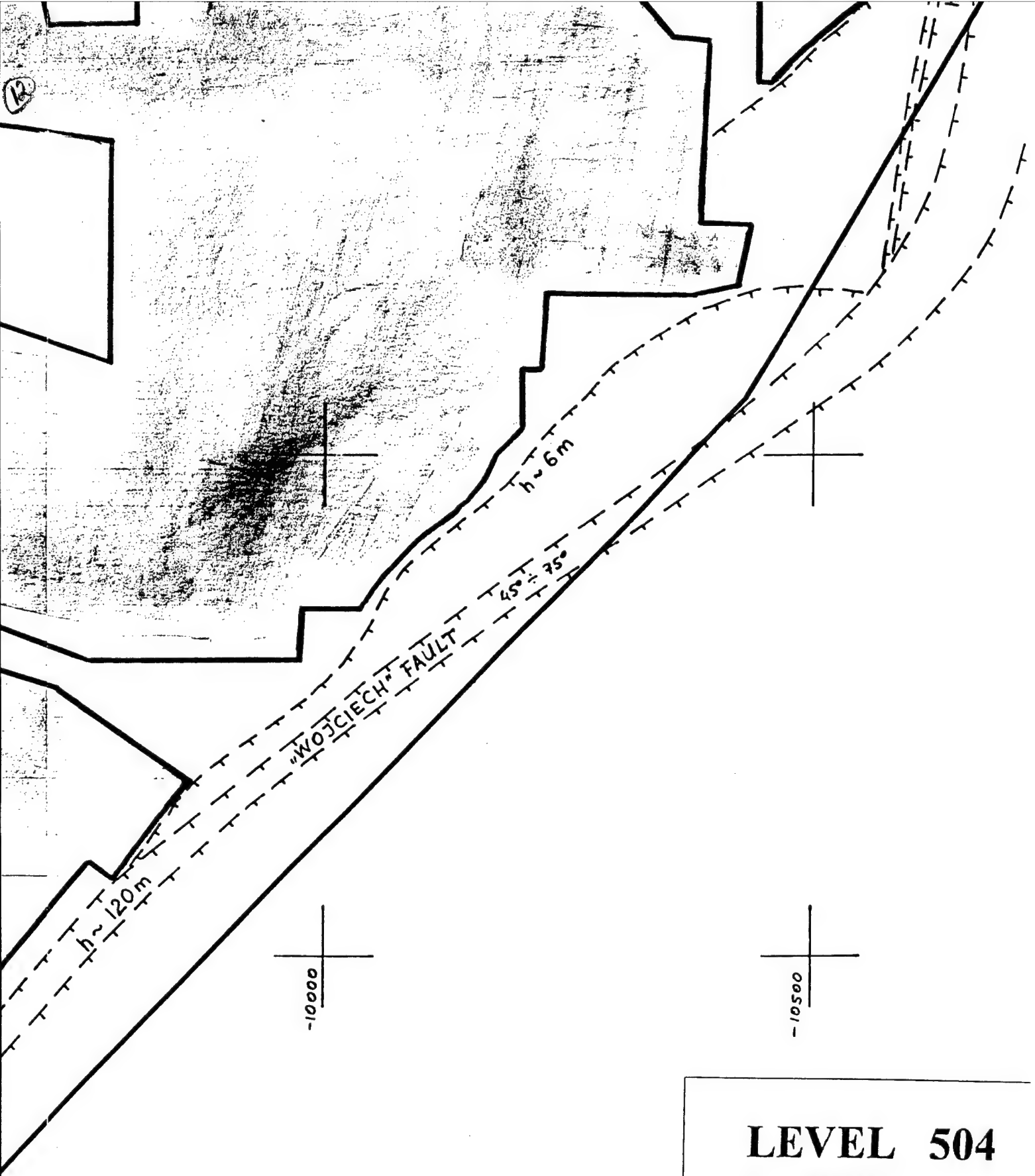

LEVEL 504
1 : 5000

APPENDIX 6

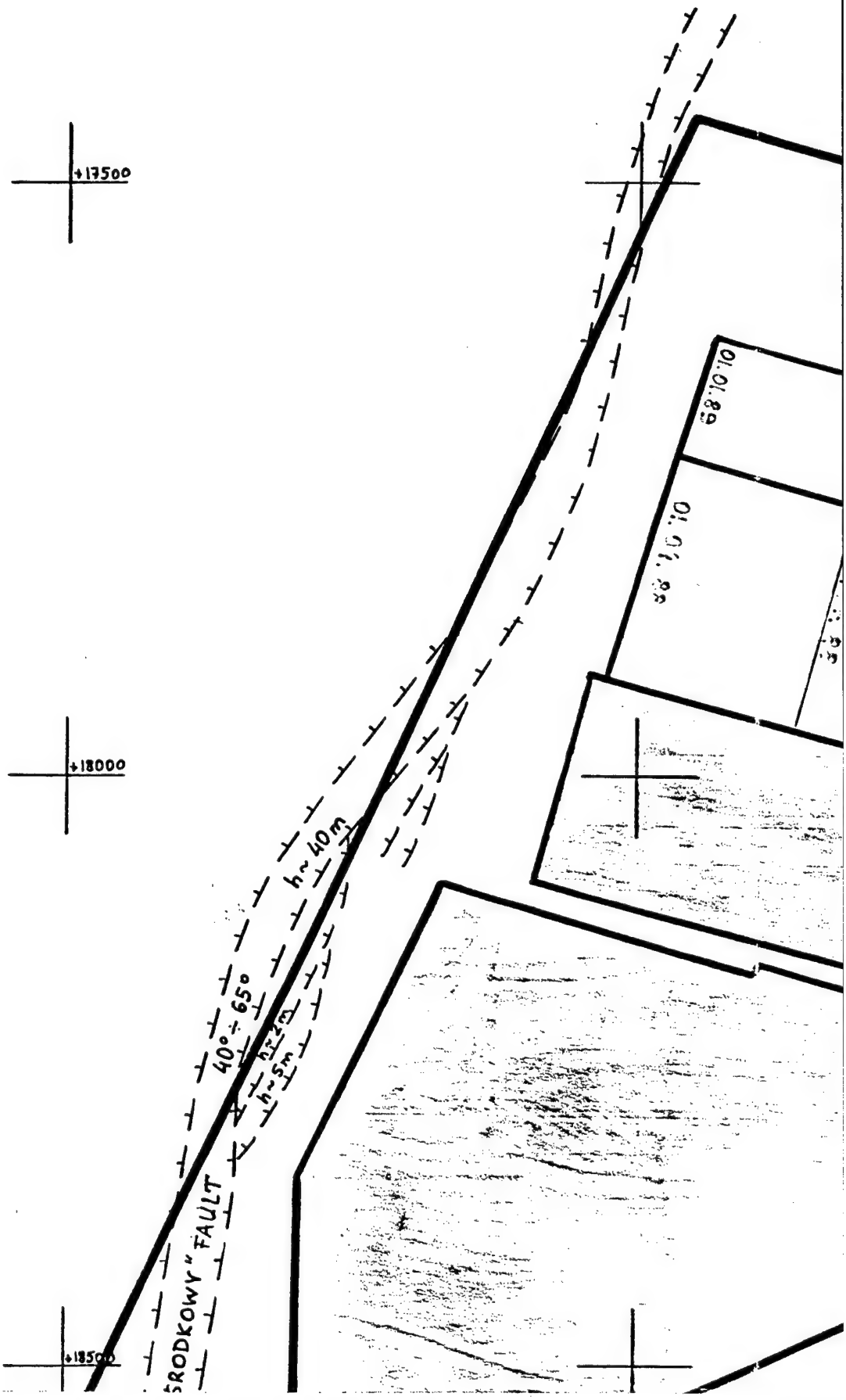
+17500
+18000
+18500
h~40m
40°÷65°
h~12m
h~5m
"ŚRODKOWY" FAULT

(2)

(3)

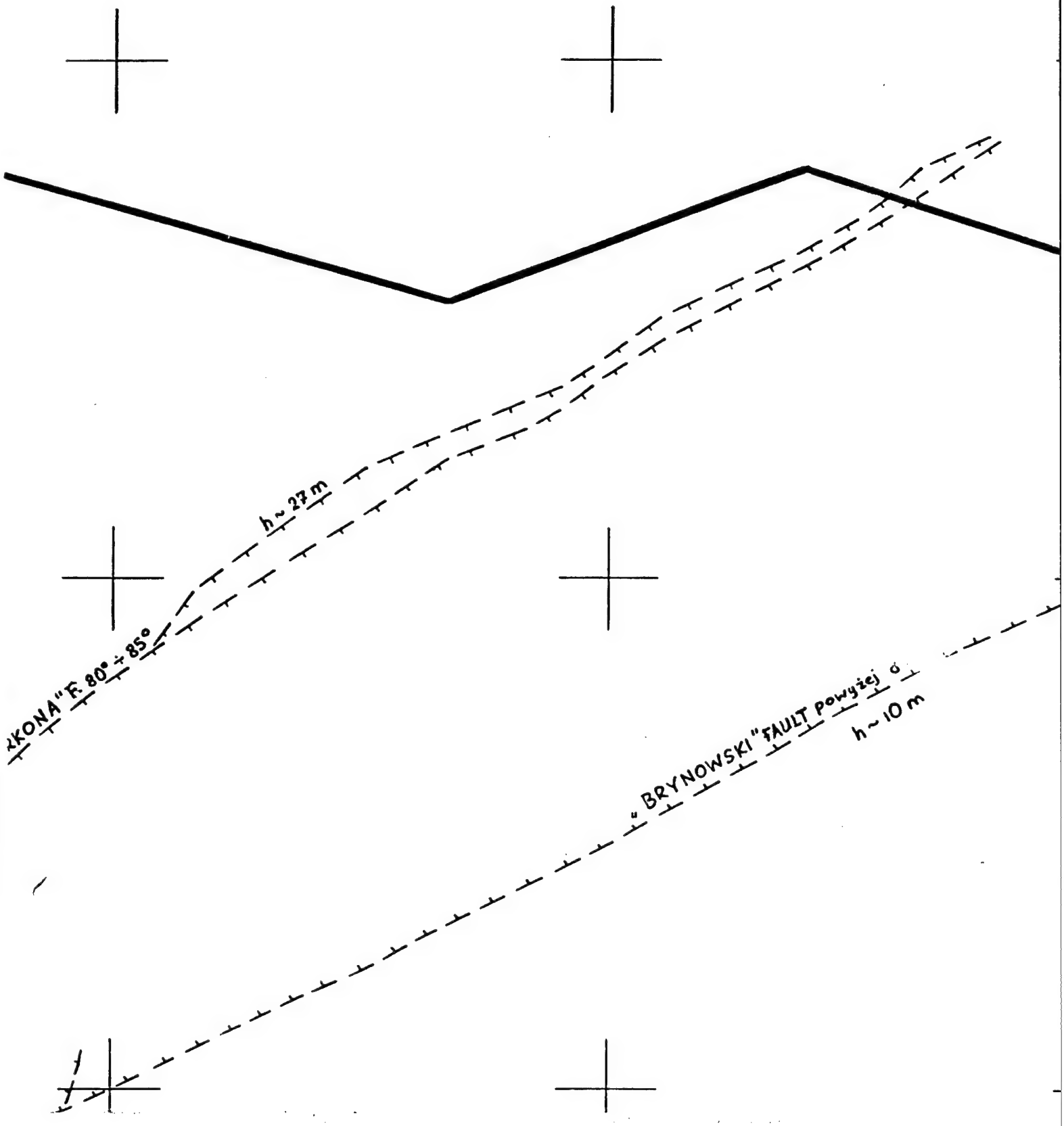

(4)

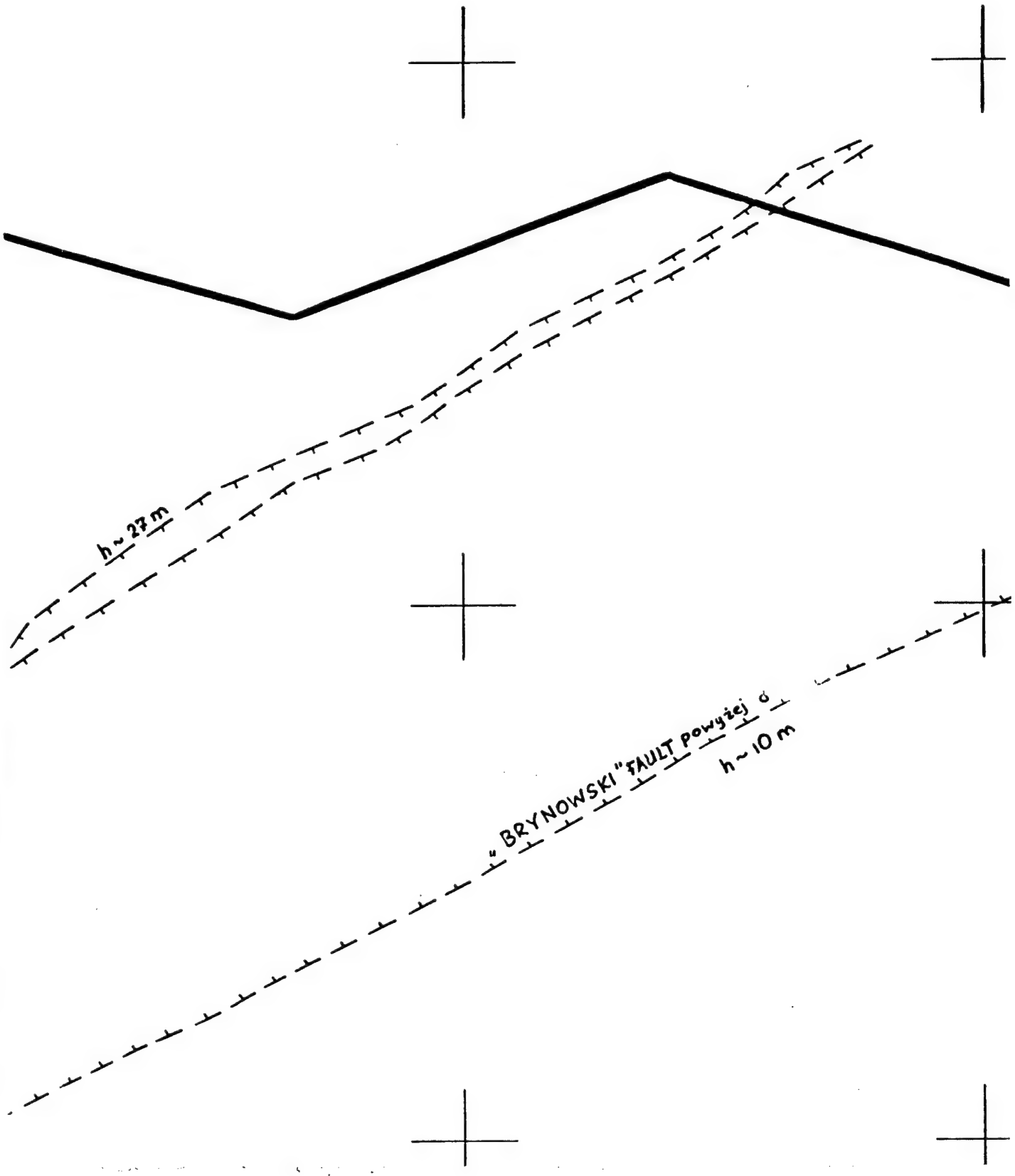

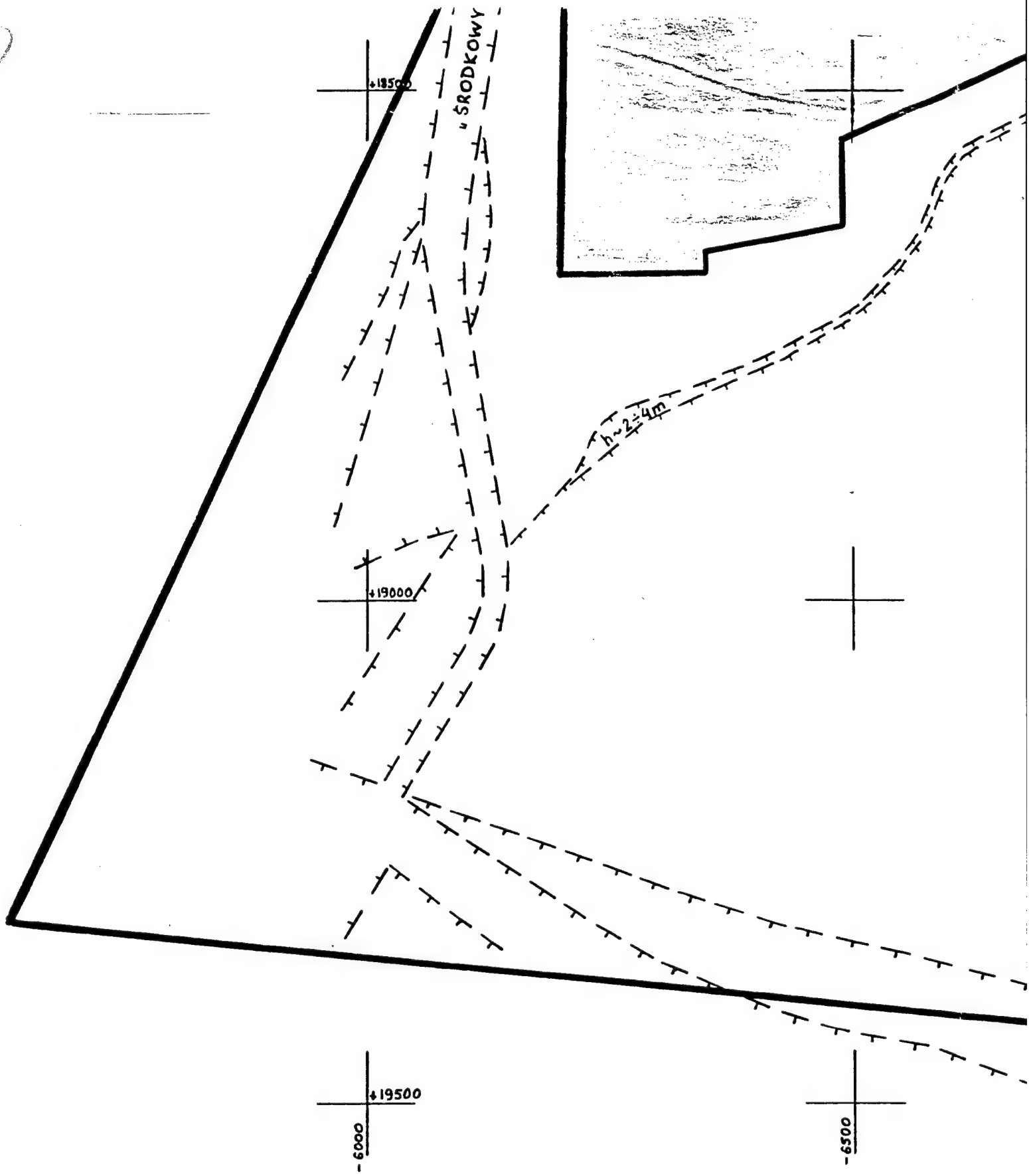

LEVEL 507
1 : 5000

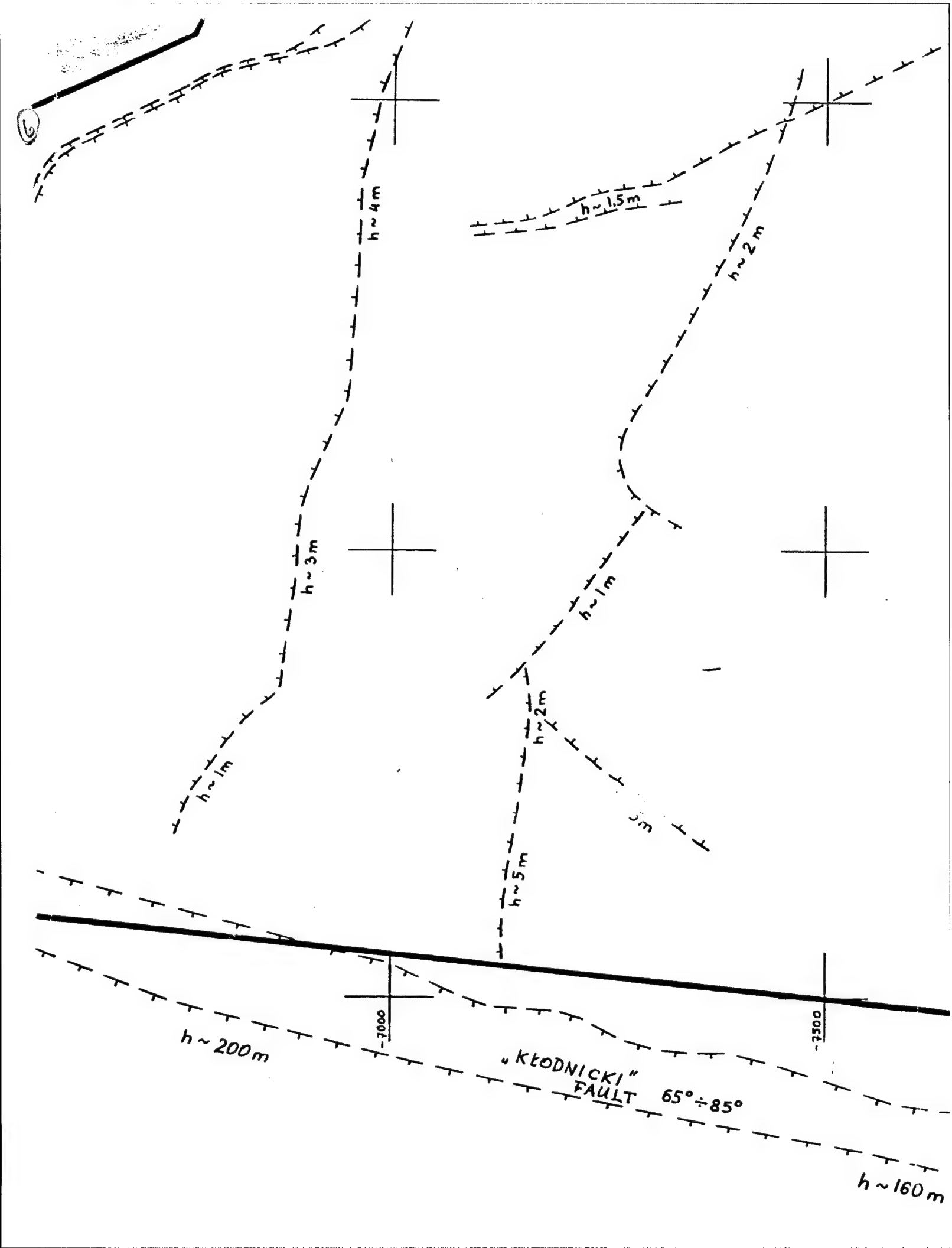
h ~ 4 m
h ~ 1.5 m
h ~ 2 m
h ~ 3 m
h ~ 1 m
h ~ 1 m
h ~ 2 m
3 m
h ~ 5 m
-7000
-7500
h ~ 200 m
„KŁODNICKI"
FAULT 65° ÷ 85°
h ~ 160 m

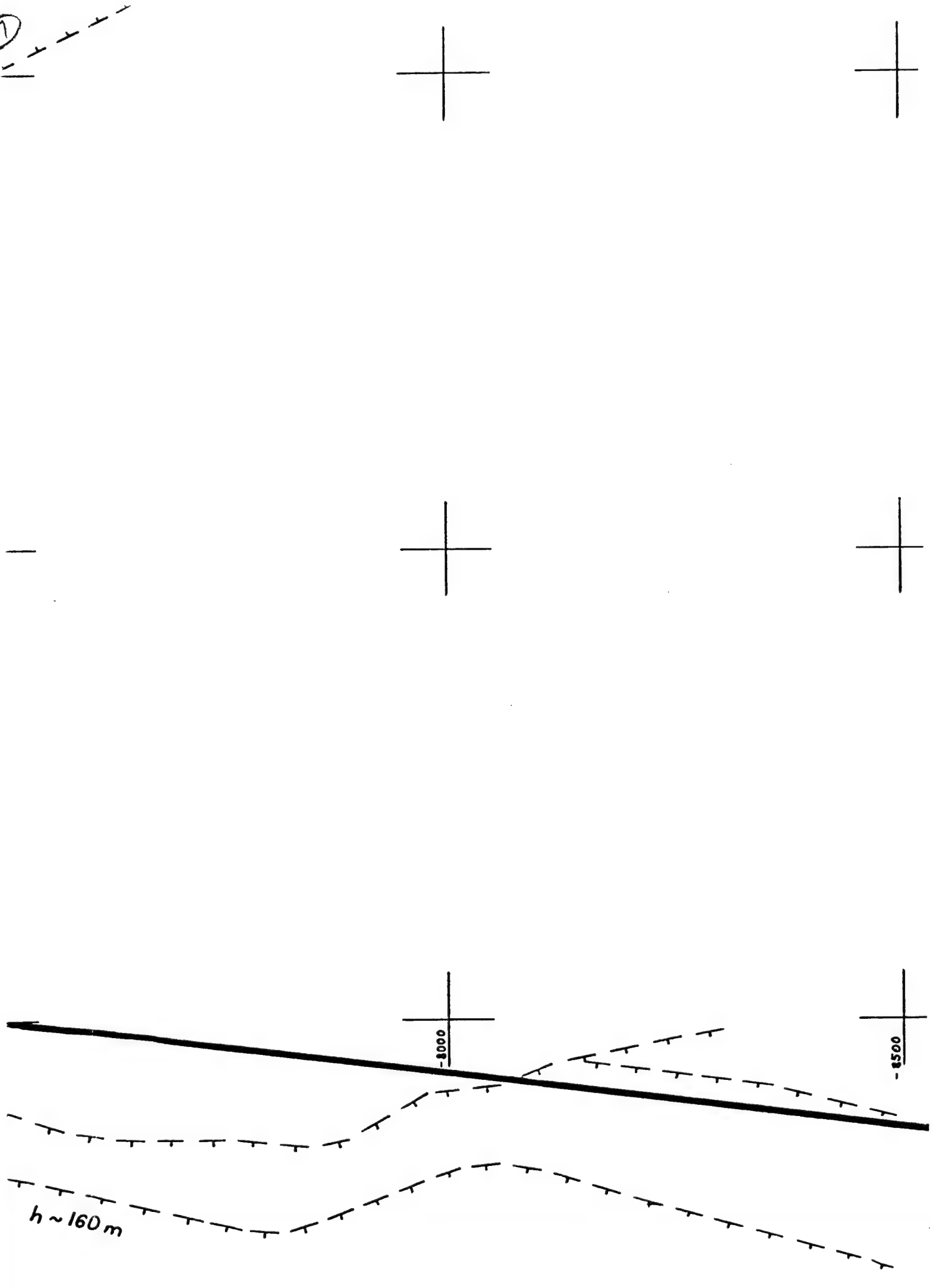
-8000
-8500
h ~ 160 m

(8)

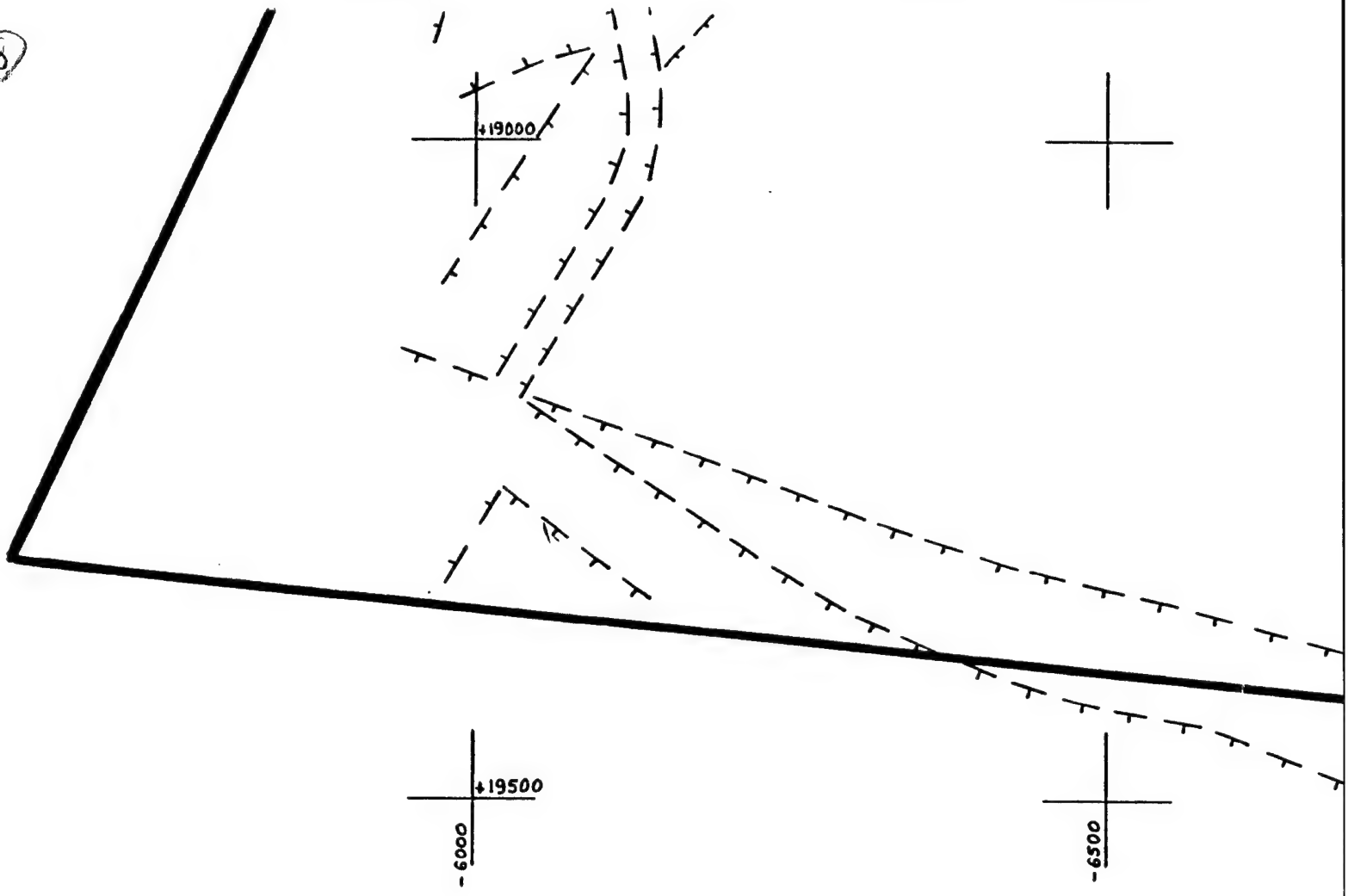

LEVEL 507
1 : 5000

APPENDIX 7

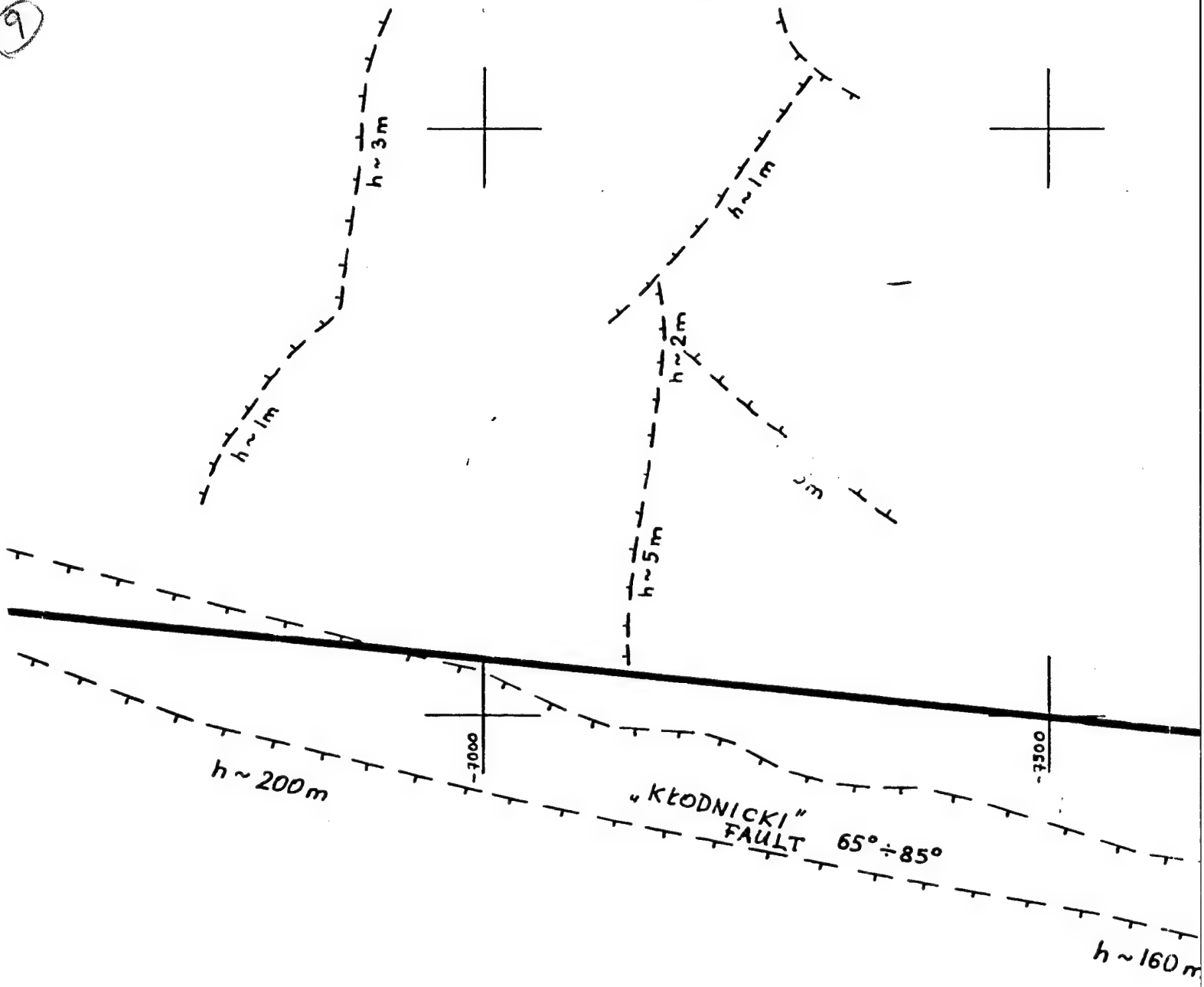
h ~ 3m
h ~ 1m
h ~ 1m
h ~ 2m
h ~ 5m
-3000
-3500
h ~ 200m
„KŁODNICKI"
FAULT 65°÷85°
h ~ 160m

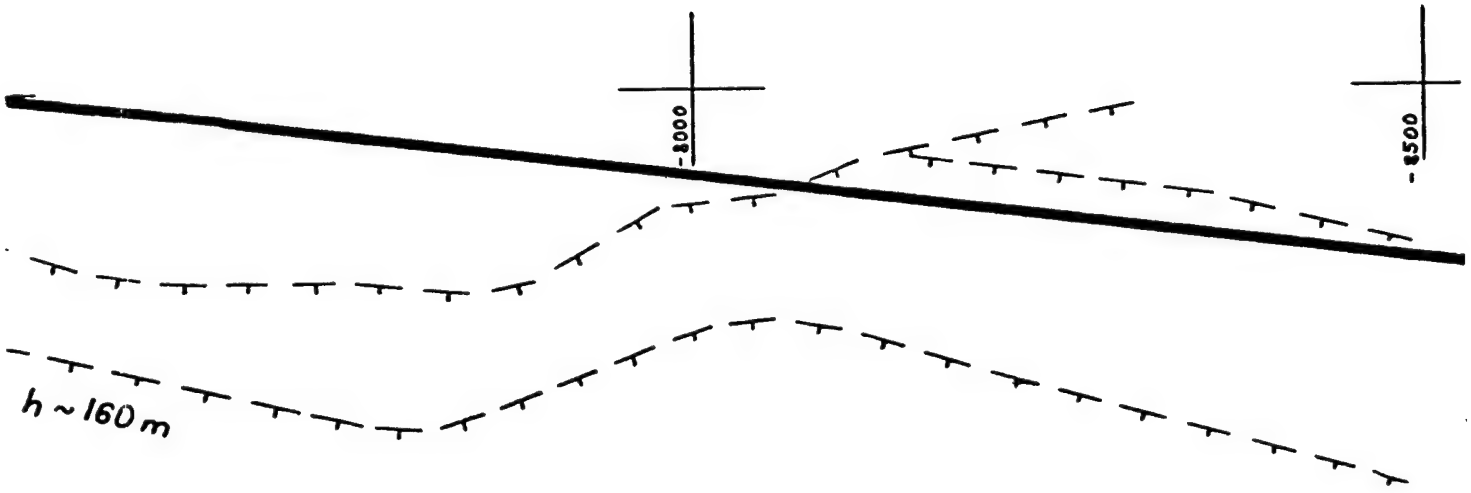
-2000
-2500
h ~ 160 m

(1)

1993

19

Sc. A II

01.10.93

01.04.93

01.10.93

01.04.93

01.10.93

01.04.93

01.10.93

Sc. A I

h ~ 0,5m

"ARKONA" FAULT

80° ÷ 85°

h ~ 2,5m

h ~ 2m

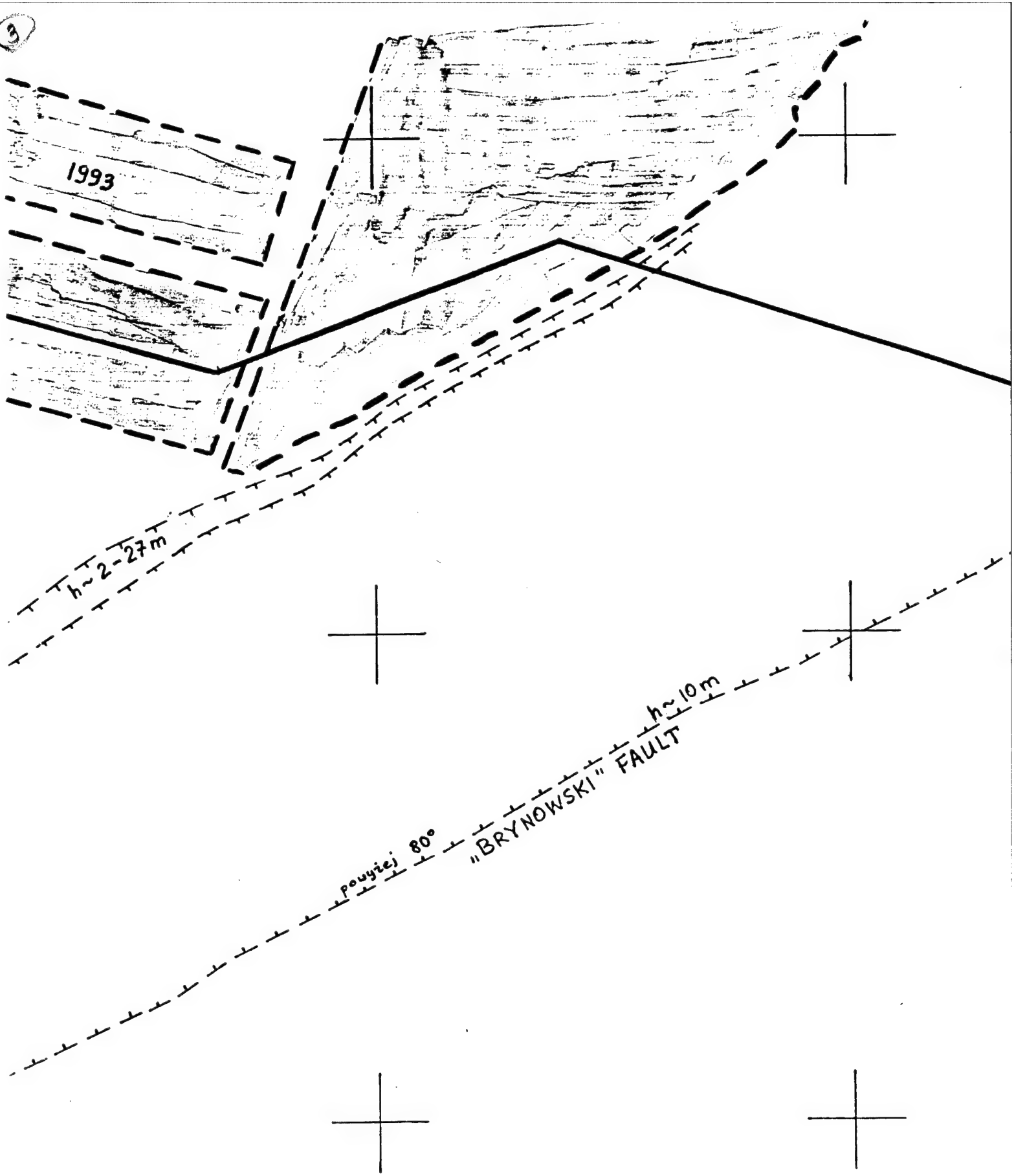
3
1993
h~2-27m
h~10m
powyżej 80°
„BRYNOWSKI" FAULT

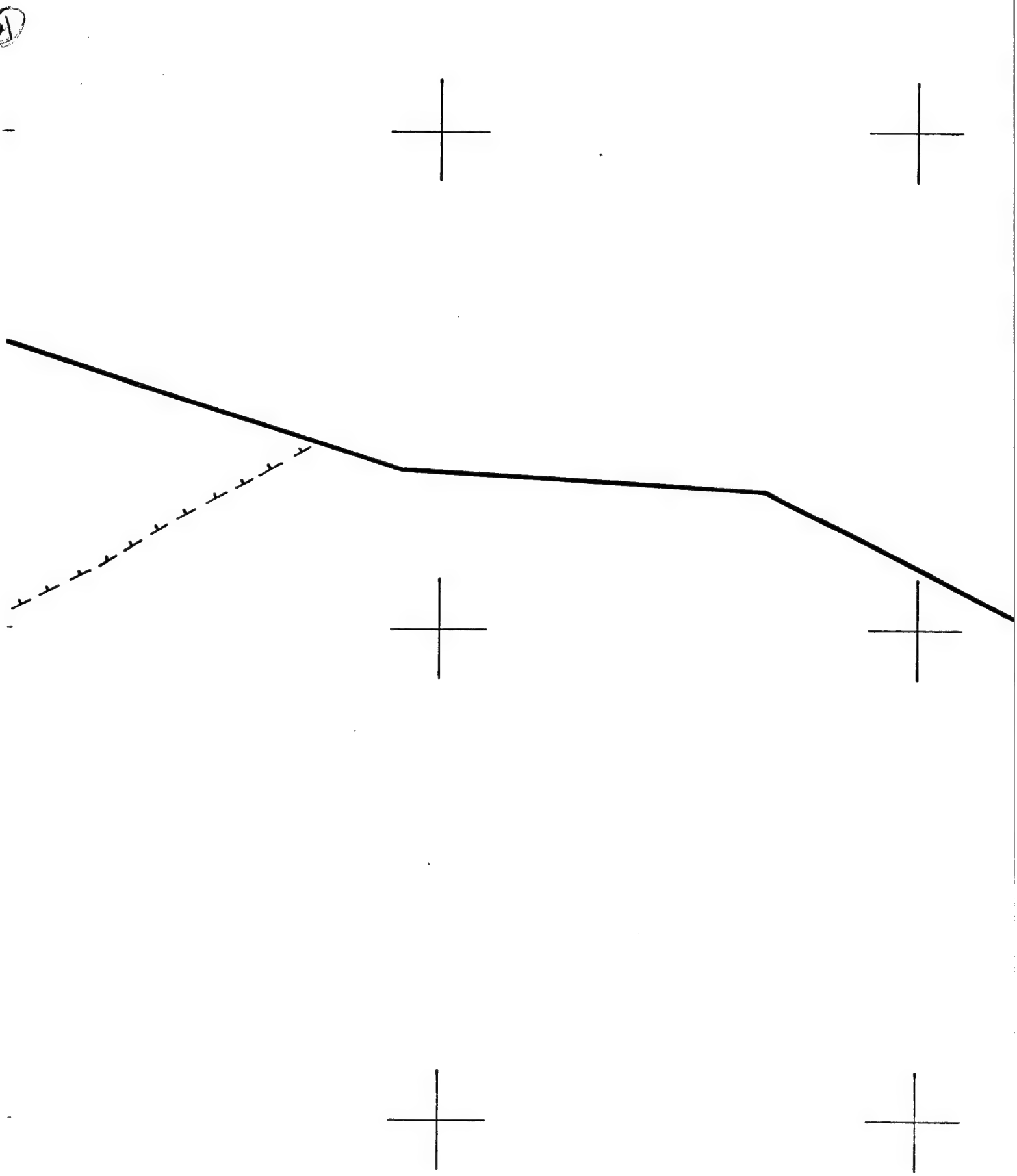

(5)

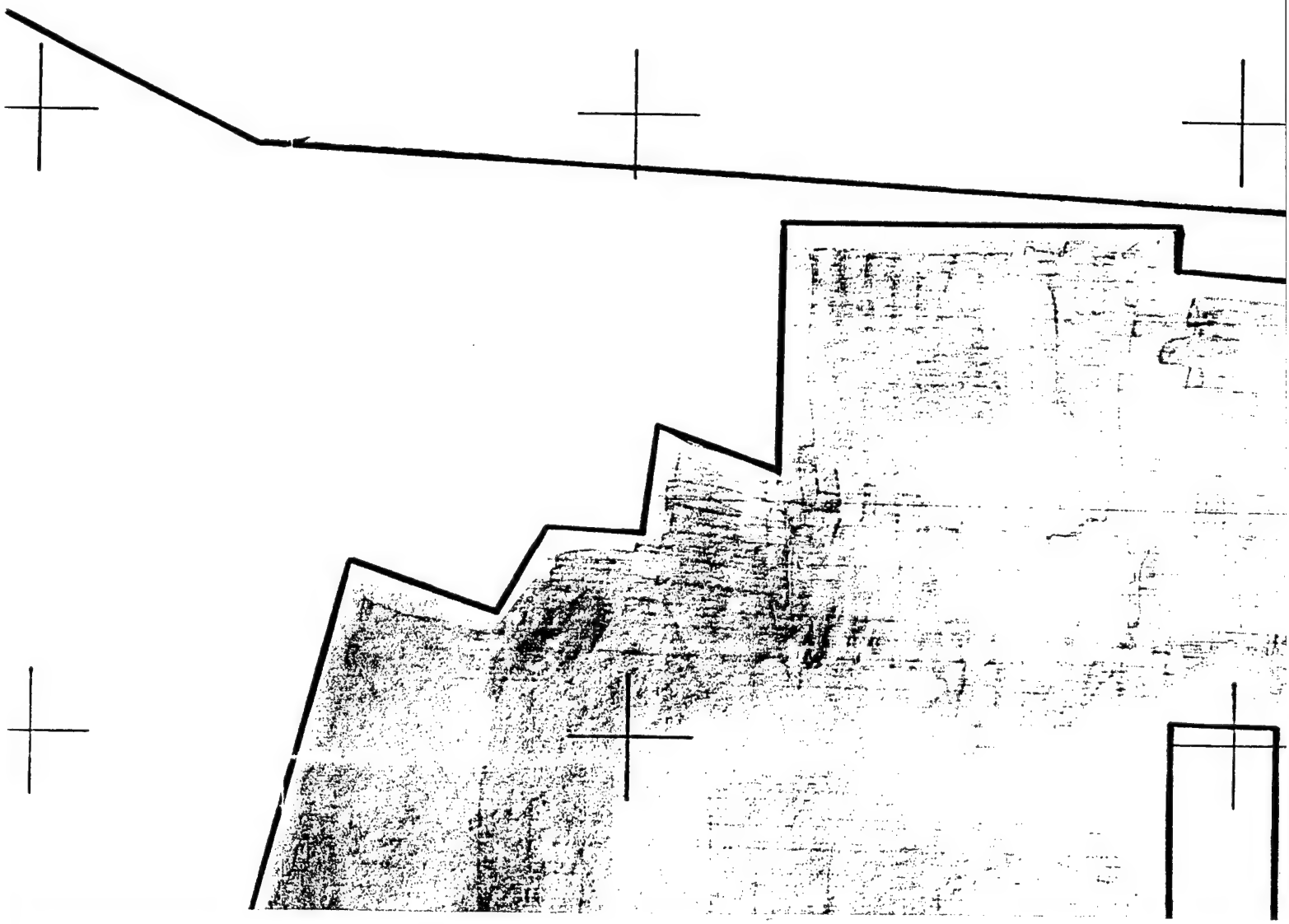

(6)

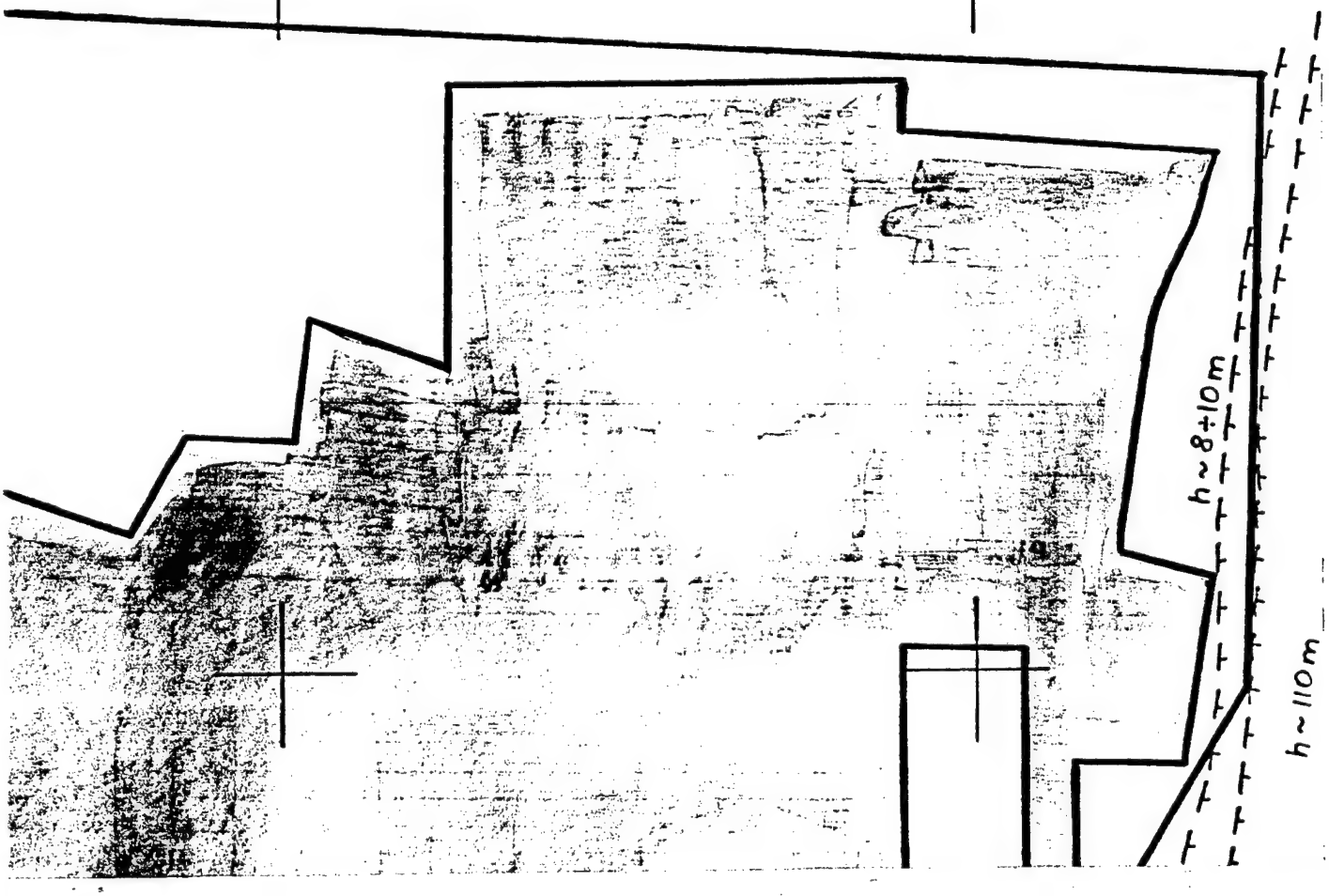

(7)

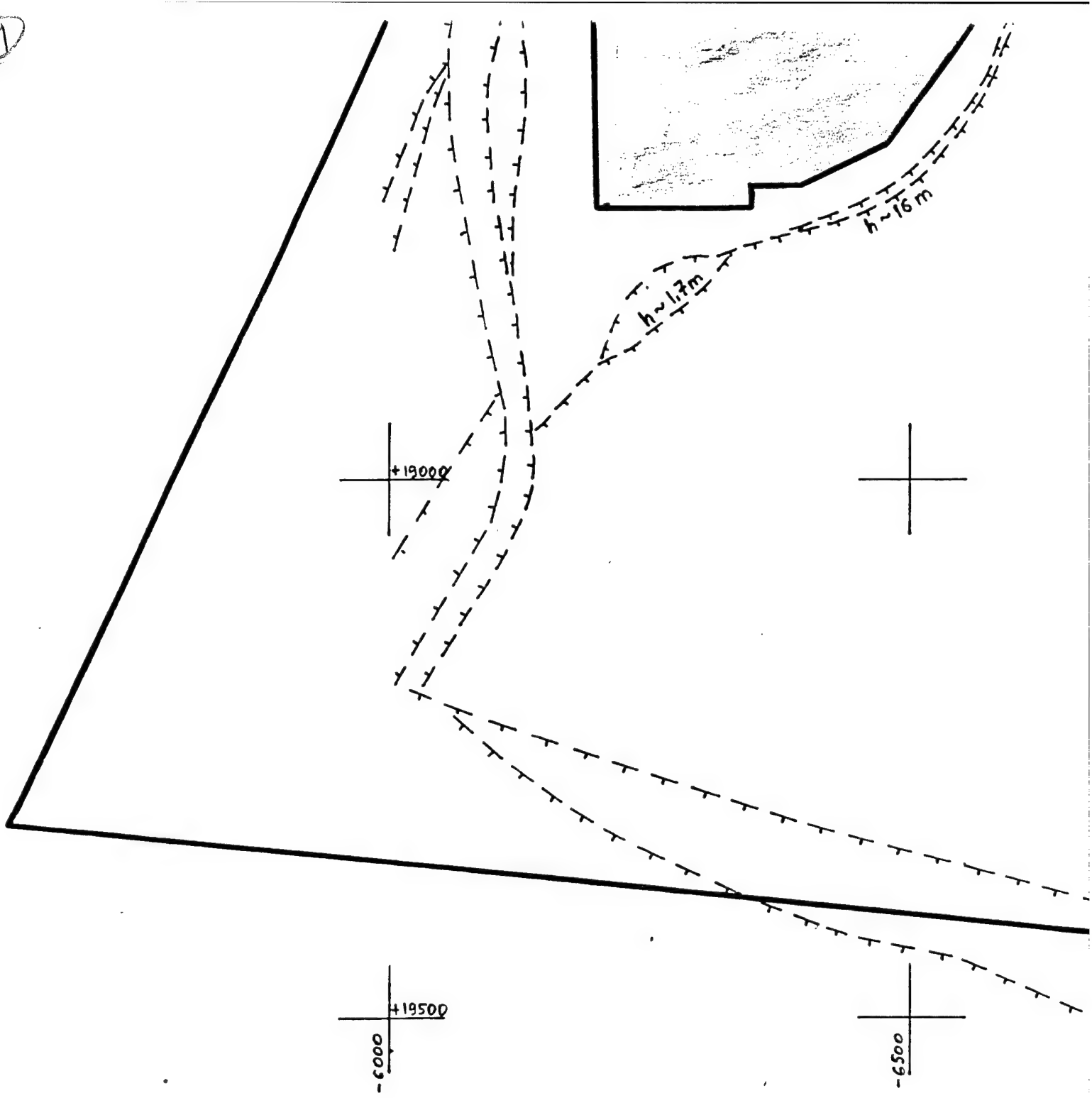

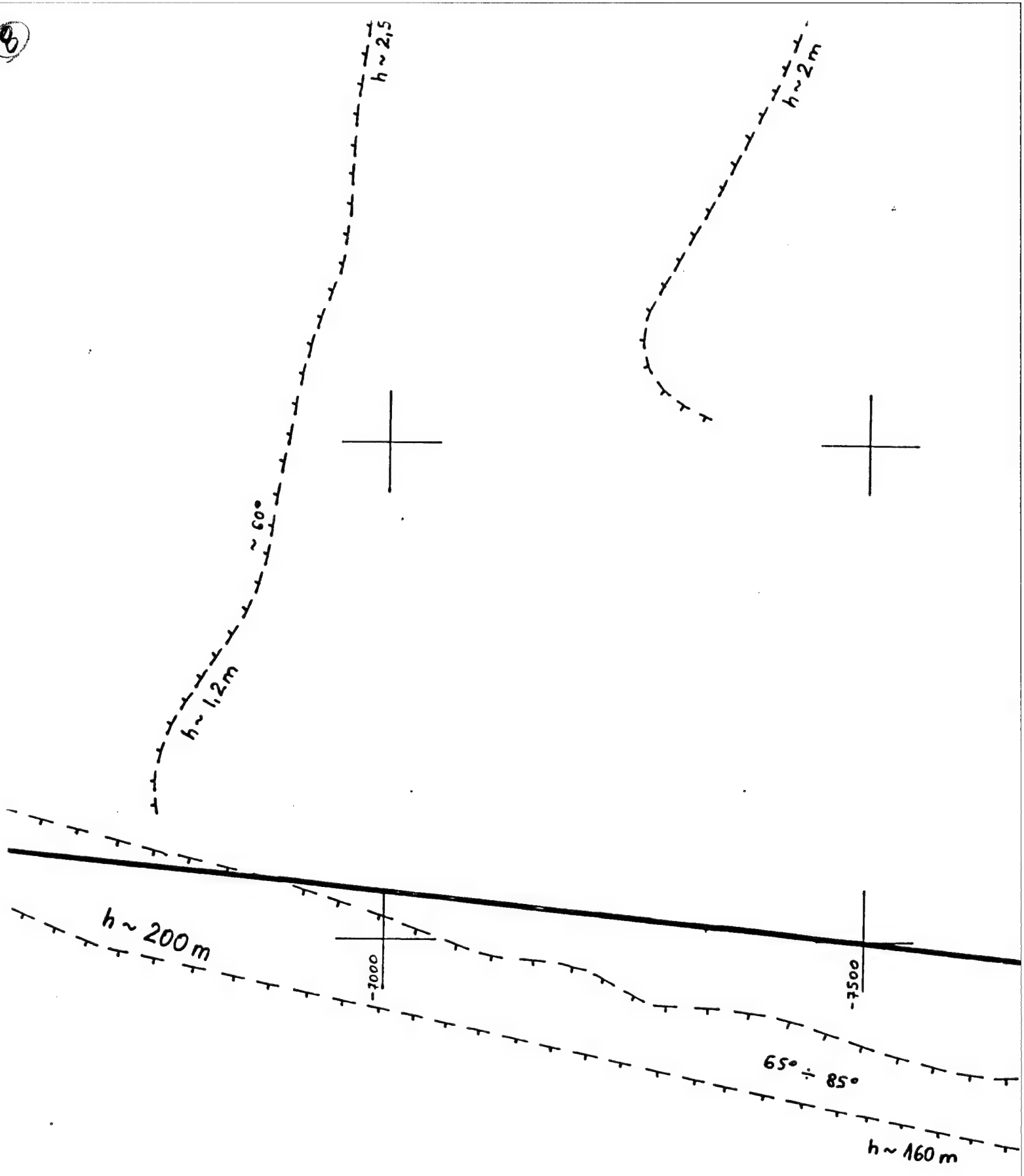
8
h ~ 2,5
h ~ 2m
~ 60°
h ~ 1,2m
h ~ 200 m
-1000
-1500
65° ÷ 85°
h ~ 160 m

(9)

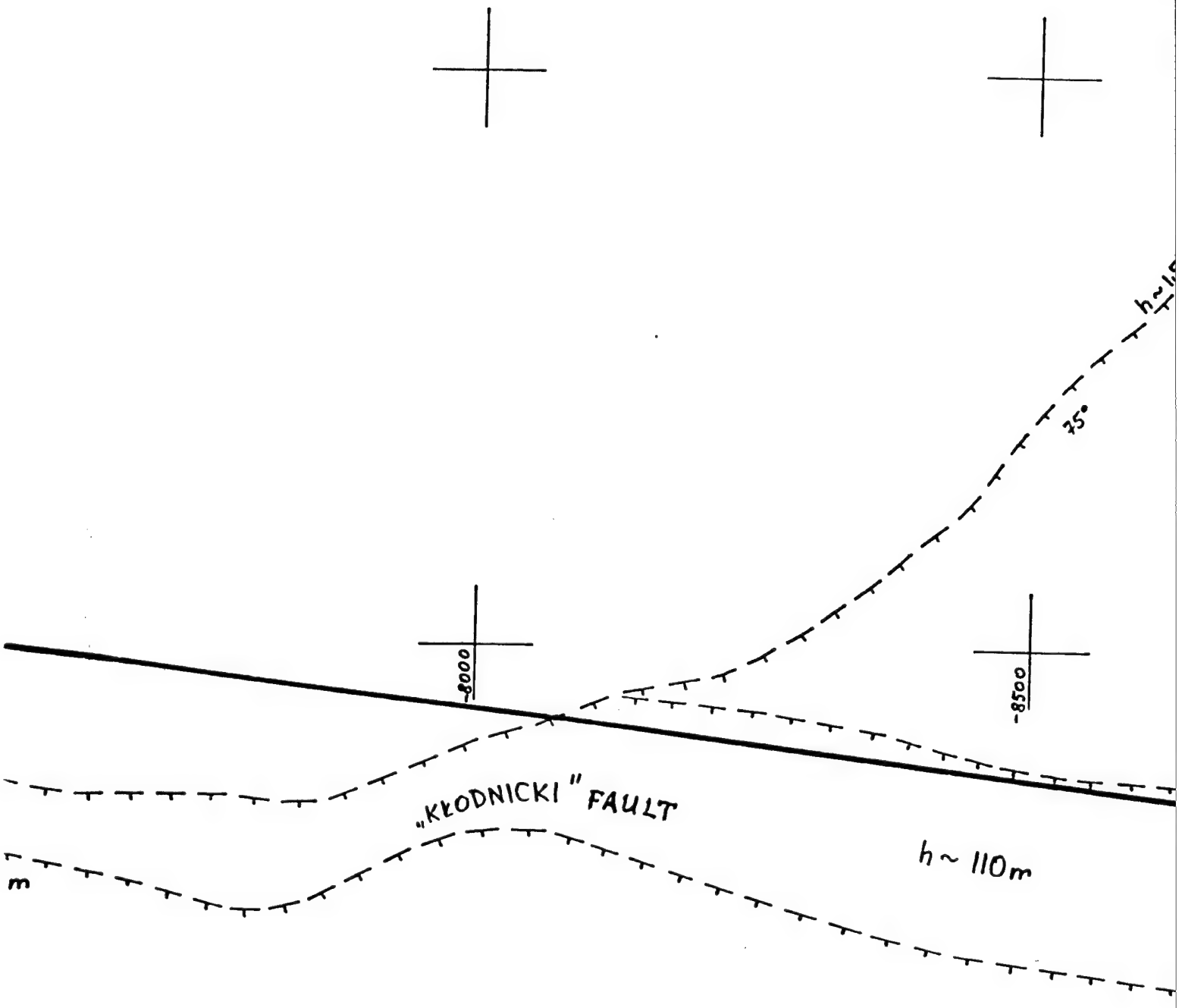

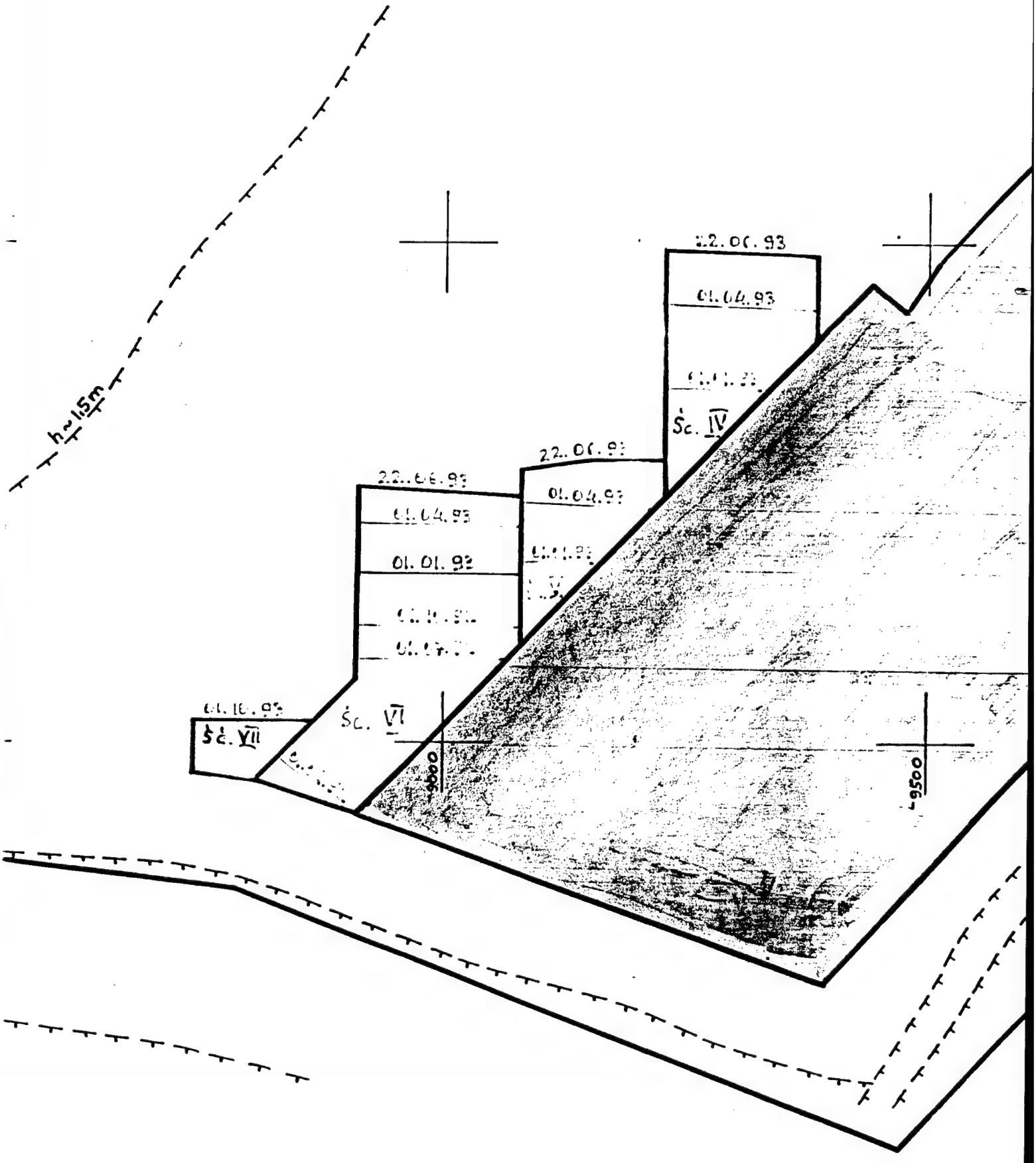
h=15m
22.06.93
01.04.93
Sc. IV
22.06.93
01.04.93
01.01.93
Sc. VI
01.10.93
Sc. VII
9800
9500

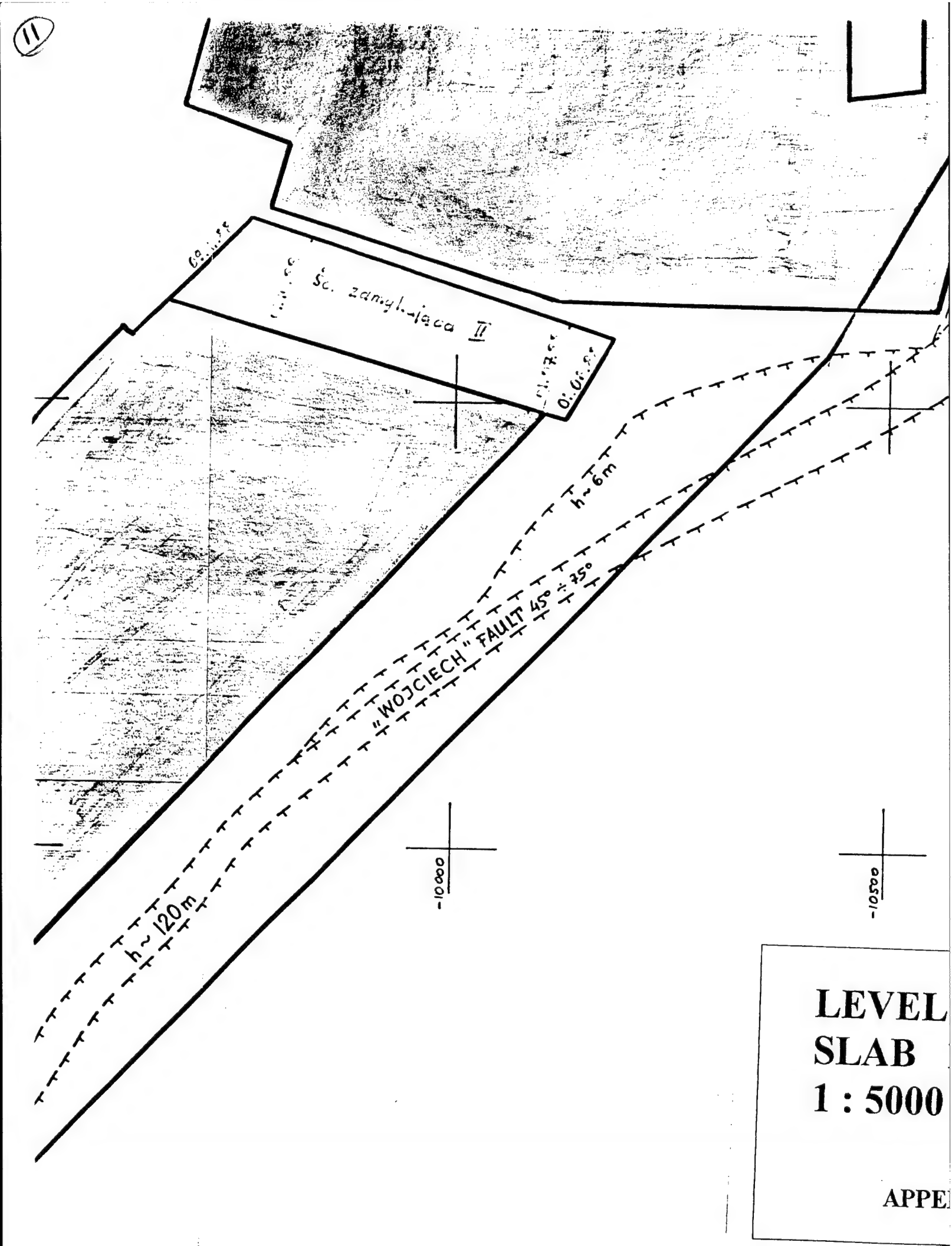

LEVEL
SLAB
1 : 5000

APPE

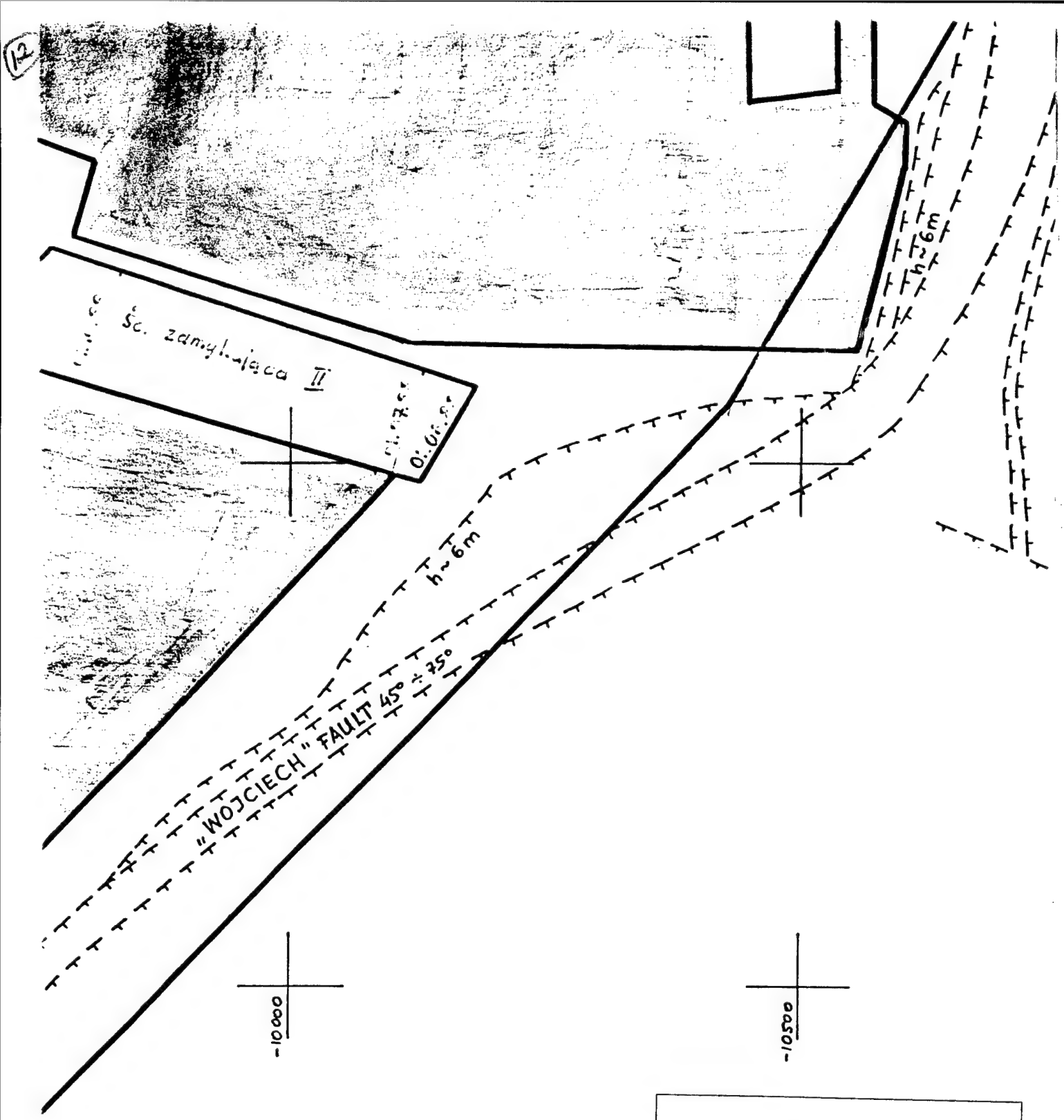

LEVEL 510
SLAB 1
1 : 5000

APPENDIX 8

9


+17500
+18000
+18500
Śc. A III a
01.10.93
Śc. A II a
01.07.91
01.10.91
h~40m
40°÷65°
"ŚRODKOWY" FAULT
~16m

(2)

Sc. A III a

01.10.93

01.01.94

Sc. A II a

01.10.91

01.01.92

01.04.92

01.07.92

01.10.92

01.01.93

01.04.93

01.07.93

01.10.93

01.01.94

Sc. A I a

01.10.91

01.01.92

01.04.92

01.07.92

01.10.92

01.01.93

01.04.93

01.07.93

01.10.93

N80°W

"ARKONA" FAULT

80° - 85°

h ~ 3,5 m

h ~ 2 m

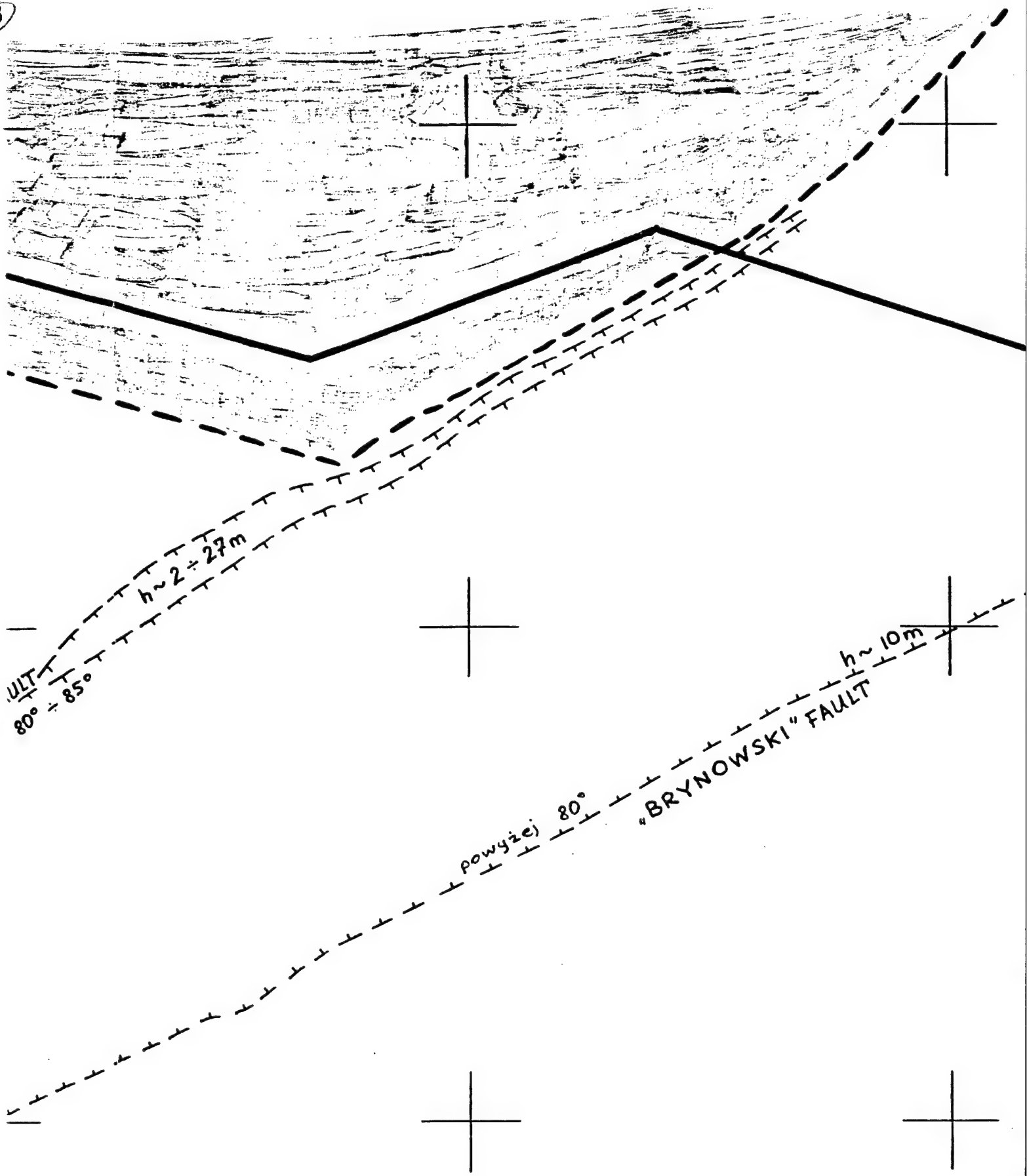
h~2÷27m
80°÷85°
powyżej 80°
h~10m
„BRYNOWSKI" FAULT

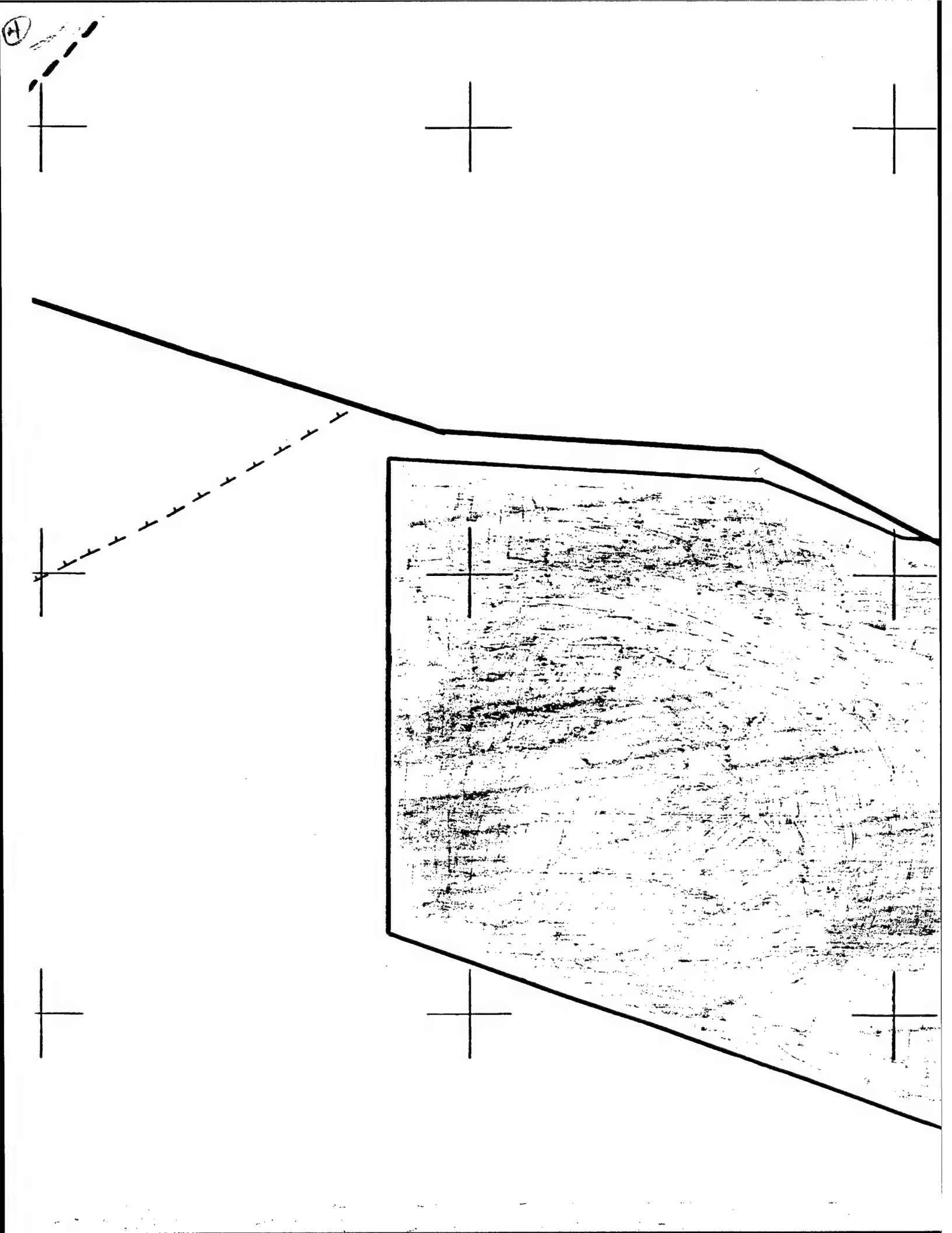

(5)

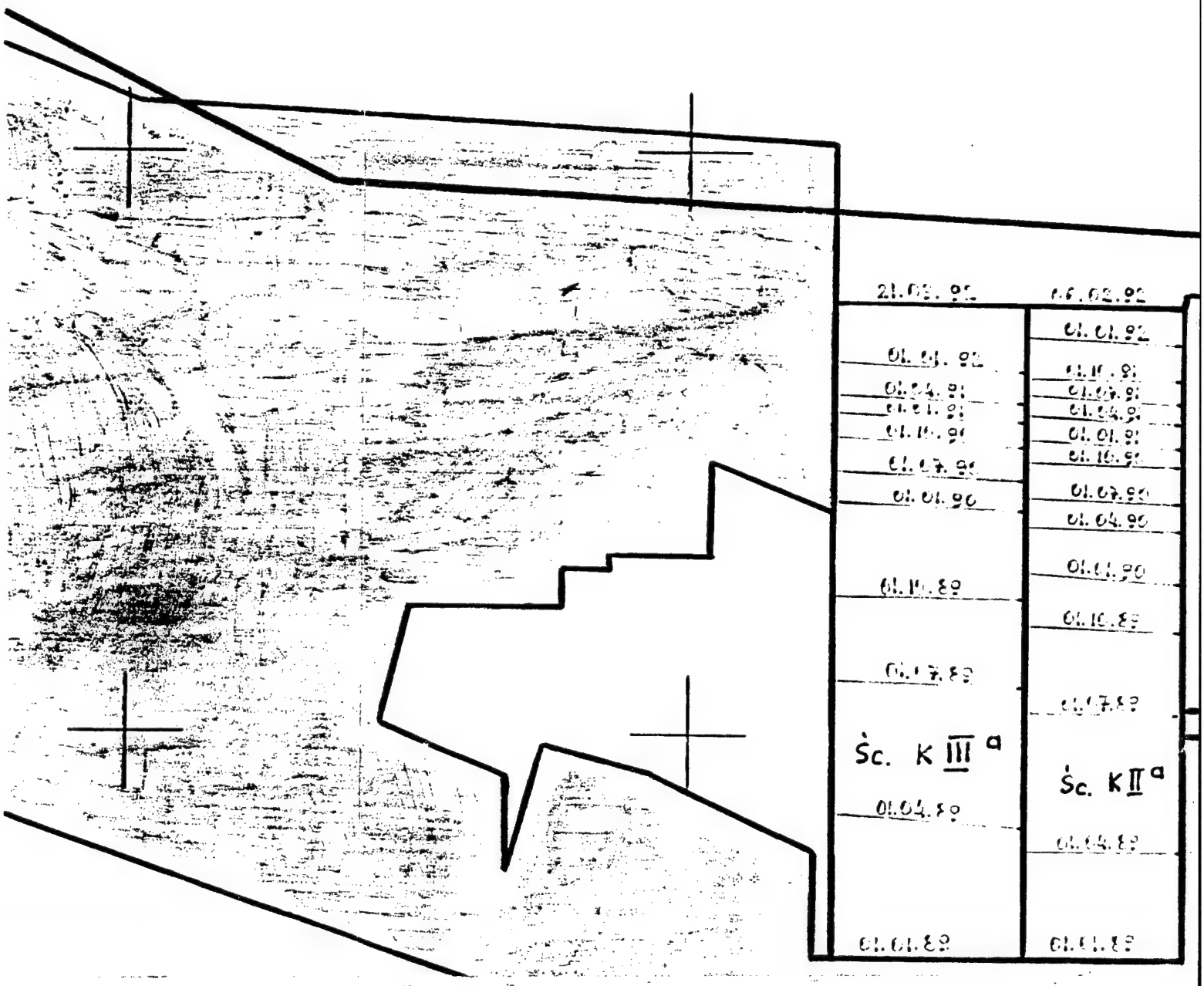

(6)

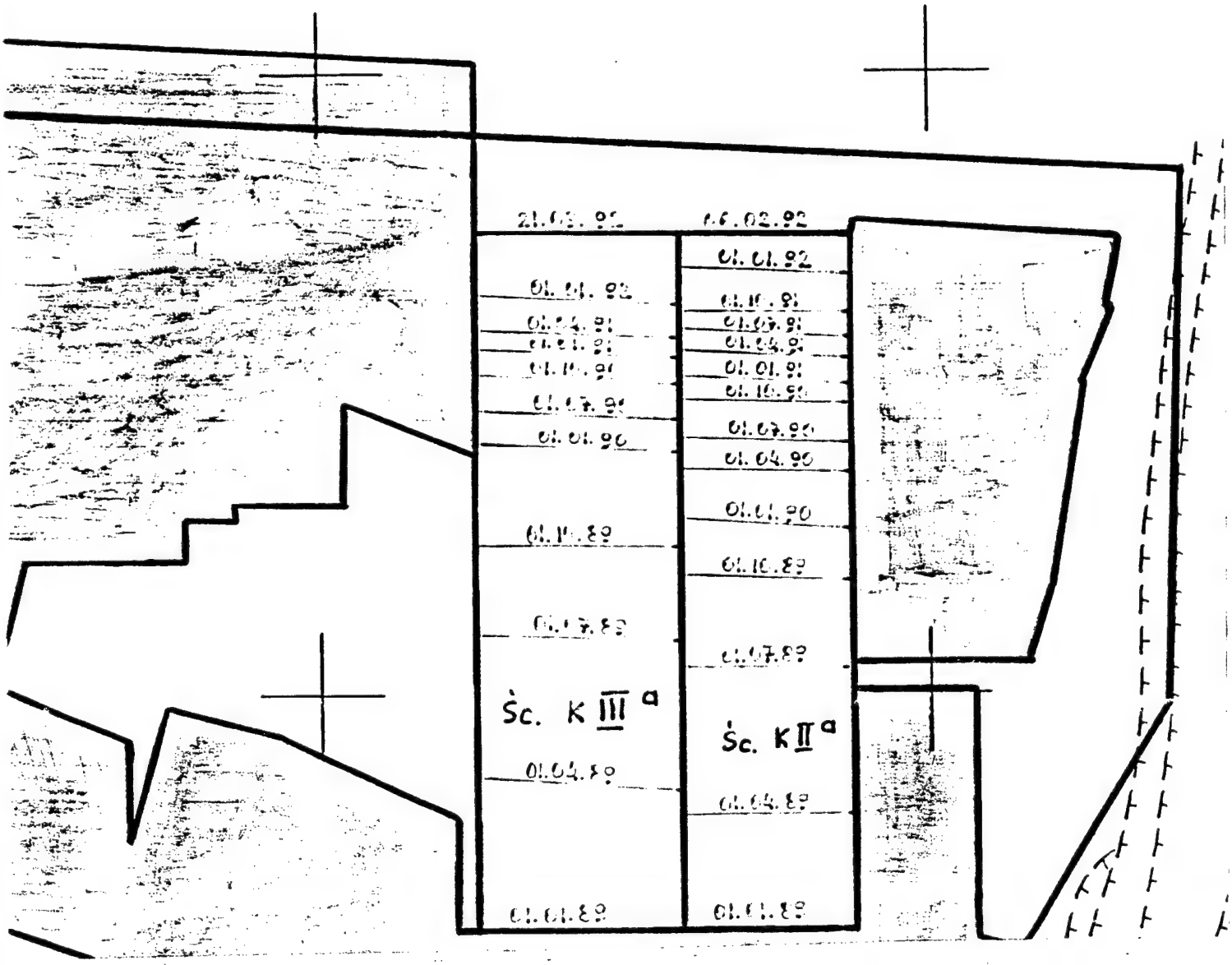

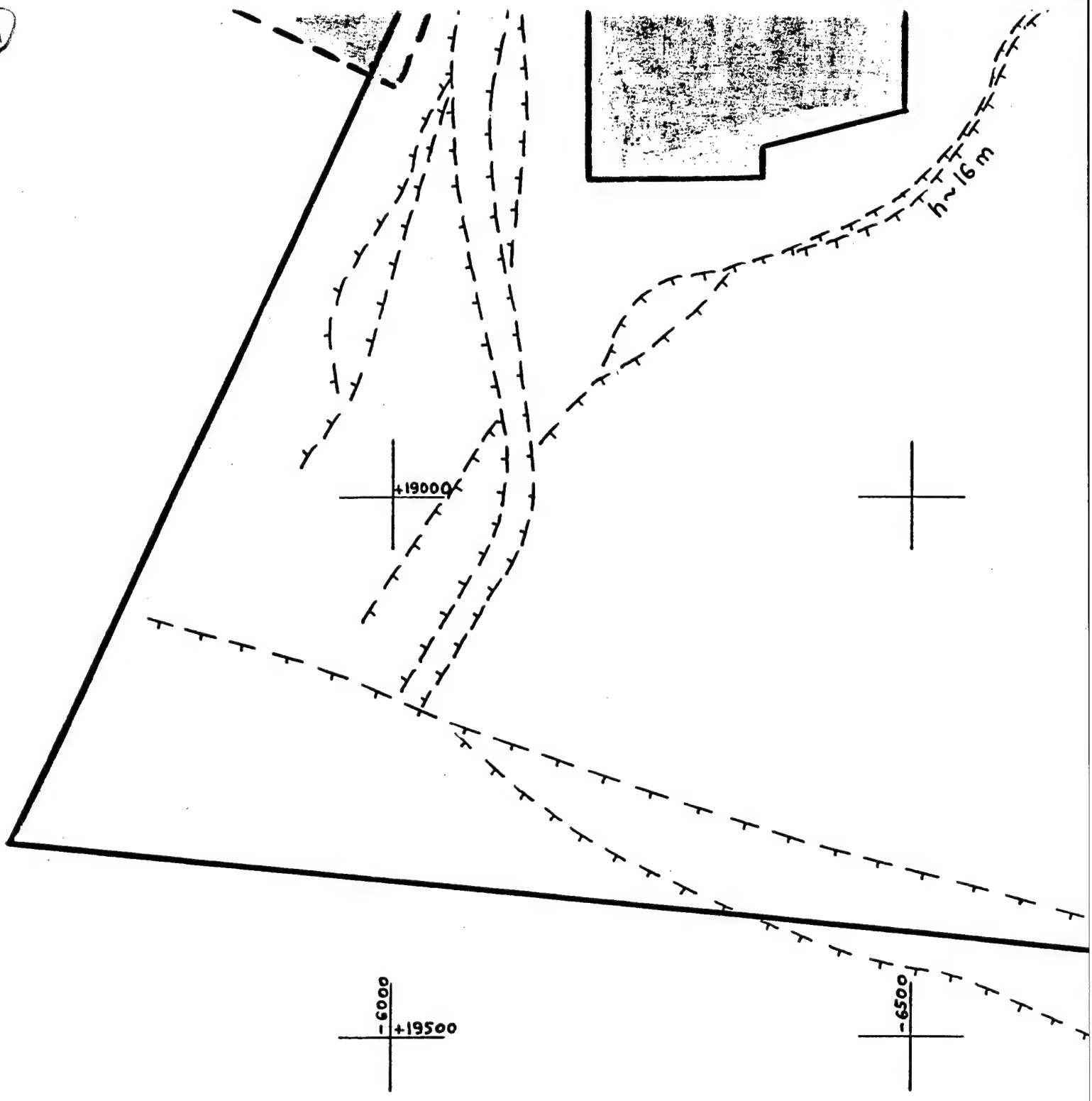
h~16 m
+19000
-6000
+19500
-6500

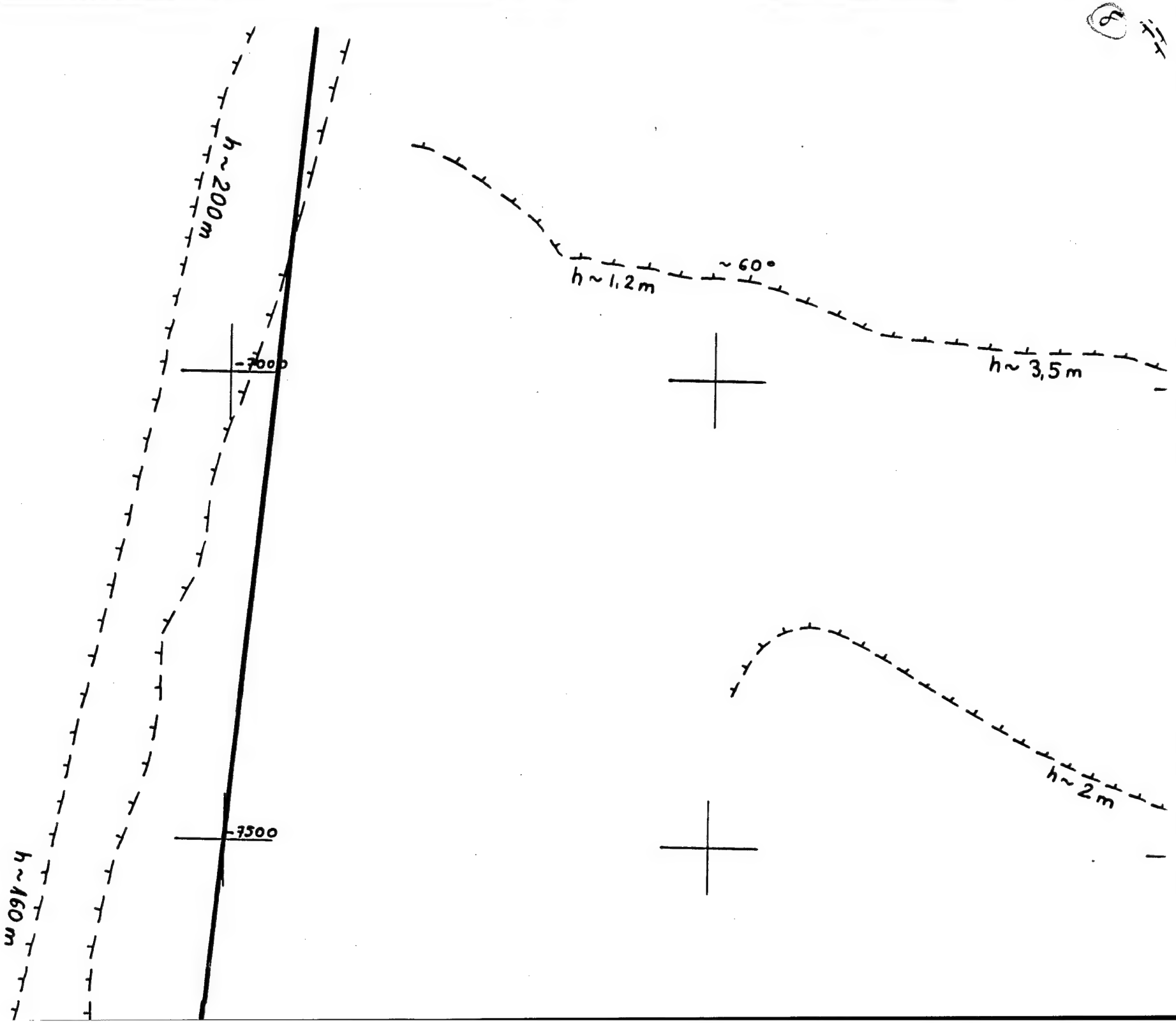
h ~ 200 m
-7000
-7500
w 091 ~ 4
h ~ 160 m
~ 60°
h ~ 1,2 m
h ~ 3,5 m
h ~ 2 m

(9)

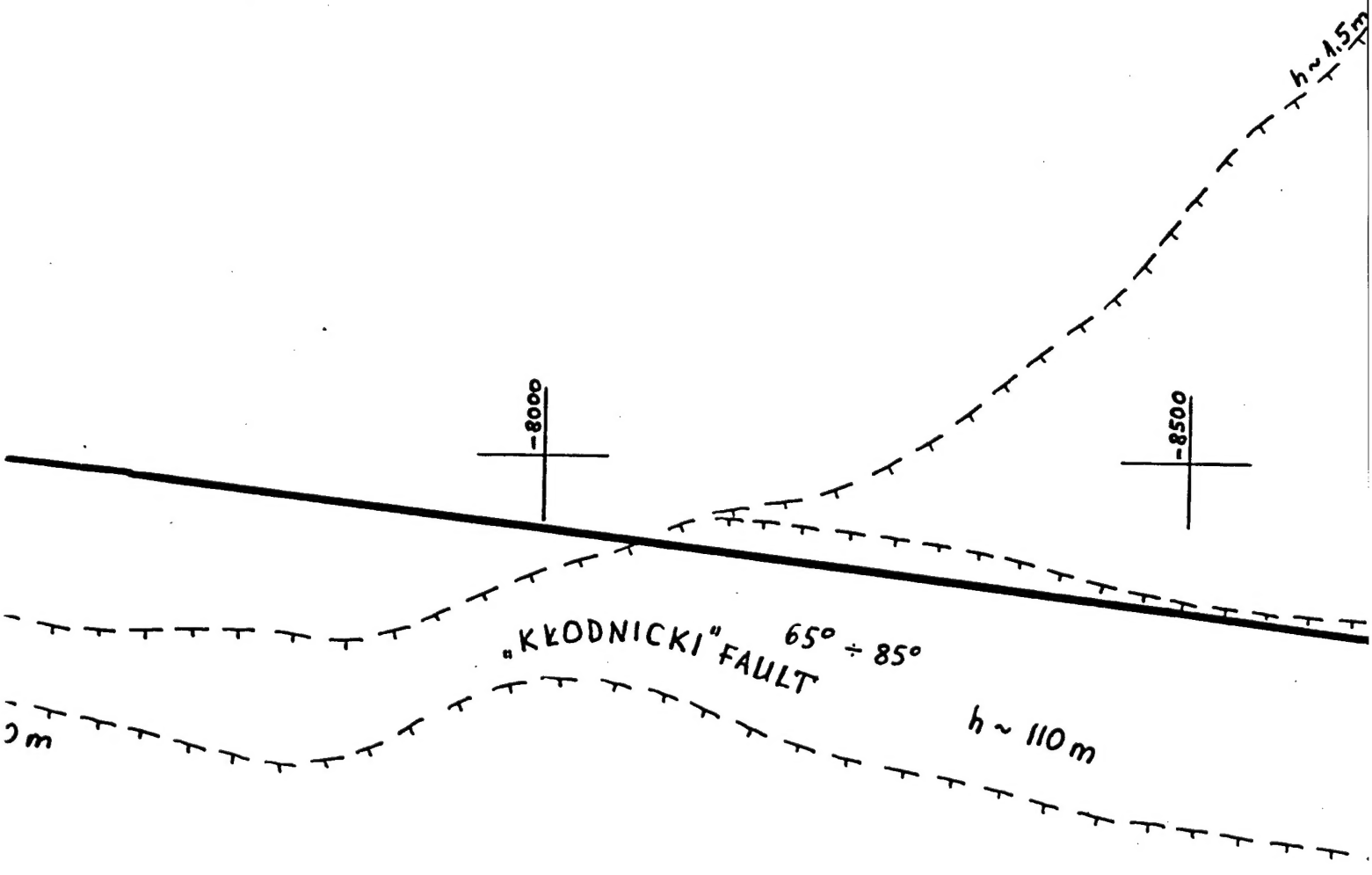

(1D)

h~1.5m

35°

01.01.94

Sc. IV a

11.07.93

Sc. III a

Sc. II a

-9000

-9500

h~12

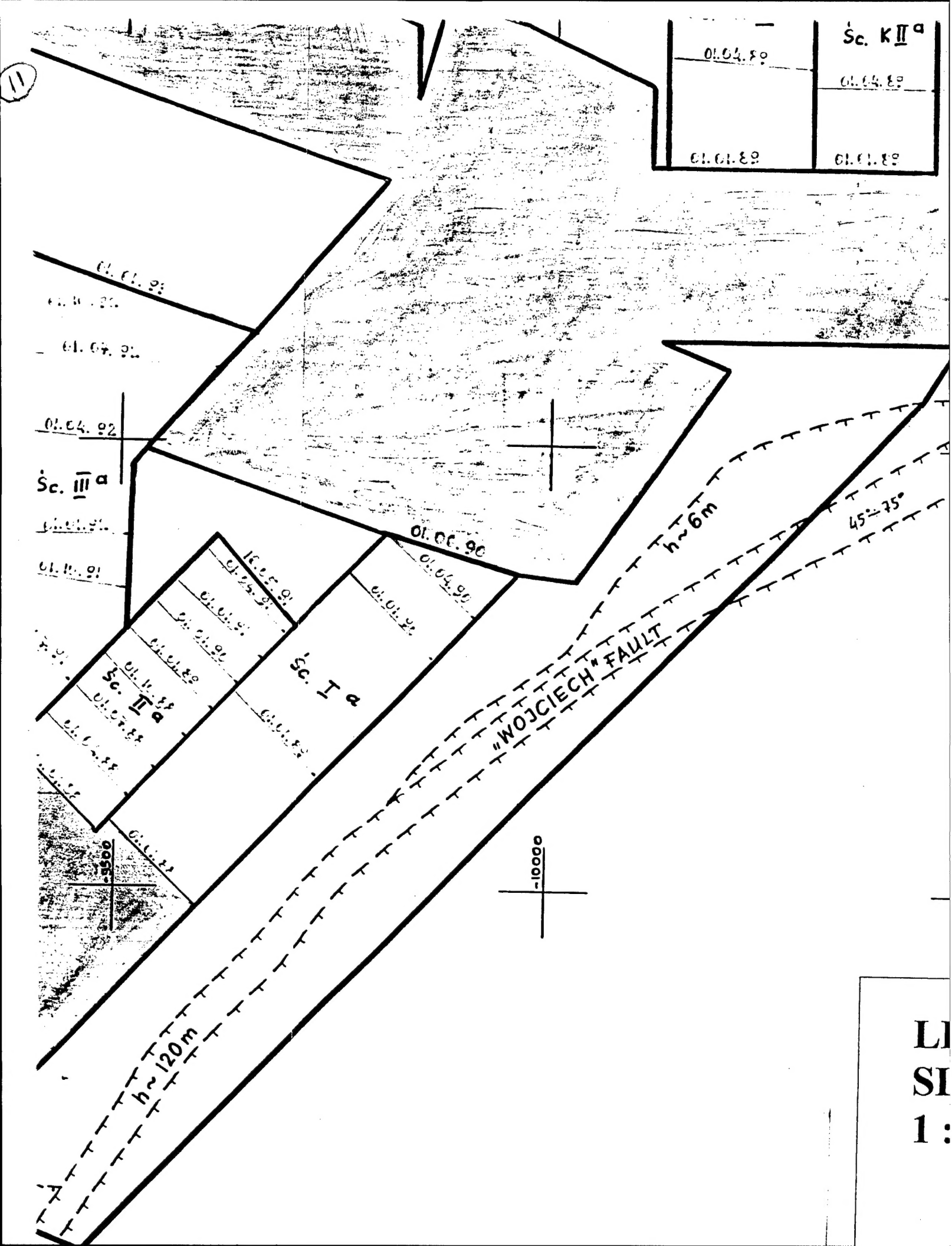
Sc. K III a
01.04.89
01.04.89
01.01.89
01.01.89
01.01.90
01.04.92
Sc. III a
01.01.90
01.04.90
Sc. II a
Sc. I a
h~6m
45°÷75°
"WOJCIECH" FAULT
h~120m
-9500
-10000

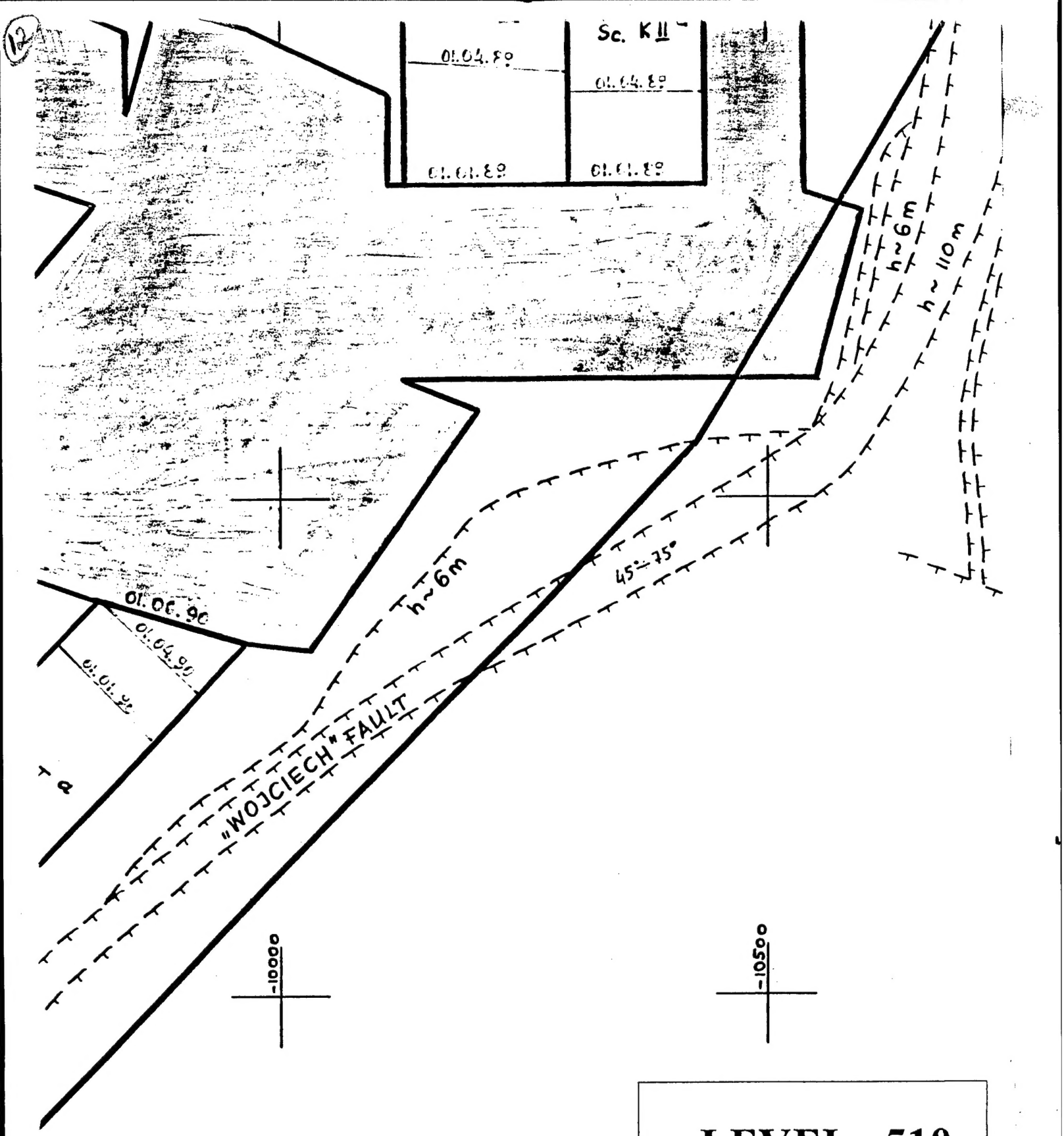

LEVEL 510
SLAB 2
1 : 5000

APPENDIX 9